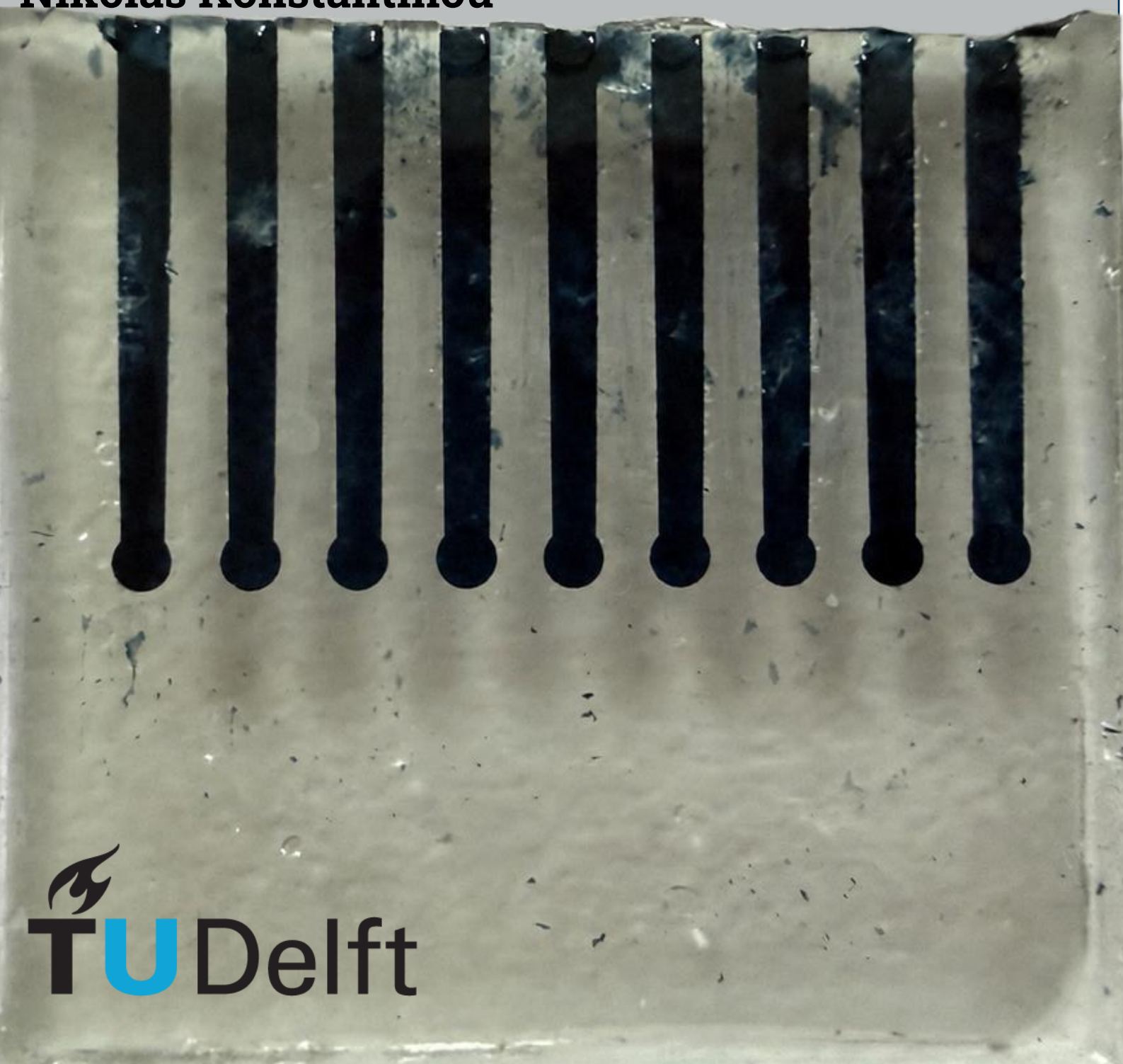
Development and Characterisation of PEDOT:PSS-Based Conductive Hydrogels for Bioelectronic Neural Interfaces

Master of Science in Biomedical Engineering

August 2026

Nikolas Konstantinou



TU Delft

Development and Characterisation of PEDOT:PSS-Based Conductive Hydrogels for Bioelectronic Neural Interfaces

by

Nikolas Konstantinou

To obtain the degree of Master of Science
at the Delft University of Technology,
to be defended publicly on Friday, August 28, 2026, at 09:00 AM.

Student Number:	6297161			
Project Duration:	January 2026 - August 2026			
Thesis committee:	Dr. Achilleas Savva	TU	Delft,	supervisor
	Dr. Tiago Costa	TU	Delft	
	Dr. Puyan Boukany	TU	Delft	

An electronic version of this thesis is available at https://repository.tudelft.nl/.

TU Delft

Abstract

Bioelectronic neural interfaces require materials that can bridge the gap between soft, hydrated biological tissue and conventional electronic systems. Conductive hydrogels are promising candidates because they combine the mechanical softness and hydration of hydrogels with electrical functionality. In this thesis, PEDOT:PSS-based conductive hydrogels were developed and characterised as soft-material candidates for bioelectronic neural interface applications. Three formulations were investigated: PEDOT:PSS-DBSA, PEDOT:PSS-PAA, and PEDOT:PSS-PEGPACHI. PEDOT:PSS-DBSA was used as a literature-based additive-induced hydrogel formulation, while PEDOT:PSS-PAA represented a polymer-network-based approach involving redox polymerisation, post-treatment, annealing, and rehydration. PEDOT:PSS-PEGPACHI was developed in this thesis as a new formulation based on PEDOT:PSS, phytic acid, chitosan, and PEGDE. The hydrogels were evaluated through physical observation, electrochemical impedance spectroscopy, cyclic voltammetry, nanoindentation, biological compatibility assessment, and preliminary device integration. The results showed that the gelation strategy and additive system strongly influenced the final material behaviour. PEDOT:PSS-DBSA showed the strongest electrochemical response and the most uniform local mechanical behaviour, but was fragile during handling. PEDOT:PSS-PAA was more robust and easier to handle, but showed a weaker electrochemical response and greater local variability. PEDOT:PSS-PEGPACHI showed an intermediate electrochemical response, soft hydrogel-like mechanical behaviour, and favourable preliminary biological compatibility. Based on the combined material and biological assessments, PEDOT:PSS-PEGPACHI was selected for preliminary integration into a PDMS hydrogel array device. The formulation could be patterned into hydrogel tracks and electrically accessed after gelation and hydration, demonstrating its potential for future soft bioelectronic platforms. Overall, this thesis demonstrates that PEDOT:PSS-based conductive hydrogels are promising materials for neural interface applications and identifies PEDOT:PSS-PEGPACHI as a strong candidate for further optimisation and biological validation.

Thesis Framework

The work presented in this MSc thesis was carried out within the Bioelectronics group at TU Delft and focused on developing soft, conductive hydrogel materials for bioelectronic neural interface applications. The thesis was motivated by the need for materials that can better bridge the mismatch between conventional electronic interfaces and soft, hydrated neural tissue. PEDOT:PSS was selected as the conductive polymer phase due to its mixed ionic-electronic transport properties, aqueous processability, and relevance to organic bioelectronics. Based on this material platform, three PEDOT:PSS-based hydrogel formulations were developed and compared: PEDOT:PSS-DBSA, PEDOT:PSS-PAA, and PEDOT:PSS-PEGPACHI. These formulations represented different gelation and material design strategies, allowing the effects of additives, processing routes, and hydrogel network formation to be evaluated. The thesis follows a material-development framework. First, the hydrogel formulations were developed and optimised. The resulting materials were then characterised physically, electrochemically, and mechanically to assess their stability, charge-transport behaviour, and hydrated stiffness. Biological compatibility was evaluated using preliminary cell culture experiments, and the most promising formulation was further integrated into a preliminary PDMS hydrogel array device. This framework allowed the thesis to progress from hydrogel formulation and optimisation towards material characterisation, biological assessment, and proof-of-concept device integration. Through this approach, PEDOT:PSS-PEGPACHI was identified as the most promising formulation for further development towards soft bioelectronic neural-interface platforms.

Acknowledgements

I would first like to express my sincere gratitude to my supervisor and thesis chair, Dr Achilleas Savva, for the opportunity to conduct this thesis work in the Bioelectronics group at TU Delft. His guidance, scientific input, and support throughout the project were essential for shaping this work. I am especially grateful for the freedom to explore different hydrogel formulations while always receiving constructive feedback and guidance when needed.

I would also like to thank my thesis committee members, Dr. Tiago Costa and Prof. Pouyan Boukany, for their time, feedback, and evaluation of this work.

I want to thank Dr. Filipe Arroyo Cardoso for his support and advice, especially regarding the cleanroom-related aspects of the project. I am also very grateful to Flavia Valente for showing me first-hand how to work with hydrogels inside the cleanroom and for sharing her practical experience. Her help made the cleanroom work much easier to approach. I would also like to thank the Else Kooi Laboratory staff and everyone involved in the cleanroom training for their technical support, guidance, and help with safe access to the cleanroom facilities.

I would like to sincerely thank Liwen Wang for all her help throughout this project. Her practical support in the lab, her experience with hydrogel preparation and biological experiments, and her work conducting cell experiments in Leiden were extremely valuable. I am also grateful to Jean-Philippe (J.P.) Frimat and the collaborators in Leiden for their contribution to the neuronal culture experiments and for providing the biological images and data used in this thesis.

I would also like to thank Mustafeez Shah for the useful discussions and advice, and Tawab Karim for his help with cleanroom equipment, PDMS-related work, and general practical support. I am also grateful to the ongoing collaborators from the Brinks Lab, especially Chris Vink, for their willingness to help with the ongoing Live/Dead assay optimisation and biological experiments.

I want to thank Maria-Ioanna Bileri and the group in Graz for their contribution to the preliminary DBSA biocompatibility work and for their support during the earlier stages of this project.

A special thank you goes to the technicians who supported this work. I want to thank Brian Nanhekhan for his help, expertise, and practical support in the wet and measurement labs. I am also very grateful to Lennart van Zanten for his help with the mechanical testing measurements and for giving me access to his lab and expertise during the nanoindentation experiments.

I would also like to thank all members of the Bioelectronics group for creating such a supportive, collaborative, and motivating research environment. I am grateful for the scientific discussions, practical advice, feedback during group meetings, and everyday help in the lab. Being part of the group made this thesis experience more enjoyable and helped me grow both scientifically and personally.

Finally, I would like to thank my family and friends for their constant support, patience, and encouragement throughout this thesis. Their support helped me stay motivated during both the successful moments and the more challenging parts of the project. This work would not have been possible without the scientific, practical, and personal support of all the people mentioned above.

Contents

Abstract 3

Thesis Framework 4

Acknowledgements 5

List of acronyms 10

1 Introduction 11
- 1.1 Bioelectronic neural interfaces 11
- 1.2 The need for soft and conductive materials 12
- 1.3 Conductive hydrogels and PEDOT:PSS 13
- 1.4 Research aim and objectives 14
- 1.5 Outline of the report 14

2 Literature Review 16
- 2.1 Neural interfaces and material requirements 16
- 2.2 Conductive hydrogels for bioelectronic interfaces 17
- 2.3 PEDOT:PSS in bioelectronics 18
- 2.4 Strategies to form PEDOT:PSS-based conductive hydrogels 20
- 2.5 Characterisation of conductive hydrogels 25
- 2.6 Summary and research gap 28

3 Materials and Methods 29
- 3.1 Materials 29
- 3.2 Preparation of PEDOT:PSS-based hydrogel formulations 30
  - 3.2.1 PEDOT:PSS-DBSA hydrogels 30
  - 3.2.2 PEDOT:PSS-PAA conductive hydrogels 31
  - 3.2.3 PEDOT:PSS-PEGPACHI conductive hydrogels 33
- 3.3 Moulding and sample preparation 35
  - 3.3.1 General moulding approaches 35
  - 3.3.2 Direct casting into electrochemical devices 35
  - 3.3.3 Sample storage and handling before characterisation 36
  - 3.3.4 Sterile handling and conditioning of conductive hydrogels for cell culture 36
- 3.4 Physical characterisation 37
  - 3.4.1 Assessment of gel formation 37
  - 3.4.2 Macroscopic appearance and handling 37
  - 3.4.3 Wet-state stability during storage 37
  - 3.4.4 Photographic documentation 37
- 3.5 Electrochemical characterisation 37
  - 3.5.1 Three-electrode measurements in the PDMS measuring platform 38
  - 3.5.2 Swagelok-based bulk conductive hydrogel measurements 38
  - 3.5.3 Electrochemical impedance spectroscopy 38
  - 3.5.4 Cyclic voltammetry 38

3.5.5 Data processing 39
3.6 Mechanical characterisation 39
3.6.1 Sample preparation for mechanical testing 39
3.6.2 Nanoindentation measurements 39
3.6.3 Mechanical indentation scans 39
3.6.4 Mechanical data processing 40
3.7 Biological characterisation 40
3.7.1 Overview of biological testing 41
3.7.2 U87 cell metabolic activity assay 41
3.7.3 Biological testing with Leiden collaborators 42
3.7.4 Live/Dead staining, immunofluorescence staining, and microscopy 42
3.8 PDMS measuring platform for electrochemical characterisation 43
3.8.1 Design rationale of the PDMS measuring platform 43
3.8.2 CAD design and 3D printing of the inverse mould 44
3.8.3 PDMS casting and curing 44
3.8.4 Hydrogel integration into the PDMS measuring platform 44
3.8.5 Electrochemical measurements in the integrated platform 44

4 Hydrogel Development and Optimisation 46
4.1 Overview of hydrogel development strategy 46
4.2 PEDOT:PSS-DBSA hydrogel development 47
4.2.1 Rationale for selecting the PEDOT:PSS-DBSA formulation 47
4.2.2 Proposed role of DBSA in PEDOT:PSS gel formation 47
4.2.3 Initial reproduction of the literature protocol 49
4.2.4 Optimisation of the mixing protocol 49
4.2.5 Effect of DBSA concentration and temperature on gelation 49
4.2.6 Importance of filtration and sample handling 50
4.2.7 Final selected PEDOT:PSS-DBSA formulation 50
4.3 PEDOT:PSS-PAA hydrogel formation 51
4.3.1 Rationale for selecting the PEDOT:PSS-PAA formulation 51
4.3.2 Proposed formation mechanism and role of the components 52
4.3.3 Cleanroom implementation and initial fabrication challenges 53
4.3.4 Optimisation of precursor mixing and gelation control 54
4.3.5 Post-treatment, annealing, and rehydration behaviour 55
4.3.6 Moulding and integration limitations 55
4.3.7 Final selected PEDOT:PSS-PAA formulation 55
4.4 PEDOT:PSS-PEGPACHI hydrogel formation 56
4.4.1 Rationale for developing the PEDOT:PSS-PEGPACHI formulation 56
4.4.2 Design logic and proposed role of each component 56
4.4.3 Initial replacement strategy-from DBSA to phytic acid 58
4.4.4 Chitosan addition and the need for a PA-chitosan stock solution 58
4.4.5 Optimisation of phytic acid and chitosan concentration 59
4.4.6 Tests with $CaSO_4$ and low DBSA addition 59
4.4.7 Addition of PEGDE and stabilisation of the final formulation 60
4.4.8 Final PEGPACHI hydrogel behaviour and selection for characterisation 60
4.5 Comparison of gel formation between formulations 61
4.6 Selection of formulations for further characterisation 62

5 Physical, Electrochemical, and Mechanical Characterisation of PEDOT:PSS-Based Hydrogels 64
5.1 Overview of characterisation strategy 64
5.2 Physical and macroscopic hydrogel characterisation 64
5.2.1 Macroscopic appearance and gel integrity 65
5.2.2 Handling and mouldability 65
5.2.3 Stability in aqueous media 66
5.2.4 Qualitative comparison of the three hydrogel formulations 66
5.3 Development and implementation of electrochemical measurement configurations 67
5.3.1 Rationale for using two electrochemical measurement configurations 67
5.3.2 PDMS measuring platform development and implementation 67
5.3.3 Swagelok-based bulk measurement setup 69
5.3.4 Comparison between the two electrochemical measurement configurations 71
5.4 Electrochemical characterisation in the PDMS measuring platform 71
5.4.1 PEDOT:PSS-DBSA electrochemical response 72
5.4.2 PEDOT:PSS-PAA electrochemical response 73
5.4.3 PEDOT:PSS-PEGPACHI electrochemical response 75
5.4.4 Comparative electrochemical evaluation of the PEDOT:PSS-based hydrogels 76
5.5 Electrochemical characterisation in the Swagelok-based bulk setup 77
5.5.1 Rationale for Swagelok bulk measurements 77
5.5.2 Comparison of PEDOT:PSS-based hydrogels in the gold-gold Swagelok configuration 78
5.5.3 Comparison of PEDOT:PSS-based hydrogels in the platinum-platinum Swagelok configuration 79
5.6 Summary of electrochemical behaviour of the PEDOT:PSS-based hydrogels 80
5.7 Mechanical characterisation by nanoindentation 81
5.7.1 Nanoindentation response of PEDOT:PSS-DBSA 81
5.7.2 Nanoindentation response of PEDOT:PSS-PAA 82
5.7.3 Nanoindentation response of PEDOT:PSS-PEGPACHI 84
5.7.4 Comparison of mechanical properties 85
5.8 Summary of mechanical behaviour 86

6 Biological Compatibility 87
6.1 Biological compatibility assessment 87
6.2 Preliminary U87 metabolic activity assessment of PEDOT:PSS-DBSA 87
6.3 Neuronal culture compatibility of PEDOT:PSS-based hydrogels 88
6.4 Live/Dead quantification of control and PEDOT:PSS-PEGPACHI cultures 90
6.5 Immunofluorescence observations 92
6.6 Overall biological compatibility discussion 93

7 PEDOT:PSS-based conducting Hydrogel electrodes - a proof of concept 95
7.1 Aim of the preliminary hydrogel-array device 95
7.2 Design development of the PDMS hydrogel-array device 95
7.3 Fabrication and PEDOT:PSS-PEGPACHI integration 97
7.4 Preliminary electrical access and measurement of PEDOT:PSS-PEGPACHI hydrogel electrodes 97
7.5 Comparison with hydrogel-based electrode-array approaches 99

7.6 Preliminary device assessment and limitations 100

8 Conclusions and Future Work 102
8.1 Main conclusions 102
8.2 Answer to the research aim 103
8.3 Limitations 103
8.4 Future work 104
8.5 Final statement 105

Appendix A. Optimised protocol for PEDOT:PSS-DBSA hydrogel preparation 107

Appendix B. EKL-approved protocol for PEDOT:PSS-PAA hydrogel fabrication 108

Appendix C. Optimised protocol for PEDOT:PSS-PEGPACHI hydrogel preparation 112

Appendix D. Additional experimental documentation of PEDOT:PSS-DBSA hydrogel optimisation 114

Appendix E. Detailed experimental log of PEDOT:PSS-PEGPACHI hydrogel optimisation 115

Appendix F. PDMS measuring platform design iterations and bonding development 119

Appendix G. Supplementary nanoindentation analysis 123

Appendix H. PEDOT:PSS-PAA hydrogel optimisation 128

Appendix I. PDMS hydrogel-array device design optimisation 131

Appendix J. Supplementary comparison with hydrogel-based electrode-array approaches 134

Appendix K. Supplementary electrochemical characterisation 136

Appendix L. Supplementary Swagelok electrochemical analysis 146

Bibliography 155

List of acronyms

Acronym	**Definition**
MEA(s)	Microelectrode Array(s)
PDMS	Polydimethylsiloxane
PEDOT:PSS	Poly(3,4-ethylenedioxythiophene):polystyrene sulfonate
EEG	Electroencephalography
ECoG	Electrocorticography
SNR	Signal-to-noise ratio
CSC	Charge storage capacity
CIC	Charge injection capacity
PPy	Polypyrrole
PANI	Polyaniline
DBSA	4-dodecylbenzenesulfonic acid
PEGDE	Poly(ethylene glycol) diglycidyl ether
PAA	Poly(acrylic acid)
AA	Acrylic acid
MBAA	N,N′-methylenebisacrylamide
H_2O_2	Hydrogen peroxide
EMIM-ES	1-ethyl-3-methylimidazolium ethyl sulfate
DMSO	Dimethyl sulfoxide
DI water	Deionised water
EKL	Else Kooi Laboratory
DPBS	Dulbecco's phosphate-buffered saline
DMEM	Dulbecco's Modified Eagle Medium
Ag/AgCl	Silver/silver chloride
hiPSC	Human induced pluripotent stem cell
EIS	Electrochemical impedance spectroscopy
CV	Cyclic voltammetry
MTS	3-(4,5-dimethylthiazol-2-yl)-5-(3-carboxymethoxyphenyl)-2-(4-sulfophenyl)-2H-tetrazolium
PA	Phytic acid
CHI	Chitosan
PBS	Phosphate-buffered saline
Eeff	Effective Young's modulus
CSC	Charge storage capacity
CIC	Charge injection capacity

1 Introduction

1.1 Bioelectronic neural interfaces

Bioelectronic neural interfaces aim to establish a functional connection between neural tissue and external electronic systems. Because neural cells communicate via electrical and electrochemical signals, these interfaces can record neural activity, deliver electrical stimulation, or enable bidirectional communication between biological tissue and electronic devices. Electronic neural interfaces have therefore been described as a direct electrical bridge between the nervous system and man-made systems, typically comprising a tissue interface, a sensing interface, and a neural signal processing unit [1].

Electrical recording and stimulation are essential to many neural engineering applications. Recording electrodes detect neural electrical activity, while stimulation electrodes deliver controlled electrical inputs to modulate excitable tissue. These principles have been applied to neural prostheses and therapies for sensory restoration, movement disorders, spinal cord injury, and other neurological conditions [2]. In this context, the electrode/tissue interface is a critical part of device performance, because it determines how efficiently ionic signals from the biological environment are converted into electronic signals, and vice versa [2].

At the same time, bioelectronic medicine has expanded the role of neural interfaces beyond passive recording. The concept of “electroceuticals” proposed that electrical impulses could be used to modulate neural circuits associated with disease, provided that the relevant circuits and intervention points can be identified [3]. This idea was further developed into the field of bioelectronic medicine, which aims to create therapeutic approaches based on targeted modulation of electrical signalling patterns in the nervous system [4]. Although this thesis is not focused on a therapeutic device, this broader field highlights the importance of developing materials that can interface effectively with neural tissue.

Microelectrode arrays (MEAs) are among the most widely used platforms for studying neural activity in vitro and in vivo. They allow simultaneous, long-term, and cell-non-invasive recordings of extracellular field potentials from multiple sites, making them valuable tools for studying neuronal networks and electrophysiological activity [5]. However, conventional extracellular electrodes mainly detect activity outside the cell and can have limitations in resolving weaker or more localized signals compared to intracellular techniques [5]. Improving the interface between electrodes and biological tissue therefore remains an important goal in neural interface development.

Despite major progress in neural recording and stimulation technologies, a persistent challenge is the mismatch between conventional electronic materials and neural tissue. Neural tissue is soft, hydrated, and chemically dynamic, while many electronic interfaces are relatively stiff and dry. This mismatch can contribute to poor long-term coupling, foreign-body responses, and reduced device performance, especially for chronic or intimate tissue-contact applications [6]. As a result, current neural interface research increasingly focuses on materials innovation, including flexible, organic, and bioinspired materials that can better match the biological environment [6]. Within this direction, organic bioelectronics has emerged as an important field because organic electronic materials can act as an interface between biological ionic signalling and electronic device operation [7], [8]. This makes them particularly attractive for bridging the gap between conventional electronics and living systems. Conductive hydrogels are promising in this context because they can combine hydration and

mechanical softness with electrical functionality, making them relevant candidates for future bioelectronic neural interfaces [9], [10].

1.2 The need for soft and conductive materials

One of the main challenges in neural interface development is not only achieving efficient electrical recording or stimulation but also creating a stable, compatible contact with neural tissue. Conventional electronic materials are usually rigid, dry, and synthetic, whereas neural tissue is soft, hydrated, and biologically dynamic. This difference in material properties can lead to poor mechanical mismatch between the device and the tissue, and in implantable systems it can contribute to tissue damage, foreign-body reactions, glial scarring, and long-term performance degradation [6], [11].

A key aspect of this challenge is the mechanical mismatch between neural tissue and everyday electronic materials. Brain tissue and neurons have elastic moduli close to the soft tissue range, while materials such as silicon, SU-8, polyimide, parylene-C, and semiconductors are several orders of magnitude stiffer. Flexible polymers can reduce this mismatch compared with rigid silicon-based materials, but their stiffness is still often much higher than that of neural tissue. Hydrogels are promising in this context because their mechanical properties can be tuned into a softer, tissue-like range, as shown in Figure 1.1 [9], [11].

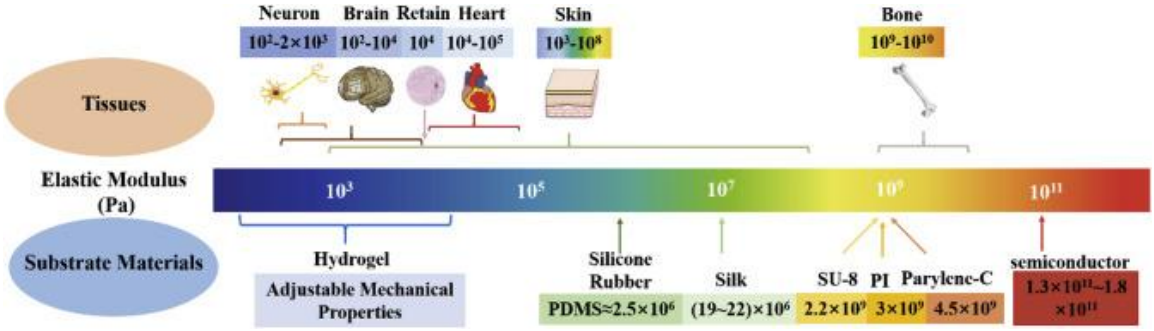


Figure 1.1: Elastic modulus mismatch between biological tissues and common substrate materials used in neural interfaces. The logarithmic scale compares the elastic modulus of soft biological tissues, including neurons and brain tissue, with commonly used substrate materials such as polydimethylsiloxane (PDMS), silicone rubber, SU-8, polyimide, parylene-C, and semiconductors. Hydrogels occupy a soft and tuneable mechanical range closer to neural tissue, highlighting their potential as mechanically compliant materials for bioelectronic neural interfaces. Reproduced from Shi et al [11].

In addition to mechanical compliance, hydrogels offer an important advantage in terms of chemical tunability. Their three-dimensional polymer networks can be modified by changing the polymer composition, crosslinking density, charge density, hydrophilicity, and functional groups. This allows properties such as swelling, ion transport, degradation, protein adsorption, and cell/material interactions to be adjusted for a specific biological application [9], [10], [12]. In contrast, conventional conductive thin films are often optimised mainly through coating thickness, morphology, dopants, and surface modification, while their interaction with the biological environment is largely limited to the film surface [13], [14]. Therefore, hydrogels provide a more versatile platform for designing soft, hydrated, and chemically adaptable bioelectronic interfaces.

However, softness and chemical tunability alone are not sufficient for neural interfaces, because these materials must also support electrical communication with the nervous system. Biological signalling is

mainly based on ionic transport in aqueous environments, whereas conventional electronic devices rely on electronic charge carriers. Therefore, an effective neural interface should support ionic-electronic coupling at the material-tissue interface. This requirement has motivated the development of soft materials that can combine tissue-like mechanical properties with electrical functionality [9], [12].

Hydrogels are promising materials for this purpose because they are crosslinked polymer networks with very high-water content, allowing them to resemble several key physical aspects of biological tissues. Their hydrated structure can provide a wet and ion-rich environment, while their chemistry can be engineered to tune mechanical properties, swelling behaviour, adhesion, degradation, and biofunctionality [9]. However, most conventional hydrogels are not electronically conductive. This limits their direct use as bioelectronic interfaces unless an electrically conductive component is incorporated. Conductive hydrogels aim to address this limitation by combining the softness and hydration of hydrogels with electrical conductivity. Depending on their composition, conductive hydrogels can support ionic conduction, electronic conduction, or mixed ionic-electronic conduction. For neural interfaces, this combination is especially relevant because it may improve the coupling between ionic signals in the biological environment and electronic signals in the connecting device. Recent reviews describe conductive hydrogels with tissue-like mechanical properties and tuneable conductivity as promising candidates for neural recording and stimulation electrodes [12].

Despite these advantages, developing conductive hydrogels for neural bioelectronics remains challenging. The material must be soft but mechanically stable, conductive but not cytotoxic, hydrated but not easily degraded, and compatible with reproducible fabrication and characterisation methods. Therefore, the design of conductive hydrogels requires balancing mechanical, electrical, chemical, and biological requirements. This thesis explores PEDOT:PSS-based conductive hydrogels as a material platform designed to achieve this balance in bioelectronic neural interfaces.

1.3 Conductive hydrogels and PEDOT:PSS

To make hydrogels suitable for bioelectronic applications, electrically active components can be incorporated into the hydrated polymer network. These components may include conductive polymers, carbon-based materials, metallic nanostructures, or ionic additives. Depending on the formulation, these conductive phases can create electrical pathways within the hydrogel, allowing the material to combine the softness and hydration of conventional hydrogels with the electrical functionality required for neural-interface applications [10], [12].

Among conductive polymers, poly(3,4-ethylenedioxythiophene):polystyrene sulfonate (PEDOT:PSS) has become one of the most widely used materials in organic bioelectronics. PEDOT:PSS is attractive because it combines aqueous processability, relatively high electrical conductivity, electrochemical stability, and compatibility with wet physiological environments. In neural interfaces, PEDOT:PSS has commonly been explored as an electrode coating to reduce impedance and improve charge transfer between biological tissue and electronic devices [7].

A key advantage of PEDOT:PSS is that it can improve the electrochemical performance of bioelectronic interfaces. Unlike conventional metallic electrodes, where charge storage is mainly limited to the electrode surface, PEDOT:PSS can contribute to charge storage throughout the polymer volume. This volumetric capacitive behaviour can increase charge storage capacity and lower impedance, making PEDOT:PSS highly relevant for neural electrodes and soft bioelectronic materials [7], [15].

Incorporating PEDOT:PSS into hydrogel systems becomes important because it may combine the electrical advantages of PEDOT:PSS with the mechanical softness, hydration, and tissue-like properties of hydrogels. However, developing stable PEDOT:PSS-based conductive hydrogels is not a straightforward procedure. The final material properties depend strongly on the formulation strategy,

including the polymer network, conductive phase, dopants, additives, crosslinkers, gelation conditions, and post-processing steps. These parameters influence not only the electrical performance, but also the mechanical stability, swelling behaviour, reproducibility, and biological compatibility of the hydrogel [9], [10], [12].

Therefore, this thesis focuses on the development and characterisation of PEDOT:PSS-based conductive hydrogels as soft material candidates for bioelectronic neural interfaces. The aim is to investigate how different formulation strategies influence the properties of the resulting hydrogels and to evaluate their potential for future integration in neural interface devices.

1.4 Research aim and objectives

The aim of this thesis is to develop and characterise poly(3,4-ethylenedioxythiophene):polystyrene sulfonate (PEDOT:PSS)-based conductive hydrogels as soft material candidates for bioelectronic neural interfaces. The work focuses on identifying formulation strategies that can combine electrical functionality with hydrogel-like mechanical and physical properties, while remaining suitable for future biological interfacing.

To achieve this aim, different PEDOT:PSS-based hydrogel systems were explored and optimised. The first objective was to investigate different gelation paths that could transform PEDOT:PSS from a conductive polymer dispersion into a stable hydrogel structure. Particular attention was given to the role of additives, crosslinkers, and processing conditions in determining whether reproducible gel formation could be achieved.

The second objective was to characterise the physical and electrochemical properties of the developed hydrogels. Since the intended application is bioelectronic neural interfacing, the materials were evaluated not only based on their macroscopic gel formation, but also on their electrical behaviour in physiologically relevant aqueous environments. Electrochemical impedance spectroscopy (EIS) and cyclic voltammetry (CV) were used to assess impedance, charge storage behaviour, and the ability of the gels to support electrical coupling at the interface.

The third objective was to assess the biological compatibility of selected hydrogel formulations. For neural-interface applications, the material should not only be conductive and mechanically suitable, but also compatible with cells and aqueous culture conditions. Therefore, cell-based experiments were used to evaluate whether selected formulations could support or maintain cell viability, providing an initial indication of their suitability for future neural bioelectronic platforms.

Finally, this thesis aimed to critically compare the different hydrogel approaches and identify the main formulation-property relationships that determine their performance. Based on this critical evaluation, the most promising gel candidate was selected for further exploration. As a proof of concept, a preliminary device platform was also developed and characterised to demonstrate the potential integration of the selected conductive hydrogel in a bioelectronic neural-interface configuration.

1.5 Outline of the report

This thesis is organised into eight chapters:

Chapter 1 introduces the motivation for developing soft conductive materials for bioelectronic neural interfaces. It presents the problem of mechanical and functional mismatch between conventional electronic materials and neural tissue, introduces conductive hydrogels and PEDOT:PSS as relevant material platforms, and defines the aim and objectives of the thesis.

Chapter 2 provides the literature background. It first discusses neural interfaces and their material requirements, followed by an overview of conductive hydrogels and PEDOT:PSS-based materials. The

chapter then reviews different strategies used to form PEDOT:PSS-based conductive hydrogels and discusses the main challenges associated with their electrochemical characterisation. Finally, the chapter identifies the research gap addressed in this thesis.

Chapter 3 describes the materials and experimental methods used in this work. This includes the preparation protocols for PEDOT:PSS-DBSA, PEDOT:PSS-PAA, and PEDOT:PSS-PEGPACHI conductive hydrogels, as well as the moulding, conditioning, physical observation, electrochemical characterisation, mechanical testing, biological compatibility assessment, and preliminary device fabrication methods.

Chapter 4 presents the development and optimisation of the three PEDOT:PSS-based conductive hydrogel formulations. The chapter describes the formulation challenges, processing decisions, and optimisation steps that led to the final selected conductive hydrogels. Special attention is given to the development of PEDOT:PSS-PEGPACHI as a new formulation based on PEDOT:PSS, phytic acid, chitosan, and PEGDE.

Chapter 5 presents the physical, electrochemical, and mechanical characterisation of the selected conductive hydrogels. The chapter compares the macroscopic behaviour, electrochemical response, and hydrated-state stiffness of PEDOT:PSS-DBSA, PEDOT:PSS-PAA, and PEDOT:PSS-PEGPACHI. It also discusses the use of different electrochemical measurement configurations, including the PDMS measuring platform and Swagelok-based bulk measurements.

Chapter 6 evaluates the biological compatibility of the PEDOT:PSS-based conductive hydrogels. It includes preliminary metabolic activity results for PEDOT:PSS-DBSA and neuronal culture compatibility assessment for PEDOT:PSS-PAA and PEDOT:PSS-PEGPACHI. Live/Dead analysis and immunofluorescence observations are used to assess the biological response to the most relevant conductive hydrogel conditions.

Chapter 7 describes the preliminary fabrication and testing of a PDMS conductive hydrogel-array device. PEDOT:PSS-PEGPACHI is integrated into patterned conductive hydrogel tracks, and the electrical accessibility of the tracks is evaluated using electrochemical measurements. The device is also positioned relative to published and ongoing conductive hydrogel-based electrode-array approaches.

Chapter 8 summarises the main conclusions of the thesis, answers the research aim, discusses the main limitations, and proposes future work. It highlights the development and first validation of PEDOT:PSS-PEGPACHI as a promising conductive hydrogel formulation for further optimisation towards soft bioelectronic neural-interface platforms.

2 Literature Review

2.1 Neural interfaces and material requirements

Neural interfaces are designed to establish communication between neural tissue and electronic systems, either by recording endogenous electrical activity, delivering electrical stimulation, or supporting bidirectional interaction with the nervous system [1], [2]. Their performance depends not only on the external recording or stimulation hardware, but also on the quality and stability of the electrode/tissue interface. Therefore, this interface controls how ionic signals from the biological environment are coupled to electronic charge transport in the device [2], [16].

Depending on the degree of invasiveness, neural recording electrodes can be classified as non-invasive, semi-invasive, or invasive interfaces, such as electroencephalography (EEG), electrocorticography (ECoG), and penetrating microelectrodes, respectively [16], [17]. In general, placing the electrode closer to the neural source can improve spatial resolution and signal amplitude, but it also increases the importance of material biocompatibility, mechanical compatibility, and long-term stability. Therefore, the requirements for a neural interface depend strongly on the intended application. Still, they usually include efficient electrical coupling, low noise, mechanical compliance, stable performance in physiological environments, and compatibility with neural cells or tissue [6], [17], [18].

For recording applications, the electrode must detect small extracellular potentials with sufficient signal quality. A low electrode impedance is generally desirable because it can reduce thermal noise and improve the signal-to-noise ratio (SNR), with impedance at 1 kHz commonly used as a practical benchmark for neural recording electrodes [2], [16], [18]. For stimulation applications, the material must also deliver charge safely to the tissue. In this case, charge storage capacity (CSC) and charge injection capacity (CIC) are important parameters, because they describe how much charge can be stored or injected without driving irreversible electrochemical reactions that may damage the electrode or surrounding tissue [2], [16], [18].

Besides electrochemical performance, mechanical properties are also a noteworthy parameter for neural interfaces. Neural tissue is soft and hydrated, whereas many conventional electrode materials, such as silicon and metals, are orders of magnitude stiffer [6], [11]. This mechanical mismatch can generate interfacial stress during tissue movement or device micromotion, which may contribute to tissue damage, inflammation, glial scarring, and physical separation between the electrode and nearby neurons [6], [11], [18]. Over time, these biological and mechanical responses can increase impedance, reduce signal quality, and limit the interface's long-term performance [6], [18], [19].

Another important parameter is stability in aqueous and physiological environments. Neural interface materials are exposed to electrolytes, proteins, cells, and mechanical deformation, all of which can affect material properties over time [18], [19]. Common failure mechanisms include corrosion, swelling, cracking, insulation leakage, delamination, and degradation of conductive coatings [19]. This is especially relevant for soft coatings and conductive hydrogel-based interfaces, where hydration and repeated electrical cycling can strongly influence the material structure and electrochemical behaviour [19], [20].

Biocompatibility must also be considered together with electrochemical and mechanical performance. In implantable systems, both the acute injury caused by insertion and the chronic presence of the device can trigger inflammatory or foreign-body responses [6], [18], [19]. In in vitro neural interface platforms, material toxicity or poor surface compatibility can affect cell viability, attachment, and

electrophysiological behaviour [18]. Therefore, a material that performs well electrically is not necessarily suitable for neural interfacing unless it also maintains stable and acceptable biological interactions [6], [16], [18].

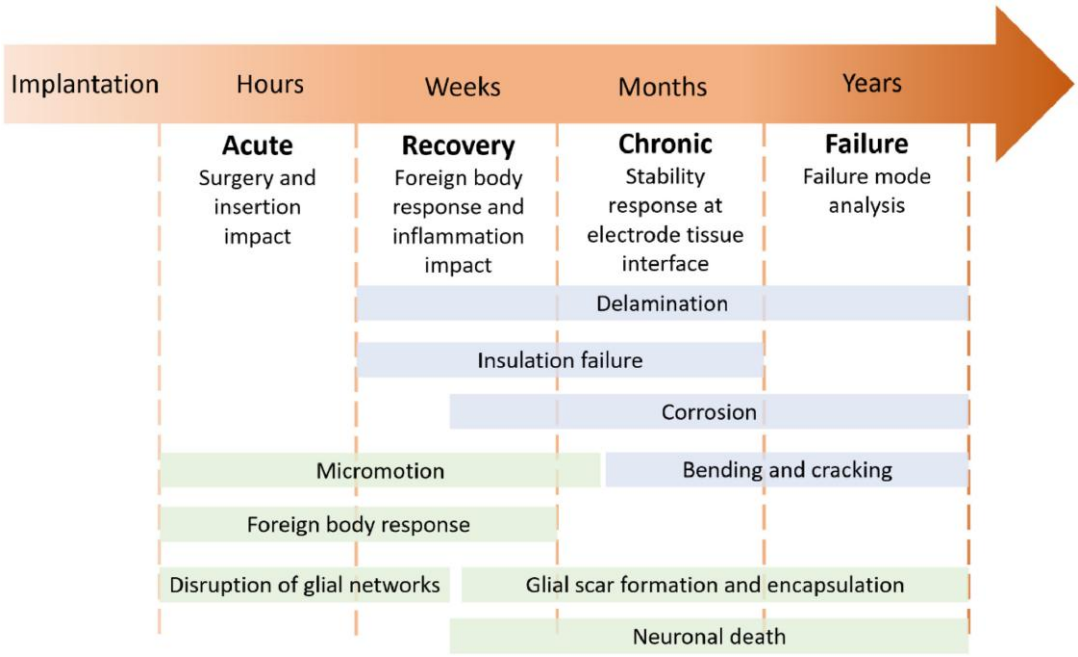


Figure 2.1: Timeline of biological responses and abiotic failure mechanisms in implantable neural electrodes. Following implantation, neural interfaces can undergo acute insertion injury, foreign body response, glial scar formation, and neuronal loss, while the device itself may experience delamination, insulation failure, corrosion, bending, and cracking over time. Reproduced from Oldroyd and Malliaras [19].

Overall, the ideal material for a bioelectronic neural interface should combine low impedance, safe charge transfer, mechanical compliance, wet-state stability, and biological compatibility [6], [16], [18]. However, achieving all these properties in a single material is challenging. Highly conductive materials are often stiff, while very soft and hydrated materials are often electrically insulating or mechanically unstable [9], [12]. This trade-off motivates the development of soft conductive materials, such as conductive hydrogels, that aim to combine tissue-like mechanical properties with the electrical functionality required for neural bioelectronics [9], [10], [12].

2.2 Conductive hydrogels for bioelectronic interfaces

According to the International Union of Pure and Applied Chemistry (IUPAC), a hydrogel is defined as a “gel in which the swelling agent is water” [21]. In practical terms, hydrogels are three-dimensional polymer networks that can absorb and retain large amounts of water while maintaining a solid-like structure. Because of this high-water content, hydrogels can resemble several physical features of biological tissues, such as softness, hydration, permeability, and deformability [9], [22]. These properties make them attractive materials for biological interfaces, especially in applications where the material needs to remain in close contact with cells or soft tissue.

Based on the material requirements discussed in Section 2.1, hydrogels are relevant for neural bioelectronics because they can provide a soft, hydrated, and permeable interface between the device and the biological environment [9], [12]. Their polymer network can be engineered to control properties

such as stiffness, swelling, degradation, and biochemical functionality, allowing the material to be adapted for different biological or bioelectronic applications [9], [22]. Therefore, hydrogels are often used not only as passive soft materials, but also as platforms that can be further modified to introduce electrical functionality.

However, conventional hydrogels are usually not sufficient on their own for bioelectronic applications. Although they can provide a favourable biological and mechanical environment, most hydrogel networks are not electronically conductive. Their water-rich structure can support ionic transport, but this does not automatically allow efficient electronic charge transport through the material. Therefore, a standard hydrogel may be useful as a soft coating, scaffold, or biological matrix, but it cannot directly replace an active electrode material unless electrical functionality is introduced [9], [10].

Conductive hydrogels aim to address this limitation by combining the softness and hydration of hydrogels with conductive components. These conductive phases can include conducting polymers, carbon-based materials such as carbon nanotubes or graphene, metallic nanostructures such as silver nanowires, or ionic additives [10], [23]. Depending on the formulation, conductivity can be introduced by blending conductive fillers into the hydrogel precursor solution, forming conducting polymers inside an existing hydrogel matrix, or creating interpenetrating networks between a soft hydrogel phase and an electroactive phase [10], [23]. In this way, conductive hydrogels can be designed to support both biological compatibility and electrical communication.

Still, conductivity alone is not enough to make a conductive hydrogel suitable for neural bioelectronics. The conductive phase must be distributed and connected well enough to allow charge transport, while the hydrogel network must still remain soft, hydrated, stable, and compatible with cells or tissue [9], [12], [20]. Increasing the amount of conductive material can improve electrical performance, but it may also affect swelling behaviour, stiffness, degradation, and cytocompatibility [10], [20], [23]. Similarly, a very soft and highly swollen hydrogel may match tissue mechanically, but it may be mechanically weak or unstable during handling and long-term use [9], [22]. Therefore, conductive hydrogel design requires a balance between electrical, mechanical, chemical, and biological properties [9], [10], [12], [20], [23].

For neural interface applications, this balance is especially important because the material must operate in a wet and physiologically relevant environment. Hydration state, ionic strength, swelling behaviour, and electrode contact can all influence the measured electrical response of the hydrogel [20]. As a result, conductive hydrogels should not be judged only by a single conductivity value, but also by their electrochemical behaviour, mechanical stability, swelling response, and biological compatibility [9], [10], [12], [20], [23]. These requirements make conductive hydrogels promising, but also more complex to develop and compare than conventional dry electrode materials.

Among the different conductive components used to produce conductive hydrogels, conducting polymers are especially attractive for bioelectronic applications because they can provide electronic functionality while remaining compatible with hydrated and soft material systems [10], [23]. Within this material family, PEDOT:PSS has become one of the most widely used conducting polymers in bioelectronics because it is available as a stable aqueous dispersion, can be processed using solution-based methods, and shows favourable electrochemical performance in wet environments [7], [24]. Therefore, the following section focuses specifically on PEDOT:PSS and its role in bioelectronic neural interfaces.

2.3 PEDOT:PSS in bioelectronics

Intrinsically conducting polymers have become important materials in bioelectronics because they can conduct electronic charge while remaining chemically tuneable and more mechanically compliant than conventional inorganic conductors [25]. Common examples include polypyrrole (PPy), polyaniline

(PANI), and PEDOT-based materials, which have been widely explored for biosensing, stimulation, recording, and tissue interfacing applications [8], [25], [26]. Their relevance in bioelectronics comes from the fact that they can operate in hydrated environments and interact with ionic biological systems more effectively than many traditional metallic or semiconductor materials [8], [26].

Within this material family, PEDOT:PSS has become one of the most widely used conducting polymers in organic bioelectronics [14], [24], [27]. PEDOT is the conjugated conducting polymer responsible for electronic transport, while PSS acts as the negatively charged counterion that balances the positively charged PEDOT chains and importantly allows the material to be dispersed in water [24], [27]. The chemical structure of PEDOT:PSS and its phase-separated morphology are shown in Figure 2.2. This distinction is important because PEDOT alone is poorly processable, whereas PEDOT:PSS can be obtained as a stable aqueous dispersion and processed using solution-based methods such as spin coating, drop casting, printing, or blending with other polymer systems [14], [24], [27].

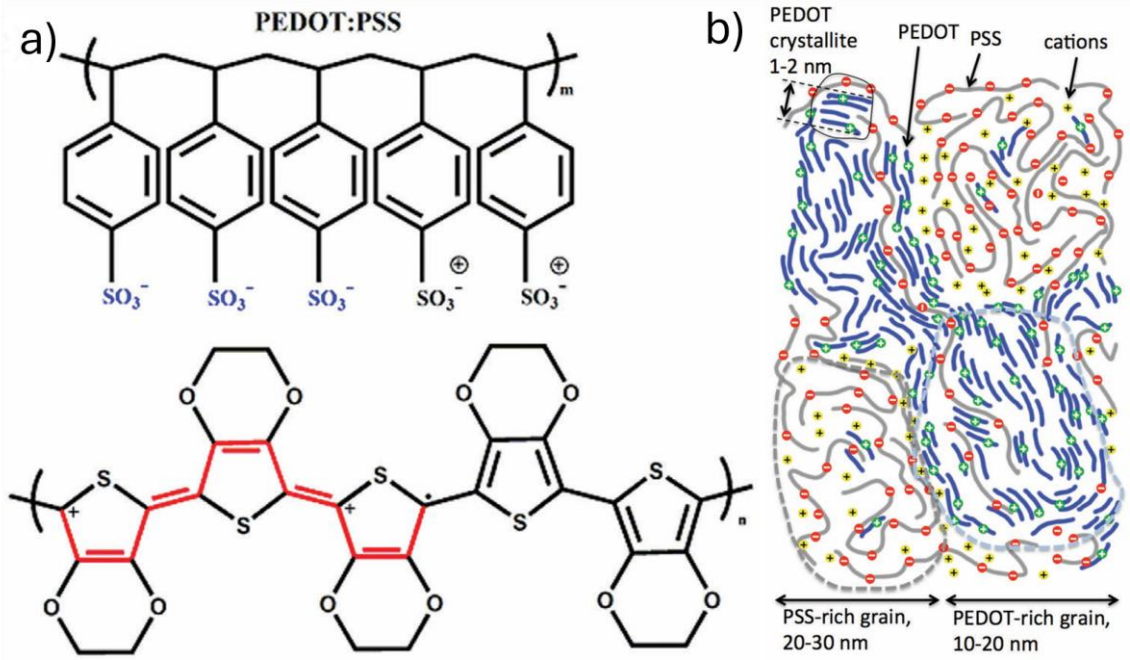


Figure 2.2: Chemical structure and phase-separated morphology of PEDOT:PSS. (a) Chemical structure of PEDOT:PSS, showing the PEDOT backbone and the PSS counterion. (b) Schematic representation of the PEDOT:PSS morphology, where PEDOT-rich regions mainly support electronic transport, while PSS-rich regions contribute to water dispersibility, ion accessibility, and electrochemical charge compensation. Adapted from [13], [14].

PEDOT:PSS is widely used in bioelectronics because it combines several properties that are difficult to obtain in a single material. PEDOT provides electronic conductivity, while PSS improves water dispersibility and enables interaction with hydrated ionic environments. As a result, PEDOT:PSS can support mixed ionic/electronic transport, which is important for coupling ionic biological signals with electronic devices [7], [8], [13]. Another important advantage of PEDOT:PSS is its aqueous processability. Because it is commercially available as a stable water-based dispersion, PEDOT:PSS can be processed using solution-based methods such as casting, spin coating, printing, and blending with other polymer or hydrogel systems [8], [13], [24]. This makes it easier to integrate into fabrication workflows compared with materials that require harsh solvents or high-temperature processing. For neural interfaces, PEDOT:PSS has often been used as a coating on metallic electrodes to improve the electrode/electrolyte interface. Compared with bare metals, PEDOT:PSS coatings can reduce

impedance and increase charge storage, which is beneficial for both neural recording and stimulation [2], [13], [14]. Its combination of conductivity, water-based processability, and compatibility with soft-material formulation also makes PEDOT:PSS a suitable platform for developing new hydrogel-based materials, including the PEDOT:PSS-based hydrogels investigated in this thesis.

A key feature of PEDOT:PSS is its ability to support both ionic and electronic processes. In hydrated environments, ions can enter and move within the PSS-rich regions of the material, while electronic transport occurs mainly through the PEDOT-rich domains [8], [13], [14]. This behaviour contributes to the high capacitance of PEDOT:PSS and allows charge to be stored not only at the outer surface, but also throughout the polymer volume [13]. As a result, PEDOT:PSS can provide a more effective electrochemical interface than purely metallic electrodes, where charge transfer is mostly limited to the electrode surface [13], [14], [28].

The electrochemical behaviour of PEDOT:PSS is strongly influenced by its internal morphology. PEDOT-rich and PSS-rich regions form a complex two-phase structure, and the accessibility of ions to these regions affects capacitance, conductivity, and charge transport [13]. Therefore, the final performance of PEDOT:PSS depends not only on the chemical composition, but also on processing conditions, additives, dopants, crosslinkers, hydration state, and post-treatment steps [13], [14], [24], [27]. This is important for bioelectronic materials because small changes in formulation can strongly affect conductivity, stability, mechanical behaviour, and biological compatibility.

Despite its advantages, PEDOT:PSS also has limitations that must be considered for neural-interface applications. In coating form, PEDOT:PSS can suffer from poor adhesion, cracking, delamination, or changes in performance after long-term exposure to aqueous environments [19], [24], [29]. In addition, although PEDOT:PSS is often considered relatively biocompatible, its biological response depends on formulation, additives, processing residues, and the specific cell or tissue model used [24], [29]. Therefore, PEDOT:PSS should not be treated as automatically suitable for all neural applications, but as a tuneable material platform that requires careful optimisation.

Traditionally, PEDOT:PSS has been mainly used as a thin film coating to improve electrode performance. However, thin films do not fully solve the mechanical and interfacial challenges discussed in the previous sections. This has motivated the development of PEDOT:PSS-based hydrogel systems, where the electrochemical advantages of PEDOT:PSS can be combined with the softness, hydration, and tissue-like properties of hydrogels. The following section therefore focuses on the main strategies used to form PEDOT:PSS-based hydrogels and their relevance for bioelectronic neural interfaces.

2.4 Strategies to form PEDOT:PSS-based conductive hydrogels

PEDOT:PSS-based conductive hydrogels can be developed through different formulation strategies. In a recent perspective on PEDOT:PSS bioelectronics, electrically active PEDOT:PSS conductive hydrogels were classified into three main formation routes: physical blending of PEDOT:PSS particles with hydrophilic polymers, in situ polymerisation of EDOT monomers within a pre-formed hydrogel matrix, and additive-induced gelation of “pure” PEDOT:PSS hydrogels [30]. In general, these strategies aim to preserve the electrochemical advantages of PEDOT:PSS while introducing hydrogel-like properties, such as high-water content, softness, swelling capacity, and three-dimensional structure [9], [10], [30]. However, the way PEDOT:PSS is incorporated into the hydrogel strongly affects the final material properties, including gel stability, conductivity, mechanical behaviour, processability, and biological compatibility [30]. In this section, the main PEDOT:PSS hydrogel formation strategies are reviewed at the literature level. The specific formulation mechanisms relevant to the hydrogels developed in this thesis, including the role of each additive and processing step, are discussed in detail

in the corresponding experimental and results sections. The main formulation routes discussed in this section are summarised in Figure 2.3.

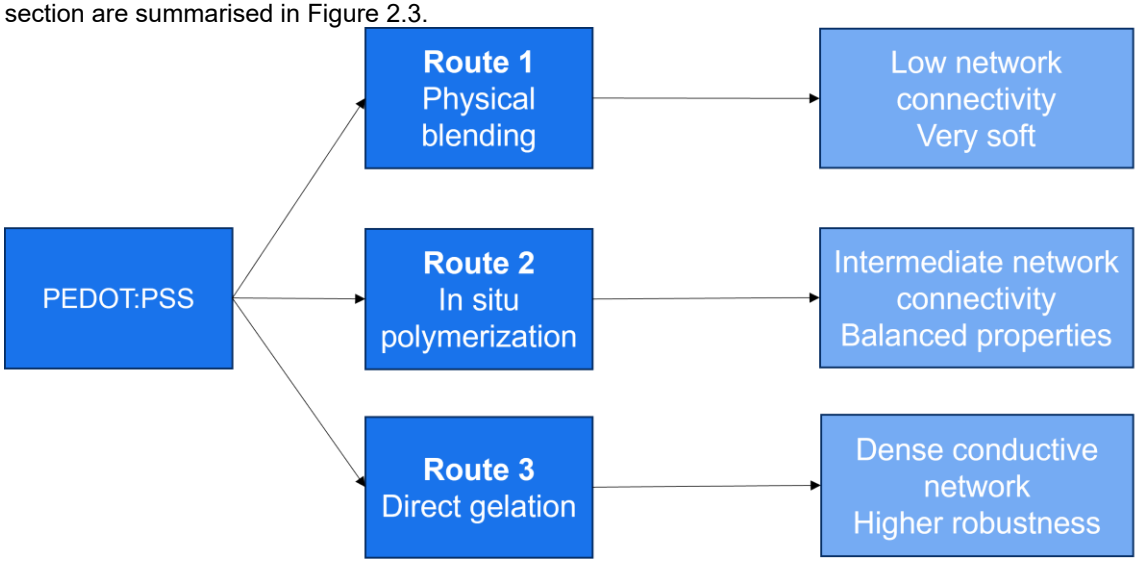


Figure 2.3: Main formulation routes for PEDOT:PSS-based conductive hydrogels. PEDOT:PSS-based hydrogels can be formed through three main routes: physical blending of PEDOT:PSS with hydrophilic polymer networks, in situ polymerisation of EDOT monomers within a pre-formed hydrogel matrix, and additive-induced direct gelation of PEDOT:PSS. These routes result in different levels of conductive network connectivity, mechanical robustness, and softness. Schematic summary created based on Ramírez et al. [30].

Route 1: Physical blending with hydrophilic polymer networks. The first route involves physically blending PEDOT:PSS particles with hydrophilic polymers, followed by crosslinking or gelation of the host polymer network [30]. In this approach, the hydrogel phase provides the soft, hydrated, and mechanically compliant structure, while PEDOT:PSS acts as the electroactive filler phase. This strategy is attractive for biological applications because the mechanical and biochemical properties can be mainly controlled by the hydrogel matrix, while the electrical functionality is introduced through the PEDOT:PSS phase [30].

A relevant example of this approach was recently reported by Wang et al., who developed electrically active hydrogels for neural cultures by embedding PEDOT:PSS particles inside an alginate-laminin hydrogel network [31]. In this design, alginate formed the primary viscoelastic hydrogel matrix, laminin provided a neural cell-adhesive secondary network, and PEDOT:PSS acted as the electrically active filler phase [31]. The inclusion of PEDOT:PSS improved the conductivity and charge storage capacitance of the hydrogels, while the materials maintained soft mechanical properties in the kPa range and remained stable under cell culture conditions for more than four weeks [31]. Importantly, the hydrogels also showed cytocompatibility with human induced pluripotent stem cell-derived cortical neurons over 28 days, highlighting the potential of matrix-based PEDOT:PSS hydrogels for neural culture applications [31]. This route is schematically illustrated in Figure 2.4, where PEDOT:PSS particles are shown as dispersed conductive domains within a soft hydrogel network.

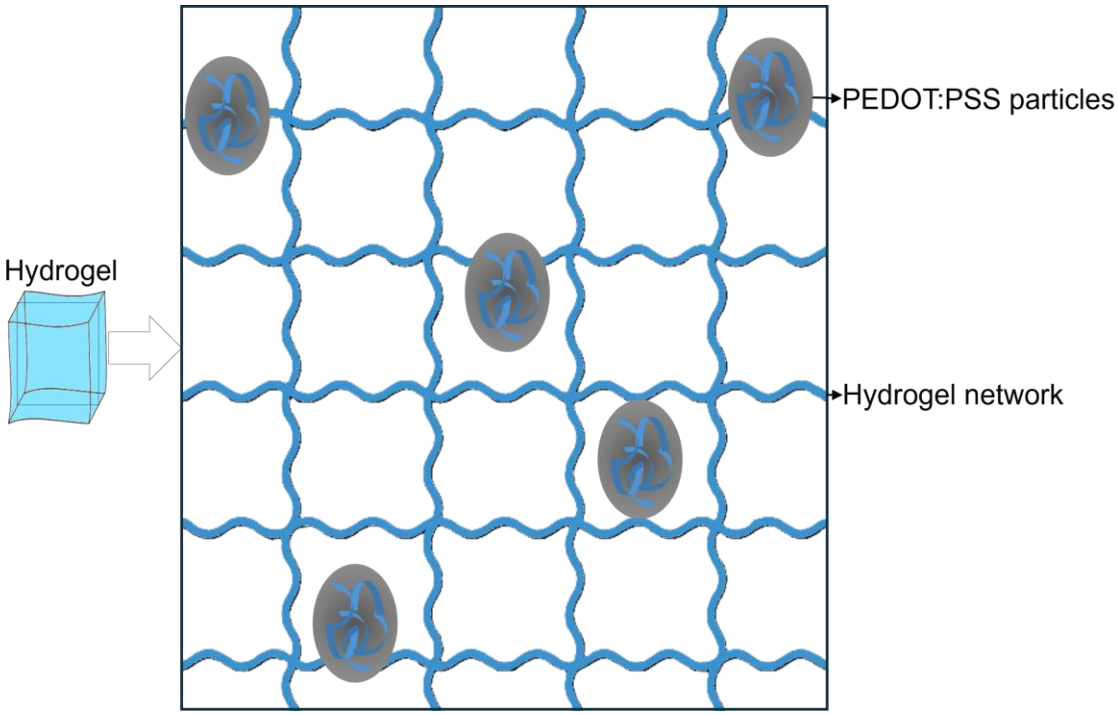


Figure 2.4: Physical blending route for PEDOT:PSS-based conductive hydrogels. Schematic representation of PEDOT:PSS particles dispersed within a hydrogel network. In this route, the hydrogel matrix provides the soft hydrated structure, while PEDOT:PSS is incorporated as separated conductive particles or domains. Because the PEDOT:PSS phase is not necessarily continuous throughout the matrix, conductive connectivity can be limited. Schematic based on the PEDOT:PSS hydrogel formation routes described by Ramírez et al. [30].

More advanced strategies use interpenetrating or double-network hydrogel systems to control the internal organisation of PEDOT:PSS. In these systems, the secondary network is not only used to improve mechanical properties, but also to guide the formation of more continuous conductive pathways. Liu et al. showed that secondary hydrogel networks such as polyethylene glycol diacrylate, polyvinyl alcohol, polyacrylamide, and especially polyacrylic acid can influence the phase continuity of PEDOT:PSS-based hydrogel semiconductors [32]. Their work also showed that porosity is an important design parameter, since higher porosity can improve ionic transport but may reduce electronic conductivity [32]. Therefore, the performance of PEDOT:PSS-based hydrogels depends not only on the presence of PEDOT:PSS, but also on the balance between electronic pathways, ionic transport, swelling, and mechanical structure.

Route 2: In situ polymerisation within a hydrogel matrix. The second route involves the in situ polymerisation of EDOT monomers within a pre-formed hydrogel matrix, resulting in an interpenetrating network between the hydrophilic polymer phase and the conducting PEDOT-based phase [30]. This approach can provide better integration of the conductive pathways within the hydrogel network compared with simple physical blending, leading to improved electrical connectivity while still retaining hydrogel-like properties [30]. This route is schematically illustrated in Figure 2.5, where the PEDOT and PSS phases are shown within the hydrogel network, representing the formation of a conductive phase inside the hydrogel matrix.

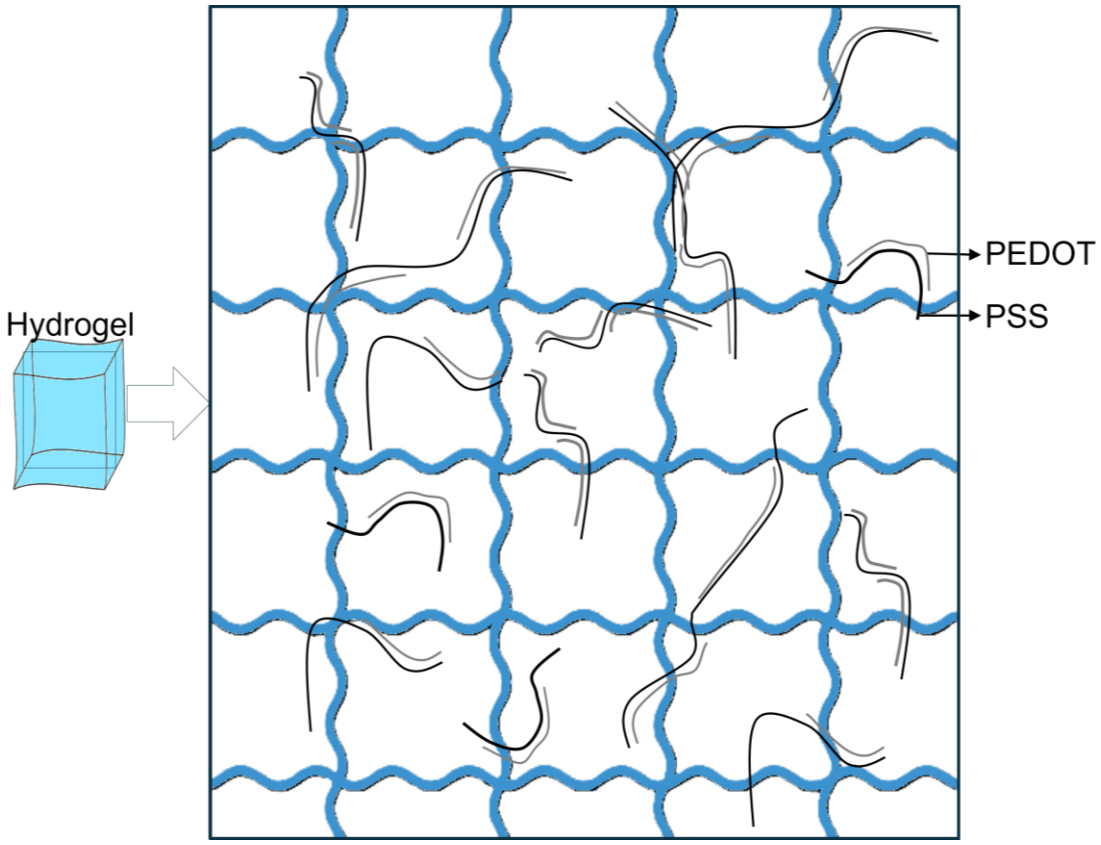


Figure 2.5: In situ polymerisation route for PEDOT:PSS-based conductive hydrogels. Schematic representation of the formation of a PEDOT:PSS-based conductive phase within a hydrogel network. In this route, the conductive polymer phase is generated inside a pre-formed or forming hydrogel matrix, producing a more integrated network than simple physical blending. This approach can improve conductive connectivity while maintaining the soft and hydrated structure of the hydrogel. Schematic based on the PEDOT:PSS hydrogel formation routes described by Ramírez et al. [30].

Feig et al. demonstrated this strategy by developing mechanically tenable conductive interpenetrating-network hydrogels, where the conducting polymer phase was formed within a soft hydrogel matrix [33]. Such systems are useful because the conductive network can be generated directly inside the hydrogel structure, allowing the electrical and mechanical properties to be tuned through both the hydrogel composition and the polymerisation conditions [33]. Related neural-electrode studies have also shown that PEDOT:PSS-based hydrogel coatings can improve porous morphology and electrochemical performance when integrated with electrode surfaces [34]. Overall, this route is particularly relevant when both conductive-network formation and hydrogel structure need to be controlled together.

Route3: Additive-induced direct gelation of PEDOT:PSS. The third route involves the formation of “pure” PEDOT:PSS hydrogels by inducing gelation of the PEDOT:PSS dispersion using additives such as DMSO or DBSA [30]. This route is schematically illustrated in Figure 2.6, where gelation additives promote the formation of a dense PEDOT:PSS network within the hydrogel structure.

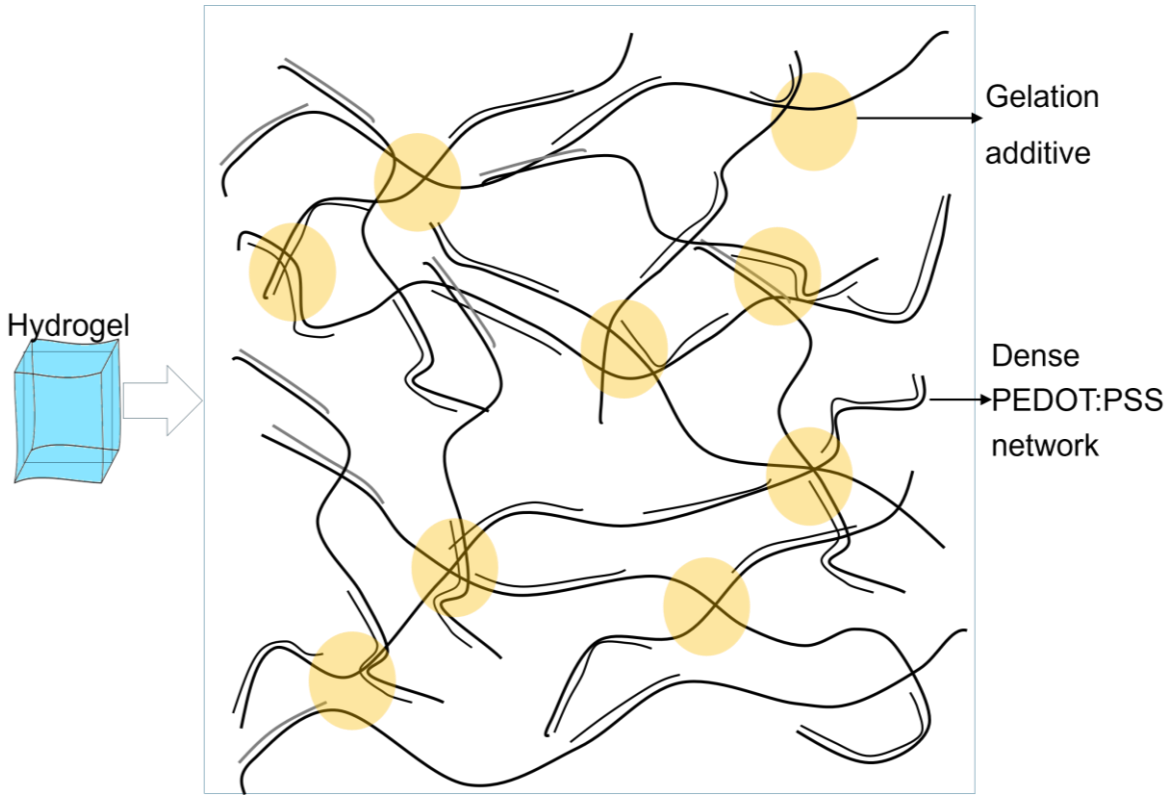


Figure 2.6: Additive-induced direct gelation route for PEDOT:PSS-based conductive hydrogels. Schematic representation of additive-induced direct gelation of PEDOT:PSS. In this route, gelation additives promote physical interactions and rearrangement within the PEDOT:PSS dispersion, resulting in a dense PEDOT:PSS-rich conductive network. Compared with physical blending and in situ polymerisation routes, this strategy can generate a more continuous conductive pathway within the hydrogel structure. Schematic based on the PEDOT:PSS hydrogel formation routes described by Ramírez et al. [30].

A key example of this strategy was reported by Zhang et al., who showed that PEDOT:PSS hydrogels can form spontaneously at room temperature after mixing PEDOT:PSS with 4-dodecylbenzenesulfonic acid (DBSA) [35]. In this system, DBSA acts as an acidic surfactant and promotes physical interactions between PEDOT:PSS-rich domains, leading to the formation of a three-dimensional conductive network. The resulting room-temperature PEDOT:PSS hydrogels were injectable, soft, and self-healable, and could also be processed into hydrogel fibres for soft bioelectronic devices [35]. This route is interesting because it is simple and does not require heating or complex chemical synthesis. However, the use of surfactants or acidic additives also means that cytocompatibility and washing/post-processing conditions must be carefully considered for biological applications.

Taken together, these studies show that PEDOT:PSS-based hydrogels can be formed through three main routes: physical blending of PEDOT:PSS particles with hydrophilic polymer networks, in situ polymerisation of EDOT monomers within pre-formed hydrogel matrices, and additive-induced gelation of “pure” PEDOT:PSS hydrogels [35]. Each strategy has advantages, but also limitations. Physical blending can provide soft and biologically relevant hydrogel matrices, but the conductive network may be less continuous. In situ polymerisation can improve the integration of conducting pathways within the hydrogel structure, but it requires more careful control of polymerisation conditions. Additive-induced gelation can produce more continuous and conductive PEDOT:PSS networks, but it may depend strongly on additives and post-processing conditions. More advanced interpenetrating or

double-network systems can further improve transport and structural control, but they also require more complex formulation and processing. Therefore, the choice of hydrogel formation strategy must be guided by the intended application and by the balance between electrical performance, mechanical properties, stability, and biocompatibility.

This thesis builds on these different formulation concepts by exploring PEDOT:PSS-based conductive hydrogels through multiple material routes. The aim is not only to obtain a gel, but to identify which formulation strategy provides the most promising balance between gel stability, electrochemical behaviour, mechanical suitability, and biological compatibility. For this reason, the developed materials are compared using a combination of physical, electrochemical, mechanical, and biological characterisation methods, which are discussed in the following section.

2.5 Characterisation of conductive hydrogels

Characterisation is a critical step in the development of conductive hydrogels for bioelectronic neural interfaces. As discussed in the previous sections, PEDOT:PSS-based hydrogels are designed to combine electrical functionality with softness, hydration, and biological compatibility. However, these properties cannot be evaluated using a single measurement. A hydrogel may appear macroscopically stable, but still show poor electrochemical performance, weak mechanical integrity, or limited cytocompatibility. Therefore, conductive hydrogels require a combination of physical, electrochemical, mechanical, and biological characterisation methods [9], [20], [31].

For conventional PEDOT:PSS thin films, electrochemical characterisation is relatively well established. Thin films are usually deposited directly onto conductive substrates, such as gold or platinum electrodes, and their geometry is typically well defined. This makes it possible to evaluate their electrode performance using techniques such as electrochemical impedance spectroscopy (EIS) and cyclic voltammetry (CV). In neural-interface studies, impedance is commonly used to evaluate the quality of the electrode/electrolyte interface, while CV is used to assess capacitive behaviour, electrochemical stability, and charge storage capacity [2], [14], [16]. Because PEDOT:PSS thin films are usually strongly associated with a defined electrode surface, the measured electrochemical response can often be linked directly to the coating, electrode area, and film thickness [14], [30].

However, the characterisation of conductive hydrogels is more complex than the characterisation of thin films. Hydrogels are soft, hydrated, three-dimensional, and deformable materials. Their properties depend strongly on water content, swelling state, electrolyte composition, sample dimensions, electrode contact, and mechanical compression [20], [36]. In addition, conductive hydrogels can contain both ionic and electronic transport pathways, meaning that a single conductivity value may not fully describe their behaviour. Depending on the measurement setup, the measured response may reflect ionic conduction through the hydrated polymer network, electronic conduction through the conductive phase, capacitive charging at the electrode interface, or a combination of all these processes [20], [36]. This makes standardization especially important when comparing hydrogel systems reported in the literature.

EIS is one of the most informative methods for analysing conductive hydrogels because it measures the frequency-dependent response of the material. At different frequency ranges, different processes can dominate the impedance response, including bulk ionic motion, interfacial charging, and electronic transport through the conductive network [20]. This is particularly important for PEDOT:PSS-based hydrogels, where the hydrogel matrix can support ionic transport while PEDOT:PSS provides an electronically active phase. By using equivalent circuit models, EIS can help separate ionic and electronic contributions and provide a more meaningful interpretation of the hydrogel's electrochemical behaviour [20]. CV complements EIS by probing capacitive charge storage and electrochemical stability

under potential cycling, making it useful for assessing whether the material can reversibly store and release charge [14], [16], [20].

A major contribution toward standardising conductive hydrogel electrochemical measurements was reported by Daso et al. [20]. In this work, the authors developed a controlled EIS-based method using a water-tight Swagelok cell with tuneable electrode distance. This configuration is important because it allows the hydrogel to be measured as a bulk hydrated material under controlled geometry and contact conditions. The study also highlighted several factors that can strongly affect conductive hydrogel measurements, including ionic strength, storage conditions, sample compression, and batch-to-batch variability [20]. Therefore, the Swagelok approach is useful not only as a measurement setup, but also as a framework for understanding why conductive hydrogel characterisation must be carefully controlled.

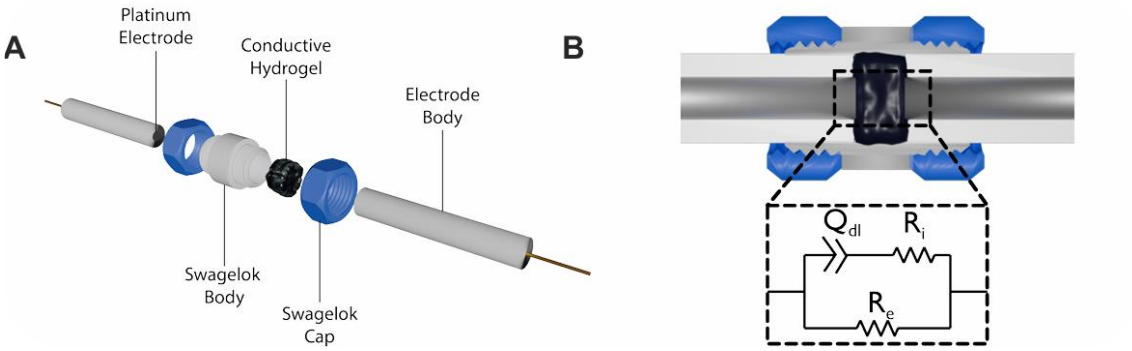


Figure 2.7: Swagelok-based electrochemical characterisation setup for conductive hydrogels. (a) Exploded schematic of the Swagelok cell used to contact a conductive hydrogel between platinum electrodes. (b) Assembled configuration and equivalent-circuit representation used to describe ionic/electronic transport and interfacial charging in the hydrogel. Adapted from Daso et al. [20].

Another relevant example was reported by Wang et al., who developed an electrochemical setup specifically for electrically active alginate-laminin-PEDOT:PSS hydrogels for neural cultures [31]. In this study, the hydrogels were cast in custom 3D-printed moulds with fixed dimensions and contacted using an integrated gold pogo pin. EIS and CV were then performed in a three-electrode configuration using the gold pogo pin as the working electrode, an Ag/AgCl reference electrode, and a platinum mesh counter electrode, with the measurements carried out in cell culture medium at physiological pH and temperature [31]. Importantly, the authors reported that simply casting the hydrogels on flat gold or indium tin oxide substrates did not give reliable electrochemical measurements because the soft hydrogels adhered weakly to the rigid electrodes, leading to delamination and inconsistent readings [31]. This example clearly shows that hydrogel electrochemical characterisation is not only about choosing EIS or CV, but also about designing a suitable hydrogel/electrode contact.

The Wang et al. study also demonstrates why measurement conditions must be kept constant when comparing hydrogel formulations. The hydrogels were immersed in cell medium before measurement to ensure homogeneous swelling, and the same medium was used during electrochemical testing to minimize osmotic differences between the hydrogel and the surrounding environment [31]. Using this controlled setup, the authors showed that incorporating PEDOT:PSS increased electronic conductivity and capacitance compared with alginate-laminin hydrogels without PEDOT:PSS, while maintaining the hydrogel under conditions relevant to neural culture [31]. This is especially relevant for bioelectronic neural interfaces, where the material must function in aqueous physiological environments rather than in dry or simplified testing conditions.



Figure 2.8: Three-electrode electrochemical setup for PEDOT:PSS-based hydrogels. Schematic, photograph, and cross-sectional representation of the custom three-electrode setup used to characterise alginate-laminin-PEDOT:PSS hydrogels in cell culture medium. The hydrogel is contacted through a gold working electrode, while Ag/AgCl and platinum electrodes are used as reference and counter electrodes, respectively. Adapted from Wang et al. [31].

In addition to electrochemical testing, physical and mechanical characterisation are necessary to evaluate whether a conductive hydrogel is suitable for handling, integration, and biological use. Physical characterisation includes observing gel formation, macroscopic stability, swelling behaviour, shape retention, and stability in aqueous media. These properties are important because excessive swelling, dehydration, or structural instability can change both the mechanical and electrochemical response of the hydrogel [9], [20], [36]. Mechanical characterisation, such as rheology, compression testing, or indentation, provides information about stiffness, viscoelasticity, and robustness. For neural-interface applications, this is important because the hydrogel should be soft enough to reduce mechanical mismatch, but stable enough to be handled and integrated with a device [9], [12], [31].

Biological characterisation is also required because good electrochemical performance does not automatically imply biological compatibility. Conductive hydrogels may contain additives, crosslinkers, acidic components, surfactants, or processing residues that can affect cell viability and behaviour. Therefore, assays such as metabolic activity measurements, Live/Dead staining, and microscopy-based evaluation of cell morphology are commonly used to assess cytocompatibility [29], [31]. In the context of neural bioelectronics, biological evaluation is especially important because the final material should be compatible with neural cells or neural-like culture environments, while maintaining its electrochemical function over time.

Overall, conductive hydrogel characterisation requires a more careful and multi-parameter approach than conventional thin film electrode characterisation. Thin films can often be evaluated through well-established electrode-based EIS and CV measurements, whereas hydrogels require additional control over hydration, sample geometry, electrode contact, swelling state, and mechanical deformation. For this reason, recent work has moved toward more controlled hydrogel-specific electrochemical setups, such as the Swagelok-based method proposed by Daso et al. and the custom three-electrode hydrogel setup reported by Wang et al. [20], [31]. In this thesis, both concepts are relevant. The developed PEDOT:PSS-based hydrogels are evaluated using electrochemical methods, including EIS and CV, together with physical, mechanical, and biological characterisation. The specific experimental configurations used in this work, including the three-electrode setup and the Swagelok-based measurement approach, are described in detail in the following chapters.

2.6 Summary and research gap

PEDOT:PSS has become one of the most important conducting polymers in bioelectronics because it combines aqueous processability, electrochemical activity, and the ability to support ionic and electronic charge transport in wet environments [14], [30]. In neural interfaces, PEDOT:PSS has been widely used as a coating material to reduce impedance, increase charge storage, and improve the electrical coupling between electrodes and biological systems [2], [14]. However, conventional PEDOT:PSS thin films do not fully address the mechanical and structural mismatch between soft neural tissue and rigid electronic devices.

Conductive hydrogels offer a promising route to address this limitation because they can combine hydration, softness, and three-dimensional structure with electrical functionality [9], [10], [12]. PEDOT:PSS-based hydrogels are especially interesting because they aim to preserve the electrochemical advantages of PEDOT:PSS while introducing hydrogel-like physical properties. As discussed in the previous sections, these materials can be formed through different strategies, including physical blending with hydrophilic polymer networks, in situ polymerisation within hydrogel matrices, and additive-induced gelation of PEDOT:PSS [30]. These routes have enabled several promising hydrogel systems, including injectable PEDOT:PSS gels, matrix-based hydrogels for neural cultures, and more advanced interpenetrating or double-network structures [31], [32], [35].

Despite this progress, several challenges remain. The final properties of PEDOT:PSS-based hydrogels depend strongly on formulation, additives, crosslinking, processing conditions, swelling state, and post-treatment steps. A formulation that improves conductivity may also affect softness, stability, or biological compatibility. Similarly, a hydrogel that is very soft and cytocompatible may not provide a sufficiently continuous conductive network. Therefore, the development of PEDOT:PSS-based hydrogels requires careful balancing of electrical, mechanical, physical, and biological properties.

Another important gap is related to characterisation. PEDOT:PSS thin films are usually measured on well-defined conductive substrates, whereas hydrogels are soft, hydrated, deformable, and often difficult to contact reproducibly. Their electrochemical response can depend on sample geometry, hydration, electrolyte composition, swelling, compression, and electrode contact [20], [36]. Recent studies have therefore highlighted the need for more controlled and standardized measurement approaches, such as Swagelok-based bulk hydrogel measurements and custom three-electrode setups for hydrogel/electrode interfaces [20], [31]. However, comparing different PEDOT:PSS hydrogel formulations remains challenging because different studies often use different geometries, electrolytes, measurement setups, and analysis methods.

Therefore, the main research gap addressed in this thesis is the need for a systematic evaluation of PEDOT:PSS-based conductive hydrogel formulations for bioelectronic neural-interface applications. Rather than focusing only on obtaining gel formation or maximizing conductivity, this thesis evaluates how different formulation routes influence gel stability, electrochemical behaviour, mechanical suitability, and biological compatibility. In addition, this work explores a PEDOT:PSS-based hydrogel formulation that, to the best of current literature knowledge, has not been previously reported for neural-interface applications. The thesis also investigates hydrogel-specific electrochemical measurement configurations, including device-relevant three-electrode measurements and controlled bulk measurements, to better understand the behaviour of these soft hydrated materials. By comparing multiple PEDOT:PSS-based hydrogel systems under a consistent experimental framework, this work aims to identify the most promising material candidate for future integration into soft bioelectronic neural-interface platforms.

3 Materials and Methods

3.1 Materials

Poly(3,4-ethylenedioxythiophene):poly(styrenesulfonate), PEDOT:PSS, was used as the main conductive polymer component for all hydrogel formulations investigated in this thesis. PEDOT:PSS aqueous dispersion, Clevios PH1000, was obtained from Heraeus Epurio GmbH. According to the safety data sheet, the material was supplied as CLEVIOS PH 1000 1KG (P1.0C) with product code 81076212.

For the PEDOT:PSS-DBSA hydrogel formulation, 4-dodecylbenzenesulfonic acid (DBSA, mixture of isomers, ≥95%, Sigma-Aldrich, product no. 44198, CAS no. 121-65-3) was used as the gelation additive. For selected crosslinked formulations, poly(ethylene glycol) diglycidyl ether (PEGDE, average Mn 500, Sigma-Aldrich, product no. 475696, CAS no. 26403-72-5) was used as a crosslinking additive.

For the PEDOT:PSS-PAA hydrogel formulation, acrylic acid (AA, Sigma-Aldrich, product no. 147230, CAS no. 79-10-7) was used as the monomer for the poly(acrylic acid) network. N,N′-methylenebisacrylamide (MBAA, Sigma-Aldrich, product no. M7279, CAS no. 110-26-9) was used as the crosslinker. Hydrogen peroxide solution (H_2O_2, 30% w/w in H_2O, Sigma-Aldrich, product no. H1009, CAS no. 7722-84-1) and L-ascorbic acid (Sigma-Aldrich, product no. A92902, CAS no. 50-81-7) were used as the redox initiation system. 1-Ethyl-3-methylimidazolium ethyl sulfate (EMIM-ES, Carl Roth, product no. 2054.1, CAS no. 342573-75-5) was used as the ionic liquid for post-gelation treatment. Dimethyl sulfoxide (DMSO, Sigma-Aldrich, product no. 472301, ACS reagent, ≥99.9%, CAS no. 67-68-5) was used as a co-solvent in the PEDOT:PSS-PAA formulation. The PEDOT:PSS-PAA protocol included PEDOT:PSS, AA, MBAA, DMSO, deionized water, H_2O_2, ascorbic acid, EMIM-ES, and DPBS rehydration steps.

For the PEDOT:PSS-phytic acid-chitosan-PEGDE hydrogel formulation, phytic acid solution (Carl Roth, product no. 260C.1, CAS no. 83-86-3), chitosan, high molecular weight (Sigma-Aldrich, product no. 419419, CAS no. 9012-76-4), and PEGDE were used. Deionized water was obtained from the Else Kooi Laboratory (EKL) cleanroom and was used for solution preparation, dilution, and washing steps unless stated otherwise.

For moulding and sample preparation, SYLGARD 184 Silicone Elastomer Kit was used to prepare polydimethylsiloxane (PDMS) moulds or chambers. Glass substrates and 3D-printed moulds were also used depending on the hydrogel formulation and characterisation method. Custom moulds were designed to control the geometry of the hydrogel samples for electrochemical, mechanical, and biological characterisation.

For aqueous handling and biological experiments, Dulbecco's phosphate-buffered saline (DPBS, 1X, no calcium, no magnesium, no phenol red, Gibco, Thermo Fisher Scientific, catalogue no. 14190144) was used for washing, hydrogel handling, storage, and electrochemical measurements where applicable. Dulbecco's Modified Eagle Medium (DMEM, high glucose, Gibco, Thermo Fisher Scientific, catalogue no. 41965039) was used as the cell culture medium. Thermo Fisher lists catalogue no. 41965039 as Gibco DMEM, high glucose.

For electrochemical characterisation, gold disk electrodes, or gold pogo pins were used as working electrode interfaces depending on the measurement configuration. Platinum mesh electrodes were used as counter electrodes, and Ag/AgCl reference electrodes (Redox.me, Silver/Silver Chloride Refillable Reference Electrode, SKU E-Ag/AgCl_30) were used as reference electrodes. A Swagelok-

based electrochemical cell was used for bulk hydrogel measurements, while a custom three-electrode setup was used for device-relevant hydrogel/electrode measurements.
For biological characterisation, selected hydrogel formulations were evaluated using cell culture-based assays. Cell viability and morphology were assessed using metabolic activity assays, fluorescence microscopy, and Live/Dead imaging. The exact biological reagents and staining protocols are described in the corresponding biological characterisation section.
All chemicals were used as received unless stated otherwise. Exact formulation ratios, processing conditions, and sample preparation steps are described in the following sections.

3.2 Preparation of PEDOT:PSS-based hydrogel formulations

3.2.1 PEDOT:PSS-DBSA hydrogels

PEDOT:PSS-DBSA conductive hydrogels were prepared using an additive-induced gelation approach adapted from the room-temperature PEDOT:PSS conductive hydrogel method reported by Zhang et al. [35]. The protocol was further optimised in this work to improve mixing, bubble removal, and reproducibility of gel formation. The final optimised formulation used 4% v/v DBSA relative to the PEDOT:PSS volume, corresponding to 40 µL DBSA per 1 mL PEDOT:PSS.
The precursor composition used for the PEDOT:PSS-DBSA conductive hydrogel preparation is summarised in Table 3.1.

Table 3.1: Precursor composition for PEDOT:PSS-DBSA conductive hydrogel preparation.

Component	Amount	Function
PEDOT:PSS PH1000	1 mL	Conductive polymer dispersion
DBSA	40 µL	Additive-induced gelation agent
1X DPBS	As required	Storage medium after gelation

PEDOT:PSS PH1000 was gently shaken before use and sonicated for 10 min using a Fisherbrand Select ultrasonic bath. The dispersion was then filtered through a 0.45 µm cellulose acetate filter to remove aggregates and improve solution homogeneity. After filtration, 1 mL of PEDOT:PSS was transferred into a clean container, followed by the addition of 40 µL DBSA.
The PEDOT:PSS-DBSA mixture was mixed using a repeated sonication and vortexing sequence. First, the mixture was sonicated for 2 min, followed by vortexing for 2 min at 800 rpm using a Fisherbrand ZX4 IR Vortex Mixer, and then sonicated again for 2 min. This mixing sequence was used to improve the distribution of DBSA within the PEDOT:PSS dispersion and to reduce visible inhomogeneities and trapped bubbles. The mixture was then carefully cast into the selected moulds and left undisturbed at room temperature. The final optimised preparation workflow used for the PEDOT:PSS-DBSA precursor is illustrated in Figure 3.1.

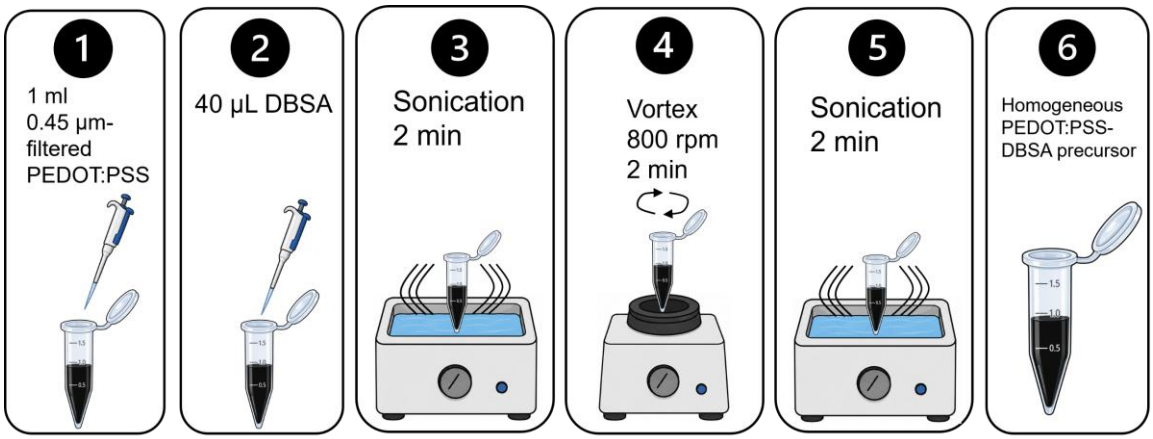


Figure 3.1: Optimised preparation workflow for PEDOT:PSS-DBSA conductive hydrogel precursor.

Schematic representation of the final optimised PEDOT:PSS-DBSA preparation sequence used in this work. First, 1 mL of 0.45 µm-filtered PEDOT:PSS dispersion was transferred to an Eppendorf tube, followed by the addition of 40 µL DBSA. The mixture was then sonicated for 2 min, vortexed at 800 rpm for 2 min, and sonicated again for 2 min to obtain a homogeneous PEDOT:PSS-DBSA precursor prior to casting and gelation.

Gelation was observed after approximately 30 min. After gelation, the samples were either used directly for characterisation or immersed in 1X DPBS and stored at approximately 5 °C until further use. PEDOT:PSS-DBSA conductive hydrogels prepared using this protocol were used for physical observation, electrochemical characterisation, mechanical testing, and biological compatibility experiments.

3.2.2 PEDOT:PSS-PAA conductive hydrogels

PEDOT:PSS-PAA conductive hydrogels were prepared using a procedure adapted from the PEDOT:PSS/PAA conductive hydrogel method reported by Liu et al. [32]. The protocol was modified according to the available processing facilities and equipment in the Else Kooi Laboratory (EKL) cleanroom. The formulation used freeze-dried PEDOT:PSS as the conducting component, acrylic acid (AA) as the monomer for the poly(acrylic acid) network, N,N′-methylenebisacrylamide (MBAA) as the crosslinker, and H_2O_2/ascorbic acid as the redox initiation system. DMSO was used as a co-solvent, while EMIM-ES was used as an ionic-liquid post-treatment to promote phase reorganisation of the PEDOT:PSS phase. The main components and workflow are consistent with the adapted protocol used for this thesis.

Unless otherwise stated, the wet-chemical preparation steps were performed in a fume hood in the EKL cleanroom. The freeze-drying step was performed in the Chemical Laboratory at Aerospace Engineering using a BÜCHI Lyovapor™ L-200 freeze dryer equipped with a 12-position manifold rack. This instrument is listed as a freeze dryer, and the 12-position manifold rack is designed for connecting multiple samples for freeze-drying.

The precursor composition used in the preparation of the PEDOT:PSS-PAA conductive hydrogel is summarised in Table 3.2. The overall preparation and post-treatment workflow used for the PEDOT:PSS-PAA conductive hydrogels is shown schematically in Figure 3.2.

Table 3.2: Formulation and post-treatment media used for PEDOT:PSS-PAA conductive hydrogel preparation.

Component	Amount	Function
Freeze-dried PEDOT:PSS	26 mg	Conductive phase
Acrylic acid	130 mg	PAA monomer
MBAA	5 mg	Crosslinker
DI water	2 g	Solvent
DMSO	0.4 g	Co-solvent
H_2O_2, 30%	15 µL	Redox initiator
Ascorbic acid, 20 wt.%	15 µL	Redox initiator
EMIM-ES	As required	Ionic-liquid post-treatment
EMIM-ES/water	70:30 v/v	Solvent-exchange treatment
1× DPBS	As required	Rehydration and storage medium

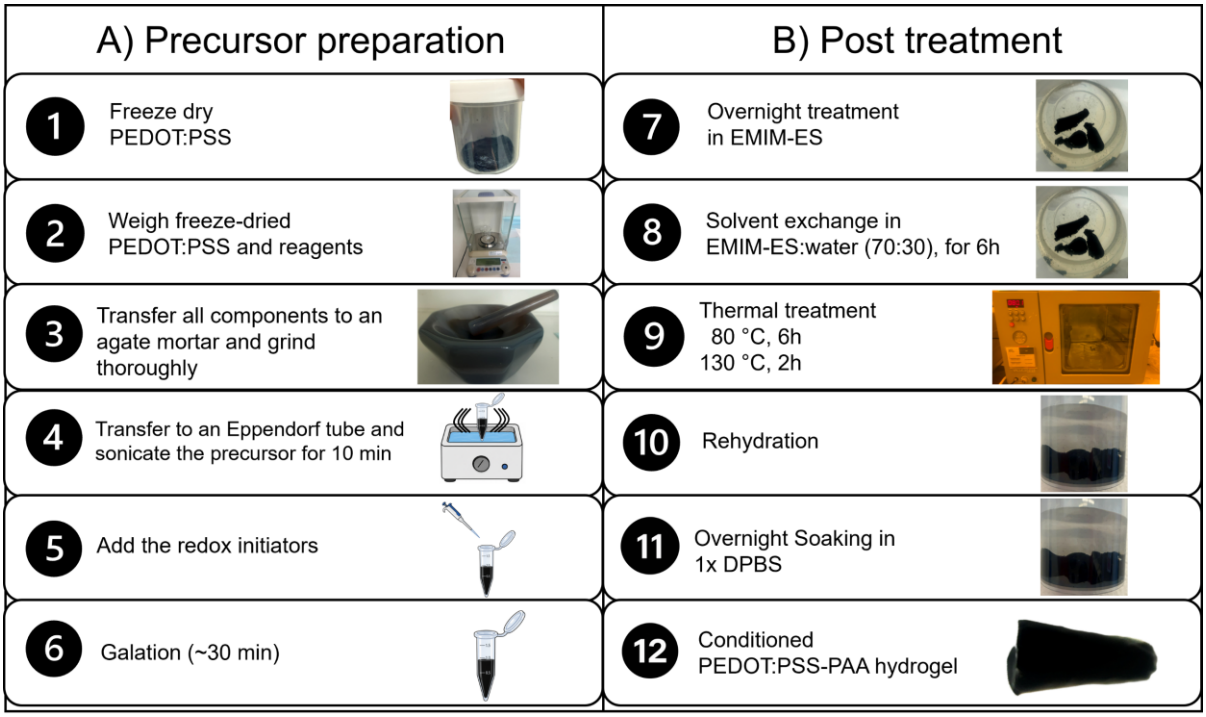


Figure 3.2: Schematic workflow for PEDOT:PSS-PAA conductive hydrogel preparation and post-treatment.

(A) Precursor preparation: PEDOT:PSS was freeze-dried, the freeze-dried PEDOT:PSS and reagents were weighed, combined in an agate mortar and ground thoroughly, transferred to an Eppendorf tube, sonicated, and then mixed with the redox initiators to induce gelation. (B) Post-treatment: the formed conductive hydrogels were treated overnight in EMIM-ES, subjected to solvent exchange in EMIM-ES:water (70:30) for 6 h, thermally treated at 80 °C for 6 h and 130 °C for 2 h, rehydrated, and soaked overnight in 1× DPBS to obtain conditioned PEDOT:PSS-PAA conductive hydrogels.

PEDOT:PSS PH1000 aqueous dispersion was first frozen and freeze-dried to obtain dry PEDOT:PSS pellets. For this step, multiple vials with 3 mL of PEDOT:PSS dispersion were frozen at −80 °C overnight and subsequently freeze-dried for 2 days. The freeze-drying run was performed using the BÜCHI

Lyovapor™ L-200 system. During operation, the freeze dryer was run under vacuum, with the condenser temperature at around −54 °C.

For each hydrogel batch, 26 mg of freeze-dried PEDOT:PSS was weighed using a Henk Maas NL analytical balance and crushed before adding the liquid components. The dry PEDOT:PSS was mixed with 2 g of DI water and 0.4 g of DMSO in an agate mortar. To improve dispersion, only a small amount of the water/DMSO mixture was initially added, and the material was ground into a smooth paste. The remaining solvent mixture was then gradually added while mixing continuously until a homogeneous, viscous suspension was obtained.

After dispersion of PEDOT:PSS, 130 mg AA and 5 mg MBAA were added to the suspension and mixed until no visible PEDOT:PSS aggregates were observed. The precursor suspension was then sonicated for 5-10 min using a Fisherbrand Select ultrasonic bath to improve homogeneity further. Before initiation, the moulds were prepared in advance so that the precursor could be cast immediately after addition of the redox initiators.

Gelation was initiated by sequential addition of 15 µL H_2O_2 and 15 µL ascorbic acid. H_2O_2 was added first, followed by ascorbic acid, after which the precursor was mixed carefully and immediately transferred into 2 mL Eppendorf tubes, which were used as moulds. The samples were left undisturbed at room temperature for 30 min to ensure complete gelation, although gel formation was observed to occur faster.

After gelation, the PEDOT:PSS-PAA conductive hydrogels were removed from the moulds and immersed in pure EMIM-ES overnight. The samples were then transferred into an EMIM-ES/water mixture at a 70:30 (v/v) EMIM-ES:water ratio for 6 h. This post-gelation treatment was used to induce phase reorganisation of the PEDOT:PSS phase before thermal annealing.

The conductive hydrogels were then annealed in two steps using a Vacuum Oven Salvislab_VC20. First, the samples were vacuum-dried and heated at 80 °C for 6 h, then heated at 130 °C for 2 h. After annealing, the samples were allowed to cool to room temperature and were then immersed in 1× DPBS until fully rehydrated. The rehydrated PEDOT:PSS-PAA conductive hydrogels were stored in 1× DPBS at approximately 5 °C until further characterisation.

PEDOT:PSS-PAA conductive hydrogels prepared using this protocol were used for physical observation, electrochemical characterisation, and mechanical testing.

The cleanroom procedure followed the EKL-approved process flowchart registered under run number P2026-13, which is provided in **Appendix B** .

3.2.3 PEDOT:PSS-PEGPACHI conductive hydrogels

A PEDOT:PSS-phytic acid-chitosan-PEGDE conductive hydrogel formulation was developed and optimised in this thesis and is referred to as PEDOT:PSS-PEGPACHI. In this name, PEG refers to PEGDE, PA refers to phytic acid, and CHI refers to chitosan. Unlike the PEDOT:PSS-DBSA and PEDOT:PSS-PAA formulations, which were adapted from previously reported protocols, the PEDOT:PSS-PEGPACHI conductive hydrogel was developed in this work as an original PEDOT:PSS-based conductive hydrogel formulation. This formulation was designed to combine PEDOT:PSS as the conductive polymer phase, PEGDE as a crosslinking additive, and a phytic acid-chitosan stock solution as an additional gel-forming component.

The formulation used in the preparation of the PEDOT:PSS-PEGPACHI conductive hydrogel is summarised in Table 3.3. The complete preparation workflow for the PEDOT:PSS-PEGPACHI conductive hydrogel, including PEGDE addition, PA-chitosan stock preparation, luer-lock syringe mixing, gelation, and DPBS conditioning, is shown schematically in Figure 3.3.

Table 3.3: Formulation used for PEDOT:PSS-PEGPACHI conductive hydrogel preparation.

Component	Amount	Function
PEDOT:PSS PH1000	1 mL	Conductive polymer dispersion
PEGDE	10 µL	Crosslinking additive
Phytic acid-chitosan stock solution	63 µL	Gel-forming additive mixture
1× DPBS	As required	Storage medium after gelation

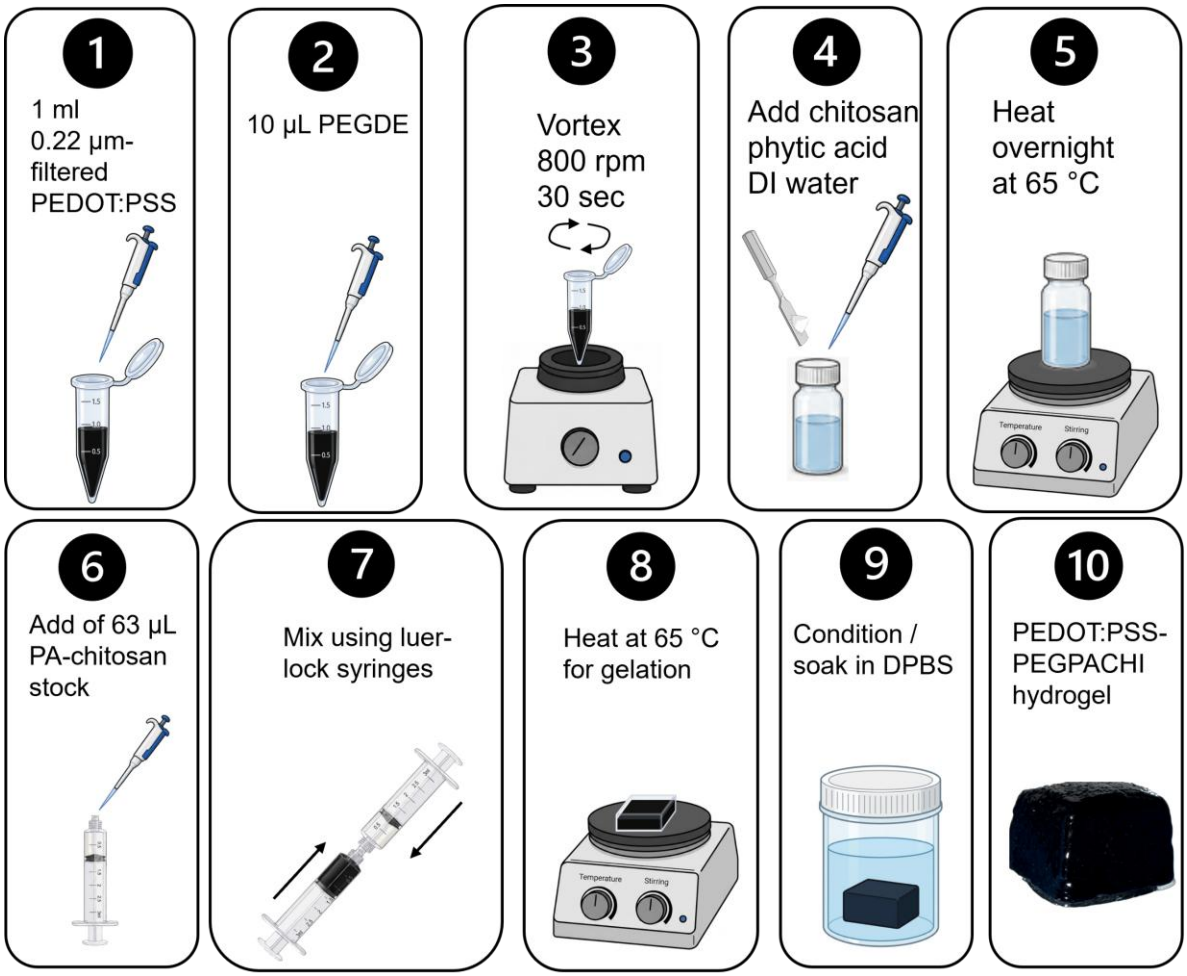


Figure 3.3: Preparation workflow for PEDOT:PSS-PEGPACHI conductive hydrogel fabrication. PEDOT:PSS was first sonicated, filtered through 0.45 µm and 0.22 µm filters, combined with PEGDE, and vortexed to form the PEDOT:PSS-PEGDE precursor. In parallel, a PA-chitosan stock solution was prepared from phytic acid, chitosan, and DI water under heating and stirring. The PA-chitosan stock was then mixed with the PEDOT:PSS-PEGDE precursor using a luer-lock syringe system. The resulting precursor was cast into moulds, heated to induce gelation, and conditioned in 1x DPBS to obtain the final PEDOT:PSS-PEGPACHI conductive hydrogel.

The phytic acid-chitosan stock solution was prepared by mixing 2 mL of phytic acid, 2 mL of DI water, and 180 mg of chitosan in a 4 mL glass vial. A magnetic stir bar was added, and the mixture was stirred overnight at 65 °C on a Thermo Scientific Cimarec hotplate/stirrer. The stirring speed was set to the maximum available setting to promote chitosan dispersion, but the exact rpm was not recorded. The resulting stock solution was used as the PA-Chi component of the PEDOT:PSS-PEGPACHI formulation.

PEDOT:PSS PH1000 was gently shaken before use and sonicated for 10 min using a Fisherbrand Select ultrasonic bath. The dispersion was then filtered sequentially through 0.45 µm and 0.22 µm filters to remove aggregates and improve solution homogeneity. After filtration, 1 mL of PEDOT:PSS was transferred into a clean syringe or container, followed by the addition of 10 µL PEGDE, corresponding to 1% v/v PEGDE relative to the PEDOT:PSS volume. The PEDOT:PSS-PEGDE mixture was then vortexed for 30 s at 800 rpm using a Fisherbrand™ ZX4 IR Vortex Mixer.

Hydrogel mixing was performed using a Luer-lock syringe mixing system. The PEDOT:PSS-PEGDE mixture was loaded into one syringe, while the phytic acid-chitosan stock solution was loaded into a second syringe. The two syringes were connected through the Luer-lock system, and 63 µL of the phytic acid-chitosan stock solution was mixed with the PEDOT:PSS-PEGDE solution by repeated transfer between the syringes. This mixing approach was used to improve contact between the two precursor solutions and promote more homogeneous hydrogel formation.

After mixing, the precursor was cast into the selected moulds and heated at 65 °C for approximately 1 h to allow gel formation. After gelation, the samples were either used directly for characterisation or immersed in 1X DPBS and stored at approximately 5 °C until further use. PEDOT:PSS-PEGPACHI conductive hydrogels prepared using this protocol were used for physical observation, electrochemical characterisation, mechanical testing, and biological compatibility experiments.

3.3 Moulding and sample preparation

After preparation of the hydrogel precursor mixtures, samples were moulded using different approaches depending on the intended characterisation method. Since the conductive hydrogels were soft and hydrated, the sample format was selected to minimise handling where possible and to improve compatibility with the planned experiment. The main moulding approaches included Eppendorf tubes, cylindrical moulds, square well-plate-type moulds, and direct casting into the PDMS measuring platform.

3.3.1 General moulding approaches

For bulk conductive hydrogel preparation, the precursor mixtures were cast into moulds immediately after mixing and then left under the gelation conditions described for each formulation. PEDOT:PSS-PAA conductive hydrogels were moulded in Eppendorf tubes. For biological testing and Swagelok-based electrochemical measurements, conductive hydrogels were prepared using cylindrical moulds with a diameter of 5 mm and height of 1 cm. These cylindrical samples were selected because they provided a defined geometry that could be transferred for later characterisation.

For mechanical testing, conductive hydrogels were prepared using a well-plate-type custom made mould containing a 4 × 2 arrangement of square wells. Each well had an approximate size of 1 × 1 × 1 cm, producing cube-like conductive hydrogel samples suitable for mechanical characterisation. The use of this mould allowed samples with similar dimensions to be prepared under comparable conditions.

3.3.2 Direct casting into electrochemical devices

For three-electrode electrochemical measurements, selected conductive hydrogels were not prepared as separate bulk samples. Instead, the precursor mixture was cast directly inside the PDMS measuring platform. Before casting, the pogo pin was inserted into the platform. The conductive hydrogel precursor was then added into the PDMS well, where it took the shape of the well and gelled around the pogo pin. This approach was used to improve contact between the conductive hydrogel and the working electrode and to reduce the need for transferring the gel after formation.

The full design and fabrication of the PDMS measuring platform are described later in Chapter 5. In this section, the platform is only introduced as one of the sample preparation methods used before electrochemical characterisation.

The approximate conductive hydrogel dimensions and volumes used for the electrochemical measurement configurations are summarised in Table 3.4. These values are important because the electrochemical response depends on the conductive hydrogel geometry, electrode contact area, and the distance between the electrodes or contact points.

Table 3.4: Approximate conductive hydrogel dimensions and volumes used for electrochemical measurements.

Measurement setup	Sample geometry	Approximate dimensions	Hydrogel volume
PDMS measuring platform	Cylindrical hydrogel well	5 mm diameter × ~3.6 mm height	70 µL/mm^3
Swagelok bulk setup	Cylindrical punched hydrogel sample	5 mm diameter × ~4 mm height	79 µL/mm^3

In the PDMS measuring platform, 70 µL of hydrogel precursor was cast into each 5 mm diameter well, corresponding to an approximate hydrogel height of 3.6 mm. For the Swagelok-based bulk setup, hydrogel samples were punched using a 5 mm diameter punch and had an approximate height of 4 mm, corresponding to an estimated hydrogel volume of 79 µL.

3.3.3 Sample storage and handling before characterisation

After gelation, hydrogel samples were either used directly or immersed in 1× DPBS and stored at approximately 5 °C until further testing. Samples were handled carefully during transfer because their hydrated and soft structure made them sensitive to deformation or breakage.

3.3.4 Sterile handling and conditioning of conductive hydrogels for cell culture

Hydrogel samples intended for biological testing were prepared and conditioned under sterile conditions before being added to cell cultures. For the PEDOT:PSS-DBSA and PEDOT:PSS-PEGPACHI conductive hydrogels, the gel preparation and subsequent washing steps were performed inside a biosafety cabinet. The PEDOT:PSS-PAA conductive hydrogels were not prepared inside the biosafety cabinet, because their fabrication protocol included a final high-temperature annealing step at 130 °C. This high-temperature treatment was considered suitable for reducing the risk of contamination before biological use. However, all subsequent washing and conditioning steps for the PEDOT:PSS-PAA conductive hydrogels were also performed inside the biosafety cabinet.

Before cell culture experiments, all hydrogel samples were washed extensively with cell culture medium. The washing was performed in sterile 15 mL Falcon tubes by immersing the gels in fresh medium and replacing the medium repeatedly. During the first medium exposure, the medium typically changed from its original pink/red colour to yellow instantly. This colour change was attributed to acidic components or soluble residues released from the conductive hydrogel samples into the phenol-red-containing culture medium. Therefore, the colour of the medium was used as a practical indicator of conductive hydrogel conditioning.

The washing procedure was continued until the colour change became progressively weaker and fresh medium remained close to its original pink/red colour after contact with the conductive hydrogels. Once this was achieved, the samples were considered sufficiently conditioned for biological testing. To further confirm that no strong colour change occurred under cell culture-like conditions, the washed conductive hydrogels were incubated in fresh culture medium at 37 °C for 4 h. After this incubation step, no visible colour change was observed. The samples were then stored overnight at approximately 5 °C in fresh medium, after which the medium still remained pink/red. After this conditioning procedure, the conductive hydrogel samples were considered ready for cell culture experiments.

3.4 Physical characterisation

Physical characterisation was performed as an initial assessment of conductive hydrogel formation, macroscopic stability, and handling behaviour. This step was used to determine whether each formulation formed a stable gel that could be transferred, stored, and used for further electrochemical, mechanical, or biological characterisation.

3.4.1 Assessment of gel formation

Gel formation was first assessed using visual inspection and a simple tilting or inversion test. After the precursor mixtures were cast into the selected moulds, samples were left under the gelation conditions described in Section 3.2. Gelation was considered successful when the material no longer flowed upon tilting or inversion and maintained a defined shape inside the mould or container.

For most formulations, the gelation behaviour was checked within the first hour after preparation. This time window was used as a practical initial assessment of whether a stable conductive hydrogel had formed.

For formulations that required additional thermal treatment, such as PEDOT:PSS-PEGPACHI, gelation was assessed after the heating step. Since the PEDOT:PSS-PEGPACHI formulation was developed and optimised in this thesis, several preliminary mixing, additive, and heating conditions were explored to identify a formulation that could form a stable gel. These optimisation steps are presented and discussed in Section 4.4.

3.4.2 Macroscopic appearance and handling

The macroscopic appearance of each conductive hydrogel was evaluated by visual inspection. Samples were examined for colour, shape retention, homogeneity, visible bubbles, cracks, fragmented regions, or non-uniform gelation. Handling behaviour was also assessed qualitatively during removal from the moulds, transfer into storage medium, or preparation for further testing.

This assessment was particularly important because some conductive hydrogels could appear gel-like inside the mould but lose their shape or break during transfer. Therefore, the physical characterisation focused not only on whether gelation occurred, but also on whether the resulting conductive hydrogel could be handled as a stable sample.

3.4.3 Wet-state stability during storage

After gelation, selected samples were immersed in 1× DPBS and stored at approximately 5 °C until further use. Wet-state stability was assessed qualitatively by observing whether the samples maintained their shape after immersion. Samples were checked for visible swelling, shrinking, fragmentation, colour changes, or loss of structural integrity.

For samples intended for biological testing, additional conditioning was performed in cell culture medium before exposure to cells, as described later in Section 3.7. In this section, medium exposure is only considered as part of the general sample handling and preparation workflow.

3.4.4 Photographic documentation

Photographs were taken during selected stages of conductive hydrogel preparation and handling to document gel formation, sample geometry, inversion behaviour, and wet-state stability. These images were used to support the qualitative comparison of the different formulations during conductive hydrogel development and optimisation.

3.5 Electrochemical characterisation

Electrochemical characterisation was performed to evaluate the impedance and electrochemical response of the PEDOT:PSS-based conductive hydrogels. Measurements were carried out using a PalmSens4 potentiostat controlled with PSTrace software. The conductive hydrogels were measured

in 1x DPBS using electrochemical impedance spectroscopy (EIS) and cyclic voltammetry (CV). Two different configurations were used: a three-electrode setup based on the PDMS measuring platform and a Swagelok-based setup.

3.5.1 Three-electrode measurements in the PDMS measuring platform

For electrochemical measurements in the PDMS measuring platform, selected conductive hydrogel formulations were cast directly inside the PDMS well. A gold pogo pin was inserted into the platform before casting and was used as the working electrode contact. The conductive hydrogel precursor was then added into the PDMS well, where it took the shape of the well and gelled around the pogo pin. This approach was used to improve the contact between the conductive hydrogel and the working electrode and to avoid transferring the gel after formation.

The electrochemical cell consisted of the gold pogo pin as the working electrode, an Ag/AgCl reference electrode, and a platinum mesh counter electrode. Measurements were performed in 1× DPBS. This configuration was used to assess the electrochemical behaviour of the conductive hydrogel when integrated directly into a device-like measurement platform. The setup was based on the principle of three-electrode conductive hydrogel characterisation used for PEDOT:PSS-based conductive hydrogels in the literature [31].

For each measurement, 70 µL of conductive hydrogel precursor was cast into a 5 mm diameter PDMS well. This corresponded to an approximate conductive hydrogel volume of 70 mm^3 and an estimated conductive hydrogel height of 3.6 mm. The gold pogo pin was inserted into the well before gelation, allowing the conductive hydrogel to form around the working electrode contact.

3.5.2 Swagelok-based bulk conductive hydrogel measurements

Hydrogel electrochemical measurements were also performed using a Swagelok-based setup. Cylindrical hydrogel samples were placed between two disk electrodes inside the Swagelok cell. Two electrode configurations were tested: one using gold disk electrodes on both sides and one using platinum disk electrodes on both sides. For these measurements, the working electrode connection from the potentiostat was connected to one side of the Swagelok cell, while the reference and counter electrode connections were connected together on the opposite side.

This configuration was used to evaluate the bulk electrochemical response of the hydrogel under a more confined geometry. The Swagelok-based approach was included because conductive hydrogel measurements are strongly affected by sample geometry and electrode contact, and similar setups have been proposed for standardised electrochemical characterisation of conductive hydrogels [20].

For the Swagelok-based measurements, cylindrical hydrogel samples were prepared using a 5 mm diameter punch. The punched samples had an approximate height of 4 mm, corresponding to an estimated hydrogel volume of approximately 79 µL, or 79 mm^3. The hydrogel was positioned between two disk electrodes, so the sample height defined the approximate distance between the electrode surfaces.

3.5.3 Electrochemical impedance spectroscopy

Electrochemical impedance spectroscopy was performed in 1x DPBS using a fixed DC potential of 0.0 V and an AC perturbation amplitude of 0.01 V. The frequency was scanned from 1 MHz to 0.1 Hz, with 57 frequency points and 8 points per decade. The impedance response was recorded to compare the frequency-dependent behaviour of the different hydrogel formulations and measurement configurations.

3.5.4 Cyclic voltammetry

Cyclic voltammetry was performed in 1x DPBS to assess the electrochemical response of the hydrogels under repeated potential cycling. The potential was swept between −0.4 V and +0.4 V, starting from 0.0 V, with a potential step of 0.01 V and a scan rate of 0.1 V s^{-1}. For each measurement, 30 cycles

were recorded. The CV measurements were used to compare the current response and capacitive behaviour of the hydrogel formulations.

3.5.5 Data processing

Electrochemical data were exported from PSTrace and processed using Origin 2024. EIS data were plotted as impedance magnitude and phase as a function of frequency, and Nyquist plots were generated where relevant. CV data were plotted as current vs potential curves and used to compare the electrochemical response of the different hydrogels. The interpretation and comparison of the electrochemical results are presented in Chapter 5.

3.6 Mechanical characterisation

Mechanical characterisation was performed to estimate the effective Young's modulus of the PEDOT:PSS-based hydrogels. Measurements were carried out using an Optics11 Life Piuma nanoindenter with the corresponding Optics11 software. The tested formulations were PEDOT:PSS-DBSA, PEDOT:PSS-PAA, and PEDOT:PSS-PEGPACHI.

3.6.1 Sample preparation for mechanical testing

Hydrogel samples for mechanical testing were prepared using the square well-plate-type mould described in Section 3.3.1. The mould consisted of a 4 x 2 array of square wells, each measuring 1 x 1 x 1 cm. This produced cube-like hydrogel samples with comparable dimensions for indentation testing. For each hydrogel formulation, three separate gel samples were prepared and tested.

Before measurement, the samples were kept hydrated in 1X DPBS. During testing, the hydrogels were handled carefully to avoid deformation or damage before positioning under the nanoindenter. The optimisation of sample preparation and handling for mechanical testing is discussed later in Section 5.7.

3.6.2 Nanoindentation measurements

Nanoindentation measurements were performed using an Optics11 Life Piuma nanoindenter. The hydrogel sample was placed under the indentation probe and measured in the hydrated state. Before measurement, the probe was cleaned and prepared according to the instrument procedure, and care was taken to avoid air bubbles or poor contact between the probe and the hydrogel surface.

A probe with a stiffness of 0.450 N/m and a tip radius of 27.5 µm was used for the measurements. The final measurements were performed using the Peak Load Poking control mode. A maximum load of 1.0 µN was applied with a piezo speed of 10 µm/s. The indentation response was fitted by the instrument software using the Hertz model, and the effective Young's modulus, Eeff, was obtained directly from the software output. The software also reported a modulus value calculated using an assumed Poisson's ratio of 0.45, but the Eeff values were used for comparison between samples. These settings were recorded in the exported Optics11 measurement files.

3.6.3 Mechanical indentation scans

In addition to single indentation measurements, matrix scans were performed to evaluate the mechanical response at different positions on the hydrogel surface. For each matrix scan, measurements were taken in a 4 × 4 grid, resulting in 16 indentation points per scan. The spacing between neighbouring measurement points was 150 µm in both the X and Y directions.

This approach was used because hydrogels can show local variations in stiffness due to differences in surface flatness, hydration, or internal structure. Measuring several positions on the same sample therefore provided a more representative estimate of the effective Young's modulus than a single indentation point.

3.6.4 Mechanical data processing

The effective Young's modulus values generated by the Optics11 software were exported from the measurement files and analysed. For each hydrogel formulation, three independent gel samples were tested, and matrix indentation measurements were collected from each sample. The software fitted the indentation response using the Hertz model and directly reported the effective Young's modulus, Eeff, which was used for the mechanical comparison between samples.

In addition to the software-reported Eeff values, the load-indentation data from the exported TXT files were plotted to visually inspect the measurement behaviour. These load-indentation curves were not re-fitted with the Hertz model during this analysis. The Hertz fitting was performed by the Optics11 software. The plotted curves were used only to identify failed or unreliable indentation measurements, such as curves with abnormal indentation depth, poor probe-sample contact, unstable loading behaviour, or clear outlier behaviour compared with the rest of the matrix scan.

A representative example of this procedure is shown in Figure 3.4. First, all exported load-indentation curves were plotted directly from the TXT file. Curves showing abnormal behaviour were then excluded, and the remaining curves were plotted again to confirm that the kept measurements showed a more consistent indentation response. The corresponding Eeff values from the retained measurements were then used to calculate the mean, standard deviation, and median values for each sample.

The full exclusion procedure, excluded values, heat maps, and additional mechanical data processing details are provided in **Appendix G**.

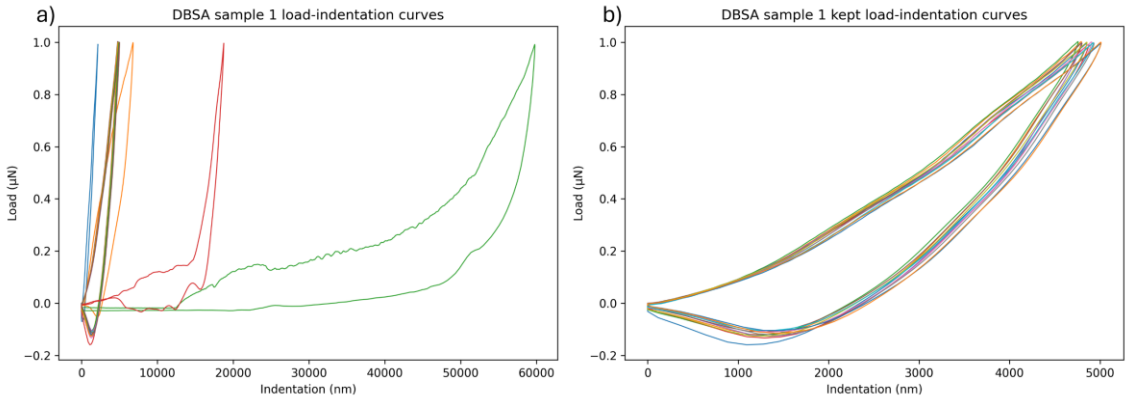


Figure 3.4: Representative load-indentation curve inspection used for mechanical data processing.

Representative load-indentation curves from PEDOT:PSS-DBSA sample 1 plotted from the exported Optics11 TXT file. (a) All measured curves before data exclusion, showing several failed or unreliable measurements with abnormal indentation depth and unstable loading behaviour. (b) Retained curves after removal of the abnormal measurements, showing a more consistent load-indentation response. These plots were used only to visually inspect measurement quality. The curves were not re-fitted during this analysis. The effective Young's modulus values used in the thesis were obtained from the Hertz-model output generated directly by the Optics11 software.

3.7 Biological characterisation

Biological characterisation was performed to evaluate the compatibility of the PEDOT:PSS-based hydrogel formulations with cell culture conditions. The biological work was carried out through collaborations with the Medical University of Graz and Leiden collaborators. The aim of these experiments was to obtain an initial assessment of the cell response to the hydrogel formulations using metabolic activity assays, Live/Dead staining, immunofluorescence staining, and microscopy. The U87

cell experiments were used as an initial cytocompatibility screening of the PEDOT:PSS-DBSA formulation, while the Leiden experiments evaluated all hydrogel formulations using human induced pluripotent stem cell-derived (hiPSC) cortical neuron cultures.

3.7.1 Overview of biological testing

Two biological testing routes were included in this thesis. First, PEDOT:PSS-DBSA hydrogels were evaluated using U87 cells in collaboration with the Medical University of Graz. This experiment was used as an initial cytocompatibility assessment of the DBSA-based hydrogel formulation using an MTS metabolic activity assay. The same collaboration also confirmed that the PEDOT:PSS-DBSA preparation protocol could be reproduced outside TU Delft and that the resulting hydrogels could be electrochemically characterised in a similar way to the samples prepared in this thesis.

Second, all hydrogel formulations were provided to collaborators in Leiden for biological testing using a protocol based on the PEDOT:PSS-based hydrogel neural culture study reported by Wang et al. [31]. In this experiment, the hydrogels were placed in contact with hiPSC-derived cortical neuron cultures and evaluated using Live/Dead staining and immunofluorescence staining at day 8.

For the Leiden experiments, hydrogel samples were conditioned before cell exposure using the sterile medium-washing procedure described in Section 3.3.3.

3.7.2 U87 cell metabolic activity assay

An initial cytocompatibility evaluation of the PEDOT:PSS-DBSA hydrogel formulation was performed using U87 cells in collaboration with the Medical University of Graz. This experiment was used to assess whether the DBSA-based hydrogel formulation could be placed in contact with cells under standard in vitro culture conditions, and whether additional hydrogel pre-conditioning steps could improve the cellular response.

Frozen U87 cells were thawed and transferred into pre-warmed complete culture medium. The cell suspension was centrifuged for 5 min at 500 rpm, after which the supernatant was removed, and the cell pellet was resuspended in fresh medium. The cells were then seeded into culture flasks and maintained under standard incubation conditions. The following day, the medium was replaced to remove residual dead cells and support cell recovery. During routine culture, cells were passaged at appropriate confluency by washing with buffer, enzymatic detachment, collection in fresh medium, and reseeding at the required density.

PEDOT:PSS-DBSA hydrogels were prepared using the transferred DBSA hydrogel protocol. The hydrogel formulation contained 4% DBSA. After gel formation, the hydrogels were washed repeatedly to remove residual components. In selected conditions, the washed hydrogels were also incubated overnight in culture medium before cell exposure. Additional preparation conditions, including GelTrex coating and conditioned-medium exposure, were also tested to investigate whether hydrogel/cell compatibility could be improved.

For direct exposure experiments, U87 cells were seeded in the presence of the DBSA-based hydrogel samples at a density of 10,000 cells per well. Cell response was evaluated using microscopy and an MTS metabolic activity assay. For the MTS assay, cells were cultured in the presence of the hydrogel samples for 24 h. At the endpoint, MTS reagent was added according to the manufacturer's protocol, and the samples were incubated for 2 h. Absorbance was then measured using a plate reader at 490 nm. Approximately 40 µL of hydrogel was used per sample. The absorbance values were used as an indirect measure of cell metabolic activity in the presence of the hydrogel formulation.

This U87 experiment was used as an initial screening assay rather than a full biological validation of the hydrogel system. The results from this experiment, including the effect of hydrogel washing, GelTrex coating, and conditioned-medium exposure, are presented and discussed in Chapter 6.

3.7.3 Biological testing with Leiden collaborators

All PEDOT:PSS-based hydrogel formulations developed in this thesis were provided to collaborators in Leiden for biological evaluation. The tested formulations included PEDOT:PSS-DBSA, PEDOT:PSS-PAA, and PEDOT:PSS-PEGPACHI hydrogels. The aim of this experiment was to evaluate whether the hydrogel samples could be kept in contact with neuronal-like cell cultures and to assess the cellular response using Live/Dead staining and immunofluorescence staining.

The biological protocol was based on the cell-hydrogel culture approach reported by Wang et al. for electrically active PEDOT:PSS-based hydrogels for neural cultures [31]. The same cell type as in the Wang study was used, namely hiPSC-derived cortical neuron cultures. In this approach, cells were cultured in the presence of hydrogel formulations to assess cytocompatibility, cell viability, and neuronal marker expression.

For the Leiden experiments in this thesis, hydrogel samples were first prepared according to the final protocols described in Sections 3.2.1-3.2.3. Before biological testing, all hydrogel samples were sterilely handled and extensively conditioned in culture medium according to the procedure described in Section 3.3.4. Only hydrogels for which the medium remained close to its original pink/red colour after repeated washing and incubation were used for cell culture experiments. After conditioning, the hydrogels were transferred to the cell culture wells under sterile conditions.

Cells were seeded first and allowed to attach for approximately 30 min before hydrogel addition. After this initial attachment period, the hydrogel samples were carefully placed on top of the cell layer in the culture medium. This approach was used to expose the cells directly to the hydrogel surface and any soluble components released from the material, while avoiding disturbance of the cells during initial attachment. Control wells containing cells without hydrogels were included for comparison. The hydrogels remained in the wells until the endpoint of the experiment.

The Leiden experiment was evaluated at day 8. At this endpoint, cell viability was assessed using Live/Dead staining. Following the Wang et al. protocol, Live/Dead staining was performed directly in the wells, after which fluorescence microscopy was used to acquire images of the control and hydrogel-containing conditions. In addition to Live/Dead staining, immunofluorescence staining was performed to evaluate cell morphology and neuronal marker expression. The results from the Leiden experiment, including representative Live/Dead and immunofluorescence images, are presented and discussed in Chapter 6.

3.7.4 Live/Dead staining, immunofluorescence staining, and microscopy

Live/Dead staining was used to evaluate cell viability in the Leiden experiment. The staining procedure followed the protocol described by Wang et al. for PEDOT:PSS-based hydrogels in neural cultures [31]. Staining was performed directly in the wells containing the cells and hydrogel samples. Live cells were identified from the green fluorescence signal, while dead cells were identified from the red fluorescence signal. After staining, the wells were imaged by fluorescence microscopy. Representative images were acquired for the control and hydrogel-containing conditions and were later used for viability analysis.

Immunofluorescence staining was also performed for the Leiden experiment. The staining procedure followed the protocol described by Wang et al. [31]. Briefly, samples were fixed, permeabilised, blocked, incubated with primary and secondary antibodies, and counterstained for nuclei before fluorescence imaging. The immunofluorescence images were used qualitatively to assess cell morphology and neuronal marker expression in the presence of the hydrogel samples. The staining results were compared between control wells and hydrogel-containing wells.

Fluorescence images from the Live/Dead assays were analysed using ImageJ/Fiji. The analysis was performed using two complementary approaches: an area-based method and a cell-counting method. For the area-based analysis, the live and dead fluorescence channels were separated, and thresholding

was applied to identify the fluorescent regions corresponding to live and dead cells. The live area was then divided by the total stained area, calculated as the sum of the live and dead areas:

$$Live\ area\ fraction\ (\%) = \frac{live\ area}{live\ area + dead\ area} \times 100$$

For the cell-counting analysis, the green and red channels were also processed separately in ImageJ/Fiji. Thresholding and particle analysis were used to estimate the number of live and dead cells. Cell viability was then calculated as:

$$Cell\ viability\ (\%) = \frac{number\ of\ live\ cells}{number\ of\ live\ cells + number\ of\ dead\ cells} \times 100$$

The ImageJ/Fiji analysis workflow was adapted from a published live/dead assay quantification guide, in which the green and red fluorescence channels are processed separately and cell viability is calculated from the detected live and dead objects [37].

Because the PEDOT:PSS-based hydrogels produced strong dark regions, uneven background, and fluorescence artefacts in some images, the analysis could not be fully automated. Regions containing obvious hydrogel artefacts, strong background fluorescence, poor focus, or areas unsuitable for reliable cell identification were manually excluded before quantification. The same exclusion approach was applied consistently across the analysed images. The final Live/Dead results were calculated using both the area-based and cell-counting methods, and the results are presented and discussed in Chapter 6.

3.8 PDMS measuring platform for electrochemical characterisation

A preliminary PDMS measuring platform was developed to support electrochemical measurements of PEDOT:PSS-based hydrogels in a controlled and reproducible geometry. The main purpose of the platform was to hold the hydrogel samples in defined wells, provide direct contact with a gold pogo pin working electrode, and allow the samples to remain hydrated during electrochemical testing. The platform was used as a measurement platform to improve hydrogel/electrode contact during electrochemical testing.

3.8.1 Design rationale of the PDMS measuring platform

The PDMS measuring platform was designed to overcome practical difficulties associated with measuring soft, hydrated hydrogels. After gelation, the hydrogels were difficult to transfer and contact reproducibly without deformation or damage. Therefore, the platform was designed so that the hydrogel precursor could be cast directly inside the measurement well and around the working electrode. This reduced sample handling after gelation and improved the stability of the electrode/hydrogel contact during electrochemical measurements.

The final platform consisted of a full-PDMS structure containing an array of cylindrical wells. The platform contained 18 wells arranged in two columns and nine rows. Each well had a diameter of 5 mm and a depth of 10 mm. The distance between neighbouring wells was 5 mm edge-to-edge. The total platform dimensions were approximately 110 mm in length, 12 mm in thickness and 26 mm in width. The platform was therefore narrow enough to be compatible with the width of standard microscope glass slides, although the final version used in this thesis did not require glass bonding.

The final design used in this thesis was a full-PDMS platform without a glass bottom. This simplified the fabrication process and avoided the need for PDMS-glass bonding. Earlier versions of the platform, including those used in the Medical University of Graz collaboration, included a glass bottom and a top

part for hydrogel thickness control. In that collaborative version, the PDMS-based device was fabricated using a 3D-printed inverse mould, a glass layer was integrated at the bottom, and a needle-made opening was used for insertion of a gold pogo pin. The platform was also used for cell experiments during the Medical University of Graz collaboration. Before U87 cell culture experiments, the PDMS platform was sterilized by ethanol washing followed by 30 min UV exposure.

3.8.2 CAD design and 3D printing of the inverse mould

The inverse mould for PDMS casting was designed in SolidWorks. The mould geometry was designed to produce the final well array in PDMS and to define the overall dimensions of the platform. The platform dimensions and well arrangement are shown in Figure 3.5.

The inverse mould was fabricated using fused deposition modelling with a Bambu Lab X1 Carbon 3D printer. Printing was prepared using Bambu Studio software. The mould was printed using Bambu PLA Basic filament, a 0.4 mm nozzle, and a 0.20 mm layer height. The initial layer height was also set to 0.20 mm. After printing, the PLA structure was used directly as the inverse mould for PDMS casting.

3.8.3 PDMS casting and curing

PDMS was prepared using the SYLGARD 184 Silicone Elastomer Kit at a 10:1 base-to-curing-agent ratio. The base and curing agent were mixed thoroughly until a homogeneous mixture was obtained. No degassing step was performed before casting.

The mixed PDMS was poured into the 3D-printed PLA inverse mould and left to cure overnight at room temperature. After curing, the PDMS platform was carefully removed from the mould. The resulting structure contained the 18-well array defined by the printed mould.

After demoulding, openings for the working-electrode contacts were created manually. A needle was used to puncture the side of the PDMS platform at the selected wells. Gold pogo pins were then inserted horizontally through the punctured openings so that each pogo pin passed into the corresponding hydrogel well. The pogo pins were connected to external wires to allow straightforward connection to the potentiostat during electrochemical measurements.

3.8.4 Hydrogel integration into the PDMS measuring platform

All three PEDOT:PSS-based hydrogel formulations were tested in the PDMS measuring platform: PEDOT:PSS-DBSA, PEDOT:PSS-PAA, and PEDOT:PSS-PEGPACHI. For each measurement, one well was used at a time.

Before casting, the gold pogo pin was inserted into the selected well. The hydrogel precursor was then added directly into the well so that it surrounded the pogo pin. For PEDOT:PSS-DBSA and PEDOT:PSS-PEGPACHI, gelation occurred directly inside the PDMS well. This produced an integrated hydrogel-pogo pin contact without the need to transfer the gel after formation.

For PEDOT:PSS-PAA, the hydrogel was prepared according to the protocol described in Section 3.2.2 and then placed in contact with the pogo pin inside the PDMS platform. After hydrogel integration, 1x DPBS was added to the well to maintain hydration and provide the electrolyte for electrochemical measurements.

Because PDMS is hydrophobic, the added DPBS formed a dome-shaped droplet above the hydrogel-containing well. This helped maintain a local electrolyte reservoir above the hydrogel and made it possible to position the Ag/AgCl reference electrode and platinum mesh counter electrode in contact with the electrolyte during measurement.

3.8.5 Electrochemical measurements in the integrated platform

Electrochemical measurements in the PDMS measuring platform were performed using the three-electrode configuration described in Section 3.5.1. The gold pogo pin embedded in the hydrogel served as the working electrode. An Ag/AgCl electrode was used as the reference electrode, and a platinum mesh electrode was used as the counter electrode. Measurements were performed in 1x DPBS.

Only one hydrogel well was measured at a time. For each measurement, the working-electrode wire connected to the selected pogo pin was connected to the potentiostat, while the reference and counter electrodes were positioned in the DPBS droplet above or near the hydrogel. Cyclic voltammetry and electrochemical impedance spectroscopy were then performed using the settings described in Sections 3.5.3 and 3.5.4.

The integrated PDMS platform was used to compare the electrochemical behaviour of the different hydrogel formulations under a consistent hydrogel-electrode contact geometry. The practical performance, advantages, and limitations of this platform are discussed in Chapter 5.3.2.

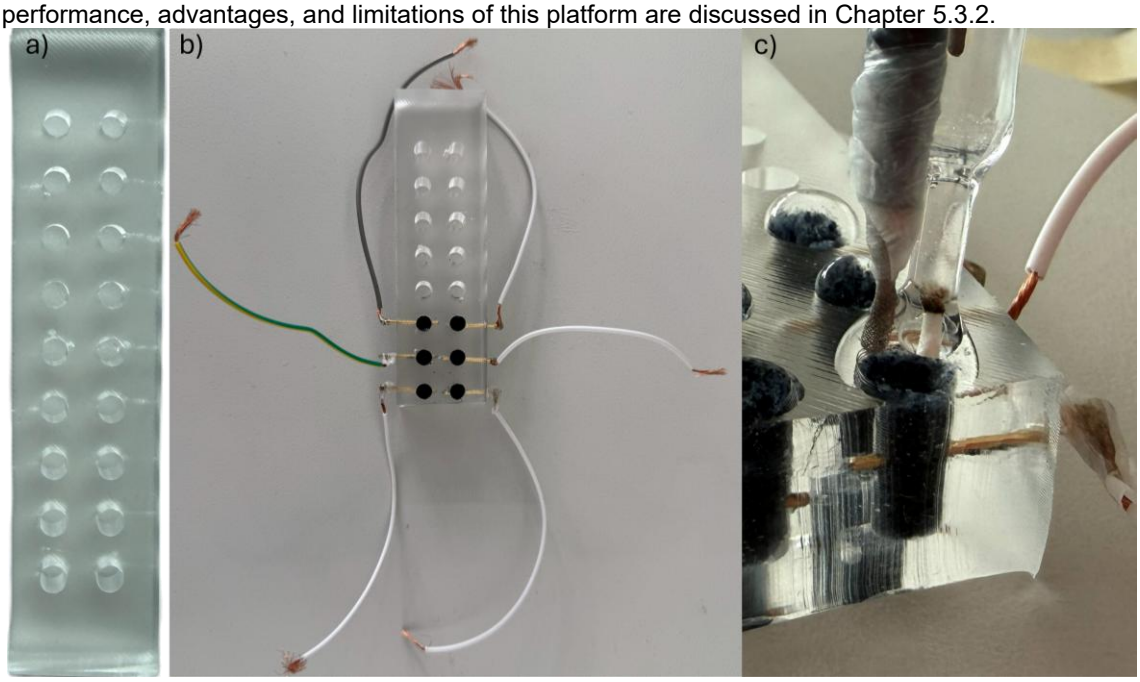


Figure 3.5: PDMS measuring platform for hydrogel electrochemical characterisation. (a) Full-PDMS platform containing an array of cylindrical wells. The platform contained 18 wells arranged in two columns and nine rows. Each well had a diameter of 5 mm and a depth of 10 mm. (b) PDMS platform after manual insertion of gold pogo pins and external wire connections. (c) Hydrogel-filled wells during electrochemical measurement. The hydrogel was integrated around the pogo pin working electrode, while 1x DPBS formed a local electrolyte reservoir above the well for positioning of the reference and counter electrodes.

4 Hydrogel Development and Optimisation

4.1 Overview of hydrogel development strategy

The aim of this chapter is to describe the development and optimisation of the PEDOT:PSS-based hydrogel formulations investigated in this thesis. Three different hydrogel systems were explored: PEDOT:PSS-DBSA, PEDOT:PSS-PAA, and PEDOT:PSS-PEGPACHI. These formulations were selected because they represent different approaches to forming conductive PEDOT:PSS-based hydrogels, with different levels of preparation complexity, chemical composition, handling behaviour, and potential biological compatibility.

The PEDOT:PSS-DBSA hydrogel was selected as the initial reference formulation. This system was based on the room-temperature PEDOT:PSS hydrogel approach reported by Zhang et al. and was used as a starting point for becoming familiar with PEDOT:PSS hydrogel preparation, gelation behaviour, moulding, handling, and electrochemical testing [35]. Since this formulation was expected to be relatively simple to prepare and optimise, it provided a useful reference against which the other hydrogel systems could be compared. In this thesis, the DBSA formulation was therefore used both as a literature-based benchmark and as a practical starting material for developing the experimental workflow.

The PEDOT:PSS-PAA hydrogel was selected as a second, more complex formulation route. In contrast to the DBSA system, this approach involved the formation of a poly(acrylic acid)-based hydrogel network containing PEDOT:PSS, followed by post-treatment steps to improve the final material properties. This route was included to investigate a different hydrogel formation strategy and to compare its behaviour with the simpler additive-induced DBSA gelation approach. The PEDOT:PSS-PAA formulation also allowed the integration of cleanroom-based processing into the thesis workflow, since its preparation involved a controlled protocol adapted for use in the Else Kooi Laboratory.

The third formulation, PEDOT:PSS-PEGPACHI, was developed and optimised in this thesis. This formulation was designed to combine some of the practical advantages of the DBSA system, such as relatively simple preparation and direct moulding, with improved suitability for biological experiments. The motivation for this formulation came from the poor biological response observed for the DBSA-based hydrogels under the tested conditions. Therefore, the PEDOT:PSS-PEGPACHI system was developed using PEGDE, phytic acid, and chitosan as additional formulation components. The goal was not only to obtain gelation, but to design a formulation in which each component had a specific role in the final material.

The optimisation work in this chapter therefore focuses on both practical hydrogel formation and material design. For each hydrogel system, the formulation strategy, proposed gelation mechanism, role of the individual components, and optimisation steps are discussed. This includes both successful and unsuccessful trials, because these experiments were important for understanding which processing conditions produced stable, handleable, and reproducible hydrogels. The comparison between the three systems was based on gelation behaviour, ease of preparation, mouldability, stability in aqueous media, handling during testing, and suitability for later electrochemical, mechanical, biological, and hydrogel-array integration experiments.

The final formulations selected from this optimisation chapter were then carried forward for detailed characterisation in the following chapters. Physical, electrochemical, and mechanical characterisation

are presented in Chapter 5, biological compatibility is discussed in Chapter 6, and preliminary integration of the hydrogels into a PDMS hydrogel-array device is presented in Chapter 7**Σφάλμα! Το αρχείο προέλευσης της αναφοράς δεν βρέθηκε.**.

4.2 PEDOT:PSS-DBSA hydrogel development

4.2.1 Rationale for selecting the PEDOT:PSS-DBSA formulation

The PEDOT:PSS-DBSA hydrogel was selected as the first hydrogel system investigated in this thesis. This formulation was chosen because it has been reported as a room-temperature-forming PEDOT:PSS hydrogel and therefore provided a useful reference system for establishing the experimental workflow. Zhang et al. reported that PEDOT:PSS hydrogels could be formed by mixing PEDOT:PSS with DBSA, with spontaneous gelation occurring once the DBSA concentration reached approximately 3 v/v%. In their work, a 4 v/v% DBSA formulation formed a hydrogel at room temperature and was used as the main hydrogel formulation.

In this thesis, the DBSA-based system was used both as a literature-based reference and as a practical starting point for learning how to prepare, mould, handle, store, and electrochemically measure PEDOT:PSS-based hydrogels. Compared with the other formulations investigated later, the DBSA system was expected to be relatively simple because gelation could occur directly after mixing PEDOT:PSS with the additive, without polymerisation, high-temperature curing, or additional network-forming steps. For this reason, it was used as the first optimisation platform before moving to more complex hydrogel systems.

4.2.2 Proposed role of DBSA in PEDOT:PSS gel formation

The formation of the PEDOT:PSS-DBSA hydrogel is based on additive-induced physical gelation, rather than covalent crosslinking. PEDOT:PSS consists of positively charged PEDOT chains that are charge-balanced and stabilised by negatively charged PSS chains. In aqueous dispersion, PSS helps to keep the material water-dispersible, while PEDOT provides the electronically conductive phase. PEDOT:PSS is therefore commonly described as a system in which PEDOT-rich conductive domains are associated with a PSS-rich phase [30], [35].

DBSA is an acidic surfactant with a hydrophobic alkylbenzene tail and a sulfonic acid head group. When DBSA is added to PEDOT:PSS at a sufficient concentration, it can influence both the ionic environment of the dispersion and the interaction between PEDOT and PSS. Zhang et al. proposed that DBSA increases the ionic strength of the system and provides protons that can protonate PSS^- groups. This weakens the electrostatic attraction between $PEDOT^+$ and PSS^- chains, allowing PEDOT-rich segments to become more exposed [35].

Once PEDOT-rich segments are more exposed, the PEDOT chains can rearrange from a more confined or coiled conformation towards a more expanded and linear structure. This conformational change increases the possibility of interchain interactions between PEDOT segments. These interactions include π-π stacking between the conjugated PEDOT backbones and hydrophobic interactions between PEDOT-rich domains. Together, these non-covalent interactions act as physical junction points within the material[35].

As the number of physical junction points increases, the PEDOT:PSS dispersion gradually loses fluidity and develops into a connected three-dimensional network. This network can trap water and form a soft hydrogel without the need for an additional covalent crosslinker. Therefore, the PEDOT:PSS-DBSA hydrogel can be understood as a physically crosslinked conductive hydrogel, where DBSA promotes PEDOT:PSS rearrangement and network formation [35].

This proposed gelation concept is illustrated schematically in Figure 4.1. The schematic is intended to summarise the possible role of DBSA in PEDOT:PSS rearrangement and hydrogel network formation, rather than to represent a directly verified molecular mechanism.

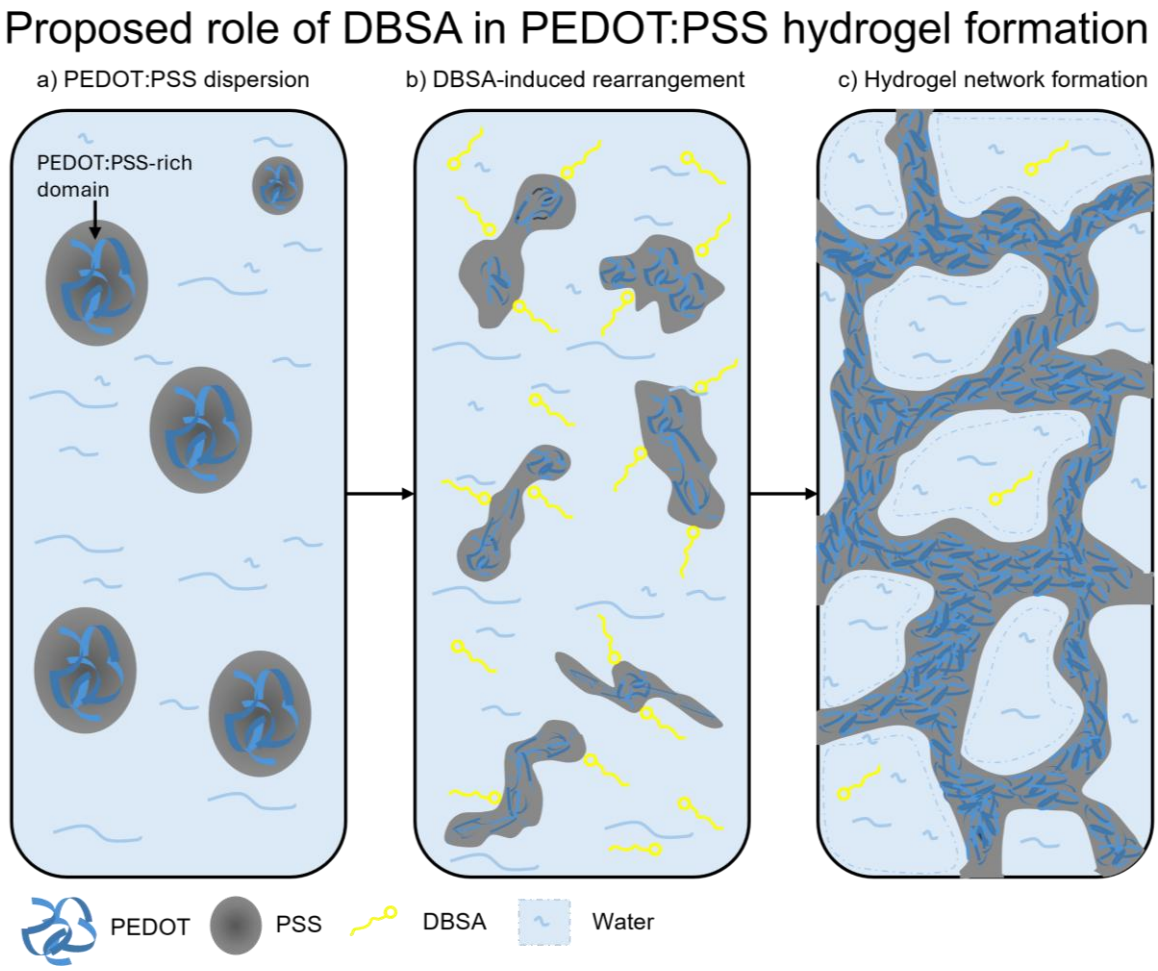


Figure 4.1: Proposed role of DBSA in PEDOT:PSS hydrogel formation. Schematic illustration of the proposed DBSA-induced gelation process. PEDOT:PSS is initially present as dispersed PEDOT:PSS-rich domains in water. After DBSA addition, the acidic surfactant is proposed to promote rearrangement and association of PEDOT:PSS-rich domains, leading to the formation of an interconnected hydrated PEDOT:PSS network. This schematic represents a proposed interpretation based on the literature and the gelation behaviour observed in this thesis, rather than a directly verified molecular mechanism.

The concentration of DBSA is a critical parameter in this mechanism. At low DBSA concentration, there may not be enough surfactant-mediated interaction to form a continuous network, and the material can remain liquid or form only a weak gel. Zhang et al. reported spontaneous gelation when the DBSA concentration reached approximately 3 v/v%, with gelation time depending on DBSA concentration [35]. In this thesis, DBSA concentration was therefore treated as an important optimisation parameter.
Mixing is also important because DBSA must be distributed homogeneously throughout the PEDOT:PSS dispersion for reproducible gelation. Insufficient mixing can lead to DBSA-rich and DBSA-poor regions, resulting in slow, incomplete, or non-uniform gel formation. However, because DBSA is a surfactant, excessive mixing can trap bubbles in the precursor and final gel. Therefore, the final preparation protocol had to balance sufficient mixing for gel formation with minimisation of bubble

formation. This was confirmed experimentally during the optimisation of the mixing sequence, where the combined sonication-vortexing-sonication procedure produced the most reliable gelation behaviour compared with sonication-only or vortex-only conditions.

4.2.3 Initial reproduction of the literature protocol

The initial objective was to reproduce the reported PEDOT:PSS-DBSA hydrogel protocol using the available equipment in the laboratory. However, the exact equipment used in the original publication was not available, and the first attempts using manual mixing were not sufficient to induce reliable gelation. The formulation remained mostly liquid or did not form a stable gel within the expected time.

Because DBSA is a surfactant, more aggressive mixing also introduced another problem. When high-speed mixing was used, the formulation became highly bubbly, and bubbles remained trapped in the hydrogel precursor and final gel. This was an important practical limitation because bubbles affected the homogeneity of the gel, the appearance of the samples, and potentially the reproducibility of later electrochemical measurements. Therefore, the optimisation focused on finding a mixing procedure that was strong enough to induce gelation, but not so aggressive that it produced excessive bubble formation.

4.2.4 Optimisation of the mixing protocol

Several mixing strategies were tested to identify a reproducible preparation method. Initial attempts included manual mixing and pipetting-based mixing, but these approaches were not sufficient to distribute DBSA homogeneously through the PEDOT:PSS dispersion and did not reliably induce gelation. After considering the properties of the formulation, especially the high viscosity and the surfactant behaviour of DBSA, mechanical mixing methods were selected as the most suitable approach. The optimisation therefore focused mainly on sonication, vortexing, and combinations of both. The tested procedures included sonication alone, vortexing alone, combined sonication and vortexing, and repeated sonication/vortexing sequences. These trials showed that the mixing sequence strongly affected the gelation time and whether a stable gel could be obtained.

In the first optimisation series, PEDOT:PSS was removed from the fridge, sonicated, filtered through a 0.45 µm filter, mixed with DBSA, and then subjected to different mixing procedures. The tested procedures included 2 min sonication only, 2 min vortexing at 800 rpm only, 2 min sonication followed by 2 min vortexing, 2 min sonication followed by 2 min vortexing and a second 2 min sonication step, and a vortex-only procedure using 800 rpm followed by 1200 rpm. The combined sequence of 2 min sonication → 2 min vortexing at 800 rpm → 2 min sonication gave the most reliable gelation behaviour, with gelation observed after approximately 20 min in that optimisation experiment. In comparison, sonication alone required approximately 50 min, vortexing alone did not form a gel after 90 min, and the sonication/vortexing sequence without the final sonication step required approximately 80 min.

Based on these results, the combined sonication-vortexing-sonication sequence was selected as the basis for the final DBSA hydrogel preparation protocol. The result suggested that both mixing intensity and mixing type were important. Sonication helped disperse DBSA into the PEDOT:PSS suspension and reduce local concentration differences, while vortexing provided additional mechanical mixing. However, vortexing alone was not sufficient under the tested conditions, and excessive mixing increased bubble formation. Representative images from the PEDOT:PSS-DBSA optimisation process are shown in Figure 4.2. Early trials showed strong bubble formation after mixing, while the optimised 4% v/v DBSA formulation produced a stable hydrogel that could be moulded and integrated into the PDMS measuring platform. Additional photographs from the DBSA optimisation process are provided in **Appendix D**.

4.2.5 Effect of DBSA concentration and temperature on gelation

After identifying a suitable mixing sequence, the effect of DBSA concentration was investigated. Different DBSA concentrations were tested to determine which formulation gave the best balance

between gelation, handling, and later electrochemical characterisation. The tested series included lower DBSA concentrations, which were expected to gel more slowly or incompletely, and higher DBSA concentrations, which were expected to gel faster but contained more surfactant.

The optimisation results confirmed that insufficient DBSA content produced weak or incomplete gelation. This was consistent with the literature, where gelation was reported to occur only above a threshold DBSA concentration of approximately 3 v/v% [35]. In the experimental optimisation series, formulations based on 2%, 3%, 4%, and 5% DBSA were tested using the selected sonication-vortexing-sonication protocol. This experiment also showed that reproducibility was affected by temperature, with colder experimental conditions associated with slower or less reliable gelation.

The final selected formulation was 4% v/v DBSA, because it gave the best overall balance between gelation time, handling, and suitability as a reference hydrogel. Lower DBSA contents were less reliable for gel formation, while higher DBSA contents gelled faster but were less attractive as a reference formulation because of the higher surfactant content and the practical difficulty of handling rapidly gelating samples. The final 4% DBSA formulation generally gelled within approximately 30 min, although the exact gelation time depended on room temperature. On colder days, gelation was slower, while warmer conditions reduced the gelation time.

4.2.6 Importance of filtration and sample handling

Filtration of the PEDOT:PSS dispersion was an important practical step in the DBSA hydrogel protocol. A 0.45 µm cellulose acetate filter was selected for the final procedure because it allowed removal of larger aggregates while still preserving the ability of the PEDOT:PSS dispersion to form a hydrogel after DBSA addition. A smaller 0.22 µm filter was also tested, but when PEDOT:PSS filtered through this filter was used in the same DBSA gelation protocol, reliable hydrogel formation was not obtained. This suggested that the filtration step could influence the final gelation behaviour, possibly by changing the effective PEDOT:PSS particle/domain population or removing components important for network formation. Therefore, 0.45 µm filtration was retained in the final optimised protocol.

Sample handling also affected the reproducibility of the DBSA hydrogels. After gelation, the hydrogels were stable when stored in 1x DPBS, but they were mechanically fragile and required careful handling. This fragility was expected for this type of physically crosslinked hydrogel, and Zhang et al. reported a Young's modulus of approximately 1 kPa for the room-temperature PEDOT:PSS-DBSA hydrogel [35]. When DBSA hydrogels were left without DPBS, they dehydrated strongly and shrank. However, rehydration in DPBS restored their hydrated appearance. This observation was not used as a primary characterisation result in this chapter, but it supported the need to store the samples in aqueous medium before testing. The electrochemical stability and behaviour of the DBSA hydrogels after storage are discussed later in Chapter 5.

4.2.7 Final selected PEDOT:PSS-DBSA formulation

Based on the optimisation process, the final PEDOT:PSS-DBSA hydrogel formulation used in this thesis consisted of PEDOT:PSS PH1000 with 4% v/v DBSA. PEDOT:PSS was first sonicated and filtered through a 0.45 µm filter. DBSA was then added, and the mixture was processed using the selected mixing sequence of sonication, vortexing at 800 rpm, and sonication. The precursor was then cast into the selected mould or directly into the PDMS measuring platform, where gelation occurred at room temperature.

The final DBSA hydrogel was reproducible enough to be used as the reference formulation for later physical, electrochemical, mechanical, biological, and measuring-platform experiments. It was simple to prepare, formed at room temperature, and showed stable gel formation when the mixing conditions were controlled. However, the later biological screening showed that the DBSA formulation had limitations in cell culture conditions. This motivated the development of the PEDOT:PSS-PEGPACHI

formulation, which aimed to retain some of the practical advantages of DBSA gelation while using components expected to be more suitable for biological testing.

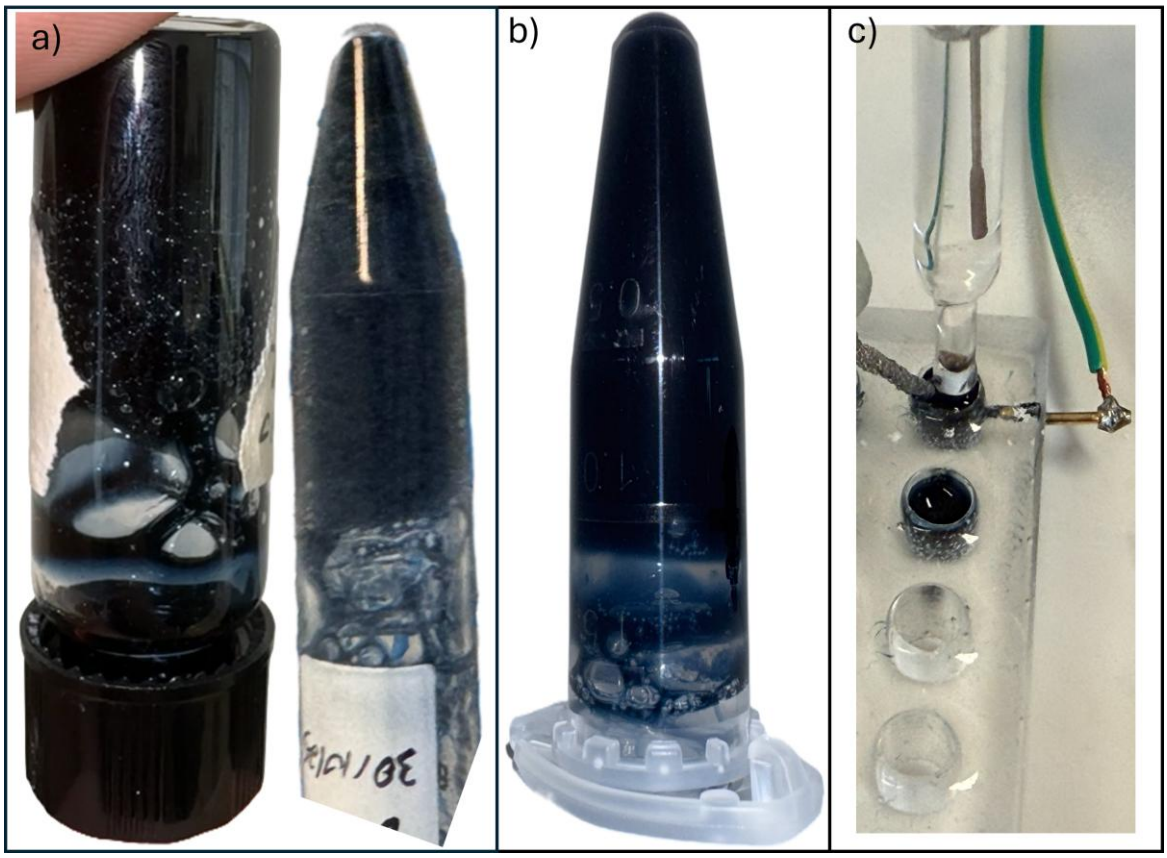


Figure 4.2: Optimisation of PEDOT:PSS-DBSA hydrogel formation and integration into the PDMS measuring platform.
(a) Early PEDOT:PSS-DBSA gelation trials showing strong bubble formation inside the hydrogel after mixing. This was one of the main practical issues observed during the first optimisation attempts. (b) PEDOT:PSS-DBSA hydrogel formed in an Eppendorf tube after optimisation of the mixing procedure, using the final 4% v/v DBSA formulation. (c) PEDOT:PSS-DBSA hydrogel cast inside the PDMS measuring platform around the gold pogo pin working electrode for electrochemical measurement.

4.3 PEDOT:PSS-PAA hydrogel formation

4.3.1 Rationale for selecting the PEDOT:PSS-PAA formulation

The PEDOT:PSS-PAA hydrogel was selected as a second literature-based formulation route in this thesis. In contrast to the PEDOT:PSSDBSA hydrogel, which was based on additive-induced physical gelation, the PEDOT:PSS-PAA system involved the formation of a polymeric hydrogel network containing PEDOT:PSS. This made it a more complex formulation and provided an opportunity to investigate a different strategy for producing conductive PEDOT:PSS-based hydrogels.

The formulation was adapted from the hydrogel semiconductor work reported by Liu et al., where PEDOT:PSS/PAA hydrogels were developed as three-dimensional hydrogel semiconductors. In that work, the PAA-containing hydrogel system was used to improve the continuity of the PEDOT-rich conducting phase and enable efficient three-dimensional ion/electron coupling in thick hydrogel structures. Liu et al. reported that secondary hydrogel networks, especially PAA, can guide the

formation of a more continuous $PEDOT^+$ phase and improve electronic conductivity and volumetric capacitance compared with pure PEDOT:PSS hydrogels [32].

In this thesis, the PEDOT:PSS-PAA formulation was included for two main reasons. First, it allowed comparison between a simple DBSA-based gelation route and a more structured polymer network-based route. Second, it allowed the integration of cleanroom-based fabrication into the project, since the formulation required controlled handling, approved materials, and post-processing steps. Therefore, the PEDOT:PSS-PAA hydrogel was used as a more technically demanding reference formulation for comparison with both PEDOT:PSS-DBSA and the thesis-developed PEDOT:PSS-PEGPACHI hydrogel.

4.3.2 Proposed formation mechanism and role of the components

The PEDOT:PSS-PAA hydrogel formation is based on the incorporation of PEDOT:PSS into a crosslinked poly(acrylic acid) network. In this formulation, PEDOT:PSS acts as the electronically conductive phase, while acrylic acid acts as the monomer used to form the PAA network. MBAA is included as a crosslinker to connect the growing PAA chains and form a three-dimensional polymer network. The combination of PEDOT:PSS with a secondary PAA network is important because the PAA network can act as a structural template that influences the organisation and continuity of the conductive PEDOT:PSS-rich phase. This is consistent with Liu et al., who showed that the secondary hydrogel network affects phase continuity and helps promote electron transport in PEDOT:PSS-based hydrogel semiconductors [32].

DMSO was included in the precursor mixture as a co-solvent and processing additive. Its role was to help produce a homogeneous PEDOT:PSS-containing precursor and support the later electrical performance of the hydrogel system. After gelation, the hydrogels were treated with EMIM-ES, a strong ionic liquid. This post-treatment step was included to promote phase reorganisation and improve the final material properties. The gels were then transferred to an EMIM-ES:water mixture to perform solvent exchange. In the cleanroom flowchart, this solvent exchange step was performed using 70:30 v/v EMIM-ES:water for 6 h.

The ionic-liquid treatment and solvent exchange steps are also relevant to the visual changes observed in the hydrogels. After EMIM-ES treatment, the surface appearance of the gels changed, and the samples visually appeared more porous or rougher. This observation was only assessed macroscopically in this thesis and should therefore be interpreted as a qualitative indication of surface and structural change rather than a quantitative porosity measurement. Liu et al. reported that solvent exchange can be used to tune the porosity of PEDOT:PSS/PAA hydrogel semiconductors and that porosity affects the balance between electronic and ionic transport [32].

Finally, the hydrogels were thermally treated and rehydrated. The annealing protocol consisted of heating at 80 °C for 6 h, followed by 130 °C for 2 h, after which the samples were rehydrated in aqueous buffer. These steps were included in the adapted protocol to complete the post-processing of the PEDOT:PSS-PAA hydrogel before later characterisations.

The proposed formation process of the PEDOT:PSS-PAA hydrogel is summarised schematically in Figure 4.3. In the precursor suspension, freeze-dried PEDOT:PSS is dispersed together with acrylic acid, MBAA, water, and DMSO. After addition of the redox initiators, acrylic acid polymerises and is crosslinked by MBAA, forming a PAA network around the dispersed PEDOT:PSS-rich particles or domains. Based on the mechanism proposed by Liu et al., the secondary PAA network can act as a template that improves the continuity of the PEDOT:PSS-rich conductive phase, supporting the formation of electron-transport pathways within the hydrogel. After EMIM-ES treatment, solvent exchange, annealing, and rehydration, a porous PEDOT:PSS-PAA hydrogel is formed. The pores support ionic transport, while the PEDOT:PSS-rich domains may provide electronic pathways through the PAA matrix.

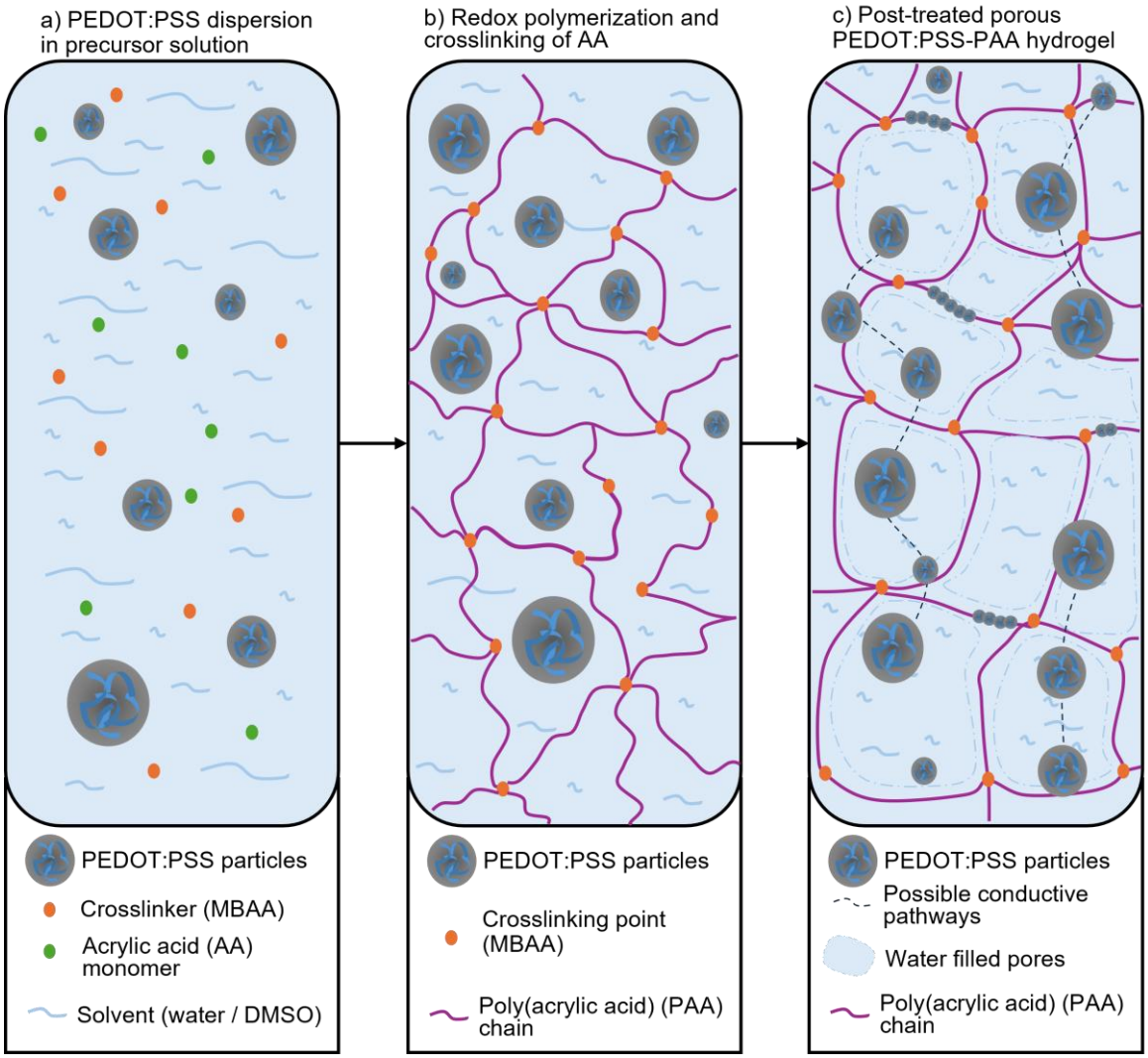


Figure 4.3: Proposed formation mechanism of PEDOT:PSS-PAA hydrogels. (a) PEDOT:PSS particles are dispersed in a precursor solution containing acrylic acid (AA), MBAA crosslinker, and solvent. (b) Redox polymerisation and crosslinking of AA lead to the formation of a poly(acrylic acid) (PAA) network, with PEDOT:PSS particles embedded throughout the matrix. (c) After post-treatment, annealing, and rehydration, a porous PEDOT:PSS-PAA hydrogel network is obtained. The PAA network is proposed to support the organisation of PEDOT:PSS-rich domains into possible conductive pathways, while the water-filled pores support ionic transport. The schematic is based on the proposed role of PAA as a secondary network in PEDOT:PSS/PAA hydrogel semiconductors and represents an interpretation of the formulation used in this thesis.

4.3.3 Cleanroom implementation and initial fabrication challenges

The PEDOT:PSS-PAA route required substantially more preparation than the DBSA formulation. Before the experimental work could be performed, the required cleanroom equipment had to be identified, training had to be completed, and an approved process flowchart had to be prepared for the Else Kooi Laboratory. The final approved flowchart was registered as P2026-13 and described the fabrication of the PEDOT:PSS/PAA hydrogel semiconductor matrix. The flowchart listed the relevant materials, cleanroom locations, and processing steps, including precursor preparation, redox-initiated gelation, EMIM-ES treatment, annealing, and rehydration.

The first major practical challenge was the preparation of dry PEDOT:PSS. Unlike the DBSA formulation, which used the PEDOT:PSS aqueous dispersion directly, the PAA protocol required PEDOT:PSS to be freeze-dried before use. The dry PEDOT:PSS then had to be weighed, crushed, and mixed with acrylic acid, MBAA, water, and DMSO to form a homogeneous viscous suspension. The base recipe used in the adapted protocol consisted of 26 mg dry PEDOT:PSS, 130 mg acrylic acid, 5 mg MBAA, 2 g DI water, and 0.4 g DMSO.

This mixing step was one of the most important practical parts of the protocol. Early experiments were performed using a large agate mortar. However, because the precursor became viscous during mixing, a significant amount of material became trapped on the walls of the mortar. This resulted in material loss and reduced the amount of precursor available for moulding. To compensate for this, some later experiments were performed using doubled quantities. In later stages, a smaller agate mortar with a more suitable surface was used, which made the original-scale formulation easier to prepare.

The second major practical challenge was the time and scheduling required for the cleanroom process. The full PAA fabrication route required approximately 2.5 days, including cleanroom precursor preparation, gelation, overnight EMIM-ES treatment, solvent exchange, annealing, and rehydration. Since the cleanroom equipment had to be reserved in advance, it was difficult to coordinate all required steps and equipment availability within the same experimental run. This made the PAA formulation more demanding to optimise than the DBSA formulation.

4.3.4 Optimisation of precursor mixing and gelation control

The first PAA fabrication trials showed that gelation occurred very rapidly after addition of the redox initiators. When a larger precursor volume was prepared as a single batch, the addition of H_2O_2 and ascorbic acid caused the material to gel too quickly. This made it difficult to transfer the precursor into the PDMS mould or PDMS measuring platform before gelation occurred. As a result, the first samples were difficult to mould and the outer surfaces appeared rough and non-uniform.

To improve the process, the precursor was divided into smaller Eppendorf tubes before initiator addition. The initiator volumes were divided proportionally between the smaller precursor portions. For example, instead of initiating the entire precursor volume at once, the total precursor was split into smaller aliquots, and the H_2O_2 and ascorbic acid volumes were also divided accordingly. This reduced the practical difficulty of handling a rapidly gelating bulk volume and produced more uniform gelation. After the first trial, this divided-volume strategy was kept as part of the optimised fabrication workflow because it consistently gave better results.

The mixing strategy was also optimised. After grinding the dry PEDOT:PSS-containing mixture in the mortar, sonication was introduced to improve homogeneity. One strategy was to sonicate the complete precursor mixture before initiator addition. Another strategy was to first mix PEDOT:PSS with water and DMSO and sonicate this dispersion before adding acrylic acid and MBAA. This second approach was tested because the precursor became more viscous after addition of acrylic acid and MBAA, making homogenisation more difficult. By improving the dispersion of PEDOT:PSS before the mixture became highly viscous, the goal was to reduce visible aggregates and obtain a more uniform precursor before gelation.

The optimisation therefore focused mainly on process control rather than changing the chemical formulation. The material composition was kept close to the literature-based formulation, while the practical workflow was modified to improve precursor homogeneity, reduce material loss, and control the rapid redox-initiated gelation step. Representative photographs from the PAA fabrication and optimisation process are shown in Figure 3.2. Additional experimental documentation is provided in **Appendix H**.

4.3.5 Post-treatment, annealing, and rehydration behaviour

After gelation, the PEDOT:PSS-PAA hydrogels were treated with pure EMIM-ES overnight, followed by solvent exchange in 70:30 v/v EMIM-ES:water for 6 h. This post-treatment step required the gels to be fully surrounded by ionic liquid or solvent-exchange medium. For this reason, samples that had been moulded directly inside PDMS structures had to be removed from the mould before treatment. This handling step was problematic because some gels were damaged during removal and transfer.

Following the ionic-liquid treatment and solvent exchange, the samples were annealed at 80 °C for 6 h and then at 130 °C for 2 h. After annealing, the gels became more stable and showed a bouncy, resilient behaviour during handling. No cracking was observed in the final samples after annealing. After rehydration, only minor swelling was observed, and some release of ionic liquid from the gel was visible. The rehydrated samples remained handleable and could be used for subsequent measurements.

The changes observed after EMIM-ES treatment, annealing, and rehydration indicated that post-processing was essential for obtaining stable PEDOT:PSS-PAA hydrogel samples. In contrast to the DBSA hydrogel, which formed directly at room temperature and could remain in the mould, the PAA formulation required several additional treatment steps before it reached its final usable form.

4.3.6 Moulding and integration limitations

A major limitation of the PEDOT:PSS-PAA hydrogel was its poor compatibility with direct integration into the PDMS measuring platform. Initially, the precursor was cast into the PDMS platform to mould the hydrogel directly. However, because the gel had to be removed again for EMIM-ES treatment and solvent exchange, the direct-moulding approach created additional handling steps. These steps increased the risk of damaging the gel and reduced the reproducibility of the final samples.

For this reason, the final approach shifted away from direct gelation inside the PDMS measuring platform. Instead, larger gel pieces were prepared in Eppendorf tubes, post-treated, annealed, rehydrated, and then cut into suitable pieces for later measurements. For electrochemical measurements in the PDMS measuring platform, the final PAA gels were punctured with the gold pin after processing rather than formed directly around the pin. This difference is important because it meant that the electrode/hydrogel contact was less controlled than for the DBSA and PEGPACHI formulations, which could gel directly around the working electrode.

This handling limitation later affected the interpretation of the electrochemical measurements obtained from the PDMS measuring platform. The PAA formulation was therefore also measured using the Swagelok-based setup, which provided a more controlled bulk-contact geometry. The influence of these measurement configurations on the electrochemical response is discussed in Chapter 5.

4.3.7 Final selected PEDOT:PSS-PAA formulation

The final PEDOT:PSS-PAA formulation used in this thesis was based on the literature formulation adapted from Liu et al. and implemented through the approved EKL cleanroom flowchart. The selected procedure used freeze-dried PEDOT:PSS, acrylic acid, MBAA, water, DMSO, H_2O_2, ascorbic acid, EMIM-ES treatment, thermal annealing, and rehydration. The main optimisation was not a change in the chemical composition, but the development of a practical workflow that allowed the viscous precursor to be mixed more uniformly, divided into smaller volumes before initiation, and processed into stable hydrogel samples.

The final PEDOT:PSS-PAA hydrogels were more difficult to fabricate than the PEDOT:PSS-DBSA hydrogels, but they provided an important comparison point because they represented a different hydrogel formation mechanism. The samples were carried forward for physical, electrochemical, mechanical, and biological characterisation. However, the limitations related to moulding and electrode integration were considered during interpretation of the later electrochemical results.

4.4 PEDOT:PSS-PEGPACHI hydrogel formation

4.4.1 Rationale for developing the PEDOT:PSS-PEGPACHI formulation

The PEDOT:PSS-PEGPACHI hydrogel was developed and optimised in this thesis as a new PEDOT:PSS-based hydrogel formulation. Unlike the PEDOT:PSS-DBSA and PEDOT:PSS-PAA hydrogels, which were adapted from previously reported protocols, the PEGPACHI formulation was developed through experimental material selection, formulation screening, and process optimisation. The name PEGPACHI refers to the main additional components used in the formulation: PEG from PEGDE, PA from phytic acid, and CHI from chitosan.

The motivation for developing this formulation came from the limitations of the PEDOT:PSS-DBSA hydrogel. The DBSA formulation was useful because it could form a hydrogel using a relatively simple mixing procedure, could be moulded directly, and could be integrated into the PDMS measuring platform. However, DBSA is an acidic surfactant, and the biological screening performed in this thesis showed poor cell compatibility under the tested conditions. Therefore, the aim was to develop a DBSA-free formulation that retained some of the practical advantages of DBSA gelation, while using components expected to be more suitable for biological testing.

The starting point for the PEGPACHI design was the DBSA mechanism. In the DBSA system, an acidic surfactant modifies the PEDOT:PSS dispersion, weakens PEDOT-PSS interactions, promotes PEDOT-rich domain interactions, and leads to physical gel formation. Therefore, the first question was whether a more biologically suitable acidic additive could partly reproduce this function. Phytic acid was selected because it is acidic, multivalent, phosphate-rich, commercially accessible, and has been used in conductive and biopolymer hydrogel systems. Sodium methyl lauroyl taurate was also considered as a possible surfactant-related alternative, but it was not selected because it was less established for this specific purpose and was more difficult to acquire.

To the best of the author's knowledge at the time of writing, the exact combination of PEDOT:PSS, phytic acid, chitosan, and PEGDE has not been previously reported as a hydrogel formulation for neural-interface applications. A targeted literature search identified related systems, including phytic-acid-induced PEDOT:PSS/PEDOT hydrogels, PEGDE-stabilised PEDOT:PSS interfaces, phytic-acid/chitosan hydrogels, and other PEDOT:PSS-based neural hydrogel systems, but not this specific PEGPACHI formulation [38], [39], [40], [41].

A detailed experimental log of the formulation-development process, including phytic acid only trials, chitosan/phytic acid mixing attempts, PA-chitosan concentration screening, $CaSO_4$ trials, low-DBSA tests, PEGDE optimisation, and additional photographs, is provided in Appendix E.

4.4.2 Design logic and proposed role of each component

The PEGPACHI formulation was designed so that each component had a specific function in the final material. PEDOT:PSS was used as the conductive phase. As in the other formulations investigated in this thesis, PEDOT:PSS provided the mixed ionic/electronic conducting component and the main electronically active material.

Phytic acid was selected as the first DBSA alternative because it is acidic, multivalent, and phosphate-rich. Phytic acid contains multiple phosphate groups, which can participate in electrostatic interactions, hydrogen bonding, and coordination-type interactions. In hydrogel systems, phytic acid has been reported to form non-covalent networks with chitosan through electrostatic interactions and hydrogen bonding. It has also been used in conductive hydrogel literature as a multivalent dopant or crosslinking component, particularly in systems involving conducting polymers [42], [43].

In the context of PEDOT:PSS, phytic acid was expected to play a role partly analogous to the acidic component of the DBSA system. The proposed function was that phytic acid could alter the ionic environment of PEDOT:PSS and promote rearrangement or phase separation of the PEDOT:PSS

dispersion. However, unlike DBSA, phytic acid does not contain a long hydrophobic surfactant tail. Therefore, it was not expected to reproduce the DBSA gelation mechanism by itself. Instead, it was used as a multivalent acidic additive that could help initiate PEDOT:PSS rearrangement and interact with an additional polymeric component.

Chitosan was selected as this polymeric component. Chitosan is a natural cationic polysaccharide that contains amine groups and is widely used in biomedical hydrogel systems because of its biocompatibility, biodegradability, and ability to form physical or chemical networks [44], [45].

In the PEGPACHI formulation, chitosan was introduced to provide a biopolymer network-forming phase. The design idea was that phytic acid could interact with both the PEDOT:PSS dispersion and the chitosan chains, while chitosan could help connect and stabilise the developing hydrogel network.

PEGDE was added as the final stabilising component. PEGDE contains two epoxy groups and has been reported as a crosslinking/stabilising additive for PEDOT:PSS interfaces. In previous PEDOT:PSS work, PEGDE was proposed to interact through epoxy-ring chemistry with sulfonic groups of excess PSS chains, improving aqueous stability and maintaining conductive behaviour [41], [46]. In this thesis, PEGDE was added after the phytic-acid/chitosan route produced gel-like materials that were not stable enough for reliable handling. The role of PEGDE was therefore to improve the integrity of the hydrogel and help stabilise the PEDOT:PSS-phytic acid-chitosan network.

The proposed mechanism of PEGPACHI gelation is therefore a combined physical and chemical stabilisation process. The proposed formation mechanism of the PEDOT:PSS-PEGPACHI hydrogel is illustrated schematically in Figure 4.4.

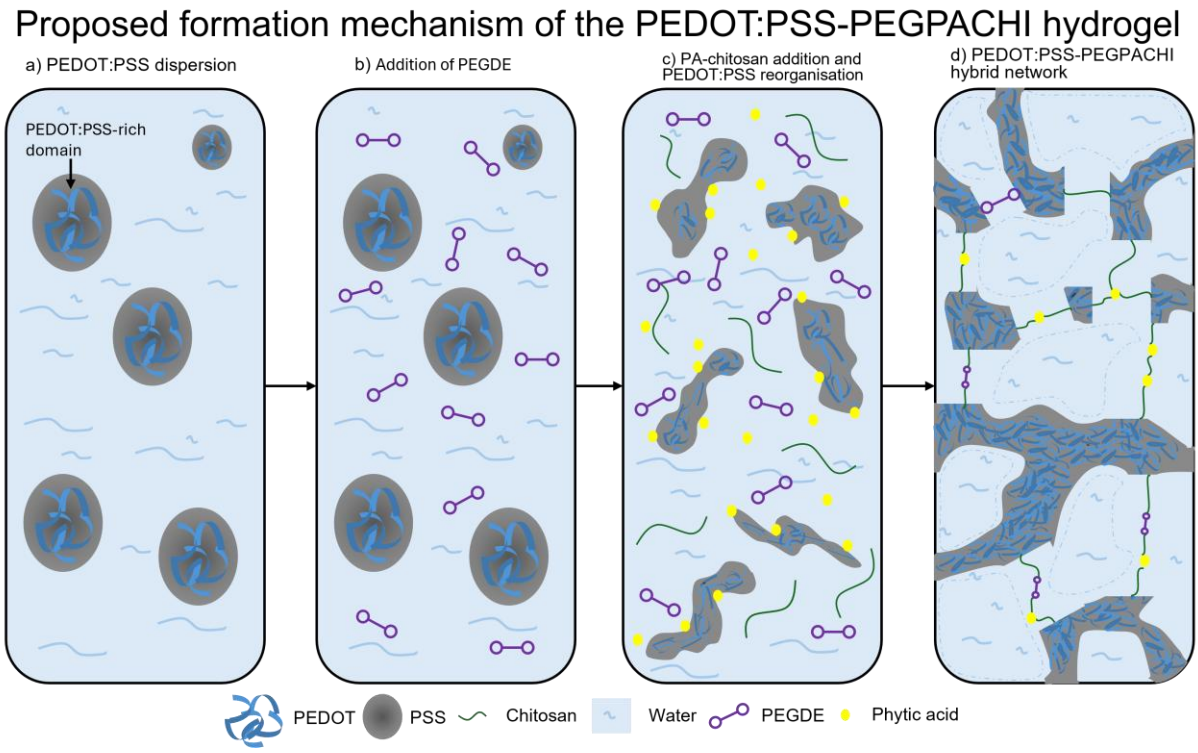


Figure 4.4: Proposed formation mechanism of the PEDOT:PSS-PEGPACHI hydrogel.
(a) PEDOT:PSS is initially present as dispersed PEDOT:PSS-rich domains in water.
(b) After PEGDE addition, no clear gelation or major structural reorganisation is expected, resulting in a PEDOT:PSS-PEGDE precursor.
(c) Upon addition of the phytic acid-chitosan stock, the ionic environment of the dispersion changes and PEDOT:PSS-rich domains are proposed to reorganise and associate. At the same time, phytic acid

and chitosan can form ionic and hydrogen-bonding interactions, while PEGDE can contribute to stabilisation of the chitosan-containing network.
(d) After heating, a hydrated PEDOT:PSS-PEGPACHI hybrid network is proposed to form, consisting of PEDOT:PSS-rich conductive regions embedded within a PA-chitosan-PEGDE-supported hydrogel matrix. The schematic represents a proposed interpretation of the gelation process rather than a directly verified molecular mechanism.

Phytic acid is expected to influence PEDOT:PSS phase organisation and interact with chitosan through multivalent ionic and hydrogen-bonding interactions. Chitosan contributes a biopolymer network that can help connect the material into a bulk hydrogel. PEGDE provides additional stabilisation, most likely by crosslinking or interacting with the chitosan-containing polymeric network rather than acting as the main gelation trigger by itself. Heating and improved mixing were then used to promote homogeneous network formation. Since this exact formulation has not been reported before, this mechanism should be considered a proposed explanation based on the known roles of the individual components and the experimental behaviour observed during formulation development.

4.4.3 Initial replacement strategy-from DBSA to phytic acid

The first stage of PEGPACHI development focused on replacing DBSA with a more biologically suitable acidic additive. Based on the DBSA mechanism, two main types of alternatives were considered: acidic surfactant-like molecules and multivalent acidic molecules. Sodium methyl lauroyl taurate was considered as a possible surfactant-related alternative, but it was not selected because it was less established for this specific PEDOT:PSS hydrogel purpose and was more difficult to acquire. Phytic acid was therefore selected as the main candidate because it was accessible and had chemical features that could plausibly influence PEDOT:PSS organisation.
Initial experiments investigated whether phytic acid alone could induce PEDOT:PSS gelation. Phytic acid volumes of 25, 50, 75, and 100 µL were added to 1 mL PEDOT:PSS using a procedure similar to the DBSA protocol. Slight gelation was observed at 75 and 100 µL phytic acid, while lower phytic acid volumes did not produce clear gel formation. Further trials using 125-200 µL phytic acid in 1 mL PEDOT:PSS with sonication at 55 °C also showed only slight gelation, and excess phytic acid remained visible.
These results suggested that phytic acid could influence PEDOT:PSS behaviour, but phytic acid alone was not sufficient to produce a homogeneous and stable bulk hydrogel. At intermediate concentrations, the material showed some sol-gel like behaviour. At higher concentrations, stronger local gelation and microgel-like domains were observed, but this was not considered suitable because it produced non-uniform samples rather than a reproducible hydrogel. This supported the idea that phytic acid could contribute to PEDOT:PSS rearrangement, but that an additional network-forming component was required.

4.4.4 Chitosan addition and the need for a PA-chitosan stock solution

Chitosan was then introduced to provide a biopolymer network-forming component. The aim was to combine the multivalent acidic character of phytic acid with the cationic polymeric structure of chitosan. In principle, this combination was expected to form a more connected network than phytic acid alone, because phytic acid can interact with chitosan through multiple non-covalent interactions, including electrostatic interactions and hydrogen bonding. Similar interaction principles have been reported for phytic-acid/chitosan hydrogel systems [43].
However, the first chitosan trials were not reproducible. Chitosan did not dissolve in phytic acid at room temperature after high-speed vortexing, and later attempts using hot-plate magnetic stirring, sonication at 55 °C, vortexing, and combined sonication/vortexing did not fully dissolve the chitosan. Visible chitosan particles remained in several mixtures. This was a major practical limitation because adding

non-homogeneous chitosan directly into PEDOT:PSS produced local clumps and made the final gelation behaviour difficult to reproduce.

To solve this, the formulation strategy was changed. Instead of adding chitosan directly into PEDOT:PSS, chitosan was first dispersed in a phytic-acid/water mixture to create a PA-chitosan stock solution. Several premixes were tested, including phytic acid/water/chitosan mixtures with different phytic acid and chitosan contents. One early premix contained 625 µL phytic acid, 375 µL DI water, and 5 mg chitosan, and other premixes varied the amount of phytic acid, water, and chitosan. These mixtures were stirred overnight at 55 °C, although some visible chitosan particles remained.

The key improvement was the development of a more reproducible PA-chitosan stock solution. The final stock used for the selected PEGPACHI formulation consisted of 2 mL phytic acid, 2 mL DI water, and 180 mg chitosan, stirred overnight at 65 °C. This step was important because it made the chitosan-containing component easier to handle and more reproducible before addition to PEDOT:PSS. The PA-chitosan stock therefore became one of the central features of the final PEGPACHI protocol.

4.4.5 Optimisation of phytic acid and chitosan concentration

A concentration-screening experiment was performed to better understand the role of phytic acid and PA-chitosan concentration in gel formation. Different phytic acid concentrations were prepared, including 0.1, 1, 2, 5, 10, and 25 wt% solutions. For the 0.1-5 wt% phytic acid solutions, volumes from 20 to 400 µL were tested in 200 µL PEDOT:PSS. For the 10 and 25 wt% solutions, additions from 20 to 50 µL were tested in 5 µL increments.

These experiments showed that gel formation was strongly dependent on both the phytic acid concentration and the amount added to PEDOT:PSS. Low concentration phytic acid solutions did not provide enough interaction to produce stable gelation. At higher phytic acid content, gel-like behaviour became more evident, but the material could also become locally gelled or non-uniform. Therefore, the concentration-screening experiments showed that phytic acid could not simply be increased indefinitely. A balance was needed between promoting gelation and maintaining a homogeneous bulk material.

The PA-chitosan formulation gave better results than phytic acid alone. In the concentration-screening experiment, gel formation was observed when 20-30 µL of a 25 wt% PA/chitosan formulation was added to 200 µL PEDOT:PSS. After addition, the samples were pipetted/mixed and heated for approximately 1 h, and some gel formation was observed in this volume range. This result supported the idea that chitosan contributed to network formation and that the PA-chitosan approach was more promising than phytic acid alone.

Further chitosan concentration tests were then performed to determine whether the amount of chitosan in the PA-chitosan stock influenced the final gel behaviour. Tested stock compositions included 1.5 mL phytic acid (25% wt), 1.5 mL DI water, and chitosan amounts corresponding to different final chitosan contents, including 13.5, 27, 67.5, and 135 mg. These trials helped guide the final stock formulation. The final stock of 2 mL phytic acid, 2 mL DI water, and 180 mg chitosan was selected because it produced a reproducible stock solution and, when added to PEDOT:PSS, gave stable macroscopic gel formation.

4.4.6 Tests with $CaSO_4$ and low DBSA addition

Additional trials were performed to test whether gelation could be improved by adding other components. $CaSO_4$ was tested because Ca^{2+} ions could, in principle, bridge negatively charged groups and help connect local gel domains into a more continuous hydrogel network. Several $CaSO_4$-containing samples were prepared using PEDOT:PSS, phytic acid, DI water, and/or PA-chitosan solution. Some samples were stored in the fridge, while others were kept at 55 °C to compare the effect of temperature. However, no gel formation was observed in the $CaSO_4$-containing trials.

A low-DBSA rescue test was also performed. In this trial, a small amount of DBSA was added to a PEDOT:PSS/phytic acid system to test whether DBSA could assist gelation after phytic acid addition. A sample containing 1 mL PEDOT:PSS, 100 µL phytic acid, and 10 µL DBSA showed mostly gelation. This confirmed that DBSA could still promote gelation, but it was not selected for the final PEGPACHI formulation because the purpose of this development route was to avoid DBSA and produce a formulation based only on PEDOT:PSS, phytic acid, chitosan, and PEGDE.

These trials were useful because they clarified the design direction. $CaSO_4$ did not improve gelation under the tested conditions, and DBSA-assisted gelation would have returned the formulation to a DBSA-containing system. Therefore, the optimisation continued with the PA-chitosan route and later PEGDE addition.

4.4.7 Addition of PEGDE and stabilisation of the final formulation

Although the PA-chitosan system improved gel formation compared with phytic acid alone, the early gels were not sufficiently stable or reproducible for later handling and testing. PEGDE was therefore added as a stabilising component. The choice of PEGDE was based on its known use as a PEDOT:PSS crosslinking/stabilising additive and on its potential to improve aqueous stability without the same limitations as DBSA. Previous work on PEDOT:PSS interfaces reported PEGDE as an effective crosslinker and conductive filler, with a proposed interaction between the epoxy groups of PEGDE and sulfonic groups of excess PSS chains [41].

Both 0.5% and 1% PEGDE were tested during optimisation. The selection was based on macroscopic observations, including gel formation, shape retention, manual handling, and apparent strength. The 1% PEGDE condition gave the best overall behaviour and was therefore selected for the final PEGPACHI formulation. Since these observations were based on macroscopic handling rather than mechanical testing, the conclusion at this stage was limited to practical process optimisation.

The final selected PEGPACHI formulation used 1 mL PEDOT:PSS, 10 µL PEGDE, and 63 µL PA-chitosan stock solution. After PEGDE addition, the PEDOT:PSS mixture was vortexed before the PA-chitosan stock was introduced. The PA-chitosan stock was added using a Luer-lock syringe mixing approach to improve homogeneity. This step was important because direct mixing could lead to non-uniform distribution of phytic acid and chitosan, resulting in local gelation or clumped regions. By repeatedly passing the formulation between connected syringes, the PA-chitosan component could be distributed more evenly throughout the PEDOT:PSS-PEGDE precursor.

After mixing, the precursor was cast into the selected mould and heated at 75 °C for approximately 1 h. Heating was included to promote gel formation and stabilisation of the network. The final hydrogels were black, macroscopically uniform, and brittle but stable enough to be removed from the mould. Compared with the earlier PA-only and PA-chitosan trials, the PEGDE-containing formulation showed improved shape retention and handling.

4.4.8 Final PEGPACHI hydrogel behaviour and selection for characterisation

The final PEDOT:PSS-PEGPACHI hydrogel was selected because it combined several practical advantages. It could be prepared from only four main components: PEDOT:PSS, PEGDE, phytic acid, and chitosan. It could be moulded into defined shapes, removed from the mould, and stored in 1x DPBS without immediate loss of structure. It was also compatible with the sterile washing and medium-conditioning procedure described in Section 3.3.3. Before PEGDE addition and stock-solution optimisation, earlier gels were less stable in DPBS and culture medium, whereas the final formulation remained macroscopically stable after washing and conditioning.

The final PEGPACHI formulation could also be cast directly inside the PDMS measuring platform. This was an important practical advantage compared with the PEDOT:PSS-PAA hydrogel, which required post-treatment and could not be reliably formed and processed entirely inside the platform. For PEGPACHI, the hydrogel precursor could be mixed, cast around the gold pogo pin, and gelled in place.

This allowed better integration into the measurement platform and supported later electrochemical testing.

Overall, the PEGPACHI formulation represented the main material-development outcome of this thesis. The optimisation process showed that none of the individual components alone reproduced the final hydrogel behaviour. Phytic acid could induce local or weak sol-gel like behaviour, chitosan introduced a possible biopolymer network but required a reproducible PA-chitosan stock, and PEGDE improved the final stability of the material. The selected formulation was therefore carried forward for physical, electrochemical, mechanical, biological, and hydrogel-array integration experiments.

The selected formulation was obtained after several preliminary formulation and processing trials. These additional experiments are summarised in **Appendix E** to document the optimisation pathway that led to the final PEDOT:PSS-PEGPACHI hydrogel.

4.5 Comparison of gel formation between formulations

The three PEDOT:PSS-based hydrogel formulations showed different formation behaviours, although two of them followed the same general gelation route. Both PEDOT:PSS-DBSA and PEDOT:PSS-PEGPACHI were based on additive-induced direct gelation of PEDOT:PSS, where additives were used to promote rearrangement of the PEDOT:PSS dispersion and formation of a hydrogel network. However, the DBSA system relied on a single acidic surfactant additive, while the PEGPACHI formulation used a multicomponent system based on phytic acid, chitosan, and PEGDE. In contrast, the PEDOT:PSS-PAA hydrogel followed a different route, where PEDOT:PSS was incorporated into a redox-polymerised poly(acrylic acid) network followed by post-treatment, annealing, and rehydration.

The DBSA formulation was the simplest and fastest system to prepare. Once the mixing sequence was optimised, the hydrogel could be formed at room temperature within approximately 30 min, although the exact gelation time depended on the room temperature. The DBSA hydrogel could be cast directly into moulds and into the PDMS measuring platform, which made it useful as an initial reference system. However, the formulation remained mechanically fragile and contained an acidic surfactant, which later became important when considering biological compatibility.

The PAA formulation was the most complex to fabricate. Unlike DBSA, it required freeze-drying of PEDOT:PSS, grinding and mixing of the dry material with acrylic acid, MBAA, water, and DMSO, redox initiation using H_2O_2 and ascorbic acid, EMIM-ES treatment, solvent exchange, annealing, and rehydration. This route produced more stable and resilient gels after post-processing, but it was less compatible with direct moulding inside the PDMS measuring platform. Since the gel had to be removed for ionic-liquid treatment and annealing, handling and electrode integration were more difficult than for the directly gelled formulations.

The PEGPACHI formulation was developed to combine some of the practical advantages of the DBSA route with a DBSA-free material composition. The final formulation could be prepared from PEDOT:PSS, PEGDE, phytic acid, and chitosan, and could be cast into moulds before heating. Compared with the early phytic acid only and PA chitosan trials, the final PEGDE-containing formulation showed improved macroscopic stability, shape retention, and handling. It was also compatible with direct casting into the PDMS measuring platform, similarly to the DBSA formulation.

Overall, the three formulations represented different balances between preparation simplicity, material stability, and integration potential. The DBSA hydrogel was the easiest to prepare and was useful as a benchmark, but it was fragile and biologically limited. The PAA hydrogel represented a more advanced literature-based polymer-network route, but its processing requirements made it more difficult to integrate into the measurement platform. The PEGPACHI hydrogel required the most formulation

development, but the final optimised version offered a practical DBSA-free route that could be moulded, handled, stored in aqueous medium, and integrated into the PDMS measuring platform.
A qualitative comparison of the main formation and handling characteristics of the three hydrogel systems is summarised in Table 4.1.

Table 4.1: Comparison of the final PEDOT:PSS-based hydrogel formulations selected for further characterisation.

Hydrogel formulation	Main gelation strategy	Preparation complexity	Gelation / processing behaviour	Handling and stability	Direct integration into PDMS measuring platform
PEDOT:PSS-DBSA	Additive-induced physical gelation	Low	Room-temperature gelation after optimised sonication-vortexing-sonication sequence. Gelation typically around 30 min	Stable in DPBS but mechanically fragile	Yes, precursor could be cast directly around the pogo pin
PEDOT:PSS-PAA	Redox-initiated PAA network formation with PEDOT:PSS	High	Rapid gelation after H_2O_2/ascorbic acid addition, required EMIM-ES treatment, annealing, and rehydration	More resilient after annealing and rehydration, but difficult to process and handle during intermediate steps	Limited, final gel had to be post-processed before contact with the pogo pin
PEDOT:PSS-PEGPACHI	Additive-induced direct gelation using a multicomponent PA-chitosan-PEGDE system	Medium/low	Required PA-chitosan stock, PEGDE addition, Luer-lock mixing, and heating at 75 °C	Black, uniform, brittle but stable, stable in DPBS and after culture-medium conditioning	Yes, precursor could be cast directly around the pogo pin

4.6 Selection of formulations for further characterisation

Based on the development and optimisation work described in this chapter, one final formulation from each hydrogel route was selected for further characterisation. The selected formulations were PEDOT:PSS-DBSA, PEDOT:PSS-PAA, and PEDOT:PSS-PEGPACHI. These three systems were

carried forward because they represented different material-design strategies and provided a useful comparison between a literature-based additive-induced hydrogel, a literature-based polymer-network hydrogel, and a thesis-developed formulation.

The final PEDOT:PSS-DBSA hydrogel was selected as the reference formulation. It was the simplest system to prepare and could form a hydrogel at room temperature using an optimised sonication-vortexing-sonication mixing sequence. The 4% v/v DBSA formulation was selected because it provided the best balance between gelation time, reproducibility, and handling compared with the other DBSA concentrations tested. Although the gel was mechanically fragile, it was stable in DPBS and could be cast directly into moulds and into the PDMS measuring platform.

The final PEDOT:PSS-PAA hydrogel was selected as the polymer-network-based comparison formulation. This system was more complex to fabricate, but it represented a fundamentally different hydrogel formation route compared with DBSA and PEGPACHI. The PAA hydrogel required freeze-dried PEDOT:PSS, redox-initiated polymerisation, EMIM-ES treatment, annealing, and rehydration. Although this made the formulation more difficult to process and less compatible with direct integration into the PDMS measuring platform, it provided an important comparison point for understanding how a secondary polymer network affects the final hydrogel behaviour.

The final PEDOT:PSS-PEGPACHI hydrogel was selected as the main thesis-developed formulation. This formulation was chosen because it achieved stable macroscopic gel formation using a DBSA-free additive system based on PEGDE, phytic acid, and chitosan. The final PEGPACHI hydrogel could be moulded, handled, stored in DPBS, conditioned in cell culture medium, and cast directly into the PDMS measuring platform. Compared with the early phytic acid only and PA-chitosan trials, the final PEGDE-containing formulation showed improved shape retention and practical stability.

Together, these three selected formulations allowed the following chapters to compare the materials from different perspectives. Chapter 5 evaluates their physical, electrochemical, and mechanical properties. Chapter 6 assesses their biological compatibility under cell culture conditions. Chapter 7 then examines the preliminary integration of PEGPACHI hydrogel into a PDMS hydrogel-array device as a proof-of-concept platform.

Overall, Chapter 4 showed that the final hydrogel formulations were not selected only because they formed gels, but because they provided different and complementary material behaviours. PEDOT:PSS-DBSA served as the simple literature-based reference, PEDOT:PSS-PAA served as the more complex polymer-network comparison, and PEDOT:PSS-PEGPACHI served as the thesis-developed formulation designed to retain direct gelation and mouldability while avoiding DBSA.

5 Physical, Electrochemical, and Mechanical Characterisation of PEDOT:PSS-Based Hydrogels

5.1 Overview of characterisation strategy

After the development and optimisation of the three PEDOT:PSS-based hydrogel formulations described in Chapter 4, the selected hydrogels were characterised to compare their physical, electrochemical, and mechanical behaviour. The formulations evaluated in this chapter were PEDOT:PSS-DBSA, PEDOT:PSS-PAA, and PEDOT:PSS-PEGPACHI.

The characterisation strategy was designed to assess the hydrogels at the material level. First, the hydrogels were compared based on their macroscopic appearance, handling behaviour, stability in aqueous media, and suitability for moulding. These observations were important because the hydrogels had to remain stable and handleable during storage, washing, electrochemical testing, mechanical testing, and later biological experiments.

Second, the electrochemical behaviour of the hydrogels was evaluated using cyclic voltammetry and electrochemical impedance spectroscopy. These measurements were performed for all three hydrogel formulations using two measurement configurations. The first configuration was the custom PDMS measuring platform, where each hydrogel was contacted through a gold pogo pin in a three-electrode setup. The second configuration was the Swagelok-based bulk measurement setup, where the hydrogel was positioned between two electrode plates and measured in a controlled bulk-contact geometry. The use of both configurations allowed the electrochemical response of the hydrogels to be evaluated under different contact and measurement conditions.

Finally, the mechanical properties of the hydrogels were evaluated using nanoindentation. The effective Young's modulus was obtained for all three formulations to compare their stiffness and assess whether the materials were within a soft mechanical range relevant for bioelectronic neural-interface applications.

Overall, this chapter provides a comparative material characterisation of the three hydrogel formulations before evaluating their biological compatibility in Chapter 6 and their integration into a preliminary PDMS hydrogel-array device in Chapter 7.

5.2 Physical and macroscopic hydrogel characterisation

After the development of the three PEDOT:PSS-based hydrogel formulations, their physical and macroscopic behaviour was evaluated before electrochemical and mechanical characterisation. This step was important because the hydrogels had to remain stable, hydrated, and handleable during transfer, storage, washing, and measurement. The three final formulations showed clear differences in appearance, mouldability, handling behaviour, and stability in aqueous media.



Figure 5.1: Macroscopic appearance of the final PEDOT:PSS-based hydrogel formulations. Representative bulk samples of (a) PEDOT:PSS-DBSA, (b) PEDOT:PSS-PEGPACHI, and (c) PEDOT:PSS-PAA hydrogels after gel formation and removal from the mould. The images show differences in shape retention, surface texture, and overall structural integrity between the three formulations.

5.2.1 Macroscopic appearance and gel integrity

The PEDOT:PSS-DBSA hydrogel formed a black and mostly uniform gel after optimisation of the preparation protocol. The final mixing procedure prevented the formation of large bubbles, which had been observed during earlier optimisation trials. The surface of the final DBSA hydrogel appeared smooth and glossy. However, compared with the other two formulations, the DBSA hydrogel showed poorer mouldability and less structural robustness. Although it could be removed from the mould relatively easily, it was the most fragile formulation and could deform or break during handling.

The PEDOT:PSS-PAA hydrogel also appeared black and relatively uniform after preparation. Before the final post-processing steps, the material was soft and mechanically weak. After ionic-liquid treatment, thermal annealing, and rehydration, the hydrogel became more stable and easier to handle. The surface became rougher and more porous after processing, which distinguished it clearly from the smoother DBSA hydrogel. Despite this rougher surface, the PAA formulation showed the best overall shape retention and appeared to be the most robust bulk hydrogel.

The PEDOT:PSS-PEGPACHI hydrogel formed a black, homogeneous, glossy, block-like gel after heating. Its surface was smoother than the PAA hydrogel but less smooth than the DBSA hydrogel. The material retained its overall moulded shape well, although some fragmentation could occur during handling or storage. Overall, the PEGPACHI hydrogel was brittle but stable when kept hydrated, making it easier to handle than DBSA but less robust than PAA.

5.2.2 Handling and mouldability

The three formulations showed different handling behaviour. PEDOT:PSS-DBSA was the easiest hydrogel to prepare, because gelation occurred directly after addition of DBSA and the material could be cast into moulds without further post-processing. However, it was also the most difficult to handle after gelation. The surfactant-based formulation made the hydrogel slippery, and it could easily slide away from tweezers during transfer. This made the DBSA hydrogel challenging to manipulate without damaging it.

PEDOT:PSS-PAA was the most difficult formulation to fabricate because it required several processing steps, including freeze-drying of PEDOT:PSS, redox polymerisation, ionic-liquid treatment, annealing, and rehydration. However, after completion of these steps, it was the easiest formulation to handle. The final hydrogel was more robust, bouncy, and stretchable compared with the other two formulations. This made it more suitable for transfer between containers and for bulk measurements where the sample had to be positioned manually.

PEDOT:PSS-PEGPACHI showed intermediate handling behaviour. It was more complex to prepare than DBSA because it required preparation of the phytic acid-chitosan stock, addition of PEGDE, syringe mixing, and heating. However, it was still easier and faster to prepare than PAA. After gelation, it could generally be removed from the mould and handled, but the material remained brittle and could fragment if excessive force was applied.

5.2.3 Stability in aqueous media

All three hydrogel formulations were stored and handled in hydrated conditions. PEDOT:PSS-DBSA was stable in 1x DPBS from the start and could remain intact for several weeks. Some swelling was observed after immersion, but this was not severe under normal hydrated storage conditions. When DBSA hydrogels were left dry in the fridge, they dehydrated and shrank. However, after DPBS was added again, the gels were able to rehydrate and partially recover their original size, while still remaining electrically active.

PEDOT:PSS-PAA was also stable in 1x DPBS after completion of the post-processing and rehydration steps. During rehydration, minor swelling was observed and the shape of the gel changed slightly. Some ionic liquid also appeared to leach out during hydration. Despite these changes, the hydrogel remained intact and showed the best overall stability among the three formulations.

PEDOT:PSS-PEGPACHI was stable when stored in 1x DPBS and in cell culture medium after sufficient washing. Minor swelling was observed, together with some fragmentation. During medium conditioning, repeated washing was required until the medium colour remained stable. After this conditioning process, no clear macroscopic degradation was observed, although fragmentation remained the main limitation of this formulation.

5.2.4 Qualitative comparison of the three hydrogel formulations

Overall, each formulation showed different advantages and limitations. PEDOT:PSS-DBSA was the simplest and fastest hydrogel to prepare, but it was also the most fragile and the most difficult to handle. PEDOT:PSS-PAA was the most complex formulation to fabricate, but after post-processing it showed the best robustness, handling behaviour, and shape retention. PEDOT:PSS-PEGPACHI provided an intermediate behaviour: it was more stable and handleable than DBSA, easier to fabricate than PAA, but still more brittle and prone to fragmentation than the PAA hydrogel.

Table 5.1: Qualitative comparison of the final PEDOT:PSS-based hydrogel formulations.

Property	Best / highest	Intermediate	Lowest / weakest
Ease of preparation	PEDOT:PSS-DBSA	PEDOT:PSS-PEGPACHI	PEDOT:PSS-PAA
Ease of handling	PEDOT:PSS-PAA	PEDOT:PSS-PEGPACHI	PEDOT:PSS-DBSA
Fragility	PEDOT:PSS-DBSA	PEDOT:PSS-PEGPACHI	PEDOT:PSS-PAA
Stability in DPBS	PEDOT:PSS-PAA	PEDOT:PSS-DBSA	PEDOT:PSS-PEGPACHI
Shape retention	PEDOT:PSS-PAA	PEDOT:PSS-PEGPACHI	PEDOT:PSS-DBSA

These physical observations were important for interpreting the later characterisation results. In particular, differences in fragility, mouldability, and hydration behaviour affected how each hydrogel could be integrated into the electrochemical measurement setups. The DBSA and PEGPACHI hydrogels were more suitable for direct casting into the PDMS measuring platform, while the PAA hydrogel was better suited for bulk measurement in the Swagelok-based setup after post-processing and rehydration.

5.3 Development and implementation of electrochemical measurement configurations

5.3.1 Rationale for using two electrochemical measurement configurations

Electrochemical characterisation of soft conductive hydrogels is strongly influenced by the measurement configuration. Unlike rigid thin films or metal electrodes, hydrogels are soft, hydrated, deformable, and difficult to contact in a fully reproducible way. Their measured response can be affected by gel geometry, electrolyte volume, electrode contact, hydration state, and handling during sample preparation. For this reason, a single measurement configuration was not considered sufficient to evaluate the electrochemical behaviour of the PEDOT:PSS-based hydrogel formulations.

Two electrochemical measurement configurations were therefore used in this thesis. The first configuration was the custom PDMS measuring platform, which was developed to measure hydrogels in a three-electrode setup using a gold pogo pin as the working electrode contact. In this setup, the hydrogel was positioned inside a PDMS well, the pogo pin contacted the hydrogel from the side, and the reference and counter electrodes were placed in the electrolyte above the gel. This configuration allowed the hydrogel to be measured in a hydrated open-well format while maintaining the same general electrochemical principle as the three-electrode hydrogel setup reported by Wang et al. [31].

The second configuration was the Swagelok-based bulk measurement setup. In this setup, the hydrogel was positioned between two electrode plates and measured in a controlled bulk-contact geometry. This configuration was used to evaluate the electrochemical response of the hydrogel material itself under a different contact condition. Compared with the PDMS measuring platform, the Swagelok setup provided a more confined geometry and a more direct electrode-hydrogel-electrode contact.

All three hydrogel formulations, PEDOT:PSS-DBSA, PEDOT:PSS-PAA, and PEDOT:PSS-PEGPACHI, were evaluated using both measurement configurations. Using both setups made it possible to compare how the same hydrogel formulation behaved under different electrochemical contact conditions. The PDMS measuring platform was useful for measurements involving a gold pogo pin working electrode in an open hydrated well, while the Swagelok setup was useful for bulk hydrogel measurements between electrode plates. Together, these configurations provided a broader understanding of the electrochemical behaviour of the hydrogels than either setup alone.

The development and implementation of the PDMS measuring platform are described first, followed by the Swagelok-based bulk measurement setup.

5.3.2 PDMS measuring platform development and implementation

Following this rationale, the first measurement configuration implemented in this thesis was the custom PDMS measuring platform. The starting point for this platform was the three-electrode hydrogel measurement approach used by Wang et al. [31], where the hydrogel is contacted through a gold pogo pin working electrode, while the reference and counter electrodes are positioned in the electrolyte above the hydrogel. Although this approach was suitable for measuring PEDOT:PSS-based hydrogels, the original setup involved several handling steps and was not ideal for testing multiple hydrogel samples in a fast and reproducible way. Therefore, a new platform was designed to preserve the same electrochemical principle while improving sample throughput, handling, and reproducibility.

The main design goal was to create a compact multi-well PDMS platform in which several hydrogels could be prepared or measured in parallel. Each well was designed to hold one hydrogel sample, while a gold pogo pin was inserted horizontally into the well to act as the working electrode contact. After gel formation, 1x DPBS could be added on top of the hydrogel, and the Ag/AgCl reference electrode and platinum counter electrode could be positioned directly in the electrolyte above the gel. In this way, each well functioned as an individual three-electrode measurement chamber.

The platform was designed in SolidWorks and fabricated using 3D-printed moulds. Several design iterations were explored before the final platform geometry was selected. The early versions were mainly used to explore the overall concept of a hydrogel-containing platform, while later versions were redesigned as practical moulds for PDMS casting. The uploaded CAD designs show this progression from early conceptual geometries to the final elongated multi-well mould format used for PDMS platform fabrication.

Two final platform versions were used. The first was a glass-bonded PDMS measuring platform, which was developed in the context of the collaboration with the Medical University of Graz. This version was intended to be sterilisable and compatible with hydrogel-based experiments under cell-culture conditions. The second was a full-PDMS measuring platform, which was used for the electrochemical measurements performed in this thesis. Both versions followed the same general well geometry. The platform contained 18 wells, arranged in nine rows and two columns. Each well had a diameter of approximately 5 mm and a depth of approximately 10 mm. The overall platform dimensions were approximately 110 mm in length and 12 mm in width.

A major challenge during development was bonding PDMS to glass. The glass-bonded version was originally designed so that the cured PDMS structure could be oxygen-plasma bonded to a glass slide. However, direct bonding was not reliable. This was attributed to the surface quality of the PDMS after curing against the FDM-printed mould. The 3D-printed mould produced microscopic surface features on the PDMS, which reduced the quality of the PDMS/glass contact and prevented consistent oxygen-plasma bonding. To overcome this, uncured PDMS was applied between the cured PDMS platform and the glass slide, and the assembly was then cured again. This created a sealed PDMS/glass platform without relying only on direct plasma bonding. The cleaning and oxygen-plasma treatment steps used during this development are included in **Appendix F**.

For the electrochemical measurements in this thesis, the full-PDMS platform was selected because it avoided the glass-bonding step completely. This made the platform simpler, faster to fabricate, and more reproducible for repeated hydrogel measurements. The mould was printed using an FDM 3D printer, and PDMS was prepared using a 10:1 base to curing agent ratio. The PDMS was poured into the mould and left to cure overnight at room temperature. After curing, the full-PDMS platform was removed from the mould and prepared for electrode integration.

Gold pogo pins were inserted manually into the side of selected wells. A needle was first used to puncture the PDMS wall and define the insertion path. The pogo pin was then pushed into the well before the hydrogel precursor integration. Electrical wires were attached to the pogo pins to allow connection to the potentiostat. This approach allowed each hydrogel to be contacted from the side while leaving the top of the well open for the addition of DPBS, reference electrode, and counter electrode.

The platform was used with all three hydrogel formulations. For PEDOT:PSS-DBSA and PEDOT:PSS-PEGPACHI, the precursor could be cast directly into the well and gelled around the pogo pin. This improved the contact between the hydrogel and the working electrode because the gel formed in direct contact with the pin. For PEDOT:PSS-PAA, integration was more difficult because the hydrogel required post-processing steps after gelation, including ionic-liquid treatment, annealing, and rehydration. Therefore, PAA samples could not be processed in the same simple direct-casting manner, and the contact with the pogo pin was less straightforward. This limitation is considered further in the electrochemical results.

One practical advantage of the platform was the behaviour of DPBS on the PDMS surface. Because PDMS is hydrophobic, the DPBS added above each well formed a dome-like droplet rather than spreading completely across the platform. This helped maintain a local electrolyte volume above the hydrogel and made it easier to position the reference and counter electrodes during measurements.

Each well was measured individually, while the multi-well layout allowed several hydrogel samples to be prepared on the same platform.
Overall, the PDMS measuring platform provided a compact and reusable configuration for three-electrode electrochemical characterisation of PEDOT:PSS-based hydrogels. Its main advantages were the controlled well geometry, the ability to test multiple hydrogel samples on one platform, easy addition of DPBS, and direct contact between the hydrogel and a gold pogo pin working electrode. However, the setup also had limitations. The pogo pin holes were created manually, which introduced some variability in the exact pin position. In addition, the quality of the measurement depended strongly on the hydrogel/pogo pin contact. Samples that were not cast directly around the pogo pin were more difficult to measure reliably. For this reason, a second electrochemical configuration, the Swagelok-based bulk measurement setup, was also implemented and is described in the following section.
The final full-PDMS measuring platform and its implementation for electrochemical testing are shown in Figure 5.2.

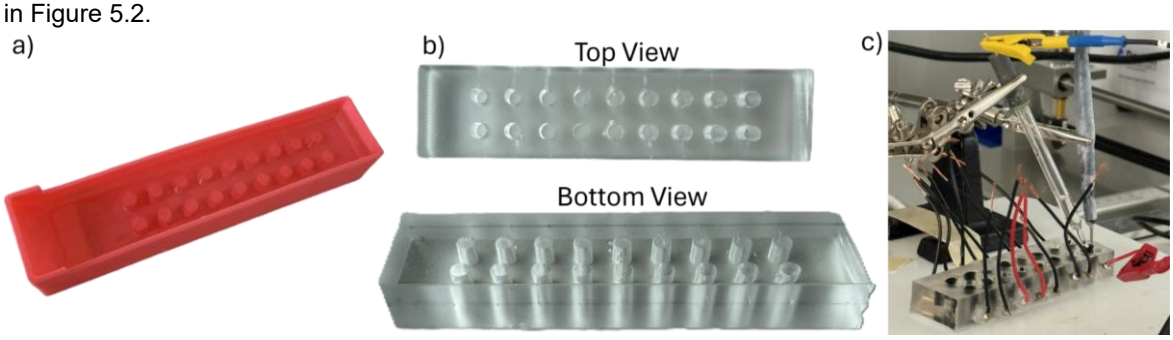


Figure 5.2: Fabrication and implementation of the full-PDMS measuring platform. (a) 3D-printed mould used for PDMS casting. (b) Top and bottom views of the demoulded full-PDMS platform, showing the 18-well layout and the well structures formed during moulding. (c) Full-PDMS measuring platform after manual pogo pin insertion, wire connection, hydrogel casting, and electrode placement for three-electrode electrochemical measurements.

5.3.3 Swagelok-based bulk measurement setup

The second electrochemical configuration used in this thesis was a Swagelok-based bulk measurement setup. This setup was introduced to provide a complementary way of measuring the hydrogels in a confined bulk-contact geometry. The design was based on the Swagelok-type hydrogel measurement approach described by Daso et al. [20], where conductive hydrogels are contacted between two electrodes to evaluate their electrochemical response under a more controlled geometry.
The main reason for implementing this setup was that not all hydrogel samples could be measured reliably in the PDMS measuring platform. The PDMS platform worked best when the hydrogel precursor could be cast directly around the gold pogo pin, as in the case of PEDOT:PSS-DBSA and PEDOT:PSS-PEGPACHI. However, when a hydrogel was formed separately and then contacted afterwards, the measurement became more dependent on the quality of the manual contact between the gel and the pogo pin. This was especially relevant for the PEDOT:PSS-PAA hydrogel, which required post-processing steps after gelation and therefore could not be prepared directly around the pogo pin in the same way. The Swagelok-based setup was therefore used to measure the bulk electrochemical response of all three hydrogels in a faster and more reproducible contact configuration.
The Swagelok-based measurements were performed using two disk electrodes placed on opposite sides of the hydrogel sample. Both gold-gold and platinum-platinum electrode configurations were tested. The disk electrodes had a 6 mm diameter PEEK body and a 3 mm gold or platinum disk. For the potentiostat connection, the working electrode was connected to one side of the hydrogel, while the reference and counter electrode leads were connected together to the opposite electrode. Therefore,

although the potentiostat was connected using the three electrode leads, the hydrogel was effectively measured in a two terminal bulk-contact configuration.

Before measurement, the hydrogel samples were soaked overnight in 1x DPBS to ensure that they were fully hydrated. The hydrated sample was then placed between the two disk electrodes inside the Swagelok cell. The cell was tightened manually until stable contact was obtained. Care was taken not to overtighten the cell, because excessive compression could deform or damage the soft hydrogel. Since the tightening was performed manually, the compression was not precisely controlled, but the same practical approach was used for all measurements by considering the approximate hydrogel dimensions and avoiding visible sample damage.

A commercial Swagelok-based cell was purchased and used for the measurements. In parallel, 3D-printed Swagelok-inspired prototypes were also designed and fabricated to better understand the internal geometry of the setup and to test whether the same measurement principle could be reproduced using a printed housing. Versions with two and three openings were designed to visualise the arrangement of the gel and electrodes inside the setup. Since the electrochemical contact was provided by the same gold or platinum disk electrodes, the 3D-printed housing produced comparable results to the purchased cell.

Overall, the Swagelok-based setup provided a useful complementary configuration to the PDMS measuring platform. The PDMS measuring platform allowed hydrogel measurements with a gold pogo pin working electrode in an open hydrated well, while the Swagelok setup allowed bulk hydrogel measurements between two disk electrodes. The Swagelok configuration was especially useful for samples that were difficult to cast directly around a pogo pin, and it provided a faster way to compare the three hydrogel formulations under similar bulk-contact conditions.

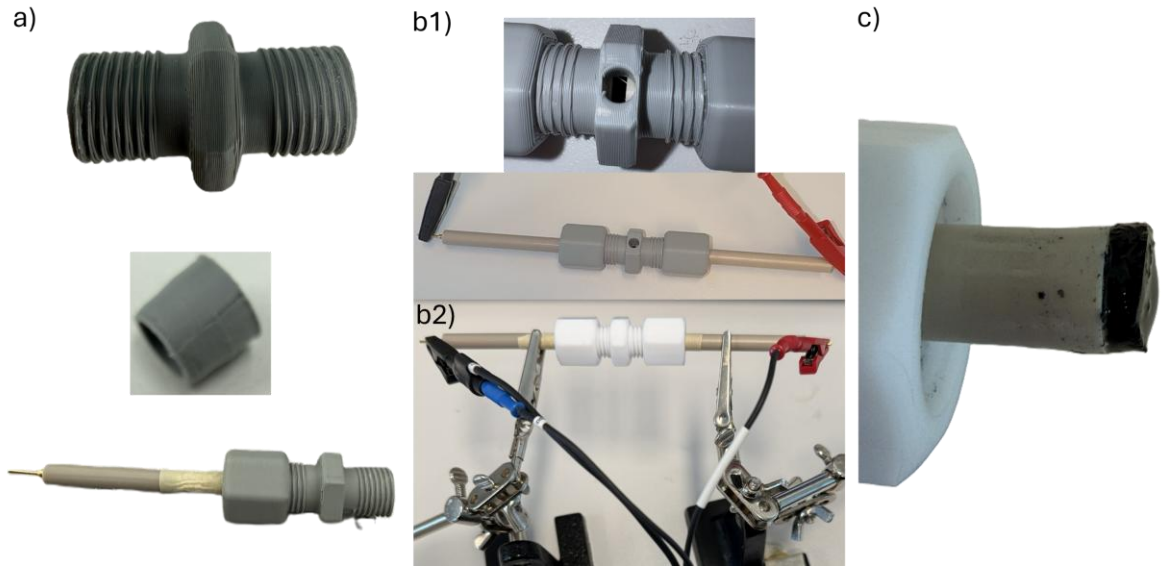


Figure 5.3: Swagelok-based bulk measurement setup for PEDOT:PSS-based hydrogels. (a) 3D-printed Swagelok-inspired prototype and electrode holder developed to reproduce the bulk-contact measurement geometry. (b1) Close-up view of the assembled 3D-printed cell showing the central hydrogel/electrode region. (b2) Swagelok-based measurement setup connected to the potentiostat using disk electrodes. (c) Hydrated hydrogel sample positioned on the disk electrode before assembly. The hydrogel was measured between two disk electrodes in a confined bulk-contact geometry. Gold-gold and platinum-platinum electrode configurations were tested, with the working electrode connected to one side and the reference and counter electrode leads connected together on the opposite side.

5.3.4 Comparison between the two electrochemical measurement configurations

The PDMS measuring platform and the Swagelok-based bulk setup were both used to characterise the electrochemical behaviour of the PEDOT:PSS-based hydrogels, but they provided different measurement conditions. The purpose of using both configurations was not to treat one setup as the only correct method, but to evaluate the hydrogels under two different contact geometries and to understand how the measurement configuration influenced the observed response.

The PDMS measuring platform allowed the hydrogels to be measured in an open well three-electrode configuration. In this setup, the hydrogel was contacted through a gold pogo pin, while the reference and counter electrodes were placed in DPBS above the gel. This configuration was particularly useful for formulations that could be cast directly around the pogo pin, such as PEDOT:PSS-DBSA and PEDOT:PSS-PEGPACHI. In these cases, the gel formed in direct contact with the working electrode, which improved integration between the hydrogel and the pogo pin.

However, the PDMS measuring platform was more sensitive to contact quality when the hydrogel was not formed directly around the pogo pin. This was especially important for PEDOT:PSS-PAA, because this formulation required post-processing steps after gelation, including ionic-liquid treatment, annealing, and rehydration. As a result, the final hydrogel had to be contacted after processing, which made the measurement more dependent on manual positioning and the quality of the contact between the hydrogel and the pogo pin.

The Swagelok-based bulk setup provided a complementary measurement configuration. In this setup, the hydrogel was placed between two disk electrodes and measured in a confined bulk-contact geometry. This made it useful for comparing the hydrogel materials themselves, especially when direct casting around a pogo pin was not practical. The Swagelok setup also allowed hydrated hydrogel samples to be measured more quickly after soaking in DPBS, while maintaining a more direct electrode-hydrogel-electrode contact.

Overall, the two setups provided complementary information. The PDMS measuring platform was useful for assessing hydrogel contact with a gold pogo pin in an open hydrated well, while the Swagelok setup was useful for bulk electrochemical comparison between hydrogel formulations. Using both configurations allowed the electrochemical behaviour of PEDOT:PSS-DBSA, PEDOT:PSS-PAA, and PEDOT:PSS-PEGPACHI to be evaluated more broadly than would have been possible using only one setup. The results obtained from these configurations are presented and compared in the following electrochemical characterisation sections.

5.4 Electrochemical characterisation in the PDMS measuring platform

Electrochemical characterisation in the PDMS measuring platform was performed using CV and EIS in 1x DPBS. In this configuration, the hydrogel was contacted through a gold pogo pin working electrode, while the Ag/AgCl reference electrode and platinum counter electrode were placed in the electrolyte above the gel. All three hydrogel formulations were evaluated in this setup. However, the measurement configuration was more suitable for hydrogels that could be cast directly around the pogo pin, such as PEDOT:PSS-DBSA and PEDOT:PSS-PEGPACHI. PEDOT:PSS-PAA required post-processing before measurement and therefore had to be contacted manually after gel formation, which made its response more dependent on the quality of the electrode/hydrogel contact. In this configuration, each hydrogel was measured in a 5 mm diameter PDMS well containing 70 µL of hydrogel, corresponding to an approximate hydrogel height of 3.6 mm.

5.4.1 PEDOT:PSS-DBSA electrochemical response

PEDOT-DBSA hydrogels were first evaluated in the PDMS measuring platform because this formulation could be cast directly around the gold pogo pin working electrode. This enabled direct contact between the hydrogel and the working electrode after gelation, reducing the need for manual positioning before measurement. The electrochemical response was evaluated using EIS and CV in 1x DPBS, as shown in Figure 5.4.

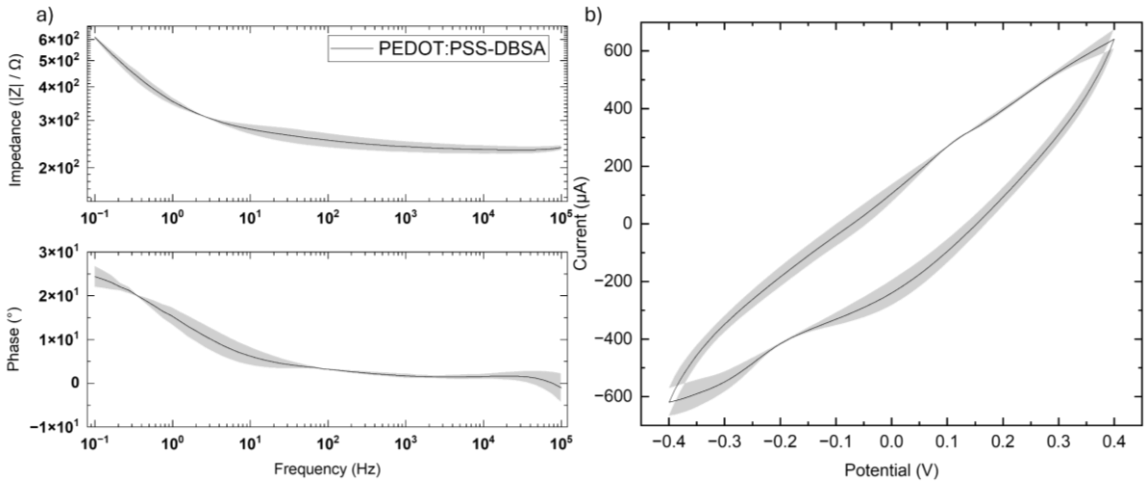


Figure 5.4: Electrochemical response of PEDOT:PSS-DBSA hydrogels measured in the PDMS measuring platform.

(a) Impedance magnitude |Z| and phase angle as a function of frequency measured by EIS in 1x DPBS. (b) Cyclic voltammetry response recorded between −0.4 and +0.4 V at 100 mV s^{-1}. The black line represents the mean response and the grey shaded area represents mean ± SD for n = 3 hydrogel samples.

Additional electrochemical experiments were also performed for PEDOT:PSS-DBSA hydrogels under different measurement conditions and sample configurations. These experiments are included in **Appendix K** to document the broader experimental evaluation of the DBSA formulation, while Figure 5.4 presents the selected averaged response used for comparison in the main text.

The EIS response showed a frequency-dependent impedance profile. The impedance magnitude was highest at low frequency and decreased with increasing frequency, reaching a lower and more stable region at higher frequencies. At 0.1 Hz, the impedance was approximately 240 Ω, while at higher frequencies the impedance decreased to approximately 230-240 Ω. Around the commonly used 1 kHz neural-electrode benchmark, the impedance was already close to the high-frequency plateau, indicating that the hydrogel/electrode contact provided a relatively low-impedance pathway under these measurement conditions.

The frequency-dependent behaviour can be interpreted in terms of the mixed ionic/electronic nature of PEDOT:PSS hydrogels. In conductive hydrogels, the low-frequency response is influenced by slower interfacial and transport processes, including electronic conduction through the conductive phase and its coupling with ionic motion in the hydrated network. In contrast, the high-frequency region is more strongly associated with faster ionic movement through the hydrated hydrogel. This interpretation is consistent with the framework discussed by Daso et al. and applied by Wang et al. for PEDOT:PSS hydrogels, where different frequency regions are used to distinguish ionic and electronic contributions to the electrochemical response [20], [31]. In the present DBSA hydrogel, the decrease in impedance

from low to high frequency therefore suggests that both hydrated ionic transport and PEDOT:PSS electronic pathways contributed to the measured response.

The phase response further supported this mixed behaviour. The phase angle was higher at low frequency, around 20-25°, and gradually approached values close to 0° at higher frequencies. This indicates that the hydrogel did not behave as a purely capacitive material. Instead, the response was dominated by a mixed resistive/capacitive behaviour, which is expected for a hydrated PEDOT:PSS hydrogel where charge transport depends on both ionic movement in the aqueous phase and electronic transport through the PEDOT-rich network.

The CV response also confirmed the electrochemical activity of the PEDOT:PSS-DBSA hydrogel. The curve showed a broad enclosed area over the −0.4 to +0.4 V potential window, with currents reaching approximately ±600 µA. This broad response indicates charge-storage behaviour within the hydrogel. However, the CV shape was tilted rather than perfectly rectangular, suggesting that the response was not purely capacitive. Instead, the hydrogel showed a mixed resistive/capacitive response, consistent with the EIS phase behaviour. The absence of sharp redox peaks also suggests that the measured current mainly originated from distributed charging and mixed ionic-electronic transport rather than a single well-defined faradaic reaction.

Overall, PEDOT:PSS-DBSA showed a stable and reproducible electrochemical response in the PDMS measuring platform. The ability to cast the hydrogel directly around the pogo pin was important for achieving consistent contact, which was reflected in the relatively narrow shaded region in both the EIS and CV measurements. These results show that the DBSA hydrogel provided a low-impedance and electrochemically active PEDOT:PSS hydrogel interface in the PDMS measuring platform.

5.4.2 PEDOT:PSS-PAA electrochemical response

The PEDOT:PSS-PAA hydrogel was also evaluated in the PDMS measuring platform using EIS and CV in 1x DPBS. However, unlike the DBSA formulation, the PAA hydrogel could not be cast directly around the gold pogo pin working electrode. This was because the PAA formulation required post-processing steps after gelation, including EMIM-ES treatment, thermal annealing, and rehydration. As a result, the final hydrogel had to be positioned and contacted manually after processing. Therefore, the electrochemical response of PEDOT:PSS-PAA in the PDMS platform was expected to be more dependent on the quality of the hydrogel/pogo pin contact.

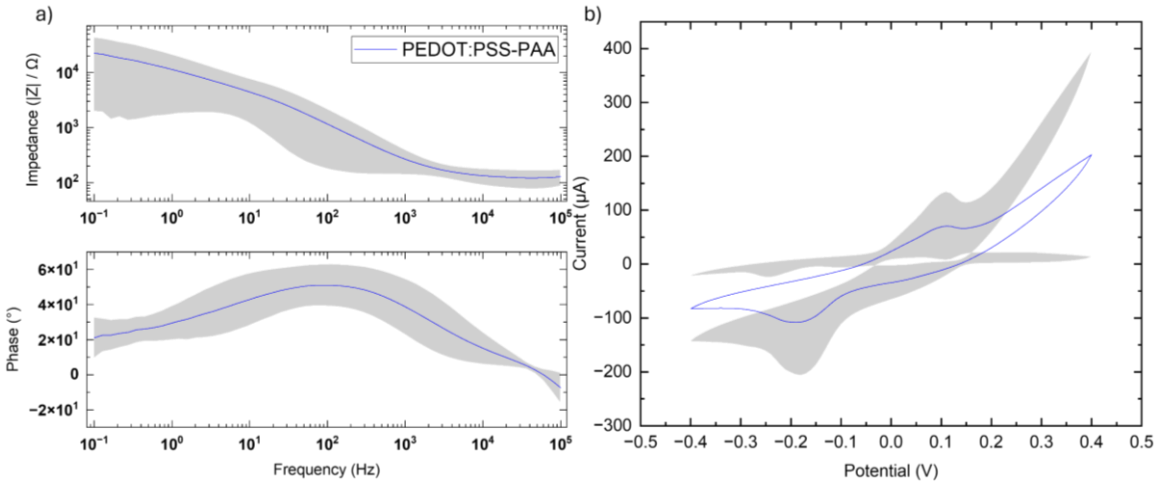


Figure 5.5: Electrochemical response of PEDOT:PSS-PAA hydrogels measured in the PDMS measuring platform.

(a) Impedance magnitude |Z| and phase angle as a function of frequency measured by EIS in 1× DPBS. (b) Cyclic voltammetry response recorded between −0.4 and +0.4 V at 100 mV s^{-1}. The black line

represents the mean response and the grey shaded area represents mean ± SD for n = 3 hydrogel samples.

Additional electrochemical experiments were also performed for PEDOT:PSS-PAA hydrogels under different measurement conditions and sample configurations. These experiments are included in **Appendix K** to document the broader experimental evaluation of the PAA formulation, while Figure 5.5 presents the selected averaged response used for comparison in the main text.

The EIS response of PEDOT:PSS-PAA showed a strong frequency dependence. The impedance magnitude was high at low frequencies and decreased substantially as the frequency increased. At low frequency, the impedance was in the range of approximately 10^4 Ω, while at high frequency it decreased towards approximately 10^2 Ω. This behaviour indicates that the PAA hydrogel provided an electrically active pathway in the PDMS measuring platform, but the large decrease in impedance across the frequency range suggests that the response was strongly influenced by frequency-dependent transport and interfacial effects.

The shaded region in the EIS plot was wider than for the DBSA hydrogel, especially in the low-frequency region. This indicates higher variability between measurements. This variability was likely related to the measurement configuration rather than only to the hydrogel material itself. Since the PAA hydrogel had to be processed separately and then contacted manually with the pogo pin, small differences in positioning, compression, hydration, and contact area could influence the measured impedance. Therefore, the PAA response in the PDMS platform should be interpreted as a contact-dependent measurement.

The phase response also differed from the DBSA hydrogel. Instead of approaching values close to 0° over most of the measured frequency range, the PAA hydrogel showed a broader phase maximum in the intermediate-frequency region. This suggests a stronger mixed resistive/capacitive contribution during the measurement. In conductive hydrogels, the frequency-dependent response can be associated with both ionic motion in the hydrated polymer network and electronic transport through the conductive PEDOT:PSS phase. As discussed by Daso et al. and Wang et al., different frequency regions can provide information about ionic and electronic contributions to charge transport in conductive hydrogels [20], [31]. In this PAA hydrogel, the broad phase response and large impedance variation suggest that both hydrogel transport properties and contact conditions contributed to the measured behaviour.

The CV response confirmed that the PEDOT:PSS-PAA hydrogel was electrochemically active in the PDMS platform, but the curve was less regular than that observed for PEDOT:PSS-DBSA. The current response was lower than DBSA, reaching approximately −100 to +200 µA in the mean curve. The CV shape was distorted and not rectangular, indicating that the response was not purely capacitive. The large shaded region, especially at positive potentials, also showed substantial variability between measurements. This again supports the interpretation that the PAA response in the PDMS measuring platform was influenced by manual hydrogel/electrode contact.

Overall, PEDOT:PSS-PAA showed measurable electrochemical activity in the PDMS measuring platform, but its response was more variable and contact-dependent than the DBSA hydrogel. This was mainly because the PAA hydrogel required post-processing before measurement and could not be gelled directly around the pogo pin. For this reason, the PDMS platform was not considered the most suitable configuration for evaluating the PAA hydrogel alone. The Swagelok-based bulk setup, presented later in this chapter, was therefore particularly important for assessing the PAA formulation under a more controlled electrode/hydrogel/electrode contact geometry.

5.4.3 PEDOT:PSS-PEGPACHI electrochemical response

PEDOT:PSS-PEGPACHI hydrogels were evaluated in the PDMS measuring platform using EIS and CV in 1x DPBS. Similar to the PEDOT:PSS-DBSA formulation, PEDOT:PSS-PEGPACHI could be cast directly inside the PDMS well around the gold pogo pin working electrode. This provided direct hydrogel/electrode contact after gelation and made the formulation suitable for measurement in the PDMS platform. The electrochemical response of PEDOT:PSS-PEGPACHI is shown in Figure 5.6.

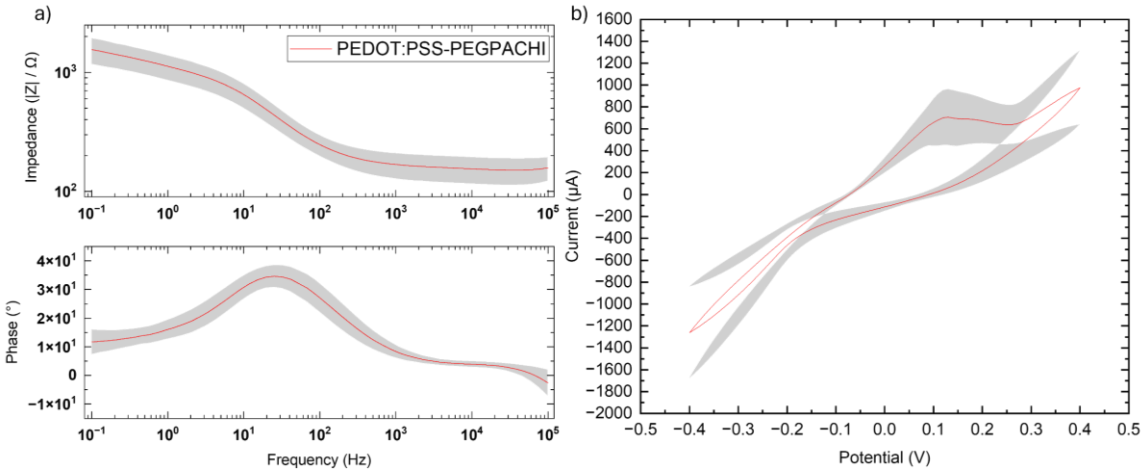


Figure 5.6: Electrochemical response of PEDOT:PSS-PEGPACHI hydrogels measured in the PDMS measuring platform.
(a) Impedance magnitude |Z| and phase angle as a function of frequency measured by EIS in 1x DPBS. (b) Cyclic voltammetry response recorded between −0.4 and +0.4 V at 100 mV s^{-1}. The black line represents the mean response and the grey shaded area represents mean ± SD for n = 3 hydrogel samples.

Additional electrochemical experiments were also performed for PEDOT:PSS-PEGPACHI hydrogels under different measurement conditions and sample configurations. These experiments are included in **Appendix K** to document the broader experimental evaluation of the PEDOT:PSS-PEGPACHI formulation, while Figure 5.6 presents the selected averaged response used for comparison in the main text.

The EIS response showed a clear frequency-dependent impedance profile. The impedance magnitude was highest at low frequency and decreased as the frequency increased. At low frequency, the impedance was in the order of 10^2-10^3 Ω, while at higher frequencies it decreased towards approximately 10^2 Ω. This indicates that the PEDOT:PSS-PEGPACHI hydrogel provided an electrically conductive pathway in the PDMS measuring platform. The decrease in impedance with increasing frequency suggests that the measured response was influenced by both ionic transport through the hydrated hydrogel network and electronic transport through the PEDOT:PSS-based conductive phase. The phase response of PEDOT:PSS-PEGPACHI showed a pronounced maximum in the intermediate-frequency region, followed by a decrease towards values close to 0° at high frequency. This indicates that the response was not dominated by a simple resistive pathway alone, but included a clear capacitive or interfacial contribution in the mid-frequency range. Compared with PEDOT:PSS-DBSA, the phase maximum was more pronounced, suggesting that the multicomponent PEGPACHI network introduced a stronger frequency-dependent response. This may be related to the hydrated PA-chitosan-PEGDE structure, although the contribution of the local hydrogel/pogo pin contact cannot be fully separated in this measurement configuration.

The CV response showed a broad current response over the −0.4 to +0.4 V potential window. The current reached approximately −1200 µA at negative potentials and up to approximately +1000 µA at positive potentials in the mean curve. This was higher than the current response observed for the PEDOT:PSS-DBSA and PEDOT:PSS-PAA hydrogels in the PDMS measuring platform. The large enclosed CV area indicates substantial charge-storage behaviour, suggesting that the PEDOT:PSS-PEGPACHI hydrogel was electrochemically active in this configuration.

However, the CV shape was not perfectly rectangular and showed some asymmetry and variability, especially at positive potentials. This indicates that the response was not purely capacitive and was likely influenced by mixed resistive/capacitive behaviour, hydrogel structure, and local electrode/hydrogel contact. The shaded region also suggests some variability between measurements, although direct casting around the pogo pin made the contact more reliable than for the PEDOT:PSS-PAA hydrogel.

Overall, PEDOT:PSS-PEGPACHI showed a strong electrochemical response in the PDMS measuring platform. The formulation could be cast directly around the pogo pin, which made it suitable for this measurement configuration. Compared with PEDOT:PSS-DBSA, PEDOT:PSS-PEGPACHI showed higher CV currents, while maintaining impedance values in the same general high-frequency range. Compared with PEDOT:PSS-PAA, the response was less dependent on post-processing-related manual contact. These results suggest that PEDOT:PSS-PEGPACHI was one of the most promising formulations for integration into the PDMS measuring platform.

5.4.4 Comparative electrochemical evaluation of the PEDOT:PSS-based hydrogels

A direct comparison of the electrochemical behaviour of the three PEDOT:PSS-based hydrogels measured on the PDMS platform is shown in Figure 5.7. Clear differences were observed in both the impedance spectra and cyclic voltammetry response, indicating that the hydrogel formulation strongly affected charge transport and electrochemical performance.

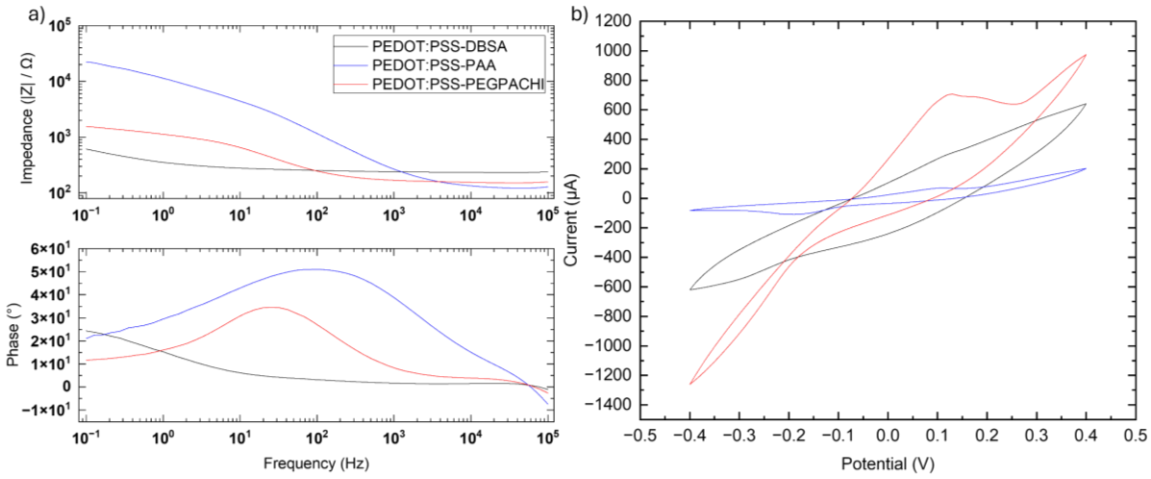


Figure 5.7: Comparative electrochemical response of the three PEDOT:PSS-based hydrogels measured using the PDMS platform.
a) Bode plots showing impedance magnitude (top) and phase angle (bottom) as a function of frequency for PEDOT:PSS-DBSA, PEDOT:PSS-PAA, and PEDOT:PSS-PEGPACHI hydrogels. b) Cyclic voltammograms of the three hydrogel formulations recorded over the same potential window. The figure highlights the differences in impedance response, phase behaviour, and charge storage characteristics among the investigated formulations.

From the EIS measurements, PEDOT:PSS-PAA exhibited the highest impedance over most of the investigated frequency range, while PEDOT:PSS-DBSA showed the lowest impedance values. PEDOT:PSS-PEGPACHI displayed an intermediate behaviour, with impedance values lower than PEDOT:PSS-PAA and closer to PEDOT:PSS-DBSA at higher frequencies. In the context of conductive hydrogels, the low-frequency region is typically associated with ionic motion through the hydrated bulk, whereas the high-frequency response is more strongly influenced by the intrinsic electronic conduction pathways of the PEDOT:PSS network, as already discussed. Based on this interpretation, the lower impedance of PEDOT:PSS-DBSA suggests more efficient overall charge transport, while the higher impedance of PEDOT:PSS-PAA indicates a less conductive electrochemical response under the tested conditions.

The phase response further highlighted these differences. PEDOT:PSS-PAA showed the most pronounced phase maximum, followed by PEDOT:PSS-PEGPACHI, whereas PEDOT:PSS-DBSA displayed the lowest and flattest phase response. This indicates that PEDOT:PSS-PAA exhibited the strongest frequency-dependent capacitive contribution, while PEDOT:PSS-DBSA behaved in a more resistive-dominant manner. At approximately 10 kHz, which is a frequency range often discussed in the context of neural interfacing, PEDOT:PSS-DBSA and PEDOT:PSS-PEGPACHI maintained lower impedance values than PEDOT:PSS-PAA, which is favourable for efficient signal transfer.

The cyclic voltammetry measurements were in agreement with the impedance trends. PEDOT:PSS-PEGPACHI showed the highest current response and the largest enclosed voltametric area, indicating the highest apparent charge storage capability among the three formulations. PEDOT:PSS-DBSA showed an intermediate response, while PEDOT:PSS-PAA exhibited the lowest currents and the smallest voltametric area. Overall, the electrochemical comparison suggests that PEDOT:PSS-DBSA provided the lowest impedance response, PEDOT:PSS-PEGPACHI provided the highest voltametric charge-handling capability, and PEDOT:PSS-PAA showed the weakest electrochemical performance among the three tested hydrogels.

5.5 Electrochemical characterisation in the Swagelok-based bulk setup

5.5.1 Rationale for Swagelok bulk measurements

Swagelok-based bulk measurements were performed to evaluate the PEDOT:PSS-based hydrogels in a more direct electrode-hydrogel-electrode geometry. In contrast to the PDMS measuring platform, where the response depended on the contact between the hydrogel and the gold pogo pin, the Swagelok setup allowed the hydrated hydrogel sample to be positioned directly between two disk electrodes. This configuration was especially useful for PEDOT:PSS-PAA, because this hydrogel required post-treatment, annealing, and rehydration, and therefore could not be cast directly around the pogo pin in the PDMS measuring platform.

Two Swagelok electrode configurations were used: gold-gold and platinum-platinum. These measurements were used to compare the relative bulk electrochemical behaviour of PEDOT:PSS-DBSA, PEDOT:PSS-PAA, and PEDOT:PSS-PEGPACHI under confined contact conditions. Individual EIS-derived plots for each hydrogel formulation and electrode configuration, including impedance magnitude, capacitance, real impedance, and Nyquist-type representations, are provided in **Appendix K-L**.

The Swagelok samples were cylindrical punched hydrogels with an approximate diameter of 5 mm and height of 4 mm, corresponding to an estimated hydrogel volume of 79 µL, or 79 mm^3.

5.5.2 Comparison of PEDOT:PSS-based hydrogels in the gold-gold Swagelok configuration

Figure 5.8 compares the bulk electrochemical behaviour of PEDOT:PSS-DBSA, PEDOT:PSS-PAA, and PEDOT:PSS-PEGPACHI hydrogels measured in the gold-gold Swagelok configuration after overnight soaking in 1x DPBS. This configuration allowed the three hydrogels to be compared under the same confined bulk-contact geometry, where the hydrogel was placed directly between two gold disk electrodes.

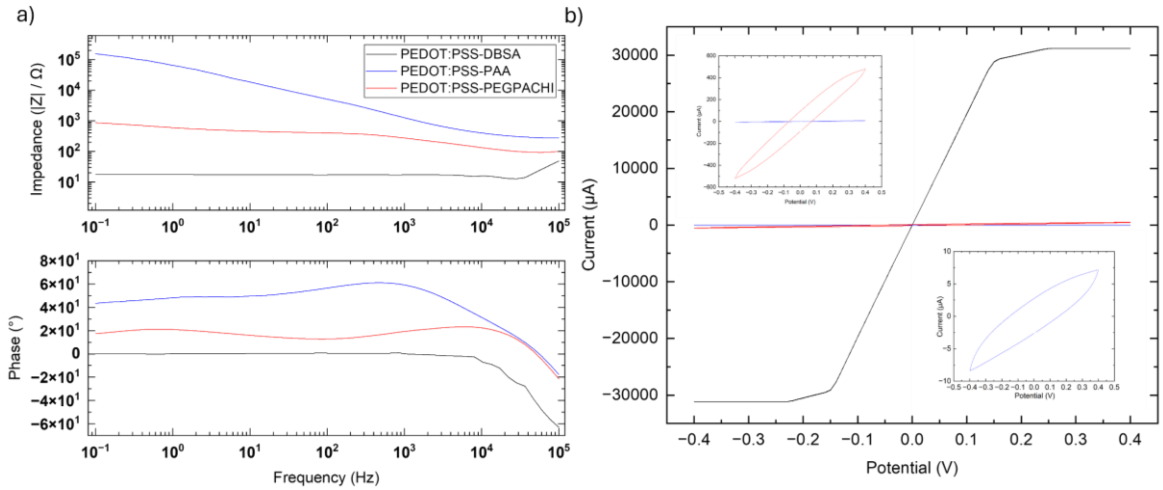


Figure 5.8: Comparison of the electrochemical response of PEDOT:PSS-DBSA, PEDOT:PSS-PAA, and PEDOT:PSS-PEGPACHI hydrogels measured in the gold-gold Swagelok configuration.

(a) Impedance magnitude |Z| and phase angle as a function of frequency measured by EIS after overnight soaking in 1x DPBS. (b) Cyclic voltammetry response recorded between −0.4 and +0.4 V. Black represents PEDOT:PSS-DBSA, blue represents PEDOT:PSS-PAA, and red represents PEDOT:PSS-PEGPACHI. Solid lines represent the mean response and the shaded areas represent mean ± SD for n = 3 hydrogel samples. Insets show the lower-current CV responses of PEDOT:PSS-PAA and PEDOT:PSS-PEGPACHI more clearly.

PEDOT:PSS-DBSA showed the lowest impedance over most of the frequency range, indicating the strongest bulk electrochemical response in the gold-gold configuration. The phase remained close to 0° across a wide frequency range, suggesting a mainly resistive response. However, the very large CV current and the almost linear CV shape are likely dominated by the low-resistance bulk pathway and the specific Swagelok contact geometry. Therefore, the apparent capacitance obtained from this response should be interpreted with caution, as it is most likely strongly affected by measurement artefacts rather than representing a purely capacitive hydrogel behaviour. Additional DBSA EIS-derived plots are provided in **Appendix K-L**.

PEDOT:PSS-PAA showed the highest impedance and the weakest CV response. The impedance decreased gradually with increasing frequency, while the phase response showed stronger frequency dependence than PEDOT:PSS-DBSA. This suggests more limited charge transport through the PAA-based hydrogel, most likely due to the polymer-network structure and the more complex fabrication route, which may have limited continuous PEDOT:PSS conductive pathways.

PEDOT:PSS-PEGPACHI showed intermediate behaviour between PEDOT:PSS-DBSA and PEDOT:PSS-PAA. Its impedance was lower than PEDOT:PSS-PAA but higher than PEDOT:PSS-DBSA, and its CV response was stronger than PEDOT:PSS-PAA while remaining much lower than the DBSA current response. This indicates that PEDOT:PSS-PEGPACHI provided measurable

electrochemical activity in the bulk Swagelok setup, while avoiding the extreme low-resistance response observed for PEDOT:PSS-DBSA.

Overall, the gold-gold Swagelok comparison showed three distinct electrochemical behaviours. PEDOT:PSS-DBSA gave the strongest but measurement-sensitive response, PEDOT:PSS-PAA gave the weakest response, and PEDOT:PSS-PEGPACHI showed an intermediate and more balanced electrochemical behaviour. The individual EIS-derived plots for each hydrogel formulation in the gold-gold configuration are provided in **Appendix K-L**.

5.5.3 Comparison of PEDOT:PSS-based hydrogels in the platinum-platinum Swagelok configuration

Figure 5.9 compares the electrochemical behaviour of PEDOT:PSS-DBSA, PEDOT:PSS-PAA, and PEDOT:PSS-PEGPACHI hydrogels measured in the platinum-platinum Swagelok configuration after overnight soaking in 1× DPBS. This configuration allowed the same three formulations to be compared under a confined bulk-contact geometry using platinum disk electrodes.

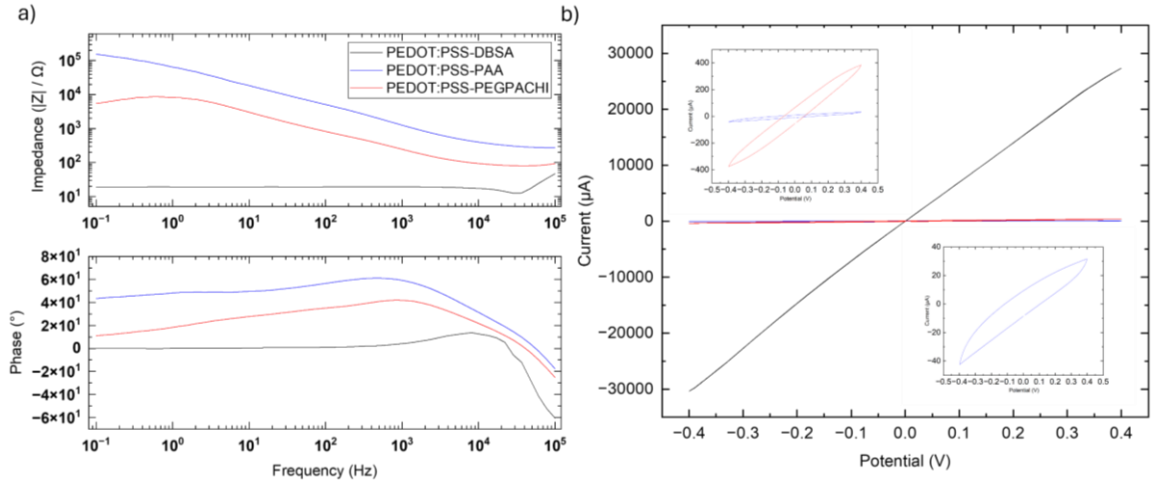


Figure 5.9: Comparison of the electrochemical response of PEDOT:PSS-DBSA, PEDOT:PSS-PAA, and PEDOT:PSS-PEGPACHI hydrogels measured in the platinum-platinum Swagelok configuration.

(a) Impedance magnitude |Z| and phase angle as a function of frequency measured by EIS after overnight soaking in 1× DPBS. (b) Cyclic voltammetry response recorded between −0.4 and +0.4 V. Black represents PEDOT:PSS-DBSA, blue represents PEDOT:PSS-PAA, and red represents PEDOT:PSS-PEGPACHI. Solid lines represent the mean response and the shaded areas represent mean ± SD for n = 3 hydrogel samples. Insets show the lower-current CV responses of PEDOT:PSS-PAA and PEDOT:PSS-PEGPACHI more clearly.

PEDOT:PSS-DBSA again showed the lowest impedance over almost the entire frequency range, confirming that it had the strongest bulk electrochemical response in the platinum-platinum configuration. The phase remained close to 0° over most of the frequency range, indicating a mainly resistive response. Similar to the gold-gold configuration, the CV response showed very high current values and an almost linear shape. Therefore, the apparent capacitance-related behaviour should be interpreted with caution, as the response was likely dominated by the low-resistance bulk pathway and the Swagelok contact geometry rather than by a clean capacitive hydrogel response.

PEDOT:PSS-PAA showed the highest impedance and the weakest CV response in the platinum-platinum configuration. The impedance decreased with increasing frequency, while the phase response showed stronger frequency dependence than PEDOT:PSS-DBSA. This again indicates more limited charge transport through the PAA-based hydrogel under the tested bulk-contact conditions.

PEDOT:PSS-PEGPACHI showed intermediate behaviour. Its impedance was lower than PEDOT:PSS-PAA but higher than PEDOT:PSS-DBSA, and its CV response was stronger than PEDOT:PSS-PAA but far below the high-current DBSA response. This supports the interpretation that PEDOT:PSS-PEGPACHI provided measurable electrochemical activity while avoiding the extreme low-resistance behaviour observed for PEDOT:PSS-DBSA.

Overall, the platinum-platinum Swagelok comparison confirmed the same general trend observed in the gold-gold configuration. PEDOT:PSS-DBSA showed the strongest but measurement-sensitive response, PEDOT:PSS-PAA showed the weakest response, and PEDOT:PSS-PEGPACHI showed an intermediate and more balanced response. The individual EIS-derived plots for each hydrogel formulation in the platinum-platinum configuration are provided in **Appendix K-L**.

5.6 Summary of electrochemical behaviour of the PEDOT:PSS-based hydrogels

The electrochemical behaviour of the three PEDOT:PSS-based hydrogels is summarised quantitatively in Table 5.2. The values were extracted from the PDMS measuring platform measurements, where each hydrogel was cast in a 5 mm diameter well with a hydrogel volume of 70 µL. The impedance values correspond to the frequency point closest to 1 kHz. The electrical conductivity was calculated as an apparent conductivity using the geometry-based equation used by Wang et al., based on the real impedance at approximately 1 kHz, the pogo pin contact area, and the estimated hydrogel height in the PDMS well. The volumetric capacitance was calculated from the EIS-derived capacitance at 0.1 Hz and normalised to the hydrogel volume. Since the PDMS measuring platform does not represent an ideal parallel-plate geometry, these values should be interpreted as apparent parameters and used mainly for comparison between formulations.

Table 5.2: Quantitative summary of the electrochemical behaviour of the PEDOT:PSS-based hydrogels measured in the PDMS measuring platform.

Hydrogel	Impedance at ~1 kHz, |Z| (Ω)	Electrical conductivity at ~1 kHz (S/m)	Volumetric capacitance from EIS at 0.1 Hz (F/cm^3)
PEDOT:PSS-DBSA	239.18 ± 10.66	0.85 ± 0.04	0.104 ± 0.010
PEDOT:PSS-PAA	255.23 ± 113.82	0.79 ± 0.35	0.014 ± 0.013
PEDOT:PSS-PEGPACHI	167.75 ± 40.38	1.21 ± 0.29	0.086 ± 0.034

The quantitative summary confirms the trends observed in the EIS and CV results. PEDOT:PSS-PEGPACHI showed the lowest impedance at approximately 1 kHz and the highest apparent electrical conductivity among the three formulations in the PDMS measuring platform. PEDOT:PSS-DBSA showed a similar impedance range and the highest volumetric capacitance, supporting its strong electrochemical activity. PEDOT:PSS-PAA showed comparable impedance values but the lowest apparent volumetric capacitance, indicating a weaker charge-storage response under the same measurement conditions. Overall, PEDOT:PSS-PEGPACHI provided the most balanced response in the PDMS measuring platform, combining low impedance, the highest apparent conductivity, and high volumetric capacitance. For this reason, it was selected as the most promising formulation for the preliminary device-integration experiments described in Chapter 7.

5.7 Mechanical characterisation by nanoindentation

Mechanical characterisation was performed to evaluate the stiffness of the PEDOT:PSS-based hydrogels under hydrated conditions. The effective Young's modulus, Eeff, was measured by nanoindentation in 1x DPBS using matrix scans on three independent hydrogel samples per formulation. For each sample, multiple indentation points were collected, and failed or unreliable measurements were excluded before analysis based on abnormal measurement behaviour, including clear outlier Eeff values, abnormal maximum load values, or poor indentation response. Several practical complications were encountered during these measurements. Because the hydrogels were soft, hydrated, and in some cases fragile or difficult to handle, the samples had to remain fully submerged while also being kept stable in one position during indentation. The available probe was also not fully ideal for all hydrogel conditions, which made careful inspection of the data necessary. In addition, each formulation presented different experimental challenges during measurement, which are described separately in the following sections. The complete exclusion tables, heat maps, and additional measurement details are provided in **Appendix G**.

5.7.1 Nanoindentation response of PEDOT:PSS-DBSA

The PEDOT:PSS-DBSA hydrogel was mechanically characterised by nanoindentation in the hydrated state. During the initial measurements, the main practical difficulty was the fragility of the hydrogel. The samples were soft and difficult to keep fixed in one position when placed directly in a Petri dish under DPBS. In addition, the hydrogel surface was not perfectly flat, which introduced local variation during indentation. To improve sample stability, the hydrogels were prepared inside a square well-plate mould and measured while remaining inside the wells. A sufficient volume of 1x DPBS was then added to fully submerge the samples during indentation. This approach allowed the hydrogels to remain hydrated and fixed in position during measurement. Additional details of the sample-positioning approach and the full exclusion tables are provided in **Appendix G**.

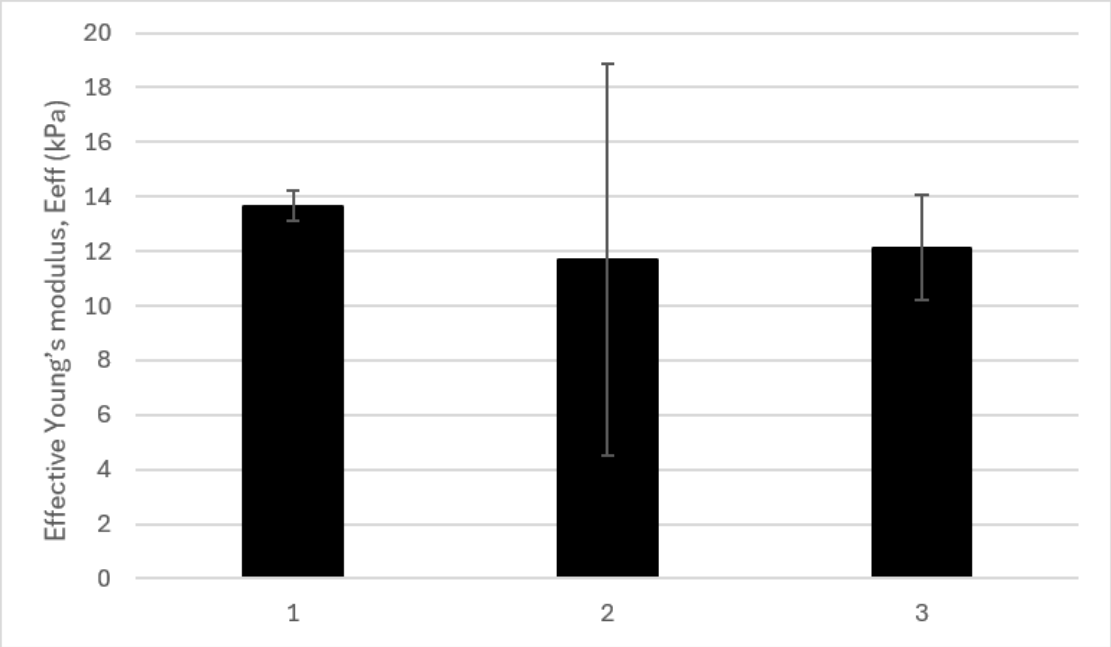


Figure 5.10: Nanoindentation response of PEDOT:PSS-DBSA hydrogels. Effective Young's modulus, Eeff, of three independent PEDOT:PSS-DBSA hydrogel samples measured by nanoindentation in 1x DPBS.
Bars show the mean Eeff of valid indentation points for each sample, and error bars represent standard deviation. Failed or unreliable indentation points were excluded before analysis based on abnormal

maximum load values, clear outlier behaviour, or poor indentation response. Full exclusion details and heat maps are provided in **Appendix G**.

The PEDOT:PSS-DBSA hydrogel showed a relatively consistent nanoindentation response across the three measured samples, with mean Eeff values in the range of approximately 11.7-13.7 kPa after exclusion of failed or unreliable indentation points. The first and third samples showed relatively small standard deviations, indicating a more uniform local mechanical response. The second sample showed a larger standard deviation, which is likely related to local surface unevenness and the sensitivity of the indentation measurement to the exact contact position on the hydrogel surface. Since nanoindentation probes only a local region of the sample, small differences in surface geometry, hydration, or contact quality can strongly affect individual indentation values.
Overall, the DBSA hydrogel behaved as a soft but measurable material. Compared with the other formulations, the heat maps showed a relatively uniform response over most of the measured area, with only a limited number of clear outliers. A possible explanation is that the PEDOT:PSS-DBSA formulation does not contain a secondary rigid polymer network or hard dispersed phase, meaning that the indented surface mainly represents the hydrated PEDOT:PSS-DBSA gel network. This may contribute to the more homogeneous local mechanical response observed for this formulation. However, because the hydrogel was fragile and the surface was not perfectly even, the obtained modulus values should be interpreted as effective hydrated-state stiffness values rather than absolute bulk mechanical constants.

5.7.2 Nanoindentation response of PEDOT:PSS-PAA

The PEDOT:PSS-PAA hydrogels were also mechanically characterised by nanoindentation in 1x DPBS. Compared with PEDOT:PSS-DBSA, the PAA-based hydrogels were easier to handle during measurement because they were more mechanically stable and remained better positioned inside the square well-plate mould during indentation. This improved sample handling made the measurement procedure more practical. However, the PAA hydrogels still showed considerable variation between indentation points, as reflected by the relatively large standard deviations observed for the three samples (Figure 5.11).

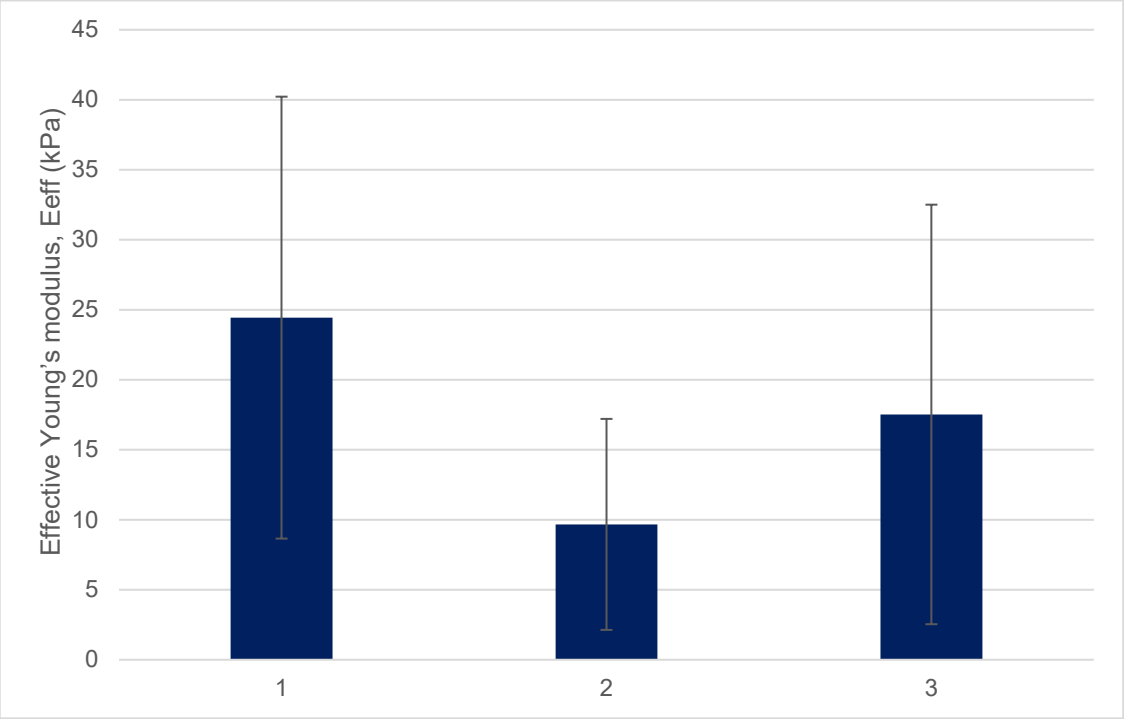


Figure 5.11: Nanoindentation response of PEDOT:PSS-PAA hydrogels. Effective Young's modulus, Eeff, of three independent PEDOT:PSS-PAA hydrogel samples measured by nanoindentation in 1x DPBS.
Bars show the mean Eeff of valid indentation points for each sample, and error bars represent standard deviation. Failed or unreliable indentation points were excluded before analysis based on abnormal maximum load values, clear outlier behaviour, or poor indentation response. Full exclusion details and heat maps are provided in **Appendix G**.

The higher variability is likely related to both the surface morphology of the PAA hydrogel and the internal structure of the material. After the post-treatment, annealing, and rehydration steps, the PAA hydrogels had a less uniform and more uneven surface compared with the PEDOT:PSS-DBSA samples. Since nanoindentation is a local measurement technique, small differences in surface height, roughness, or contact quality can strongly influence the measured Eeff value. In addition, the PEDOT:PSS phase was incorporated into the PAA network from freeze-dried and manually processed PEDOT:PSS material. This may have resulted in PEDOT:PSS domains or aggregates with different local sizes within the hydrogel matrix. As a result, the nanoindenter probe may have contacted regions with different local compositions, for example areas richer in PAA network or areas containing larger PEDOT:PSS-rich domains. This could explain the large spread in measured values within the same sample.
The PAA formulation therefore behaved differently from the DBSA hydrogel. While PEDOT:PSS-PAA was more robust and easier to handle during testing, its local mechanical response was less uniform. This is consistent with the more complex fabrication route of this hydrogel, which included freeze-drying, manual grinding, redox polymerisation, EMIM-ES treatment, annealing, rehydration, and cutting/handling before measurement. Each of these steps could contribute to structural heterogeneity in the final hydrogel. Therefore, the measured values should be interpreted as effective local hydrated-state stiffness values rather than a fully homogeneous bulk modulus. The complete exclusion tables and heat maps are provided in **Appendix G**.

5.7.3 Nanoindentation response of PEDOT:PSS-PEGPACHI

The PEDOT:PSS-PEGPACHI hydrogels were mechanically characterised by nanoindentation in 1x DPBS using the same hydrated measurement approach. Similar to PEDOT:PSS-DBSA, the PEGPACHI samples were soft and not straightforward to measure directly in a Petri dish. However, once the samples were prepared and measured inside the square well-plate mould, they remained sufficiently stable and submerged during indentation. The hydrogel surface appeared macroscopically continuous, but it was still locally uneven, which is important because nanoindentation is sensitive to the exact contact point between the probe and the hydrogel surface.

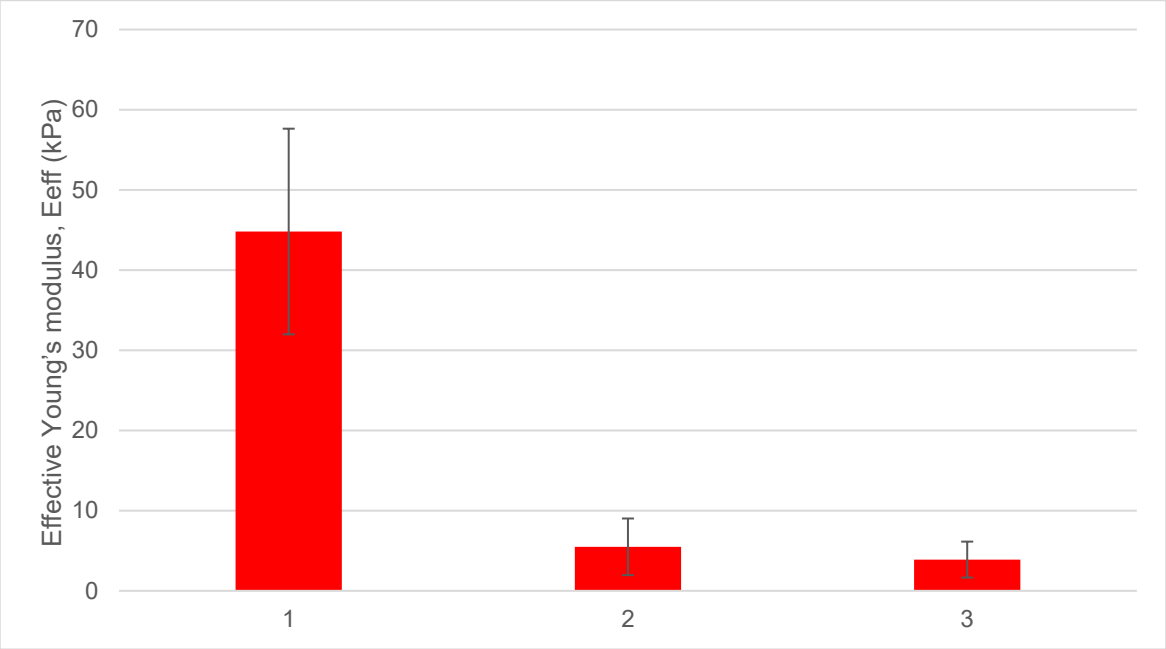


Figure 5.12: Nanoindentation response of PEDOT:PSS-PEGPACHI hydrogels. Effective Young's modulus, Eeff, of three independent PEDOT:PSS-PEGPACHI hydrogel samples measured by nanoindentation in 1x DPBS.
Bars show the mean Eeff of valid indentation points for each sample, and error bars represent standard deviation. Failed or unreliable indentation points were excluded before analysis based on abnormal maximum load values, clear outlier behaviour, or poor indentation response. Full exclusion details and heat maps are provided in **Appendix G**.

The PEGPACHI formulation showed a clear difference between the first sample and the other two samples (Figure 5.12). Sample 1 showed a higher mean Eeff value, while samples 2 and 3 showed much lower values. This indicates that the PEGPACHI hydrogels had stronger sample-to-sample variability than PEDOT:PSS-DBSA and PEDOT:PSS-PAA under the tested conditions. One possible explanation is the multicomponent nature of the formulation. PEDOT:PSS-PEGPACHI contains PEDOT:PSS, phytic acid, chitosan, and PEGDE, and although the final mixing protocol produced macroscopically homogeneous gels, local microscale differences may still exist within the hydrated network. For example, the nanoindenter probe may locally contact regions with slightly different surface morphology or composition, such as areas enriched in chitosan-containing network or PEDOT:PSS-rich domains. These local differences would not necessarily be visible macroscopically but could influence the measured Eeff values.
The difference between sample 1 and samples 2-3 may also be partly related to local surface unevenness. If the probe contacted a denser or less swollen region in sample 1, this could result in

higher apparent stiffness. In contrast, samples 2 and 3 may have been measured in softer or more hydrated regions of the gel. Therefore, the PEGPACHI results suggest that, while the formulation could be measured in the hydrated state, its local mechanical response was more variable than expected. As with the other hydrogels, the values should be interpreted as effective local hydrated-state stiffness values rather than absolute bulk moduli. The full exclusion tables and heat maps are provided in **Appendix G**.

5.7.4 Comparison of mechanical properties

To compare the mechanical behaviour of the three formulations, the median Eeff value of each independent hydrogel sample was used. These sample medians were plotted as a box-and-whisker plot to show both the central tendency and the sample-to-sample variability between the three hydrogels. Since only three independent samples were measured per formulation, the plot was used as a descriptive comparison and no statistical significance is claimed.

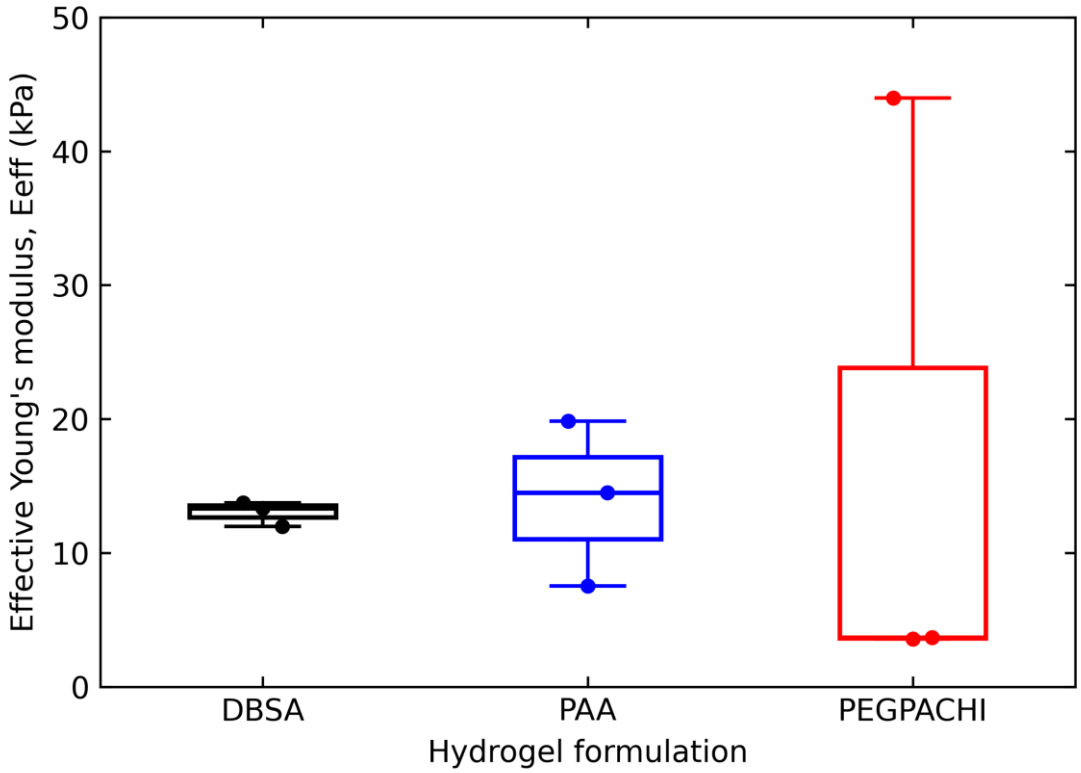


Figure 5.13: Box-and-whisker comparison of effective Young's modulus of PEDOT:PSS-based hydrogels.

Effective Young's modulus, Eeff, of PEDOT:PSS-DBSA, PEDOT:PSS-PAA, and PEDOT:PSS-PEGPACHI hydrogels measured by nanoindentation in 1× DPBS. Each data point represents the median Eeff value of one independent hydrogel sample calculated from valid indentation points. Whiskers represent the minimum and maximum sample median values. The plot is intended as a preliminary comparison of hydrated-state stiffness, and no statistical significance is claimed. The comparison is intended as a preliminary assessment of hydrated-state stiffness and no statistical significance is claimed. Full exclusion tables and heat maps are provided in **Appendix G**.

The box-and-whisker plot highlights that PEDOT:PSS-DBSA showed the most consistent mechanical response, while PEDOT:PSS-PAA showed larger sample-to-sample variability. PEDOT:PSS-

PEGPACHI showed the widest spread, mainly because one sample had a much higher Eeff value than the other two. Therefore, the PEGPACHI average should be interpreted carefully and the result should be viewed as preliminary hydrated-state stiffness information rather than a definitive bulk modulus comparison.

No statistical significance is claimed from these measurements, because the number of independent hydrogel samples was limited and the results were strongly affected by local surface conditions, sample hydration, and probe-sample contact. Therefore, the mechanical characterisation should be interpreted mainly as a preliminary assessment of the hydrated stiffness range of the hydrogels, rather than as a definitive comparison of bulk mechanical properties. Nevertheless, the results provide useful information on the relative mechanical behaviour of the three formulations and confirm that all materials were within a soft kPa-range relevant for hydrogel-based bioelectronic interfaces.

5.8 Summary of mechanical behaviour

The mechanical behaviour of the three PEDOT:PSS-based hydrogels is summarised quantitatively in Table 5.3. The values were extracted from the hydrated nanoindentation measurements presented above. For each hydrogel formulation, three independent gel samples were measured, and multiple indentation points were collected from each sample. Failed or unreliable indentation points were excluded before analysis, as described in Appendix G. To compare the formulations, the median Eeff value of each independent gel sample was used, and the final value is reported as the mean ± standard deviation of the sample medians. This approach avoids overinterpreting multiple indentation points from the same gel as fully independent replicates.

Table 5.3: Quantitative summary of the mechanical behaviour of the PEDOT:PSS-based hydrogels.

Hydrogel	Sample median Eeff values (kPa)	Mean sample median Eeff (kPa)	Overall behaviour
PEDOT:PSS-DBSA	13.73, 13.34, 11.97	13.01 ± 0.91	Most uniform local mechanical response
PEDOT:PSS-PAA	19.83, 7.54, 14.49	13.95 ± 6.16	More robust material, but higher local variability
PEDOT:PSS-PEGPACHI	43.98, 3.58, 3.68	17.08 ± 23.32	Soft hydrogel response, but strong sample-to-sample variability

Overall, all three hydrogels showed effective Young's modulus values in the soft kPa range under hydrated nanoindentation conditions. PEDOT:PSS-DBSA showed the most consistent mechanical response, with similar median Eeff values across the three samples. PEDOT:PSS-PAA showed a comparable average stiffness but larger variability, which is consistent with its more complex fabrication and post-treatment process. PEDOT:PSS-PEGPACHI showed the highest mean sample median Eeff, but this was mainly influenced by one stiffer sample, while the other two samples were much softer. Therefore, the mechanical results should be interpreted as a preliminary comparison of effective hydrated-state stiffness rather than as a definitive comparison of bulk mechanical properties. The full exclusion tables, heat maps, and additional data-processing details are provided in **Appendix G**.

6 Biological Compatibility

6.1 Biological compatibility assessment

After the physical, electrochemical, and mechanical characterisation of the PEDOT:PSS-based hydrogels, their biological compatibility was evaluated under cell-culture conditions. This step was important because materials intended for bioelectronic neural interfaces must not only provide suitable electrical and mechanical properties, but also remain stable in aqueous biological environments and avoid causing strong negative effects on nearby cells.

The biological evaluation in this thesis was performed in two stages. First, PEDOT:PSS-DBSA was tested in a preliminary U87 metabolic activity assay in collaboration with the Medical University of Graz. This experiment was used as an initial screening step to evaluate whether the DBSA-based hydrogel could be placed in contact with cells after washing and medium conditioning. Since DBSA is a surfactant-based additive, this formulation was expected to present potential biological compatibility concerns, and therefore required early evaluation.

Second, all three final hydrogel formulations, PEDOT:PSS-DBSA, PEDOT:PSS-PAA, and PEDOT:PSS-PEGPACHI, were tested using iPSC-derived neuronal cultures in collaboration with the Leiden group. After this first mention, these cultures are referred to as neurons for simplicity. In this experiment, the hydrogels were placed directly in contact with the neurons after initial cell attachment and remained in the wells until day 8. Cell response was assessed using Live/Dead staining and immunofluorescence imaging, following the general biological testing approach used for PEDOT:PSS-based hydrogels by Wang et al. [31].

This chapter presents the biological response of the different hydrogel formulations. First, the conditioning procedure used before cell exposure is summarised. The preliminary U87 results for PEDOT:PSS-DBSA are then presented, followed by the neuronal culture results for the three final hydrogels. All hydrogels were conditioned before cell exposure using the medium-washing procedure described in Section 3.3.4. The chapter concludes by comparing the biological compatibility of the formulations and identifying which hydrogel showed the most promising behaviour for further development toward bioelectronic neural-interface applications.

6.2 Preliminary U87 metabolic activity assessment of PEDOT:PSS-DBSA

As an initial biological screening step, PEDOT:PSS-DBSA hydrogels were evaluated using U87 cells in collaboration with the Medical University of Graz. This experiment was performed before the final neuronal culture experiments and was used to assess whether the DBSA-based hydrogel could be considered for further biological testing.

U87 cells were seeded in well plates and exposed to PEDOT:PSS-DBSA hydrogels. A second DBSA condition was included in which the hydrogel was washed and conditioned for 96 h before cell exposure. Several additional preliminary conditions were also tested during this screening stage, including hydrogel coating and conditioned-medium approaches, but these were not included in the main figure because they were exploratory and did not change the overall conclusion.

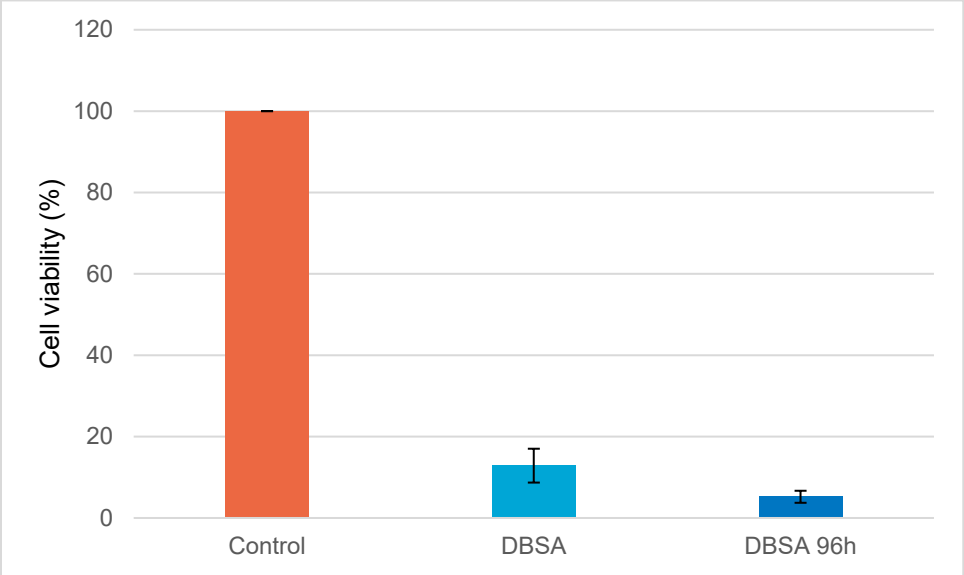


Figure 6.1: Preliminary U87 metabolic activity assessment after exposure to PEDOT:PSS-DBSA hydrogel conditions.
U87 cell viability measured using the MTS assay after exposure to PEDOT:PSS-DBSA hydrogels. Cells were exposed to either directly prepared PEDOT:PSS-DBSA hydrogels or PEDOT:PSS-DBSA hydrogels washed and conditioned for 96 h before exposure. Cell viability was normalised to the untreated control, which was set to 100%. The results show a strong reduction in metabolic activity for both DBSA conditions. **Graph provided by the Waldherr Lab, Medical University of Graz, and adapted for this thesis.**

The MTS results showed a strong reduction in metabolic activity for both PEDOT:PSS-DBSA conditions compared with the control (Figure 6.1). Direct exposure to PEDOT:PSS-DBSA resulted in low cell viability, while the 96 h washed condition also showed poor metabolic activity. This indicated that washing and conditioning improved the condition only slightly and was not sufficient to make the DBSA-based hydrogel suitable for further biological experiments.
Overall, this preliminary result suggested that the PEDOT:PSS-DBSA formulation had poor biological compatibility under the tested conditions. Although PEDOT:PSS-DBSA showed strong electrochemical performance in Chapter 5, the U87 results indicated that the DBSA-based formulation was not suitable for direct biological contact without further modification. This result supported the development and evaluation of alternative PEDOT:PSS-based hydrogel formulations, especially PEDOT:PSS-PEGPACHI, in the subsequent neuronal culture experiments.

6.3 Neuronal culture compatibility of PEDOT:PSS-based hydrogels

The biological compatibility of the final PEDOT:PSS-based hydrogel formulations was further evaluated using iPSC-derived neuronal cultures in collaboration with the Leiden group. After initial cell attachment, the hydrogels were added to the wells and remained in the culture medium until day 8. The tested formulations were PEDOT:PSS-DBSA, PEDOT:PSS-PAA, and PEDOT:PSS-PEGPACHI. A cell-only condition was included as the control.
The purpose of this experiment was to obtain an initial indication of how the hydrogels behaved under neuronal culture conditions. The assessment was based on the available microscopy images, including brightfield, immunofluorescence, and Live/Dead staining images depending on the formulation.

Representative microscopy images of neuronal cultures after exposure to the different hydrogel formulations. Representative brightfield images from the neuronal culture experiment are shown in Figure 6.2. Brightfield imaging was available for all conditions and was used as the first qualitative comparison between the cell-only control and the hydrogel-exposed cultures.
In the control condition, the neurons showed the expected cell coverage and morphology after 8 days in culture. This provided the baseline for comparing the response of the hydrogel-exposed conditions. The control images were also used later for Live/Dead quantification, as described in Section 7.
For the PEDOT:PSS-DBSA condition, only brightfield images were available.

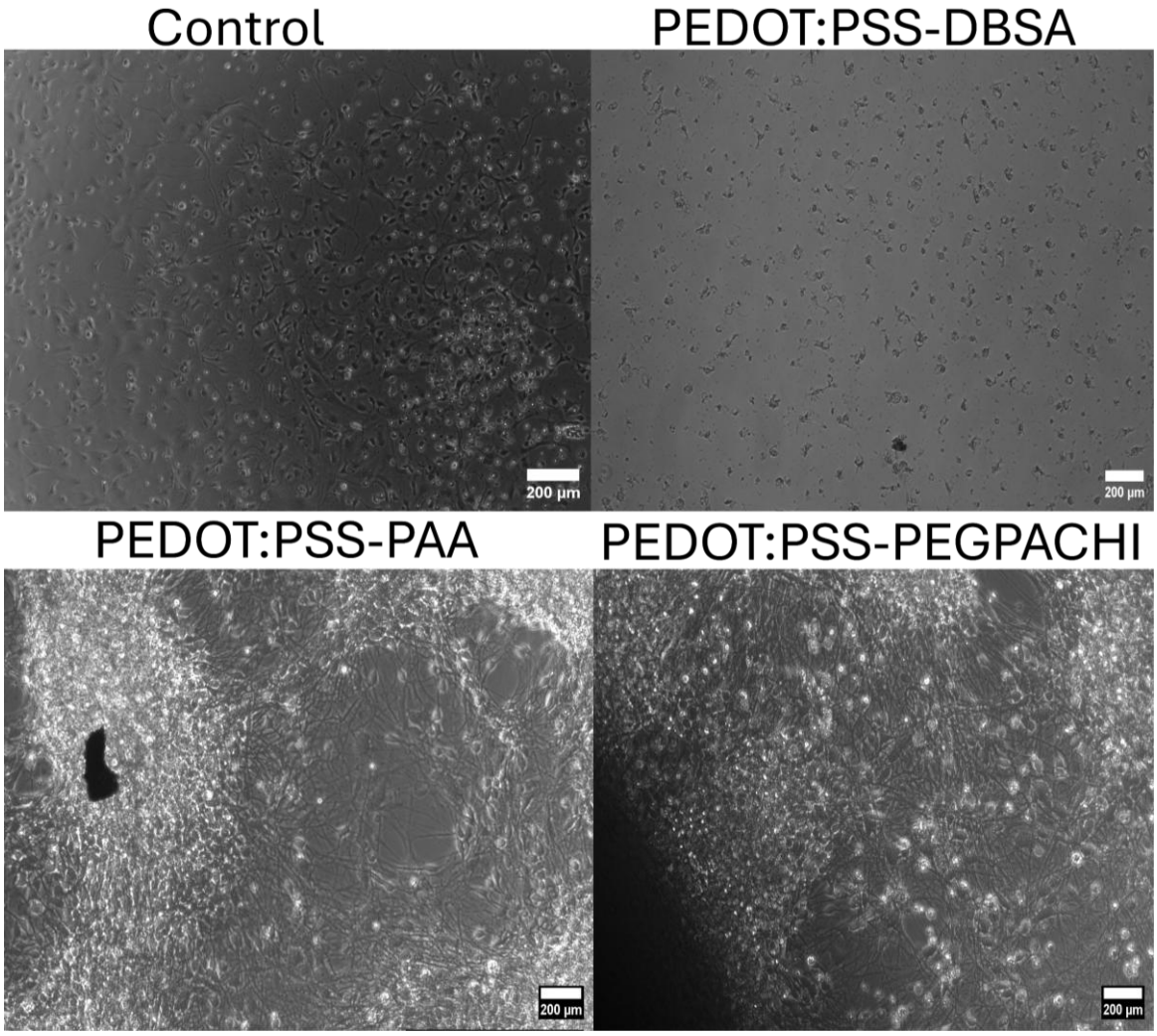


Figure 6.2: Brightfield assessment of neuronal cultures exposed to PEDOT:PSS-based hydrogels after 8 days.
Representative brightfield images of the cell-only control and neuronal cultures exposed to PEDOT:PSS-DBSA, PEDOT:PSS-PAA, and PEDOT:PSS-PEGPACHI. PEDOT:PSS-DBSA showed a poor cell response, while cells remained visible in the PEDOT:PSS-PAA and PEDOT:PSS-PEGPACHI conditions. Images were provided by the Leiden collaborators and adapted for this thesis.

These images showed a poor cell response, with no clear healthy neuronal culture visible in the analysed regions. Live/Dead quantification was not performed for the PEDOT:PSS-DBSA condition because the collaborators' brightfield observations indicated severe loss of cell viability and no clear

live-cell population to quantify. This result was consistent with the preliminary U87 MTS assay, where PEDOT:PSS-DBSA caused a strong reduction in metabolic activity. Together, these observations indicate that the DBSA-based formulation was not biologically suitable under the tested culture conditions.

For the PEDOT:PSS-PAA condition, brightfield and immunofluorescence images were available. These images did not indicate the same severe negative response observed for PEDOT:PSS-DBSA. However, Live/Dead quantification was not available for PEDOT:PSS-PAA due to experimental time limitations during the collaborator workflow. Therefore, this formulation was assessed qualitatively from the available microscopy images. In addition, the PEDOT:PSS-PAA hydrogel was observed to float in the medium and did not remain in stable direct contact with the neurons. As a result, the experiment should be interpreted mainly as an indirect exposure condition rather than as a definitive direct-contact compatibility test.

For PEDOT:PSS-PEGPACHI, brightfield, immunofluorescence, and Live/Dead images were available. The images suggested that the neuronal culture remained present after exposure to the hydrogel condition, without the severe loss of cells observed for PEDOT:PSS-DBSA. However, similar to PEDOT:PSS-PAA, the PEDOT:PSS-PEGPACHI hydrogel was floating in the medium and did not remain in stable direct contact with the cells. Therefore, the results indicate that PEDOT:PSS-PEGPACHI did not show strong toxicity under the tested indirect-exposure conditions, but they do not fully demonstrate stable direct cell-hydrogel contact.

Overall, the qualitative neuronal culture observations showed clear differences between the hydrogel formulations. PEDOT:PSS-DBSA showed poor compatibility, supporting the conclusion from the U87 metabolic activity assay. In contrast, PEDOT:PSS-PAA and PEDOT:PSS-PEGPACHI did not show obvious severe toxicity in the available microscopy images. The next section therefore focuses on the Live/Dead quantification that was available for the control and PEDOT:PSS-PEGPACHI conditions.

6.4 Live/Dead quantification of control and PEDOT:PSS-PEGPACHI cultures

Live/Dead quantification was performed for the cell-only control and PEDOT:PSS-PEGPACHI conditions. Quantification was not performed for PEDOT:PSS-DBSA because the collaborators' brightfield observations indicated severe loss of cell viability and no clear live-cell population to quantify. PEDOT:PSS-PAA was assessed qualitatively because Live/Dead quantification was not available due to experimental time limitations during the collaborator workflow.

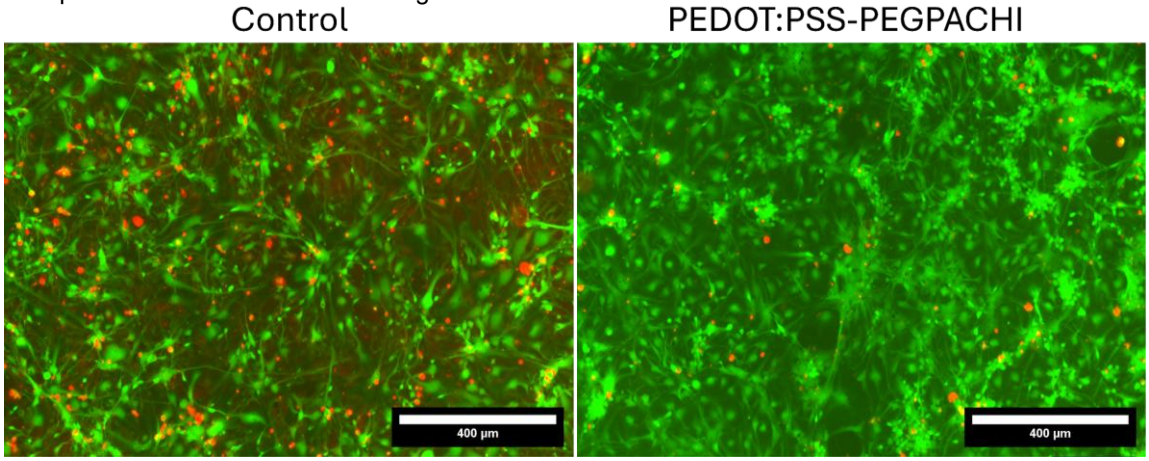


Figure 6.3: Live/Dead assessment of neuronal cultures exposed to PEDOT:PSS-PEGPACHI. Representative Live/Dead images and area-based quantification of the cell-only control and

PEDOT:PSS-PEGPACHI condition after 8 days. Green signal indicates live cells and red signal indicates dead cells. Bars represent mean live-cell area and error bars represent standard deviation. Images were provided by the Leiden collaborators and quantified using ImageJ/Fiji.

Representative Live/Dead images of the control and PEDOT:PSS-PEGPACHI conditions are shown in Figure Figure **6.4**. In both conditions, the staining was dominated by green signal, indicating the presence of a high proportion of viable cells, while only a limited number of red-stained dead cells were observed. Qualitatively, the PEDOT:PSS-PEGPACHI condition appeared comparable to the control, which was consistent with the quantitative viability analysis.
For PEDOT:PSS-PEGPACHI, the available Live/Dead images were analysed using ImageJ/Fiji. Green fluorescence was used as the live-cell signal, while red fluorescence was used as the dead-cell signal. The analysis was performed using an area-based approach, where the live-cell area was calculated relative to the total stained area. The available PEDOT:PSS-PEGPACHI conditions were combined into one group for comparison with the control.

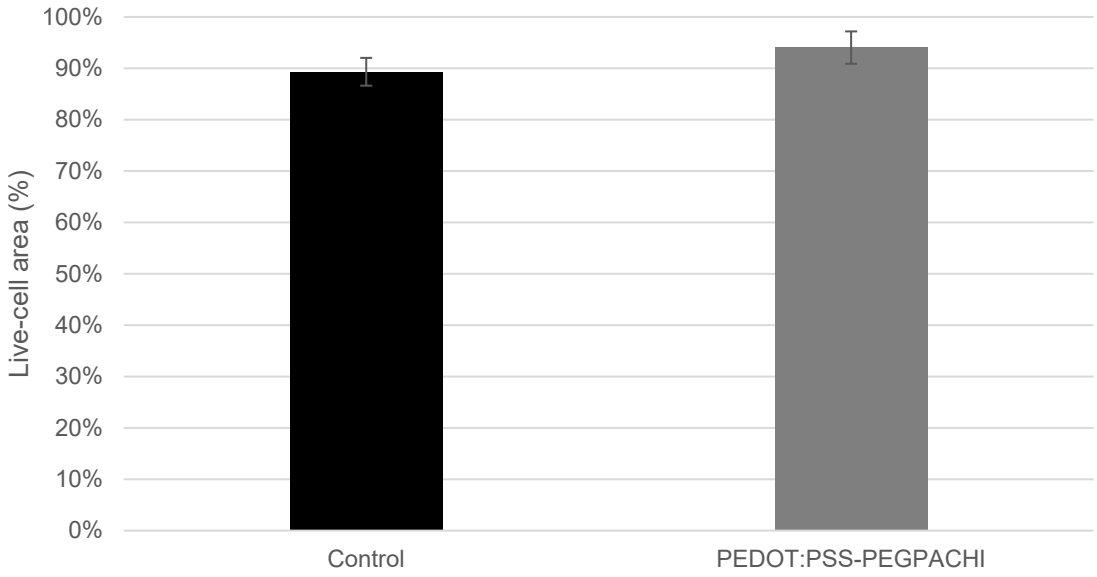


Figure 6.4: Live/Dead quantification of neuronal cultures exposed to PEDOT:PSS-PEGPACHI. Area-based Live/Dead quantification of neuronal cultures after 8 days. The control condition represents cell-only cultures, while the PEDOT:PSS-PEGPACHI condition combines the available PEGPACHI-related samples. Bars represent mean live-cell area and error bars represent standard deviation. The analysis was performed from Live/Dead images provided by the Leiden collaborators and quantified using ImageJ/Fiji.

Representative immunofluorescence images of the control, PEDOT:PSS-PAA, and PEDOT:PSS-PEGPACHI conditions are shown in Figure 6.5. The images were used to assess whether neuronal marker staining and nuclei remained visible after exposure to the hydrogel conditions.
The control condition showed a mean live-cell area of approximately 89%, indicating that most of the stained cell area corresponded to live cells after 8 days in culture. The combined PEDOT:PSS-PEGPACHI condition showed a mean live-cell area of approximately 94%, with a small standard deviation. This suggests that, under the tested conditions, PEDOT:PSS-PEGPACHI did not reduce the live-cell signal compared with the cell-only control.

However, this result should be interpreted carefully. As described in Section 6.3, the PEDOT:PSS-PEGPACHI hydrogels were observed to float in the culture medium and did not remain in stable direct contact with the neurons. Therefore, the Live/Dead result mainly reflects the effect of indirect exposure to the hydrogel in the culture medium, rather than a definitive direct-contact compatibility test.
Overall, the Live/Dead quantification supported the qualitative microscopy observations. PEDOT:PSS-PEGPACHI did not show obvious toxicity under the tested indirect-exposure conditions and showed a live-cell area comparable to the control. In contrast to PEDOT:PSS-DBSA, which showed poor biological compatibility in both the U87 and neuronal culture observations, PEDOT:PSS-PEGPACHI appeared more biologically favourable under the available testing conditions. Further experiments with improved hydrogel positioning would be needed to confirm its compatibility under stable direct cell-hydrogel contact.

6.5 Immunofluorescence observations

Immunofluorescence imaging was used to further assess the morphology of the neuronal cultures after exposure to the hydrogel conditions. The staining followed the approach used by Wang et al. [31]. Neuronal structures were labelled using mouse monoclonal anti-βIII-tubulin as the primary antibody, followed by goat anti-mouse Alexa Fluor 488 as the secondary antibody, giving the green fluorescence signal. Cell nuclei were counterstained with NucBlue, giving the blue fluorescence signal. In the Live/Dead images, Calcein AM was used as the live-cell indicator shown in green, while BOBO-3 iodide was used as the dead-cell indicator shown in red.

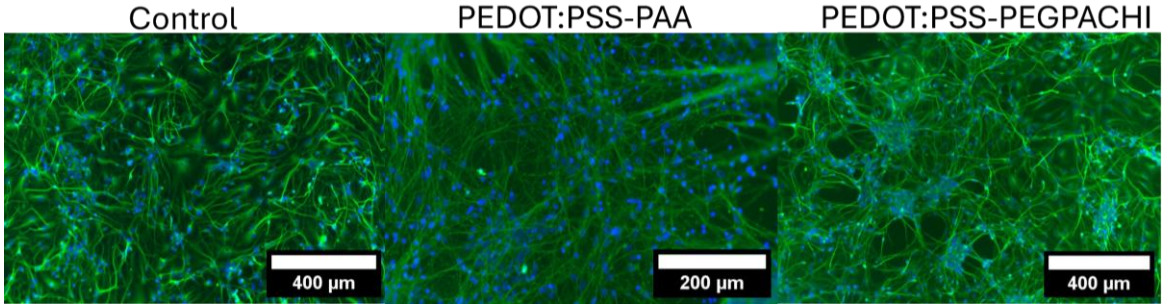


Figure 6.5: Immunofluorescence assessment of neuronal cultures exposed to PEDOT:PSS-based hydrogels after 8 days.
Representative immunofluorescence images of the cell-only control and neuronal cultures exposed to PEDOT:PSS-PAA and PEDOT:PSS-PEGPACHI. βIII-tubulin staining is shown in green and NucBlue nuclear counterstaining is shown in blue. PEDOT:PSS-PAA and PEDOT:PSS-PEGPACHI showed visible neuronal marker staining and nuclei after 8 days. Images were provided by the Leiden collaborators and adapted for this thesis.

The control condition showed a dense neuronal culture with clear green neuronal staining and visible blue nuclei throughout the image. Neurite-like structures were spread across the field of view, forming a connected network. This confirmed that the cell-only control supported neuronal survival and network formation over the 8-day culture period.
For the PEDOT:PSS-PAA condition, neuronal marker staining and nuclei were still visible, indicating that cells remained present after exposure to the hydrogel condition. The images showed neurite-like structures and cell bodies, although the culture appeared more heterogeneous than the control in some regions. This suggests that PEDOT:PSS-PAA did not cause the same severe loss of cells observed for PEDOT:PSS-DBSA. However, as discussed in Section 6.3, the PEDOT:PSS-PAA hydrogel was

floating in the culture medium and did not remain in stable direct contact with the neurons. Therefore, the immunofluorescence results mainly indicate that PEDOT:PSS-PAA did not cause obvious toxicity under indirect-exposure conditions.

For PEDOT:PSS-PEGPACHI, the immunofluorescence images also showed clear neuronal staining and nuclear signal. Neurite-like structures were visible across the images, and the culture remained present after exposure to the hydrogel condition. The morphology appeared broadly comparable to the control in the available images, supporting the Live/Dead results presented in Section 6.4. However, similar to PEDOT:PSS-PAA, the PEDOT:PSS-PEGPACHI hydrogel did not remain in stable direct contact with the cells. Therefore, these observations support the conclusion that PEDOT:PSS-PEGPACHI did not show strong indirect toxicity, but they do not fully demonstrate compatibility under stable direct cell/hydrogel contact.

Overall, the immunofluorescence observations supported the qualitative and Live/Dead results. PEDOT:PSS-PAA and PEDOT:PSS-PEGPACHI both showed remaining neuronal cultures with visible neuronal marker staining and nuclei after 8 days, while PEDOT:PSS-DBSA was not further assessed by immunofluorescence due to the poor brightfield response. These results suggest that the DBSA-free formulations were more biologically favourable than PEDOT:PSS-DBSA under the tested conditions, although further experiments are needed with improved hydrogel positioning to confirm direct-contact compatibility.

6.6 Overall biological compatibility discussion

The biological compatibility results showed clear differences between the three PEDOT:PSS-based hydrogel formulations. Although all three materials were developed as conductive hydrogel candidates for bioelectronic neural-interface applications, their biological responses were not equivalent. The results suggest that electrochemical performance alone was not sufficient to identify the most suitable formulation, since the strongest electrochemical response did not necessarily correspond to the most favourable biological behaviour.

PEDOT:PSS-DBSA showed the poorest biological compatibility. In the preliminary U87 MTS assay, all PEDOT:PSS-DBSA-related conditions resulted in strongly reduced metabolic activity compared with the untreated control. Direct exposure to PEDOT:PSS-DBSA resulted in low viability, and this decreased further after longer exposure. GelTrex coating produced only a limited short-term improvement, while the conditioned-medium experiment also showed low viability, suggesting that soluble components released from the hydrogel contributed to the negative cell response. This was consistent with the neuronal culture observations, where the available brightfield images showed a poor cell response and no clear healthy neuronal culture. Therefore, despite its strong electrochemical behaviour, PEDOT:PSS-DBSA was excluded from further biological consideration in this thesis

PEDOT:PSS-PAA showed a more favourable biological response than PEDOT:PSS-DBSA in the available neuronal culture images. Brightfield and immunofluorescence images showed that cells remained present after exposure to the PEDOT:PSS-PAA condition, with visible neuronal marker staining and nuclei. However, the interpretation of this formulation remained limited because Live/Dead quantification was not available. As a result, PEDOT:PSSPAA can be considered potentially more compatible than PEDOT:PSS-DBSA, but its biological response was not quantified in this experiment and should therefore be treated as inconclusive.

PEDOT:PSS-PEGPACHI showed the most promising biological response among the formulations tested. The qualitative microscopy images showed remaining neuronal cultures with visible immunofluorescence staining, and Live/Dead quantification showed a live-cell area comparable to the cell-only control. The control showed a mean live-cell area of approximately 89%, while the combined

PEDOT:PSS-PEGPACHI condition showed approximately 94%. This suggests that PEDOT:PSS-PEGPACHI did not reduce the live-cell signal under the tested conditions and appeared more biologically favourable than PEDOT:PSS-DBSA.

Overall, the biological results support PEDOT:PSS-PEGPACHI as the most promising formulation from the available cell-culture data. PEDOT:PSS-DBSA combined strong electrochemical performance with poor biological compatibility, making it unsuitable for further biological development in its current form. PEDOT:PSS-PAA appeared less harmful than PEDOT:PSS-DBSA, but the lack of quantitative Live/Dead data limited the strength of the conclusion. PEDOT:PSS-PEGPACHI provided the best balance in this chapter, showing no obvious severe toxicity in the available neuronal culture images and maintaining a live-cell area comparable to the control. Therefore, based on the biological compatibility results, PEDOT:PSS-PEGPACHI was selected as the most favourable formulation for further consideration.

7 PEDOT:PSS-based conducting Hydrogel electrodes - a proof of concept

7.1 Aim of the preliminary hydrogel-array device

After the material development, characterisation, and biological compatibility assessment described in the previous chapters, PEDOT:PSS-PEGPACHI was selected as the most suitable formulation for preliminary device integration. This formulation showed direct gelation behaviour, could be patterned into defined structures, showed measurable electrochemical activity, and gave the most favourable biological response among the tested PEDOT:PSS-based hydrogels.

The aim of this chapter was to demonstrate the preliminary integration of PEDOT:PSS-PEGPACHI into a PDMS hydrogel-array device and to evaluate whether the patterned hydrogel tracks could be electrically accessed. The device was designed as a proof-of-concept platform containing nine parallel hydrogel tracks with rounded electrode-site regions. The PDMS structure was placed on glass during filling to define the hydrogel pattern, after which the filled device could be peeled off for further handling and testing.

This chapter focuses on the development of the PDMS hydrogel-array device, including the design iterations, fabrication challenges, and practical limitations encountered during hydrogel integration. Preliminary electrical measurements were also performed to assess whether the PEDOT:PSS-PEGPACHI tracks could be contacted after integration into the device. The purpose was not to produce a final neural interface device, but to demonstrate a first step toward integrating the selected conductive hydrogel formulation into a patterned device structure.

7.2 Design development of the PDMS hydrogel-array device

The PDMS hydrogel-array device was developed through several design iterations in SolidWorks before the final geometry was selected. The overall aim was to create a PDMS structure containing defined hydrogel tracks and electrode-site regions that could be filled with PEDOT:PSS-PEGPACHI. Resin 3D printing was used to fabricate the moulds, because the device required small features that were difficult to produce using standard FDM printing. The main text focuses on the final design and the key design decisions, while additional SolidWorks designs, preliminary moulds, and early filling trials are provided in **Appendix I**.

The first design approach used small resin-printed pillars with a diameter of approximately 200 µm. These pillars were intended to form holes or electrode-site openings in the PDMS after curing. Although the Asiga resin printer was able to produce the small features and the printed structures were mechanically stable, this design was not considered practical for PDMS casting. The main limitation was demoulding: removing cured PDMS from many small 200 µm pillars would be difficult and could damage either the PDMS structure or the fine features of the mould. Therefore, this design was not selected for further device fabrication.

A second design was then developed using an array layout with raised electrode-site regions and narrow hydrogel tracks and electrode sites. In this design, the electrode-site regions were made higher than the tracks, with the aim of forming defined contact regions at the ends of the hydrogel structures. Microfluidic-style tracks were included so that the PEDOT:PSS-PEGPACHI precursor could flow

through the device and fill the patterned geometry. This approach worked in principle, because the precursor could enter the channels and move through the array. However, the filling process was not fully reliable. Some tracks did not fill completely, and the needle did not seal tightly inside the inlet region, causing part of the precursor to leak out instead of flowing through the tracks. In addition, after gelation/annealing of PEDOT:PSS-PEGPACHI at 75 °C, the hydrogel did not always remain as one continuous structure inside the small channels. Instead, separation of the hydrogel was observed, suggesting that the geometry was too small to support reliable formation of a continuous hydrogel track. Based on these limitations, the final design was enlarged to improve filling and hydrogel continuity. The final PDMS hydrogel-array device consisted of nine parallel tracks, each with a width of 1 mm, a thickness of 200 µm, and a length of 1 cm. Each track ended in a rounded electrode-site region with a diameter of 1.2 mm. A larger inlet chamber was added at the beginning of the array to improve precursor loading. During filling, the thick PDMS wall near this chamber was punctured and the PEDOT:PSS-PEGPACHI precursor was injected into the device. This allowed the precursor to flow more uniformly across the array and fill the tracks and electrode-site regions.

When the track thickness was not sufficient after the first filling step, additional PEDOT:PSS-PEGPACHI precursor was added manually near the tracks. A blade was then used in a doctor-blade like manner to push the precursor into the patterned regions and improve filling. This manual step helped obtain more complete hydrogel tracks and filled electrode-site regions. After filling, the PEDOT:PSS-PEGPACHI hydrogel was gelled using the same thermal treatment as the bulk formulation.

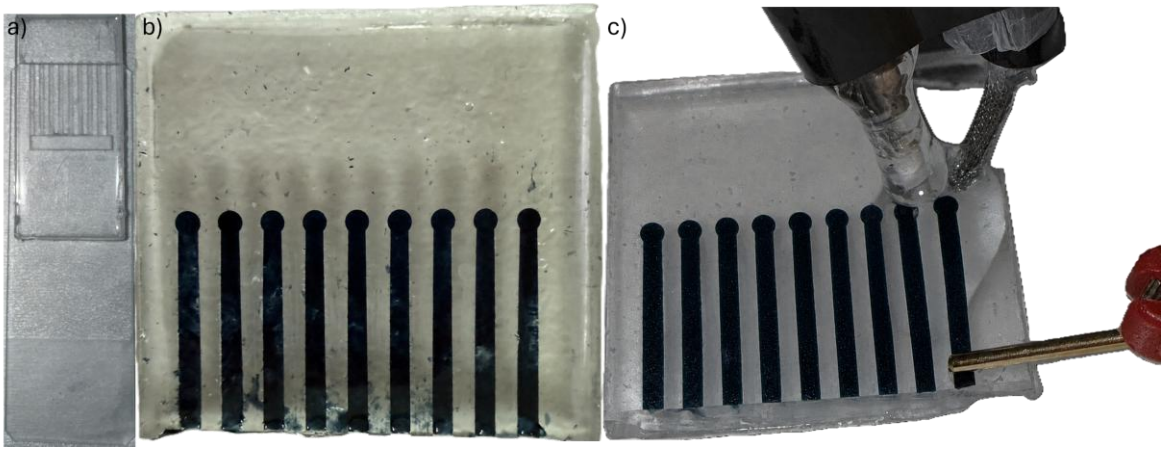


Figure 7.1: Final PDMS hydrogel-array device design and PEDOT:PS-PEGPACHI integration. (a) Final array design containing nine parallel PDMS-defined channels with rounded electrode-site regions. (b) Fabricated PDMS hydrogel-array device after filling with PEDOT:PSS-PEGPACHI, forming patterned hydrogel electrodes. (c) Preliminary electrical access of the PEDOT:PSS-PEGPACHI hydrogel electrodes during testing. Final design used 1 mm wide, 200 µm thick, and 1 cm long electrode lines with 1.2 mm diameter electrode-site regions.

Overall, the design development showed that the device geometry had to be large enough to allow reliable PDMS demoulding, precursor filling, and continuous hydrogel formation. The final enlarged design provided a more practical geometry for integrating PEDOT:PSS-PEGPACHI into a patterned PDMS array and was therefore selected for preliminary electrical testing.

7.3 Fabrication and PEDOT:PSS-PEGPACHI integration

After selecting the final device geometry, the PDMS hydrogel-array device was fabricated using the resin-printed mould. PDMS was prepared using a 10:1 base-to-curing-agent ratio, poured into the mould, and cured overnight. When faster fabrication was required, the uncured PDMS was first degassed in a desiccator to remove trapped air bubbles and then cured on a hot plate at 90 °C for approximately 1.5 h.

After curing, the PDMS structure was carefully removed from the resin mould. The demoulded PDMS device contained the negative features of the mould, forming the hydrogel tracks and electrode-site regions. The device was then temporarily placed on a clean glass substrate during filling. No plasma bonding was used. Instead, the clean PDMS surface adhered sufficiently to the glass to create a temporary seal, which allowed the hydrogel precursor to be introduced into the patterned regions without permanent bonding.

PEDOT:PSS-PEGPACHI precursor was then introduced into the device through the inlet chamber. The thick PDMS wall near the chamber was punctured, and the precursor was injected so that it could flow through the array and fill the nine parallel tracks and rounded electrode-site regions. In some cases, additional PEDOT:PSS-PEGPACHI precursor was added near the tracks and manually pushed into the patterned regions using a blade in a doctor-blade-like manner. This step was used to improve filling when the initial precursor volume did not fully occupy the track thickness.

After filling, the PEDOT:PSS-PEGPACHI precursor was gelled using the same thermal treatment as the bulk formulation, at 75 °C for approximately 1 h. After gelation, the filled PDMS device was peeled from the glass substrate. The patterned PEDOT:PSS-PEGPACHI hydrogel tracks remained inside the PDMS structure, forming the preliminary hydrogel-array device shown in Figure 7.1. The device was then stored overnight in 1x DPBS before preliminary electrical testing.

Overall, this fabrication approach allowed PEDOT:PSS-PEGPACHI to be integrated into a patterned PDMS structure without permanent glass bonding. The temporary glass support was useful during filling because it helped seal the bottom of the PDMS features, while still allowing the device to be removed after hydrogel formation. This provided a simple proof-of-concept method for producing PEDOT:PSS-PEGPACHI hydrogel tracks inside a PDMS hydrogel-array device.

7.4 Preliminary electrical access and measurement of PEDOT:PSS-PEGPACHI hydrogel electrodes

After fabrication and overnight storage in 1x DPBS, the PEDOT:PSS-PEGPACHI hydrogel-array device was evaluated to determine whether the patterned hydrogel tracks could be electrically accessed. This step was important because the previous sections demonstrated hydrogel integration visually, but the device also needed to show that the patterned PEDOT:PSS-PEGPACHI structures could function as conductive tracks.

Each hydrogel track was measured separately using EIS and CV. Electrical contact was made using a gold pogo pin connected to the potentiostat through a crocodile clip. During measurement, the pogo pin was manually positioned so that it pressed gently against the rounded hydrogel electrode-site region at the end of each track. A small amount of force was applied to maintain contact, while avoiding excessive deformation or damage to the hydrogel. The reference and counter electrodes were placed in contact with the electrolyte above the hydrogel region, following the same general measurement principle used for the PDMS measuring platform.

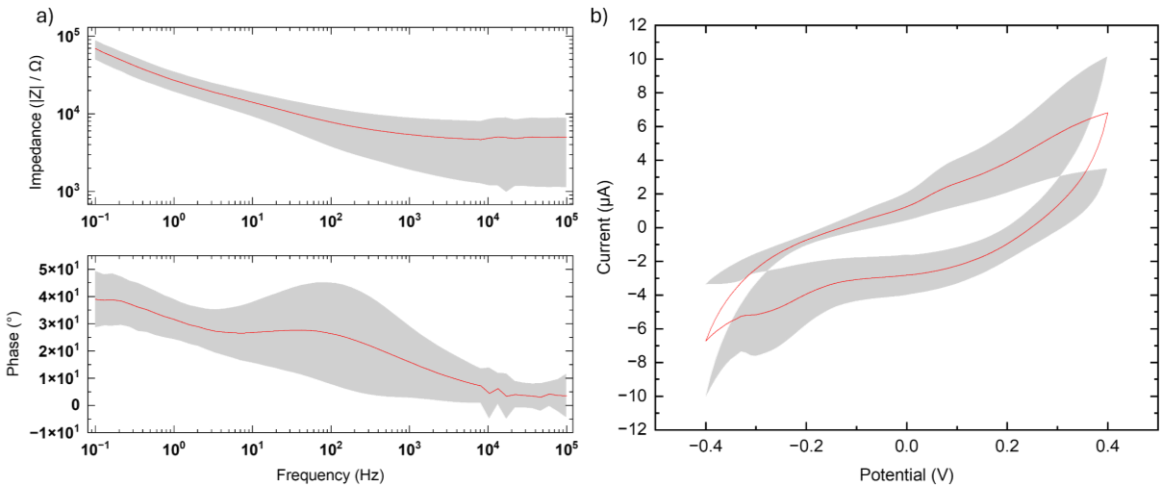


Figure 7.2: Preliminary electrochemical measurement of PEDOT:PSS-PEGPACHI tracks integrated into the PDMS hydrogel-array device.
(a) Impedance magnitude |Z| and phase angle as a function of frequency measured by EIS in 1x DPBS. (b) Cyclic voltammetry response recorded between −0.4 and +0.4 V. The red line represents the mean response and the grey shaded area represents mean ± SD for individually measured PEDOT:PSS-PEGPACHI tracks. Measurements were performed after overnight storage in 1x DPBS using a manually positioned gold pogo pin to contact the rounded hydrogel electrode-site regions.

Additional EIS-derived plots for the PEDOT:PSS-PEGPACHI hydrogel tracks integrated into the PDMS hydrogel-array device, including capacitance, real impedance, and Nyquist-type response, are provided in **Appendix K**.

The EIS response showed that the patterned PEDOT:PSS-PEGPACHI tracks could be electrically measured after integration into the PDMS hydrogel-array device. The impedance decreased with increasing frequency, from values in the order of 10^4-10^5 Ω at low frequency to approximately 10^3-10^4 Ω at higher frequency. This frequency-dependent response indicates that the hydrogel tracks were conductive, but that the electrical pathway was more resistive than in the bulk hydrogel measurements presented in Chapter 5. This was expected because the hydrogel was confined within narrow patterned tracks and was contacted manually through the rounded electrode-site regions.

The phase response also showed a frequency-dependent behaviour. The phase angle was positive at low frequency and gradually decreased towards values closer to 0° at higher frequency. This suggests that the integrated hydrogel tracks did not behave as purely resistive conductors, but still showed a mixed resistive/capacitive response. The relatively broad grey region indicates variability between individual tracks, which was likely influenced by differences in local filling, hydrogel continuity, hydration, and manual pogo-pin contact.

The CV response further confirmed that the PEDOT:PSS-PEGPACHI tracks were electrically accessible. The current remained in the microampere range, reaching approximately −7 to +7 μA in the mean response. This current was much lower than that measured for bulk PEDOT:PSS-PEGPACHI samples, but it was still measurable and showed an enclosed voltametric response. The lower current is consistent with the smaller hydrogel volume, thinner track geometry, and manual external contact used in the array device.

Overall, the preliminary electrical measurements demonstrated that PEDOT:PSS-PEGPACHI could be integrated into patterned PDMS tracks while maintaining measurable electrochemical activity. The results confirm that the hydrogel tracks could be contacted individually and that the array design provided electrical access to the integrated material. However, the relatively high impedance and

variability show that this remains an early proof-of-concept device. The response was likely limited by manual pogo-pin contact, track-to-track filling differences, and the small hydrogel geometry.

7.5 Comparison with hydrogel-based electrode-array approaches

To position the preliminary PDMS hydrogel-array device within the broader field of soft conductive electrode arrays, the impedance response of the PEDOT:PSS-PEGPACHI hydrogel tracks was compared with selected hydrogel-based and PEDOT:PSS-based electrode-array approaches. This comparison is not intended as a direct performance ranking, because the systems differ in material composition, electrode geometry, contact method, electrolyte environment, and device maturity. Instead, the comparison provides context for the order of magnitude of the impedance response achieved in this thesis.

Tringides et al. reported a fully viscoelastic surface electrode array based on conductive hydrogel tracks made from an alginate matrix loaded with carbon nanomaterials. Their device included conductive hydrogel tracks, viscoelastic encapsulation layers, electrode openings, and a flexible connector. The electrode sites had a diameter of 700 µm, corresponding to an electrode surface area of approximately 0.38 mm^2. The reported median impedance at 1 kHz was 167 ± 40 kΩ for five devices containing 40 tracks. The same work also demonstrated intertrack resistance in the MΩ range, stability in PBS, mechanical cycling, and in vivo recording and stimulation, showing that this was a fully developed hydrogel-based electrode-array platform rather than only a proof-of-concept device [47].

Ongoing work within the Bioelectronics group by Mustafeez Shah is exploring microfabricated full PEDOT:PSS thin-film electrodes for transparent and stable bioelectronic interfaces. These structures are relevant because microfabricated thin-film electrode arrays represent a more established device architecture for neural recording and stimulation. Based on the 1 mm electrode structure shown in the group data, the impedance at 1 kHz is approximately in the 10 kΩ range. This system is closer to the present thesis in terms of using PEDOT:PSS as the conductive material, but it differs because the electrodes consist of full PEDOT:PSS thin-film structures rather than PEDOT:PSS incorporated into a hydrogel formulation. In contrast, the device developed in this thesis uses PEDOT:PSS-PEGPACHI as a soft conductive hydrogel patterned into PDMS-defined electrode channels, forming hydrogel electrodes after gelation.

Table 7.1: Comparison of the PEDOT:PSS-PEGPACHI hydrogel-array device with hydrogel-based and PEDOT:PSS-based electrode-array approaches.

System	Conductive material	Device stage	Electrode/track geometry	Impedance at ~1 kHz	Main relevance
Tringides et al.	Alginate-carbon conductive hydrogel	Fully viscoelastic electrode array	700 µm diameter electrode sites; electrode area ≈ 0.38 mm^2	167 ± 40 kΩ	Published hydrogel-array benchmark
Ongoing group work	Full PEDOT:PSS	Patterned PEDOT:PSS electrode platform	1 mm PEDOT:PSS electrode structure	~10 kΩ	Relevant PEDOT:PSS-track comparison
This thesis	PEDOT:PSS-PEGPACHI hydrogel	Preliminary PDMS hydrogel-array device	PDMS-defined hydrogel tracks and electrode sites	5.36 ± 3.50 kΩ	First PEGPACHI hydrogel-electrode array

The PEDOT:PSS-PEGPACHI hydrogel tracks developed in this thesis showed an impedance of 5.36 ± 3.50 kΩ at approximately 1 kHz, which is lower than the impedance reported for the viscoelastic alginate-carbon hydrogel array by Tringides et al. and in a similar order of magnitude to the full PEDOT:PSS electrode structures being developed within the group. However, this comparison should be interpreted carefully. The Tringides et al. device is a fully assembled and validated array with integrated contacts, encapsulation, stability testing, and in vivo functionality, whereas the PDMS hydrogel-array device in this thesis is still a preliminary platform with manually contacted hydrogel tracks. Similarly, the ongoing full PEDOT:PSS electrode work uses a different material architecture from the PEDOT:PSS-PEGPACHI hydrogel used here.

Therefore, the main significance of the present device is not that it outperforms existing systems, but that it demonstrates that the PEDOT:PSS-PEGPACHI hydrogel can be patterned into electrically accessible tracks with impedance values in a relevant range for soft bioelectronic electrode-array development. This supports the potential of the PEGPACHI formulation for further device optimisation, especially if future designs include integrated electrodes, improved track reproducibility, and more controlled hydrogel-electrode contact.

7.6 Preliminary device assessment and limitations

The PDMS hydrogel-array device successfully demonstrated the preliminary integration of PEDOT:PSS-PEGPACHI into a patterned device structure. In the final design, all nine hydrogel tracks could be filled, gelled, removed from the temporary glass support, stored overnight in 1x DPBS, and electrically measured. Compared with the earlier smaller designs, the enlarged 1 mm-wide track geometry provided a more stable and practical structure for hydrogel integration.

Electrical measurements were performed on three different devices, with each hydrogel track measured individually. The EIS and CV results confirmed that the patterned PEDOT:PSS-PEGPACHI tracks remained electrically accessible after fabrication and hydration. This showed that the hydrogel could form continuous conductive structures inside the PDMS array and that the rounded electrode-site regions could be used for external electrical contact.

However, the measurements also showed variability between tracks. Some tracks gave lower impedance and clearer electrochemical responses, while others showed much higher impedance. This was most likely related to the manual contact between the gold pogo pin and the hydrogel electrode-site region. Because the pogo pin had to be positioned by hand and pressed gently against the hydrogel, small differences in contact pressure, contact area, and alignment could strongly influence the measured response. Therefore, part of the variability was likely caused by the measurement approach rather than only by differences in the hydrogel tracks themselves.

The main limitation of the current device was therefore not the filling of the final 1 mm tracks, which was relatively stable, but the way the tracks were electrically contacted. The use of a manually positioned pogo pin allowed rapid proof-of-concept testing, but it did not provide a fully reproducible or permanently integrated electrode interface. As a result, the device was useful for demonstrating electrical access to the PEDOT:PSS-PEGPACHI tracks, but it was not yet suitable for highly reproducible device-level electrochemical characterisation.

The comparison with previously reported hydrogel-based electrode arrays showed that the PEDOT:PSS-PEGPACHI tracks had impedance values within a relevant range for soft electrode-array development, although direct comparison is limited by differences in device geometry, electrode area, conductive material, and contact configuration.

Overall, the preliminary device results showed that PEDOT:PSS-PEGPACHI can be integrated into a patterned PDMS hydrogel-array device and retain measurable electrochemical activity after hydration. The device should therefore be considered a successful proof-of-concept platform for hydrogel integration. At the same time, the variability between tracks shows that future versions should focus on improving the electrical contact strategy, especially by replacing manual pogo-pin contact with integrated electrode structures.

8 Conclusions and Future Work

8.1 Main conclusions

This thesis focused on the development, optimisation, and characterisation of PEDOT:PSS-based conductive hydrogels for bioelectronic neural-interface applications. Three hydrogel formulations were investigated: PEDOT:PSS-DBSA, PEDOT:PSS-PAA, and PEDOT:PSS-PEGPACHI. These formulations represented different material-design strategies and allowed comparison between a literature-based additive-induced hydrogel, a polymer-network-based hydrogel, and a DBSA-free hydrogel formulation developed in this thesis.

The first main conclusion is that all three PEDOT:PSS-based hydrogel systems could be prepared as soft, hydrated materials, but their formulation behaviour was clearly different. PEDOT:PSS-DBSA was the most straightforward formulation to prepare and showed fast gelation after optimisation of the DBSA concentration and mixing sequence. PEDOT:PSS-PAA required a more complex fabrication route, including freeze-drying, redox polymerisation, post-treatment, annealing, and rehydration. PEDOT:PSS-PEGPACHI was developed as a new DBSA-free formulation based on PEDOT:PSS, phytic acid, chitosan, and PEGDE. This formulation was especially important because it provided an alternative direct-gelation route without relying on DBSA.

Electrochemical characterisation showed that the three hydrogels had distinct charge-transport behaviour. PEDOT:PSS-DBSA gave the strongest electrochemical response, with the lowest impedance and highest CV current response. PEDOT:PSS-PAA showed the weakest electrochemical response, which suggests that the PAA network and processing route may have limited the formation of continuous PEDOT:PSS conductive pathways. PEDOT:PSS-PEGPACHI showed intermediate electrochemical behaviour, with clearer activity than PEDOT:PSS-PAA while avoiding the DBSA-based formulation route.

Mechanical characterisation showed that all three formulations had effective Young's modulus values in the soft kPa range under hydrated nanoindentation conditions. PEDOT:PSS-DBSA showed the most uniform local mechanical response, although it was fragile during handling. PEDOT:PSS-PAA was easier to handle and more mechanically stable, but showed higher local variability, likely due to its more complex processing route and heterogeneous structure. PEDOT:PSS-PEGPACHI also remained in the kPa range but showed sample-to-sample variability, probably related to the multicomponent nature of the formulation.

The biological compatibility results showed clear differences between the formulations. PEDOT:PSS-DBSA showed poor compatibility in the preliminary metabolic activity assessment, supporting the need for a DBSA-free alternative. In contrast, PEDOT:PSS-PAA and PEDOT:PSS-PEGPACHI supported visible neuronal cultures after exposure. PEDOT:PSS-PEGPACHI showed high Live/Dead viability compared with the control condition, making it the most promising formulation from the combined material and biological assessment.

Finally, PEDOT:PSS-PEGPACHI was successfully integrated into a preliminary PDMS hydrogel-array device. The hydrogel precursor could be patterned into tracks, and the resulting hydrogel structures were electrically accessible after gelation and hydration. The impedance values measured from the PEDOT:PSS-PEGPACHI tracks were in a relevant range when positioned against hydrogel-based and PEDOT:PSS-based electrode-array approaches. However, the comparison also showed that the device remains at an early proof-of-concept stage, especially because it does not yet include integrated electrodes, encapsulation, or long-term device validation. Overall, this result demonstrated that the

thesis-developed PEDOT:PSS-PEGPACHI formulation could be transferred from bulk hydrogel preparation towards preliminary patterned device integration.

8.2 Answer to the research aim

The aim of this thesis was to develop and characterise PEDOT:PSS-based conductive hydrogels as soft material candidates for bioelectronic neural-interface applications. Based on the results presented in this work, this aim was achieved at the level of material development, characterisation, biological screening, and preliminary device integration.

Overall, the results show that PEDOT:PSS-based conductive hydrogels are promising materials for bioelectronic neural-interface applications. However, their suitability depends strongly on the formulation strategy, additive selection, processing route, and integration method. The comparison between PEDOT:PSS-DBSA, PEDOT:PSS-PAA, and PEDOT:PSS-PEGPACHI showed that the presence of PEDOT:PSS alone is not enough to define the final material performance. Instead, the surrounding hydrogel network and gelation chemistry strongly influence electrochemical behaviour, mechanical handling, biological response, and device compatibility.

A key outcome of this thesis was the development of the PEDOT:PSS-PEGPACHI formulation. Although PEDOT:PSS-DBSA showed the strongest electrochemical response, its overall suitability was limited by practical and biological concerns. PEDOT:PSS-PAA provided better mechanical robustness, but its electrochemical response was weaker and its fabrication route was more complex. In contrast, PEDOT:PSS-PEGPACHI provided a more balanced material profile. It showed measurable electrochemical activity, remained within the soft hydrogel stiffness range, supported favourable biological results, and could be integrated into a preliminary PDMS hydrogel-array device.

Therefore, the thesis demonstrates that PEDOT:PSS-based conductive hydrogels can be developed as relevant soft material candidates for bioelectronic neural interfaces. Among the formulations studied, PEDOT:PSS-PEGPACHI emerged as the most promising overall candidate because it combined a DBSA-free formulation route with electrochemical functionality, hydrogel-like mechanical behaviour, biological compatibility, and preliminary device integration potential. This suggests that the new PEDOT:PSS-PEGPACHI formulation could be a strong candidate for further optimisation towards future soft bioelectronic neural-interface platforms.

8.3 Limitations

Although this thesis demonstrated the potential of PEDOT:PSS-based conductive hydrogels for bioelectronic neural-interface applications, several limitations should be considered when interpreting the results. These limitations do not invalidate the findings, but they define the level at which the conclusions can be made. Overall, the work should be viewed as material development and preliminary validation rather than final device-level optimisation.

One limitation was related to formulation reproducibility. The three hydrogel systems showed different levels of sensitivity to processing conditions, including mixing, temperature, gelation time, post-treatment, and handling. This was especially important for PEDOT:PSS-PAA and PEDOT:PSS-PEGPACHI, which required more complex processing than PEDOT:PSS-DBSA. The PEGPACHI formulation was developed in this thesis and therefore its gelation mechanism remains a proposed explanation based on the known roles of PEDOT:PSS, phytic acid, chitosan, and PEGDE, together with the observed experimental behaviour. Further chemical and structural characterisation would be needed to confirm the exact interactions responsible for gel formation and stabilisation.

The electrochemical measurements also had limitations. The measured response was strongly affected by the measurement configuration, hydrogel geometry, hydration state, and electrode-hydrogel contact. The PDMS measuring platform and Swagelok-based setup provided useful comparative information, but they were not fully equivalent measurement systems. In addition, conductivity and capacitance values were not extracted in this thesis because the setups were mainly used to compare the relative electrochemical behaviour of the formulations. Therefore, the EIS and CV results should be interpreted as comparative electrochemical characterisation rather than absolute material constants.

Mechanical characterisation was limited by the local nature of nanoindentation. The hydrogels were soft, hydrated, and in some cases fragile or difficult to position during testing. Surface unevenness, local hydrogel heterogeneity, and probe-sample contact could influence the measured effective Young's modulus values. As a result, the mechanical results represent effective local hydrated-state stiffness values rather than absolute bulk Young's moduli. The measurements were useful for comparing the relative stiffness range of the formulations, but more extensive mechanical testing would be needed to fully characterise their bulk behaviour.

The biological compatibility assessment was also preliminary. The experiments provided important first indications of how the different hydrogels behaved under cell culture conditions, but the number of tested conditions and replicates was limited. PEDOT:PSS-DBSA was assessed using a preliminary metabolic activity assay, while neuronal culture experiments were performed for PEDOT:PSS-PAA and PEDOT:PSS-PEGPACHI. Live/Dead quantification was performed for PEDOT:PSS-PEGPACHI, but not for all formulations under the same conditions. Therefore, the biological results support the potential of PEGPACHI, but further biological validation would be needed before making stronger conclusions about long-term neural compatibility.

Finally, the PDMS hydrogel-array device was a proof-of-concept platform. Although PEDOT:PSS-PEGPACHI could be integrated into patterned hydrogel tracks and electrically accessed, the device was not yet a fully optimised neural-interface platform. Electrode contact was still performed manually, and reproducible track filling, hydrogel continuity, and permanent electrode integration require further development. In addition, the comparison with published and ongoing electrode-array approaches should be interpreted as a positioning comparison rather than a direct performance comparison, because the materials, electrode dimensions, contact methods, and device architectures were different. Longer and more systematic stability testing under relevant operating and culture conditions would also strengthen the device-level conclusions.

Together, these limitations show that the thesis provides a foundation for PEDOT:PSS-based conductive hydrogel development, but further optimisation and validation are required before these materials can be translated into more advanced neural-interface platforms. These limitations provide the basis for the future work proposed in the following section.

8.4 Future work

Future work should focus mainly on the further optimisation of the PEDOT:PSS-PEGPACHI hydrogel, since this formulation showed the most promising overall balance between material properties, biological compatibility, and device-integration potential. The formulation could be optimised by systematically varying the ratios of phytic acid, chitosan, and PEGDE, as well as the mixing method, heating temperature, gelation time, and conditioning procedure. This would help improve gel uniformity, reduce sample-to-sample variability, and increase reproducibility between batches.

A second important direction is to better understand the formation mechanism and internal structure of the PEDOT:PSS-PEGPACHI hydrogel. In this thesis, the proposed gelation mechanism was based on the known roles of the individual components and the observed experimental behaviour. Future studies

should investigate this mechanism more directly using chemical and structural characterisation methods such as FTIR, SEM or cryo-SEM, swelling analysis, water-content measurements, and leaching studies. These experiments would help clarify how PEDOT:PSS, phytic acid, chitosan, and PEGDE interact within the final hydrogel network.

Further mechanical characterisation is also needed. Nanoindentation provided useful information about the local hydrated stiffness of the hydrogels, but additional testing would give a more complete understanding of their mechanical behaviour. Future work should include bulk rheology, compression testing, tensile testing where possible, stress-relaxation measurements, cyclic loading, swelling-related mechanical changes, and long-term mechanical stability under hydrated conditions. These tests would allow the mechanical behaviour of the hydrogels to be evaluated more broadly and compared more directly with the requirements of soft neural-interface materials.

Biological testing should also be expanded. The initial results showed that PEDOT:PSS-PEGPACHI supported favourable neuronal culture outcomes, but more systematic validation is needed. This work is already ongoing with collaborators in Applied Sciences, where the protocol for culturing cells together with the hydrogels is currently being optimised to obtain more robust and publishable biological results. Future studies should include more replicates, longer culture periods, Live/Dead quantification for all relevant conditions, immunostaining, direct-contact studies, and possibly encapsulation or 3D culture approaches. This would provide a stronger assessment of the suitability of PEDOT:PSS-PEGPACHI for neural bioelectronic applications.

The PDMS hydrogel-array device should also be further developed. The proof-of-concept device demonstrated that PEDOT:PSS-PEGPACHI could be patterned into hydrogel tracks and electrically accessed, but the platform still requires optimisation. Future versions should include more reliable hydrogel filling, improved track continuity, better control of hydrogel dimensions, and integrated or permanent electrodes instead of manually positioned contacts. Sterilisation-compatible fabrication and miniaturisation should also be considered if the platform is to be used for biological experiments or more advanced neural-interface studies.

In the longer term, the PEDOT:PSS-PEGPACHI formulation could be developed further as a soft conductive material for in vitro neural-interface platforms and, more cautiously, for future implantable neural-interface applications. Before this can be achieved, the formulation would need more extensive validation of its reproducibility, stability, electrochemical behaviour, mechanical performance, and biological response. The results of this thesis, together with the ongoing biological work with the Applied Sciences collaborators, provide a basis for preparing this work for publication and for further developing PEDOT:PSS-PEGPACHI as a candidate material for soft bioelectronic neural interfaces.

8.5 Final statement

This thesis demonstrates that PEDOT:PSS-based conductive hydrogels can be developed as soft and hydrated material candidates for bioelectronic neural-interface applications. By comparing PEDOT:PSS-DBSA, PEDOT:PSS-PAA, and PEDOT:PSS-PEGPACHI, the work showed that the final performance of these materials depends strongly on the gelation strategy, processing route, and additive system. Among the formulations investigated, PEDOT:PSS-PEGPACHI emerged as the most promising overall candidate because it combined a DBSA-free formulation, measurable electrochemical activity, soft hydrogel-like mechanical behaviour, favourable preliminary biological compatibility, and successful proof-of-concept device integration.

The main contribution of this thesis is therefore the development and first validation of PEDOT:PSS-PEGPACHI as a new conductive hydrogel formulation for soft bioelectronic applications. Although

further optimisation and validation are required, the results provide a strong foundation for future work towards publishable biological studies and more advanced hydrogel-based neural-interface platforms.

Appendix A. Optimised protocol for PEDOT:PSS-DBSA hydrogel preparation

A.1 Purpose

This protocol describes the optimised preparation of PEDOT:PSS-DBSA hydrogels used in this thesis. The formulation was adapted from the room-temperature PEDOT:PSS hydrogel method reported by Zhang et al. and optimised for reproducible gel formation, mixing, and mould casting.

A.2 Materials

- PEDOT:PSS PH1000
- 4-dodecylbenzenesulfonic acid (DBSA)
- 1X DPBS for storage
- Deionised water, if used for cleaning or dilution

A.3 Equipment and labware

- Fisherbrand Select ultrasonic bath
- Fisherbrand ZX4 IR Vortex Mixer
- Micropipettes and tips
- 0.45 µm cellulose acetate filters
- Moulds for hydrogel casting
- Refrigerator set to approximately 5 °C

A.4 Final optimised formulation

- For each hydrogel batch, 40 µL DBSA was added to 1 mL PEDOT:PSS PH1000, corresponding to 4% v/v DBSA relative to PEDOT:PSS volume.

A.5 Procedure

1. Gently shake the PEDOT:PSS PH1000 dispersion to obtain a homogeneous suspension.
2. Sonicate the PEDOT:PSS dispersion for 10 min.
3. Filter the PEDOT:PSS dispersion through a 0.45 µm cellulose acetate filter.
4. Transfer 1 mL of filtered PEDOT:PSS into a clean container.
5. Add 40 µL DBSA to the PEDOT:PSS dispersion.
6. Sonicate the mixture for 2 min.
7. Vortex the mixture for 2 min at 800 rpm.
8. Sonicate the mixture again for 2 min.
9. Carefully cast the mixture into the selected moulds, avoiding bubble formation where possible.
10. Leave the samples undisturbed at room temperature until gelation is observed. Gelation occurred after approximately 30 min.
11. Use the gels directly for characterisation or immerse them in 1X DPBS and store at approximately 5 °C until further use.

A.6 Notes

The final protocol was selected after optimisation of the mixing sequence and DBSA concentration. Preliminary trials included different DBSA concentrations, but the final formulation used for characterisation was 4% v/v DBSA.

Appendix B. EKL-approved protocol for PEDOT:PSS-PAA hydrogel fabrication

Run number: P2026-13
Protocol title: PEDOT:PSS/PAA Hydrogel Semiconductor Matrix Fabrication
Valid from: February 2026

This appendix contains the EKL-approved process flowchart used for the preparation of PEDOT:PSS-PAA hydrogels in the cleanroom. The protocol includes the approved chemical list, cleanroom handling remarks, precursor preparation, redox-initiated gelation, EMIM-ES treatment, solvent exchange, thermal annealing, and rehydration steps. The flowchart lists PEDOT:PSS PH1000, acrylic acid, MBAA, DMSO, H_2O_2, L-ascorbic acid, EMIM-ES, and PBS as the starting materials, and describes the key fabrication steps including 15 µL H_2O_2 followed by 15 µL ascorbic acid, EMIM-ES overnight soaking, 70:30 v/v EMIM-ES:water solvent exchange for 6 h, annealing at 80 °C for 6 h and 130 °C for 2 h, and final rehydration in PBS.

GENERAL REMARKS

1. Always follow the "Security and Behavior" rules when working in the Dimes cleanrooms.
2. Always handle wafers with care during processing. Use cleanroom gloves and work as clean as possible.
3. Always check equipment and process conditions before starting a process.

   Directly notify the responsible person(s) **and** other users when there are problems with equipment operation or contamination. Do not try to repair or clean unknown equipment yourself, and never try to refresh a contaminated etch or cleaning bath !
4. Always clean wafers after several hours of storage **before** performing a coating, furnace, epitaxy or deposition step. Wafers do not have to be cleaned **after** a furnace or epitaxy step if the next process step is carried out immediately.

   Use the correct cleaning procedure:

- Acetone or Tepla stripper	for photoresist removal
- HNO_3 100%	for wafers which do not need a HNO_3 65% step
- HNO_3 100% metaal	for wafers which are or have been in contact with a metal
- HNO_3 100% and HNO3 65%	for all other wafers

5. Wafers that are covered with a resist or a metal layer may **never** be processed in a furnace. Only alloying is allowed for wafers with an aluminium layer.
6. It is allowed to use the Leitz MPV-SP or SOPRA measurement system for layer thickness measurements on the wafers of a process batch. These measurements are non-destructive and without contact to the wafer surface. If these methods

cannot be used on your wafer, or when sheet resistance and/or junction depth measurements must be performed, an extra wafer has to be processed for measuring.

7. All substrates, layers and chemicals which are not standard being used in the Dimes 01/02/03/04 or Dimos 01 production processes are considered to be "non-standard" materials, and can be possibly contaminating.

   The use of those materials for processing in the class 100 cleanroom and SAL must **always** be evaluated and approved by the PAC committee. It is strictly forbidden to use "non-standard"materials without permission.

   Check the PAC "Rules & Instructions" - available on the internet - for more details.

8. Wafers that are contaminated may never be processed in any of the equipment without permission of the PAC committee. Special precautions may have to be taken, like the use of a special substrate holder or container.

9. **Always perform all the measurements and inspection steps, and write down the results in your journal and in the result tables in the cleanroom !!** The results can be used to check the condition of processes and/or equipment.

STARTING MATERIAL

1. Chemical List

PEDOT:PSS PH 1000 - [Poly(3,4-ethylenedioxythiophene)-poly(styrenesulfonate)]
Supplier: Heraeus
Product code: 81076212-1000ML
Phase: Liquid
Storage location: Firdge 2-5 oC
CAS no. 155090-83-8

Acrylic acid (AA) - monomer (for PAA network)
Supplier: Sigma-Aldrich (Merck)
Product code: 147230 (anhydrous, MEHQ inhibited)
Phase: Liquid
CAS no.: 79-10-7

MBAA - N,N′-Methylenebisacrylamide
Supplier: Sigma-Aldrich (Merck)
Product code: M7279
Phase: Powder
CAS no.: 110-26-9

DMSO - Dimethyl sulfoxide
Supplier: Sigma-Aldrich (Merck)
Product code: 472301
Phase: Liquid
CAS no.: 67-68-5

Hydrogen peroxide solution (H_2O_2)
Supplier: Sigma-Aldrich (Merck)
Product code: H1009 (30% w/w in H_2O)
Phase: Liquid
Storage temp: 2–8 °C
CAS no.: 7722-84-1

L-Ascorbic acid
Supplier: Sigma-Aldrich (Merck)
Product code: A92902
Phase: Powder
CAS no.: 50-81-7

EMIM-ES (1-ethyl-3-methylimidazolium ethyl sulfate)
Supplier: Carl Roth
Article no.: 2054.1
Phase: Ionic liquid
CAS no.: 342573-75-5

PBS (0.1 M)
Supplier: In stock / prepared in-house
Phase: Liquid solution

Mixing
PEDOT: PSS dry pellets + Acrylic Acid (AA) + MBAA + DI water + DMSO + H_2O_2 (30% v/v) + ascorbic acid (20 wt%)
Soaking overnight with EMIM-ES
Making PEDOT: PSS/PAA hydrogel and soaking overnight
Solvent exchange EMIM-ES: water = 70:30 (v/v) for 6 hours
Solvent exchange for PEDOT:PSS/PAA hydrogels

1. Bring PEDOT: PSS dry pellets (NOT IN EKL)

Freeze-dry PEDOT: PSS (PH1000) to obtain dry pellets.
NOTE: This will be done prior of mixing in different lab and brought in the clean room!

2. Make viscous precursor suspension (base recipe)

Location: Chemical Lab (Class 10 000 cleanroom), Fume hood 5
Equipment name: Agate Mortar (I will bring the agate mortar and pestle into the cleanroom), Scale

Weigh and add into agate mortar:

- 26 mg PEDOT: PSS dry pellets
- 130 mg Acrylic Acid (AA)
- 5 mg MBAA
- 2 g DI water + 0.4 g DMSO

Grind until a homogeneous viscous suspension is obtained.
Take the appropriate beakers. Clean the station after usage.

3. Gel Initiation - In situ Polymerization

Location: Chemical Lab (Class 10 000 cleanroom)
Equipment name: Micropipettes, timer

1. Add initiators sequentially to the viscous suspension:
    - 15 µL H_2O_2 (30% v/v) then 15 µL ascorbic acid (20 wt%)
2. Mix quickly and proceed immediately to molding (gel sets fast).
3. Leave in mold at room temperature for 20 minutes to complete gelation.

4. Ionic-Liquid Treatment

Location: Chemical Lab (Class 10 000 cleanroom)
Equipment name: Beaker, tweezers

1. Remove gel from PDMS mold and soak gel in **pure EMIM-ES overnight**.
2. Transfer to **EMIM-ES: water = 70:30 (v/v)** for **6 hours** (solvent exchange).

5. Annealing

Location: Polymer Lab (Class 100 cleanroom)
Equipment name: Vacuum Oven, Beaker to withstand the temperature.

1. 80 °C for 6 h
2. 130 °C for 2 h

6. Rehydration

Location: Wet bench (Class 100 cleanroom)
Equipment name: Beaker

1. Soak in **0.1 M PBS** until fully rehydrated.

Appendix C. Optimised protocol for PEDOT:PSS-PEGPACHI hydrogel preparation

C.1 Purpose

This protocol describes the optimised preparation of PEDOT:PSS-PEGPACHI hydrogels developed and optimised in this thesis. PEDOT:PSS-PEGPACHI refers to an original PEDOT:PSS-phytic acid-chitosan-PEGDE hydrogel formulation developed in this work. In this name, PEG refers to PEGDE, PA refers to phytic acid, and CHI refers to chitosan. The protocol was optimised for reproducible gel formation, mixing, and mould casting.

C.2 Materials

- PEDOT:PSS PH1000
- Poly(ethylene glycol) diglycidyl ether (PEGDE)
- Phytic acid
- Chitosan, high molecular weight
- Deionised water
- 1X DPBS for storage

C.3 Equipment and labware

- Fisherbrand Select ultrasonic bath
- Fisherbrand ZX4 IR Vortex Mixer
- Thermo Scientific Cimarec hotplate/stirrer
- Magnetic stir bar
- 4 mL glass vial
- Micropipettes and tips
- 0.45 µm filter
- 0.22 µm filter
- Luer-lock syringes
- Moulds for hydrogel casting
- Refrigerator set to approximately 5 °C

C.4 Final optimised formulation

- For each hydrogel batch, 10 µL PEGDE was added to 1 mL PEDOT:PSS PH1000, corresponding to 1% v/v PEGDE relative to PEDOT:PSS volume.
- 63 µL PA-Chi stock solution was then mixed with the PEDOT:PSS-PEGDE precursor.
  The PA-Chi stock solution was prepared using:
- 2 mL phytic acid
- 2 mL deionised water
- 180 mg chitosan

C.5 Procedure

1. Add 2 mL phytic acid, 2 mL deionized water, and 180 mg chitosan into a 4 mL glass vial.
2. Add a magnetic stir bar and stir the mixture overnight at 65 °C using a Thermo Scientific Cimarec hotplate/stirrer.
3. Gently shake the PEDOT:PSS PH1000 dispersion to obtain a homogeneous suspension.
4. Sonicate the PEDOT:PSS dispersion for 10 min.

5. Filter the PEDOT:PSS dispersion through a 0.45 µm filter, followed by a 0.22 µm filter.
6. Transfer 1 mL of filtered PEDOT:PSS into a clean syringe or container.
7. Add 10 µL PEGDE to the PEDOT:PSS dispersion.
8. Vortex the PEDOT:PSS-PEGDE mixture for 30 s at 800 rpm.
9. Load the PEDOT:PSS-PEGDE mixture into one Luer-lock syringe.
10. Load 63 µL of the PA-Chi stock solution into a second Luer-lock syringe.
11. Connect the two syringes using the Luer-lock system and mix by repeated transfer between the syringes.
12. Carefully cast the mixed precursor into the selected moulds, avoiding bubble formation where possible.
13. Heat the samples at 75 °C for approximately 1 h to allow gel formation.
14. Use the gels directly for characterisation or immerse them in 1X DPBS and store at approximately 5 °C until further use.

B.6 Notes

The final protocol was selected after optimisation of the phytic acid-chitosan stock solution, PEGDE concentration, mixing method, and thermal gelation conditions. Preliminary trials included different phytic acid concentrations, chitosan contents, mixing approaches, and heating conditions, but the final formulation used for characterisation was based on 1 mL PEDOT:PSS PH1000, 10 µL PEGDE, and 63 µL PA-Chi stock solution.

Appendix D. Additional experimental documentation of PEDOT:PSS-DBSA hydrogel optimisation

This appendix contains additional photographs from the PEDOT:PSS-DBSA hydrogel optimisation process. The images document early gelation trials, bubble formation during mixing, DBSA concentration screening, tube inversion tests, and preliminary moulding attempts. These photographs support the optimisation process described in Section 4.2 but are included in the appendix to keep the main text focused on the final selected formulation.



Figure A 1: Additional photographs from PEDOT:PSS-DBSA hydrogel optimisation.
Photographs showing early PEDOT: PSS-DBSA gelation trials, bubble formation after mixing, tube inversion tests, and preliminary moulding attempts. These observations were used to optimise the mixing procedure and support the final selection of the 4% v/v DBSA formulation.

Appendix E. Detailed experimental log of PEDOT:PSS-PEGPACHI hydrogel optimisation

This appendix summarises the detailed experimental optimisation pathway used during development of the PEDOT:PSS-PEGPACHI hydrogel formulation. The appendix includes preliminary phytic acid only trials, chitosan/phytic acid mixing attempts, PA-chitosan premix experiments, $CaSO_4$ and low-DBSA trials, phytic acid concentration screening, chitosan concentration screening, PEGDE optimisation, and additional photographic documentation. These experiments support the formulation-development discussion in Section 4.4 but are included in the appendix to keep the main text focused on the final selected PEGPACHI formulation.

Table A 1: Experimental optimisation pathway for the development of the PEDOT:PSS-PEGPACHI hydrogel formulation

The table summarises the main formulation trials, processing conditions, macroscopic observations, and outcomes that guided the selection of the final PEDOT:PSS-PEGPACHI hydrogel composition.

Stage	Formulation / condition tested	Observation	Outcome
Phytic acid only	25, 50, 75, and 100 µL PA in 1 mL PEDOT:PSS	Slight gelation at 75 and 100 µL PA	PA could influence PEDOT:PSS, but was not enough for stable bulk gelation
Higher PA volume	125-200 µL PA in 1 mL PEDOT:PSS, sonication at 55 °C	Slight gelation, with visible excess PA	Not homogeneous enough
Chitosan directly in PA	Chitosan mixed with PA using vortexing, hot-plate stirring, sonication, and combined mixing	Chitosan did not fully dissolve; visible particles remained	Needed a better PA-chitosan stock approach
PA-chitosan premixes	PA/DI water/chitosan mixtures, including 625 µL PA + 375 µL DI + 5 mg chitosan	Almost mixed, but some chitosan particles remained	Improved handling but not yet reproducible
Low-DBSA rescue	PEDOT:PSS/PA system with 10 µL DBSA	Some or mostly gelation observed	Not selected because final goal was DBSA-free formulation
$CaSO_4$ trials	PEDOT:PSS/PA ± $CaSO_4$ and PEDOT:PSS/PA-chitosan ± $CaSO_4$	No gel formation observed	$CaSO_4$ was not used further

PA concentration screen	0.1, 1, 2, 5, 10, and 25 wt% PA solutions added to PEDOT:PSS	Gelation depended on PA concentration and aliquot volume	Guided the useful PA concentration range
PA-chitosan screen	25 wt% PA/chitosan formulation added to 200 µL PEDOT:PSS	Gelation observed for 20-30 µL additions	PA-chitosan route selected for further optimisation
Chitosan concentration screen	PA/water stocks with 13.5, 27, 67.5, and 135 mg chitosan	Different macroscopic behaviours observed	Helped guide final stock formulation
Final PA-chitosan stock	2 mL PA + 2 mL DI water + 180 mg chitosan, stirred overnight at 65 °C	More reproducible PA-chitosan stock	Selected for final PEGPACHI formulation
PEGDE optimisation	0.5% and 1% PEGDE	1% gave better macroscopic stability and handling	1% PEGDE selected
PEDOT:PSS amount / PA volume screen	200 µL PEDOT:PSS with 25-50 µL PA, pipette mixing only	No clear improvement observed	PA amount alone was not enough to obtain reliable gelation
Unfiltered PEDOT:PSS trials	1 mL unfiltered PEDOT:PSS with 50, 75, or 100 µL PA; sonicated and stored in fridge	No gel formation observed	Unfiltered PEDOT:PSS was not selected
Small-volume PA trials	200 µL PEDOT:PSS with 25-50 µL PA in small Eppendorf tubes, stored in fridge	Some gel-like behaviour for 25, 30, and 35 µL PA	Suggested that PA amount and sample volume influenced gel-like behaviour
Heating comparison	200 µL PEDOT:PSS with 25 or 35 µL PA, left at 55 °C	No gel formation observed	Heating alone did not solve PA-only gelation
Stepwise PA addition	200 µL PEDOT:PSS with sequential PA additions over time	No gel formation observed	Gradual PA addition was not enough to produce a bulk gel
Diluted PA addition	Diluted PA solution added stepwise into PEDOT:PSS	No gel formation observed	Dilution/stepwise addition did not improve gelation under the tested conditions
Component-control experiment	PEDOT:PSS combined with PA-only, PA-chitosan, PA-PEGDE, PEGDE-only, and PA-chitosan-PEGDE conditions	Individual or incomplete component combinations did not reproduce the final gel behaviour. Gelation was mainly observed when the required components were combined, with the PA-	Supported the final four-component PEGPACHI formulation

		chitosan-PEGDE condition showing the most stable macroscopic gel formation	

Component-control experiment for PEGPACHI formulation design

A component-control experiment was performed to evaluate whether the final PEDOT:PSS-PEGPACHI gelation behaviour resulted from the combined effect of the selected additives rather than from one component alone. In this experiment, different partial formulations were prepared and compared macroscopically. The tested conditions included phytic acid alone, PA-chitosan, PA-PEGDE, PEGDE alone, and the full PA-chitosan-PEGDE combination.

The purpose of this experiment was to test the design logic of the PEGPACHI formulation. Phytic acid was expected to influence the PEDOT:PSS dispersion, chitosan was introduced to contribute a biopolymer network-forming component, and PEGDE was added to improve stability and handling. Therefore, comparing the individual and partial combinations helped confirm whether stable gel formation required the combined presence of these components.

As shown in Figure A 2, the individual or incomplete component combinations did not reproduce the final hydrogel behaviour. Phytic acid only and PEGDE-only conditions did not produce a stable macroscopic gel comparable to the final formulation. PA-chitosan and PA-PEGDE conditions showed some gel-like behaviour, but the most stable and handleable gel was observed when PA, chitosan, and PEGDE were all included. This supported the final formulation strategy, where PA, chitosan, and PEGDE were combined with PEDOT:PSS to obtain the PEDOT:PSS-PEGPACHI hydrogel.

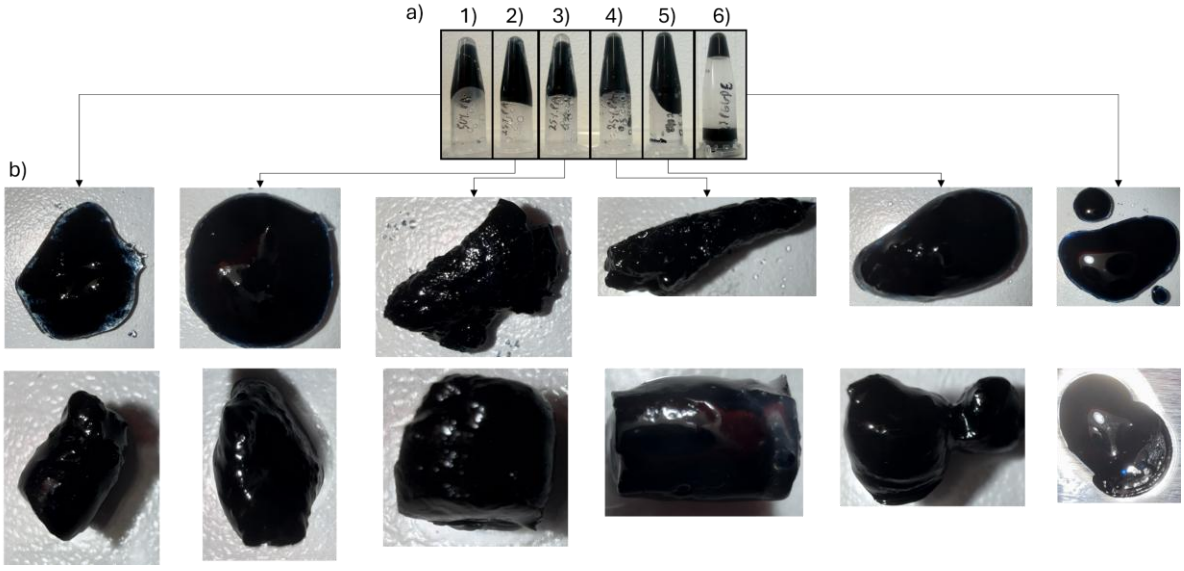


Figure A 2: Component-control experiment during PEDOT:PSS-PEGPACHI hydrogel development.

(a) PEDOT:PSS-based formulations prepared with different additive combinations: (1) 50% PA-63 µL, (2) 25% PA-63 µL, (3) 25% PA + 0.5% chitosan, (4) 25% PA + 0.5% chitosan + 0.5% PEGDE-63 µL, (5) 25% PA + 0.5% PEGDE-63 µL, and (6) 0.5% PEGDE. (b) Macroscopic appearance of the corresponding samples after gelation/removal from the tubes. The component-control experiment showed that the individual or incomplete additive combinations did not reproduce the final PEGPACHI

hydrogel behaviour. More stable and handleable gel formation was observed when phytic acid, chitosan, and PEGDE were combined, supporting the final multicomponent formulation strategy.

Appendix F. PDMS measuring platform design iterations and bonding development

This appendix summarises the design iterations and bonding-development steps used during fabrication of the PDMS measuring platform. The platform was developed to simplify three-electrode electrochemical measurements of PEDOT:PSS-based hydrogels while keeping the principle of a gold pogo pin working electrode and reference/counter electrodes placed in electrolyte above the hydrogel. Several SolidWorks designs were prepared before two final platform versions were selected: a glass-bonded PDMS platform for collaborative cell culture related experiments and a full-PDMS platform for electrochemical measurements in this thesis.

Table A 2: Summary of PDMS measuring platform design iterations.

Design stage	Design purpose	Main features	Outcome
Early conceptual designs	Initial representation of the hydrogel measurement platform	Multi-well layout based on the idea of contacting hydrogels with pogo pins and placing electrodes above the gel	Used to define the general platform concept
Intermediate mould designs	Translation of the platform idea into moulds suitable for PDMS casting	SolidWorks moulds with well-forming pillars and rectangular platform geometry	Helped optimise the platform layout and fabrication approach
Glass-bonded PDMS platform	Sterilisable platform for collaborative cell culture related experiments	PDMS structure bonded to a glass slide, designed to allow hydrogel experiments under cell-culture conditions	Worked after bonding strategy was modified using uncured PDMS as an intermediate sealing layer
Full-PDMS measuring platform	Platform used for electrochemical measurements in this thesis	Full PDMS structure without glass bonding, 18 wells arranged in 9 rows x 2 columns, pogo pins inserted manually from the side	Selected for thesis electrochemical measurements because it was faster, simpler, and avoided PDMS-glass bonding problems

Several design iterations were explored during development of the PDMS measuring platform. The first stage consisted of conceptual designs for how the PDMS platform could be arranged, including the number of wells, the position of the hydrogel chambers, and the general approach for integrating pogo pins. These early designs were useful for defining the overall platform idea, but they were not yet practical moulds for reproducible PDMS casting.

The first printed moulds were then fabricated using FDM 3D printing. These moulds showed that the general concept was possible, but the PDMS could not be removed reliably after curing. This was mainly due to the close spacing between the well-forming pillars and the limited clearance around the

structures. In addition, the mould geometry did not initially allow PDMS to flow easily to the opposite side of the mould. A later version therefore included an additional filling/flow feature at the end of the mould to improve PDMS distribution. However, even with this modification, the spacing between the structures remained too small, and demoulding was still unreliable.

A two-part “LEGO-like” mould concept was then tested. This design included a bottom part containing the well-forming structures and a top part intended to guide PDMS filling. In theory, this approach allowed better control over mould assembly and filling. However, in practice, sealing was difficult because of the surface quality and dimensional limitations of the FDM-printed parts. As a result, leakage and incomplete sealing made this version unsuitable for reproducible platform fabrication.

The next design stage focused on producing a full-PDMS platform in which the PDMS could be cast and cured together with a glass slide. This design was considered promising because it could, in principle, create a glass-bottom PDMS platform without requiring a separate bonding step after curing. However, practical implementation was difficult. The glass had to be positioned level with the mould, the PDMS had to contact the glass uniformly, and bubbles or incomplete contact could prevent proper sealing. For the collaborative cell-culture-related work, an array with larger spacing between wells was also considered to meet the experimental needs of the Medical University of Graz project.

A resin-printed mould was also explored to improve the surface quality of the mould and increase the chance of successful oxygen-plasma bonding between PDMS and glass. However, the available resin printer build plate limited the size of the mould. The resulting mould was too small, and the reduced dimensions again made PDMS removal difficult. Therefore, this route was not selected.

The final glass-bonded design was based on the most practical geometry obtained during the design process. Since direct oxygen-plasma bonding between the FDM-moulded PDMS and glass was not reliable, the final approach used uncured PDMS as an intermediate sealing layer between the cured PDMS platform and the glass slide, followed by curing. In parallel, a full-PDMS version was selected for the electrochemical measurements in this thesis because it avoided glass bonding completely and was easier to fabricate reproducibly.

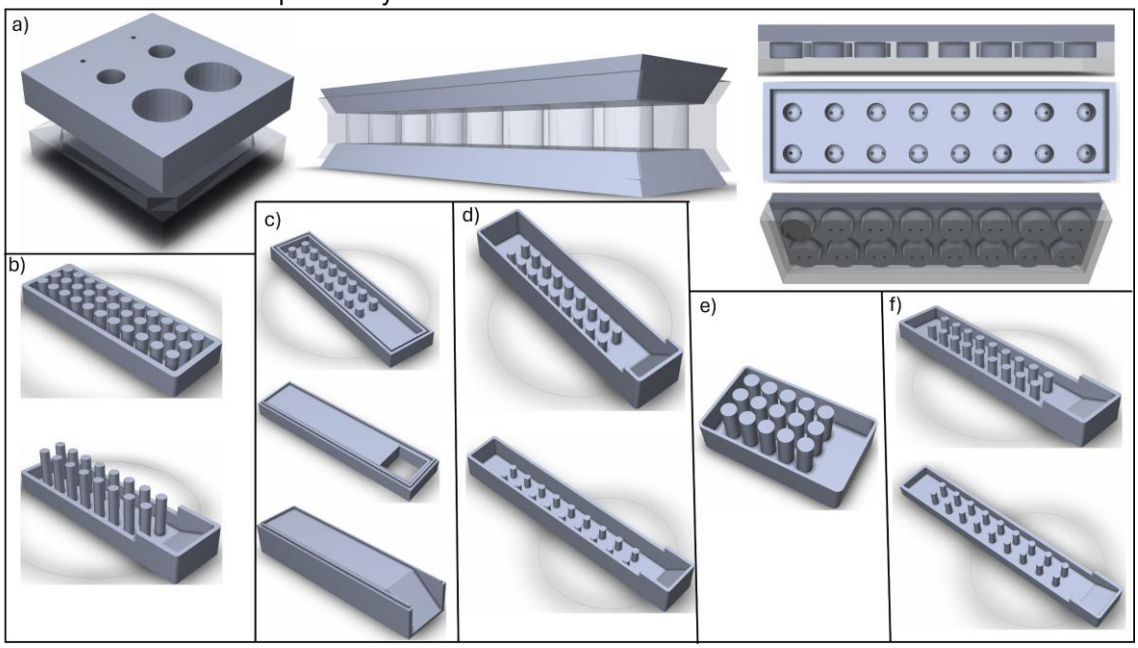


Figure A 3: Design iterations during development of the PDMS measuring platform. (a) Initial design ideas for the PDMS platform, showing different possible arrangements for the hydrogel wells and overall platform geometry. (b) Early FDM-printed mould designs. These versions demonstrated the feasibility of PDMS casting but had insufficient clearance between the well-forming

structures, making demoulding difficult. A later version included an additional filling/flow feature to help PDMS reach the opposite side of the mould, but demoulding remained unreliable. (c) Two-part LEGO-like mould concept, consisting of a bottom mould and top filling component. Although this design was promising in principle, sealing was limited by the surface quality and dimensional accuracy of the FDM-printed parts. (d) Full-PDMS/glass-assisted mould concept, designed so that PDMS could be cured together with a glass slide. This approach was difficult to implement reproducibly because uniform glass contact, levelling, and bubble-free filling were challenging. (e) Resin-printed mould concept developed to improve surface quality for oxygen-plasma bonding. This approach was limited by the resin printer build size and the small mould dimensions, which again made PDMS removal difficult. (f) Final glass-bonded PDMS platform design selected after optimisation, where uncured PDMS was used as an intermediate sealing layer between the cured PDMS platform and glass.

F2 Oxygen-plasma bonding attempt for glass-bottom PDMS platforms

Oxygen-plasma bonding was tested during development of the glass-bottom PDMS measuring platform, which was intended to support collaborative experiments performed at the Medical University of Graz. The aim of this step was to bond the cured PDMS platform to a glass slide, creating a sealed platform with optical access through the glass base. Before oxygen-plasma treatment, both the glass slide and the cured PDMS platform were cleaned using ethanol and water. The cleaning protocol consisted of 10 min in 99% ethanol, 5 min in water, and 1 min in ethanol, followed by drying with nitrogen and then putting it inside the oxygen plasma chamber.

After cleaning and drying, the glass and PDMS surfaces were treated in the oxygen-plasma reactor. The plasma process used O_2 gas, with a gas supply period of 1 min, a plasma treatment period of 2 min, and a venting period of 1 min. The process pressure was approximately 0.22 mbar and the plasma power was set to 10%. Immediately after plasma exposure, the PDMS platform was placed in contact with the glass slide. A metal block was placed on top of the assembly to increase contact between the PDMS and glass during bonding.

Although oxygen-plasma bonding was expected to improve adhesion between the PDMS and glass, the bonding was not reliable for these platforms. The main limitation was likely the surface quality and dimensional accuracy of the FDM-moulded PDMS structures. Small surface irregularities prevented uniform contact between the PDMS and glass, even when a metal block was used to apply pressure. As a result, the plasma-bonded platforms did not consistently seal. Because of this, the final glass-bottom platform design used uncured PDMS as an intermediate sealing layer between the cured PDMS platform and the glass slide, followed by curing. This approach gave a more practical and reproducible seal for the final glass-bottom platform.

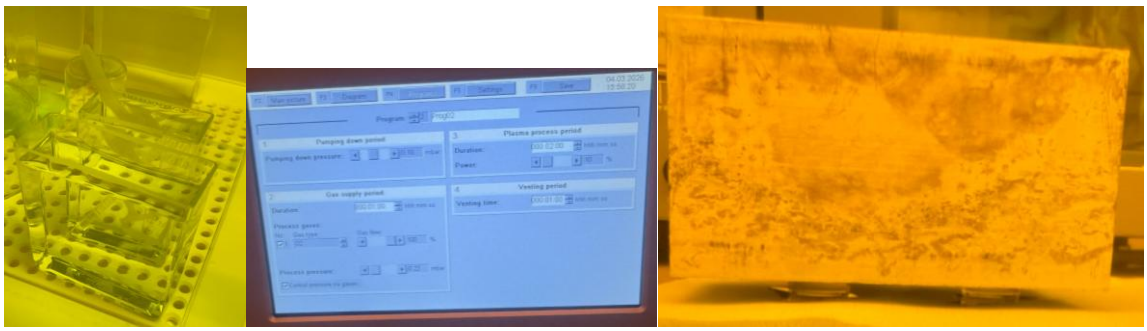


Figure A 4: Cleaning and oxygen-plasma bonding attempt for the glass-bottom PDMS measuring platform.

(a) Cleaning of the cured PDMS platform and glass slide before plasma treatment. The cleaning sequence consisted of 10 min in 99% ethanol, 5 min in water, and 1 min in ethanol, followed by drying

with nitrogen. (b) Oxygen-plasma reactor settings used for the bonding attempt, including O_2 plasma treatment for 2 min at 10% power. (c) A metal block was placed on top of the PDMS/glass assembly to improve contact during bonding. Although the approach helped press the surfaces together, reliable bonding was not achieved, most likely due to non-uniform contact caused by the surface quality of the FDM-moulded PDMS platform.

Appendix G. Supplementary nanoindentation analysis

G1 Practical nanoindentation setup and hydrated sample positioning

During the nanoindentation measurements, the hydrogels had to remain fully hydrated while also being kept stable in one position. This was challenging because the PEDOT:PSS-based hydrogels were soft, hydrated, and in some cases fragile. When the samples were placed directly in a Petri dish with DPBS, they could move during measurement, which made stable probe contact difficult. In addition, the hydrogel surfaces were not perfectly flat, which could influence the local contact between the nanoindenter probe and the sample surface.

An initial approach was tested in which a metallic ring was incorporated into the hydrogel so that the sample could be magnetically held at the bottom of the dish during measurement. This approach was successful in keeping the hydrogel attached to the bottom surface. However, it did not provide the most reliable measurement configuration. The final approach used a square well-plate mould, in which the hydrogels were prepared and measured while remaining inside the wells. A sufficient volume of 1x DPBS was added to fully submerge the samples during indentation. This configuration reduced sample movement, maintained hydration, and improved measurement stability.

The nanoindentation setup, software interface, square well-plate mould, and preliminary magnetic-fixation approach are shown in Figure A 5.

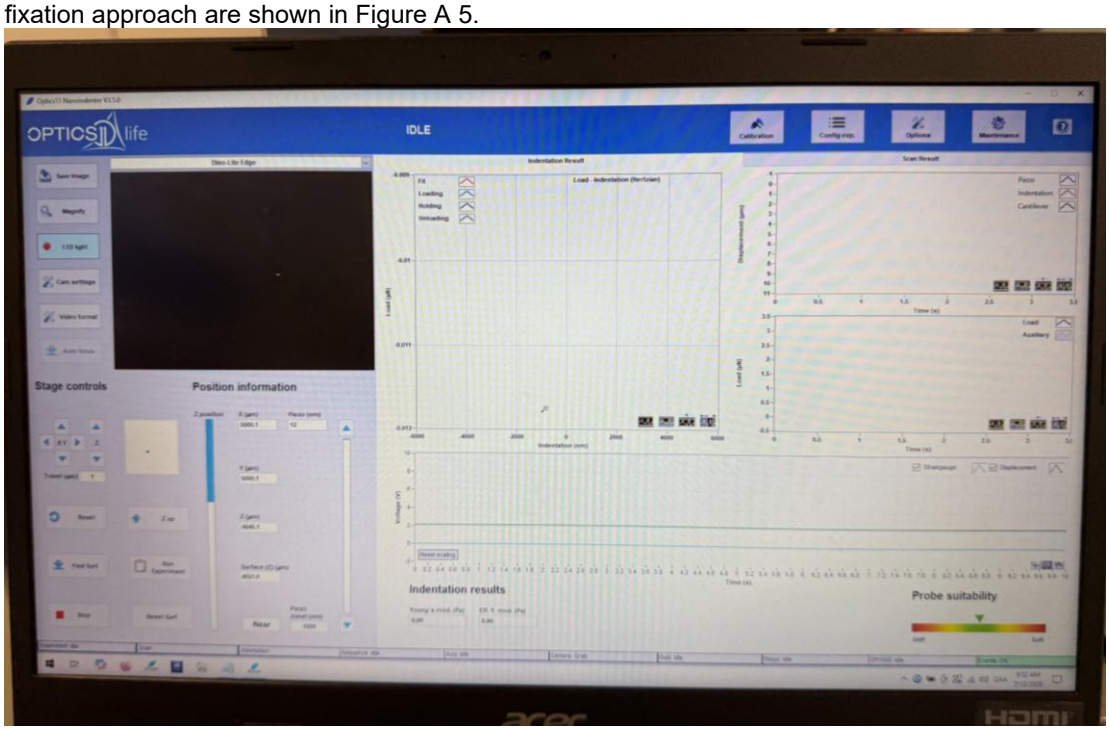




Figure A 5: Practical setup used for hydrated nanoindentation measurements. Representative photographs of the nanoindentation workflow. The hydrogel samples were prepared inside a square well-plate mould to improve sample stability during measurement. Measurements were performed using the Optics11 Piuma nanoindenter while the hydrogels were fully submerged in 1x DPBS. The software interface was used to monitor the indentation response during testing. A preliminary approach using a metallic ring incorporated into the hydrogel was also tested to magnetically fix the sample to the bottom of the dish. Although this approach helped keep the gel in position, the square well-plate mould provided a more practical and reproducible configuration for the final measurements.

G2 Data processing and exclusion criteria

Effective Young's modulus values were exported from the Optics11 Piuma software as Eeff values and converted from Pa to kPa. For each hydrogel sample, multiple indentation points were collected using matrix scans. The raw exported values were first inspected, and failed or unreliable indentation points were excluded before calculating the final values reported in the main text.

Measurements were excluded when they showed abnormal behaviour, including extremely low or high Eeff values, abnormal maximum load values, or poor indentation response. The excluded values were retained in the raw data tables for transparency but were not included in the mean, standard deviation, or median calculations. Heat maps were generated to visualise the spatial distribution of Eeff values across each matrix scan.

For the individual hydrogel sections in Chapter 5, the mean and standard deviation were calculated from the valid indentation points of each sample. For the final comparison between hydrogel formulations, the median Eeff value of each independent hydrogel sample was used. This was done to avoid treating multiple indentation points from the same hydrogel as independent material replicates.

G3 Excluded values and summary statistics

G3.1 PEDOT:PSS-DBSA

Sample	Excluded Eeff values (kPa)	Reason	Valid points	Mean ± SD Eeff (kPa)	Median Eeff (kPa)
DBSA 1	62.06, 17.26, 0.16, 0.52	clear outlier / failed indentation	12/16	13.66 ± 0.55	13.73
DBSA 2	180.56	clear high outlier	15/16	11.70 ± 7.17	13.34
DBSA 3	24.37, 24.38, 5.93	clear high/low outliers	13/16	12.13 ± 1.91	11.97

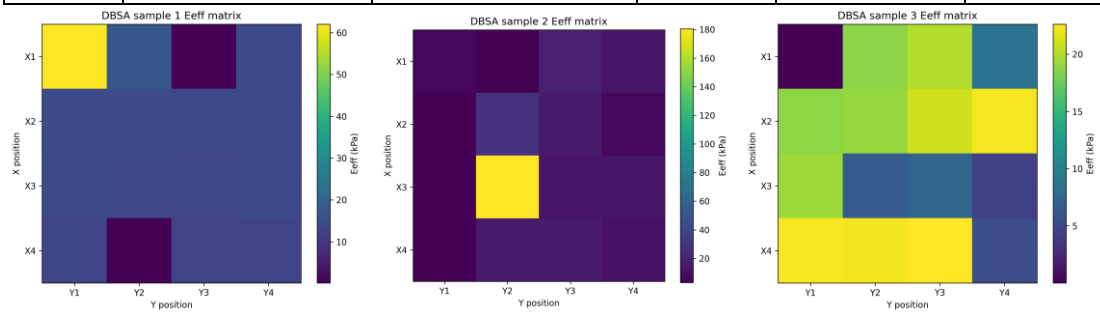


Figure A 6: Heat maps of PEDOT:PSS-DBSA nanoindentation measurements. Heat maps showing the spatial distribution of Eeff values obtained from matrix scans of three independent PEDOT:PSS-DBSA hydrogel samples. Excluded indentation points are listed in the table above.

G3.2 PEDOT:PSS-PAA

Sample	Excluded Eeff values (kPa)	Reason	Valid points	Mean ± SD Eeff (kPa)	Median Eeff (kPa)
PAA 1	273.50	clear high outlier	15/16	24.44 ± 15.78	19.83
PAA 2	0.001, 92.90, 0.0004	abnormal maximum load / clear outlier	13/16	9.67 ± 7.54	7.54
PAA 3	347.78, 135.57, 136.45	clear high outliers	13/16	17.52 ± 14.99	14.49

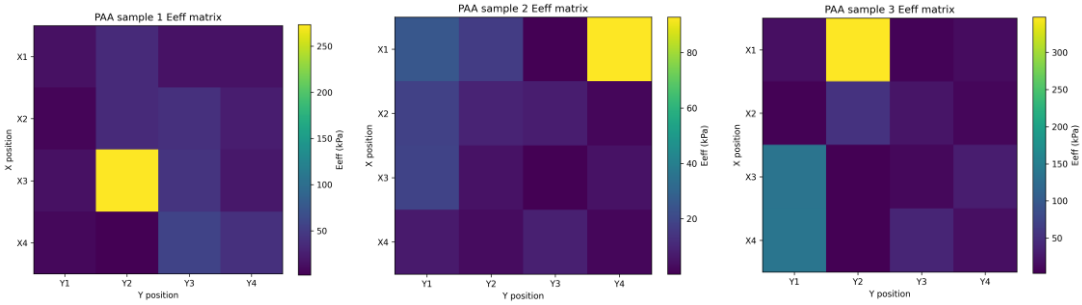


Figure A 7: Heat maps of PEDOT:PSS-PAA nanoindentation measurements. Heat maps showing the spatial distribution of Eeff values obtained from matrix scans of three independent PEDOT:PSS-PAA hydrogel samples. The PAA hydrogels showed larger local variability than PEDOT:PSS-DBSA, likely due to surface unevenness and structural heterogeneity introduced by the fabrication and post-treatment process. Excluded indentation points are listed in the table above.

G3.3 PEDOT:PSS-PEGPACHI

Sample	Excluded Eeff values (kPa)	Reason	Valid points	Mean ± SD Eeff (kPa)	Median Eeff (kPa)
PEGPACHI 1	0.23, 0.01	failed/very low indentation values	14/16	44.81 ± 12.83	43.98
PEGPACHI 2	0.002	abnormal measurement behaviour	15/16	5.49 ± 3.53	3.58
PEGPACHI 3	0.03	abnormal measurement behaviour	15/16	3.89 ± 2.24	3.68

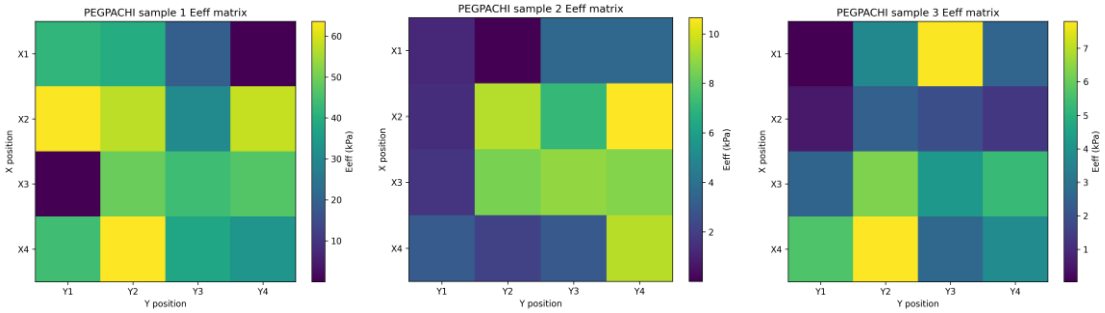


Figure A 8: Heat maps of PEDOT:PSS-PEGPACHI nanoindentation measurements. Heat maps showing the spatial distribution of Eeff values obtained from matrix scans of three independent PEDOT:PSS-PEGPACHI hydrogel samples. The PEGPACHI formulation showed clear sample-to-sample variability, with one stiffer sample and two softer samples. Excluded indentation points are listed in the table above.

G4 Notes on interpretation

The nanoindentation measurements were used to obtain a preliminary estimate of the hydrated mechanical response of the PEDOT:PSS-based hydrogels. Since nanoindentation is a local measurement technique, the measured Eeff values depend strongly on the local surface condition, probe-sample contact, hydration state, and microscale structure of the hydrogel.

This was especially important because the hydrogel surfaces were not perfectly flat and the materials were measured in the fully hydrated state. For PEDOT:PSS-PAA and PEDOT:PSS-PEGPACHI,

additional local variability may also arise from their more complex internal structures, including polymer networks, PEDOT:PSS-rich domains, or multicomponent formulation effects. Therefore, the values reported in the main text should not be interpreted as absolute bulk Young's modulus values. Instead, they represent effective local hydrated-state stiffness values that allow a qualitative comparison between the three hydrogel formulations under the same measurement conditions.

Appendix H. PEDOT:PSS-PAA hydrogel optimisation

H1 Purpose of the optimisation

The PEDOT:PSS-PAA hydrogel required a more complex preparation route than the PEDOT:PSS-DBSA and PEDOT:PSS-PEGPACHI formulations. The aim of the optimisation was not to introduce a new final composition, but to make the preparation procedure more reproducible and easier to handle. In particular, the optimisation focused on the freeze-drying of PEDOT:PSS, grinding and dispersion of the dried PEDOT:PSS material, handling of the precursor before gelation, and the practical limitations of casting the PAA hydrogel directly into the PDMS measuring platform.

The final working protocol used for PEDOT:PSS-PAA hydrogel preparation is described in Chapter 3. This appendix provides additional photographic documentation of the optimisation process and explains the practical observations that led to the final approach.

H2 Freeze-drying of PEDOT:PSS

Freeze-drying was used to obtain dry PEDOT:PSS material before preparation of the PEDOT:PSS-PAA precursor. The PEDOT:PSS dispersion was first frozen and then transferred to the freeze-dryer. After freeze-drying, the dried PEDOT:PSS material was collected and used in the next preparation step. This step was necessary because the PAA formulation required PEDOT:PSS to be incorporated into the precursor as a dry material before polymerisation.



Figure A 9: Freeze-drying of PEDOT:PSS for PEDOT:PSS-PAA hydrogel preparation. Photographs showing the freeze-drying setup used to obtain dry PEDOT:PSS material before preparation of the PEDOT:PSS-PAA precursor. The dried PEDOT:PSS was later collected, ground, and incorporated into the PAA precursor mixture.

H3 Grinding and precursor preparation

After freeze-drying, the dried PEDOT:PSS had to be manually processed before it could be incorporated into the PAA precursor. During the first trials, the precursor appeared highly non-uniform, with visible large PEDOT:PSS-rich particles or aggregates. This indicated that the dried PEDOT:PSS was not sufficiently dispersed in the precursor mixture.

Manual grinding was therefore used to improve incorporation of the freeze-dried PEDOT:PSS into the precursor. However, the early use of a relatively large mortar made handling difficult, because a noticeable amount of material remained attached to the mortar walls during grinding. This caused material loss and made the procedure less reproducible. The grinding and mixing step was therefore identified as an important part of the PAA optimisation process.

After optimisation of the mixing procedure, the precursor appeared more homogeneous and more liquid-like compared with the first trials (Figure A 10). This suggested improved dispersion before gelation. Nevertheless, because the PEDOT:PSS phase was introduced from freeze-dried and manually processed material, local PEDOT:PSS-rich regions or particles with different sizes could still be present in the final hydrogel. This was considered when interpreting the later characterisation results, especially the local variability observed during nanoindentation.

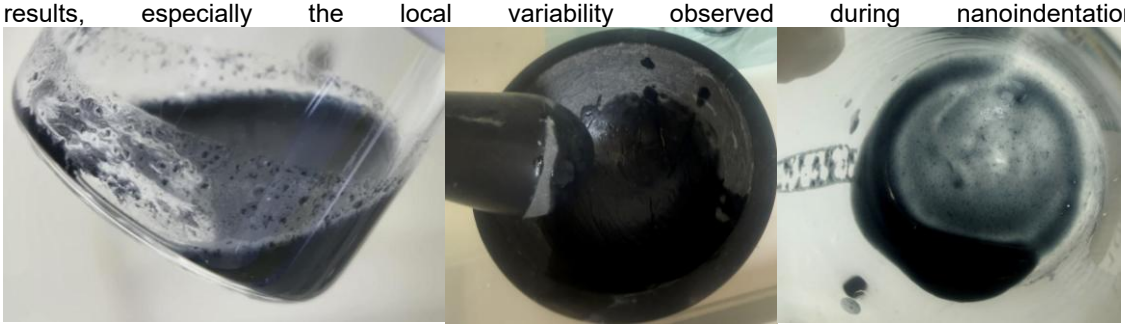


Figure A 10: Optimisation of PEDOT:PSS-PAA precursor mixing. Photographs showing the PEDOT:PSS-PAA precursor during the grinding and mixing optimisation process. In the early trials, the precursor appeared non-uniform and contained visible large PEDOT:PSS-rich particles or aggregates. Manual grinding in the mortar helped incorporate the freeze-dried PEDOT:PSS into the precursor, but material loss on the mortar walls was observed. After optimisation of the mixing procedure, the precursor appeared more homogeneous and more liquid-like, indicating improved dispersion before gelation.

H4 First attempt to cast PEDOT:PSS-PAA directly in the PDMS measuring platform

An early optimisation trial attempted to form the PEDOT:PSS-PAA hydrogel directly inside the PDMS measuring platform. This was tested because direct casting inside the platform would have simplified later electrochemical measurements by allowing the hydrogel to form around the electrode contact. However, this approach was not practical for the PAA formulation.

The main limitation was that the PEDOT:PSS-PAA hydrogel required post-treatment, annealing, and rehydration after gelation. These steps were difficult to perform reliably when the gel was formed directly inside the PDMS measuring platform. In addition, removing the PAA gel from the PDMS structure after gelation was difficult and caused damage to the gel. For this reason, direct casting of PAA into the PDMS measuring platform was not used as the final approach.

Instead, the PAA hydrogels were prepared as bulk samples, treated and rehydrated separately, and then handled or cut for later characterisation. This approach was more suitable for the PAA formulation because it allowed the post-treatment steps to be performed more reliably.

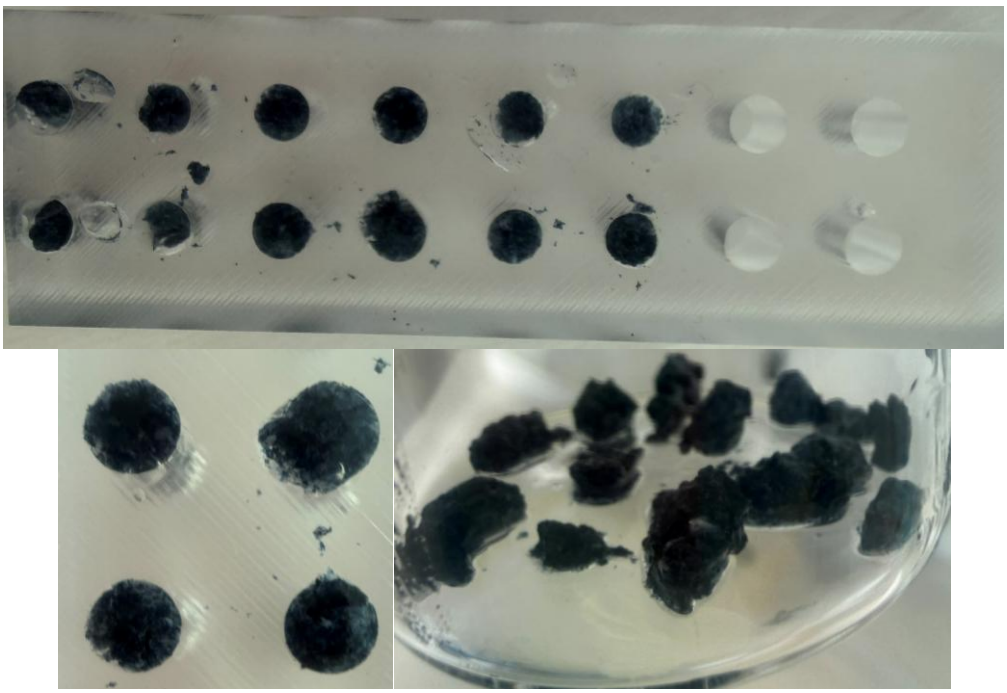


Figure A 11: First attempt to form PEDOT:PSS-PAA hydrogel directly inside the PDMS measuring platform.

Photographs showing an early trial in which the PEDOT:PSS-PAA precursor was cast directly into the PDMS measuring platform. Although gel formation was achieved, this approach was not practical because the PAA hydrogel required post-treatment, annealing, and rehydration after gelation. Removal from the PDMS platform also damaged the gel, so this approach was not selected for the final protocol.

H5 Outcome of the optimisation

The PAA optimisation showed that the main challenges were related to processing and handling rather than only gel formation. Freeze-drying was necessary to obtain dry PEDOT:PSS, but the following grinding step introduced practical difficulties and possible material loss. Direct formation of the hydrogel inside the PDMS measuring platform was also not suitable because the PAA formulation required additional post-treatment steps after gelation.

Based on these observations, the final PAA preparation strategy used bulk hydrogel formation followed by post-treatment, annealing, rehydration, and later sample preparation for characterisation. This made the fabrication process more practical and reduced the risk of damaging the hydrogel during processing. However, the optimisation also showed that the PAA route remained more complex than the DBSA and PEGPACHI formulations, which may have contributed to the variability observed during later mechanical and electrochemical characterisation.

Appendix I. PDMS hydrogel-array device design optimisation

I1 Purpose of the device optimisation

The PDMS hydrogel-array device was developed as a preliminary platform to integrate PEDOT:PSS-based hydrogel tracks into a patterned structure. The aim of the optimisation was to identify a design that could be fabricated reproducibly, demoulded without damaging the PDMS structure, filled with hydrogel precursor, and used for preliminary electrical access of the hydrogel tracks.

Several design iterations were tested before selecting the final device design used in Chapter 7**Σφάλμα! Το αρχείο προέλευσης της αναφοράς δεν βρέθηκε.**. The optimisation focused mainly on the geometry of the hydrogel tracks, the formation of electrode-access regions, and the practical limitations of mould fabrication and PDMS demoulding.

I2 First design with pillar-defined electrode holes

The first design included small resin pillars intended to define electrode-access holes in the PDMS after curing. The idea was that, after PDMS curing and demoulding, the hydrogel tracks would remain connected to small openings that could later be used for electrode access. However, the pillar dimensions were too small for reliable demoulding. Because the pillars were approximately 200 µm in size, it was likely that they would either break during PDMS removal or damage the surrounding PDMS structure. This would make it difficult to obtain intact holes and reproducible electrode-access regions. For this reason, the pillar-based design was not selected for the final device. Although the concept was useful for defining the first layout, the fabrication risk was too high for reliable PDMS device production.



Figure A 12: First PDMS hydrogel-array device design with pillar-defined electrode holes. Photographs showing the first device design, where small resin pillars were included to form electrode-access holes in the PDMS after curing. Although this design provided a first strategy for defining hydrogel tracks and electrode-access regions, the small pillar size made demoulding unreliable. The resin pillars were expected to be difficult to remove without breaking or damaging the surrounding PDMS, so this design was not selected for the final device.

I3 Track-based device design without pillar-defined holes

A second design was then developed using a simpler track-based geometry. In this version, the device focused on forming continuous hydrogel tracks without relying on small pillar-defined electrode holes. This reduced the risk of damaging the PDMS during demoulding and made the overall structure easier to fabricate.

The track-based design improved the practicality of the device fabrication process, because the PDMS structure could be removed more easily from the mould. However, this version still required further optimisation to improve hydrogel filling and continuity across the patterned tracks. In some cases, the hydrogel precursor did not form a fully continuous track after gelation, which limited the reliability of the design for electrical measurements.

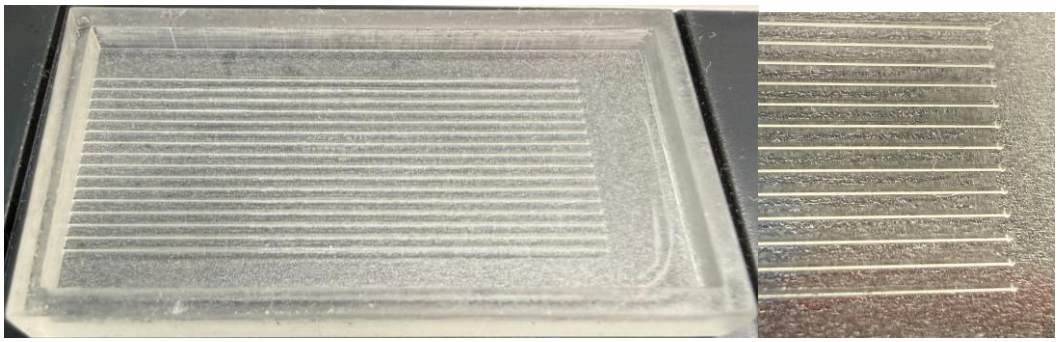


Figure A 13: Track-based PDMS hydrogel-array device design.
Photographs showing the second design iteration, where the device was simplified by removing the small pillar-defined electrode holes and focusing on continuous hydrogel tracks. This design improved PDMS demoulding compared with the pillar-based version, but further optimisation was still required to improve hydrogel filling and track continuity.

I4 Microfluidic-track device design

A further design iteration used a microfluidic-track layout to improve hydrogel patterning and guide the precursor through smaller defined channels. This design avoided the fragile pillar-defined electrode holes used in the first version and was easier to demould from the PDMS mould. The microfluidic layout was therefore more practical than the first pillar-based design.

However, this version was still not selected as the final device. The main limitation was hydrogel continuity inside the small tracks. During filling and gelation, the precursor did not always form continuous hydrogel tracks, and after heating some regions appeared separated or disconnected. This made the design unreliable for consistent electrical measurements.

For this reason, the microfluidic-track design was considered an intermediate optimisation step. The final device used in Chapter 7**Σφάλμα! Το αρχείο προέλευσης της αναφοράς δεν βρέθηκε.** was therefore developed further with larger and more accessible hydrogel tracks, as described in the main text.

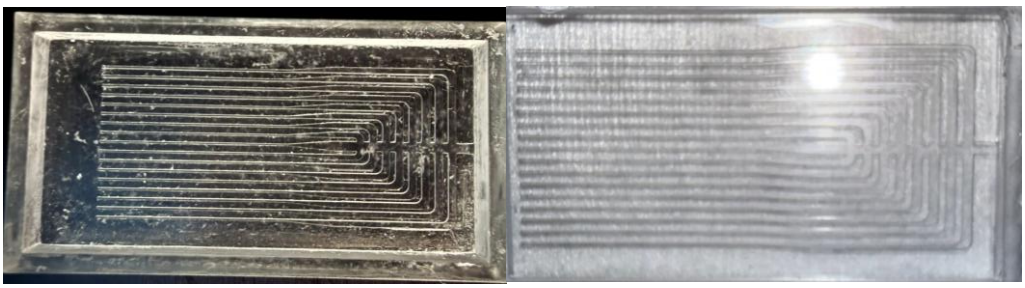


Figure A 14: Intermediate PDMS hydrogel-array device design with microfluidic tracks.
Photographs showing the intermediate microfluidic-track device design tested during PDMS hydrogel-array optimisation. This design improved fabrication compared with the first pillar-based version because it avoided fragile small resin pillars. However, the small microfluidic tracks did not always fill uniformly with the PEDOT:PSS-PEGPACHI precursor, and hydrogel continuity after gelation was not reliable. Therefore, this design was not selected as the final device.

I5 Outcome of the design optimisation

The device optimisation showed that the main limitation of the first design was the practical difficulty of fabricating and demoulding very small pillar-defined features. The following track-based and microfluidic designs improved fabrication by removing these fragile features, but hydrogel filling and continuity remained challenging in the smaller patterned structures.

Therefore, the final device used in Chapter 7 was developed with larger and more accessible hydrogel tracks. This final design represented a compromise between fabrication simplicity, hydrogel patterning,

and electrical accessibility. It was suitable for preliminary hydrogel integration and electrical testing, but further optimisation would be needed to improve reproducibility, track continuity, and electrode integration in future device versions.

Appendix J. Supplementary comparison with hydrogel-based electrode-array approaches

This appendix provides the supporting impedance graphs used to position the preliminary PEDOT:PSS-PEGPACHI hydrogel-array device developed in this thesis relative to hydrogel-based and PEDOT:PSS-based electrode-array approaches. The comparison is intended to provide context for the order of magnitude of the impedance response. It should not be interpreted as a direct performance ranking, because the systems differ in conductive material, device geometry, electrode area, electrolyte environment, and electrode-contact configuration.

J1 Published viscoelastic hydrogel electrode-array benchmark

Tringides et al. developed a fully viscoelastic surface electrode array based on conductive hydrogel tracks made from an alginate matrix loaded with carbon nanomaterials. Their device included conductive hydrogel tracks, viscoelastic encapsulation layers, electrode openings, and a flexible connector. In their device characterisation, the impedance response was measured for five devices from five distinct batches, with the mean and standard deviation plotted for 40 electrodes. The same figure also reports ageing in PBS, mechanical cycling, comparison with a clinical grid, and charge storage capacity, showing that this was a fully developed and validated hydrogel-based electrode-array platform [47].

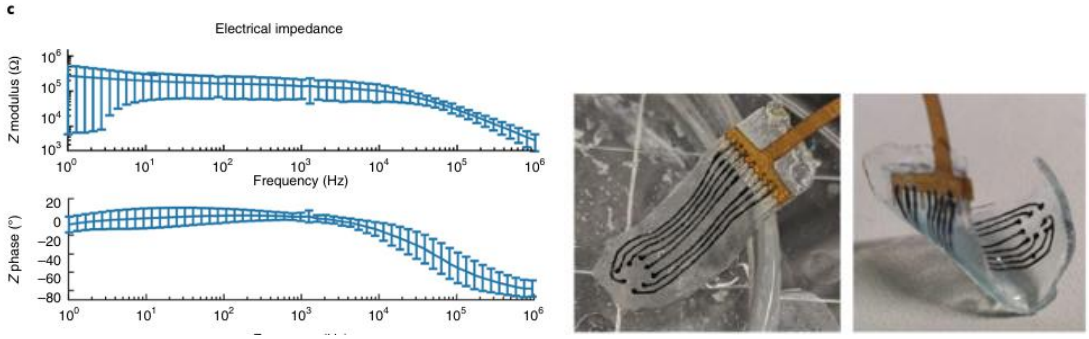


Figure A 15: Published viscoelastic hydrogel electrode-array benchmark. Impedance and device-characterisation data reported by Tringides et al. for a fully viscoelastic surface electrode array based on alginate-carbon conductive hydrogel tracks. The published device included integrated conductive tracks, encapsulation layers, electrode openings, and a flexible connector. The impedance response at 1 kHz was used in Chapter 7 as a published hydrogel-array benchmark for positioning the PEDOT:PSS-PEGPACHI hydrogel-array device developed in this thesis. Reproduced from Tringides et al. [47].

J2 Ongoing PEDOT:PSS electrode work within the Bioelectronics group

Ongoing work within the Bioelectronics group is exploring microfabricated full PEDOT:PSS thin-film electrodes for transparent and stable bioelectronic interfaces. These electrode structures are relevant to neural recording and stimulation because microfabricated thin-film electrode arrays represent a more established device architecture for interfacing with neural tissue. In this work, PEDOT:PSS is used directly as the electrode material, rather than being incorporated into a hydrogel network.

The data shown in Figure A 16 were generated by Mustafeez Shah as part of ongoing work within the Bioelectronics group. This system is relevant to the present thesis because it provides a PEDOT:PSS-based electrode comparison from the same research environment. However, it differs from the PEDOT:PSS-PEGPACHI device developed in this thesis because the group work is based on microfabricated full PEDOT:PSS thin-film electrodes, while this thesis uses PEDOT:PSS incorporated into a soft PEGPACHI hydrogel formulation. Therefore, the comparison is used only to position the order of magnitude of the impedance response, not as a direct performance comparison.

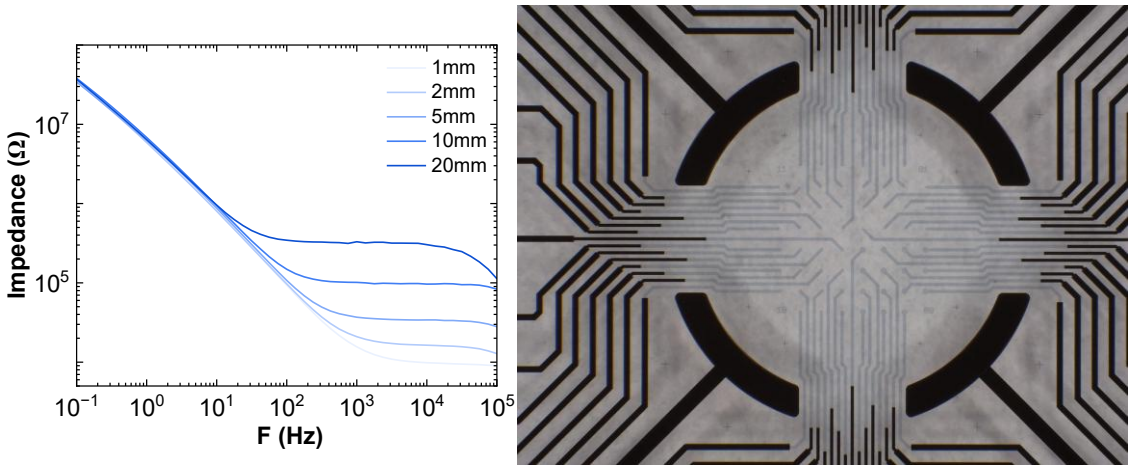


Figure A 16: Ongoing microfabricated full PEDOT:PSS thin-film electrode work within the Bioelectronics group.
Representative impedance data and optical image of patterned full PEDOT:PSS thin-film electrode structures developed within the Bioelectronics group. The 1 mm electrode structure was used as a relevant PEDOT:PSS-based comparison for the PEDOT:PSS-PEGPACHI hydrogel electrodes developed in this thesis. Unlike the present work, these electrodes are based on microfabricated full PEDOT:PSS thin films rather than PEDOT:PSS incorporated into a hydrogel formulation. Data generated by Mustafeez Shah. Reproduced with permission from Shah, Wang, Frimat, and Savva, in preparation.

J3 Positioning of the PEDOT:PSS-PEGPACHI hydrogel-array device

The PEDOT:PSS-PEGPACHI hydrogel-array device developed in this thesis showed an impedance of 5.36 ± 3.50 kΩ at approximately 1 kHz. This value was compared with the Tringides et al. hydrogel-array benchmark and the ongoing full PEDOT:PSS electrode work to position the device within the broader context of soft electrode-array development. However, the comparison remains qualitative because the systems differ in device maturity, electrode geometry, contact method, and conductive material. Therefore, the main conclusion is not that the PEDOT:PSS-PEGPACHI device outperforms existing systems, but that the hydrogel tracks showed impedance values in a relevant range for further development of soft bioelectronic electrode arrays.

Appendix K. Supplementary electrochemical characterisation

K1 Supplementary EIS analysis of PEDOT:PSS-DBSA

Supplementary EIS-derived plots were generated for the PEDOT:PSS-DBSA hydrogel to provide a more complete view of its electrochemical behaviour. In addition to the impedance magnitude shown in the main text, the capacitance, real impedance, and Nyquist-type response were plotted to support the interpretation of the DBSA formulation.

The PEDOT:PSS-DBSA hydrogel showed a relatively low impedance response over the measured frequency range. The impedance and real impedance decreased with increasing frequency and reached a more stable response at higher frequencies. The capacitance was highest at low frequencies and decreased rapidly with increasing frequency, indicating that charge-storage behaviour was more pronounced at lower frequencies. The Nyquist-type plot showed a compact response, supporting the interpretation that the PEDOT:PSS-DBSA hydrogel behaved as a highly conductive formulation under the tested conditions.

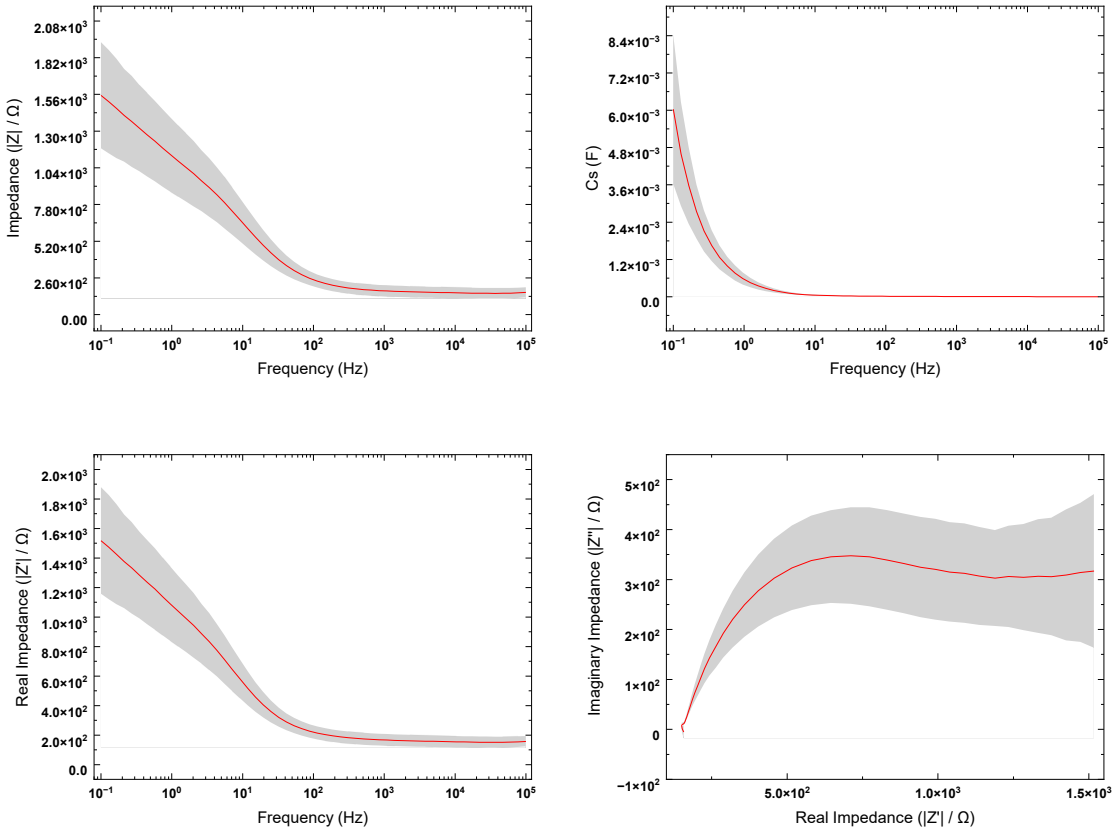


Figure A 17: Supplementary EIS analysis of PEDOT:PSS-DBSA hydrogel. Supplementary electrochemical impedance analysis of PEDOT:PSS-DBSA hydrogel measured in 1x DPBS. The plots show impedance magnitude, capacitance, real impedance, and the corresponding Nyquist-type representation. The black line represents the mean response and the grey shaded region represents the standard deviation between measured samples. These plots support the PEDOT:PSS-DBSA electrochemical characterisation presented in Chapter 5.

K2 Supplementary EIS analysis of PEDOT:PSS-PAA

Supplementary EIS-derived plots were generated for the PEDOT:PSS-PAA hydrogel to support the electrochemical characterisation presented in Chapter 5. In addition to the impedance magnitude response, the capacitance, real impedance, and Nyquist-type response were plotted to provide a more complete overview of the behaviour of the PAA-based formulation.

The PEDOT:PSS-PAA hydrogel showed a higher impedance response than the other formulations, especially at low frequencies. The impedance and real impedance decreased with increasing frequency, but the response also showed a large standard deviation, indicating variability between measured samples. The capacitance was highest at low frequencies and rapidly decreased with increasing frequency, while the Nyquist-type plot showed a broad and variable response. This supports the interpretation that PEDOT:PSS-PAA had weaker and less reproducible electrochemical behaviour under the tested conditions, likely due to the more complex fabrication route, hydrogel handling, and electrode-contact variability.

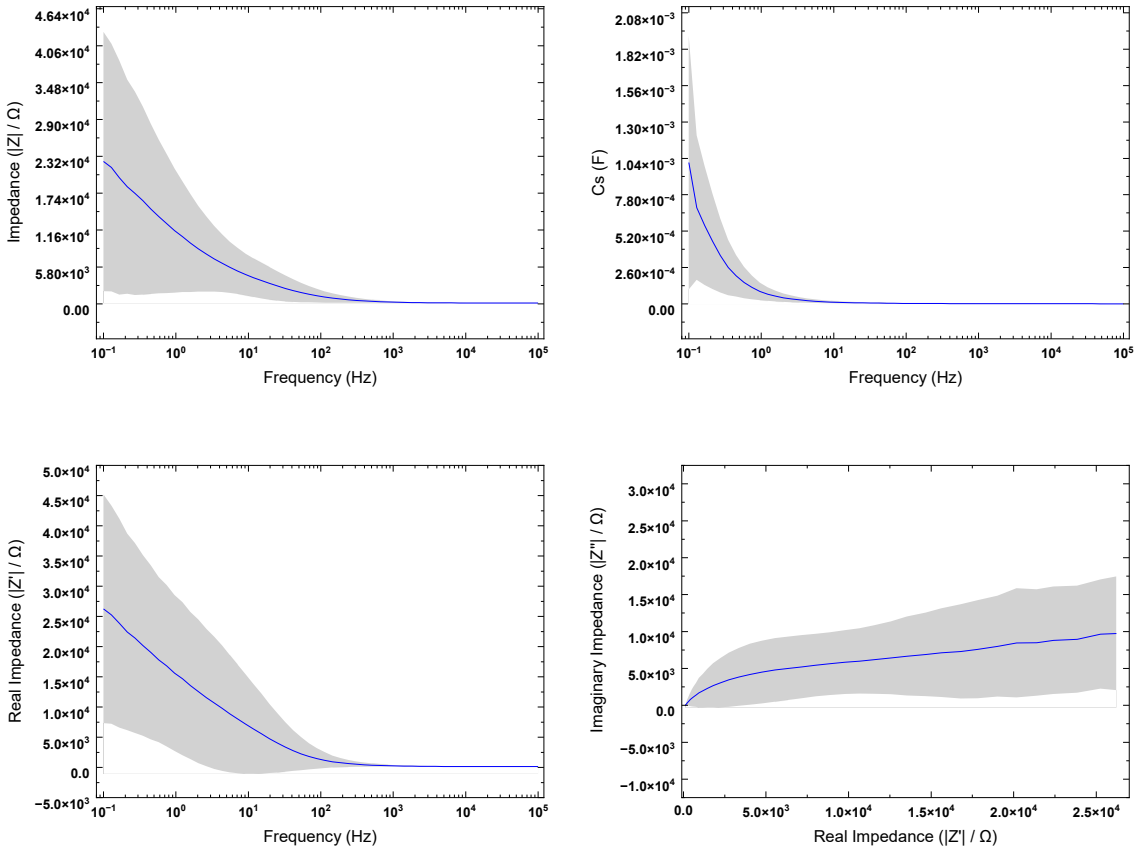


Figure A 18: Supplementary EIS analysis of PEDOT:PSS-PAA hydrogel. Supplementary electrochemical impedance analysis of PEDOT:PSS-PAA hydrogel measured in 1x DPBS. The plots show impedance magnitude, capacitance, real impedance, and the corresponding Nyquist-type representation. The blue line represents the mean response, and the grey shaded region represents the standard deviation between measured samples. These plots support the PEDOT:PSS-PAA electrochemical characterisation presented in Chapter 5.

K3 Supplementary EIS analysis of PEDOT:PSS-PEGPACHI

Supplementary EIS-derived plots were generated for the PEDOT:PSS-PEGPACHI hydrogel to further support the electrochemical characterisation presented in Chapter 5. The impedance magnitude,

capacitance, real impedance, and Nyquist-type response were plotted to provide a more complete overview of the electrochemical behaviour of the thesis-developed formulation.

The PEDOT:PSS-PEGPACHI hydrogel showed an intermediate impedance response compared with PEDOT:PSS-DBSA and PEDOT:PSS-PAA. The impedance and real impedance decreased with increasing frequency, indicating measurable charge transport through the hydrated hydrogel. The capacitance was highest at low frequencies and decreased rapidly as frequency increased, suggesting that charge-storage behaviour was mainly present in the low-frequency region. The Nyquist-type plot showed a more defined response than PEDOT:PSS-PAA, although variability between samples was still observed. This supports the interpretation that PEDOT:PSS-PEGPACHI showed clearer electrochemical activity than PEDOT:PSS-PAA, while remaining less conductive than PEDOT:PSS-DBSA.

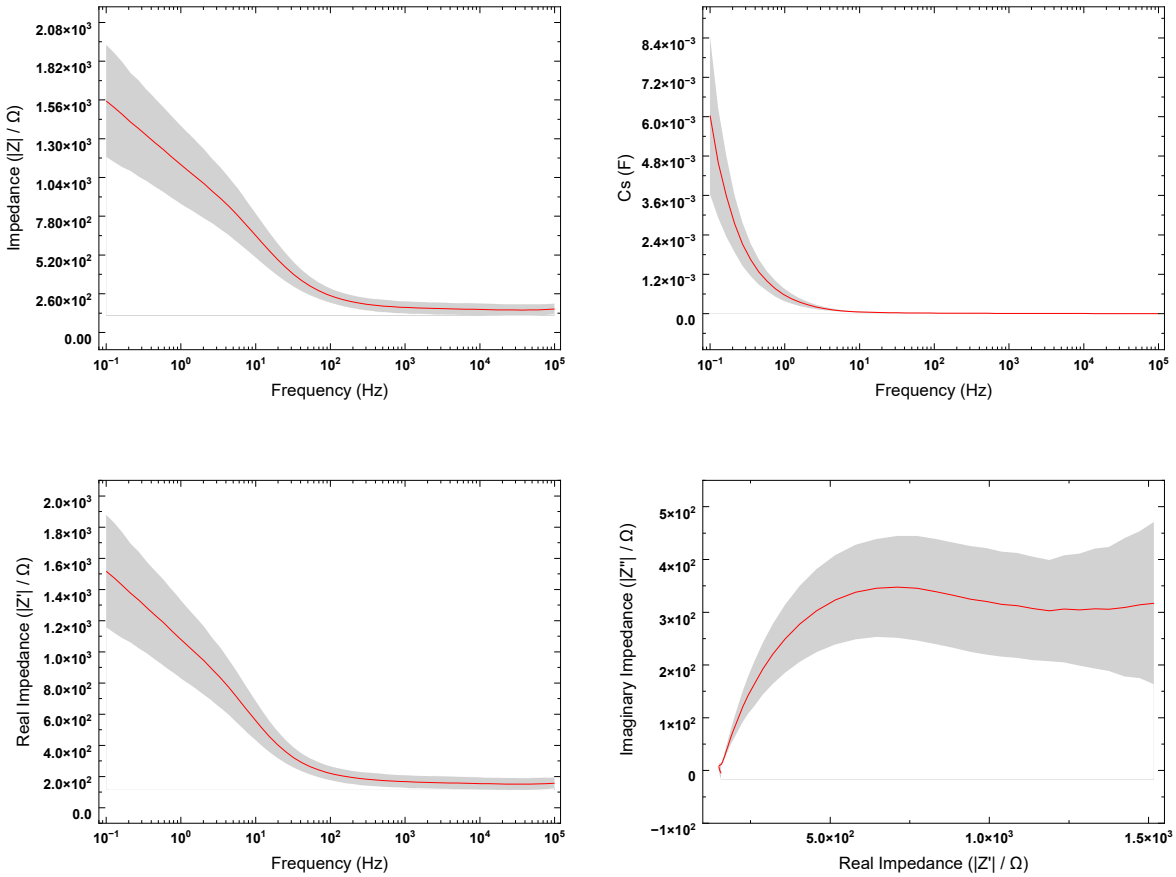


Figure A 19: Supplementary EIS analysis of PEDOT:PSS-PEGPACHI hydrogel. Supplementary electrochemical impedance analysis of PEDOT:PSS-PEGPACHI hydrogel measured in 1x DPBS. The plots show impedance magnitude, capacitance, real impedance, and the corresponding Nyquist-type representation. The red line represents the mean response and the grey shaded region represents the standard deviation between measured samples. These plots support the PEDOT:PSS-PEGPACHI electrochemical characterisation presented in Chapter 5.

K4 Supplementary EIS analysis of PEDOT:PSS-DBSA in Swagelok configurations

Supplementary EIS-derived plots were generated for PEDOT:PSS-DBSA measured in the Swagelok-based configurations to compare the response obtained with different electrode materials. The hydrogel was measured between either gold-gold or platinum-platinum electrodes, and the impedance

magnitude, capacitance, real impedance, and Nyquist-type response were plotted for each configuration.

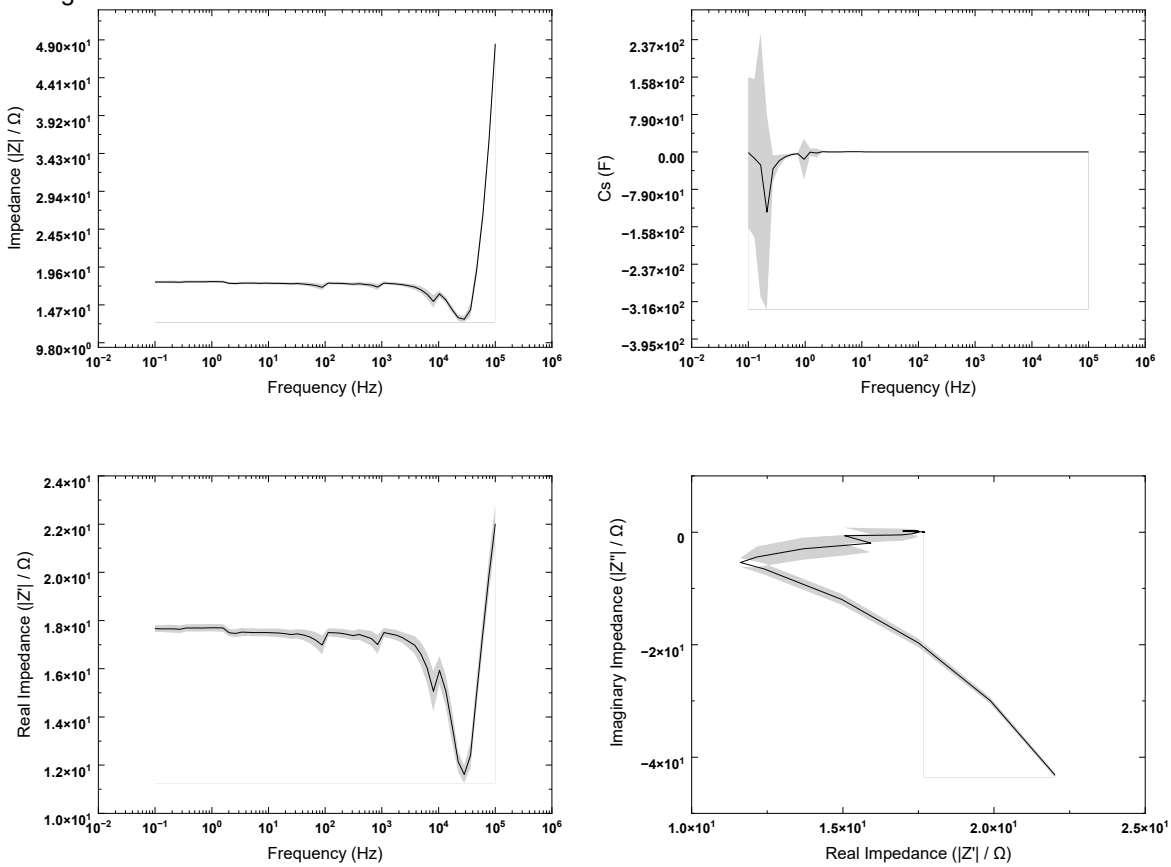


Figure A 20: Supplementary EIS analysis of PEDOT:PSS-DBSA hydrogel measured in gold-gold Swagelok configuration.

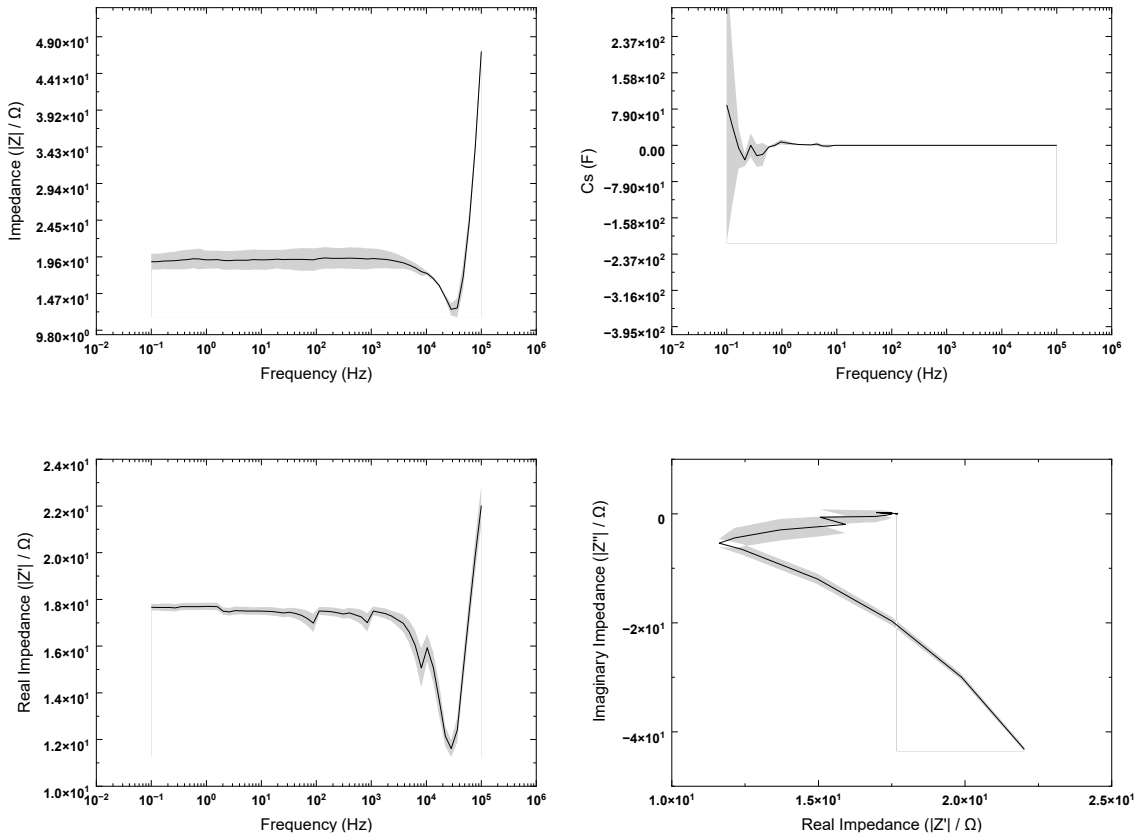


Figure A 21: Supplementary EIS analysis of PEDOT:PSS-DBSA hydrogel in the platinum-platinum Swagelok configuration.

K5 Supplementary EIS analysis of PEDOT:PSS-PAA in Swagelok configuration

Supplementary EIS-derived plots were generated for PEDOT:PSS-PAA measured in the Swagelok-based configurations to compare the response obtained with different electrode materials. The hydrogel was measured between either gold-gold or platinum-platinum electrodes, and the impedance magnitude, capacitance, real impedance, and Nyquist-type response were plotted for each configuration.

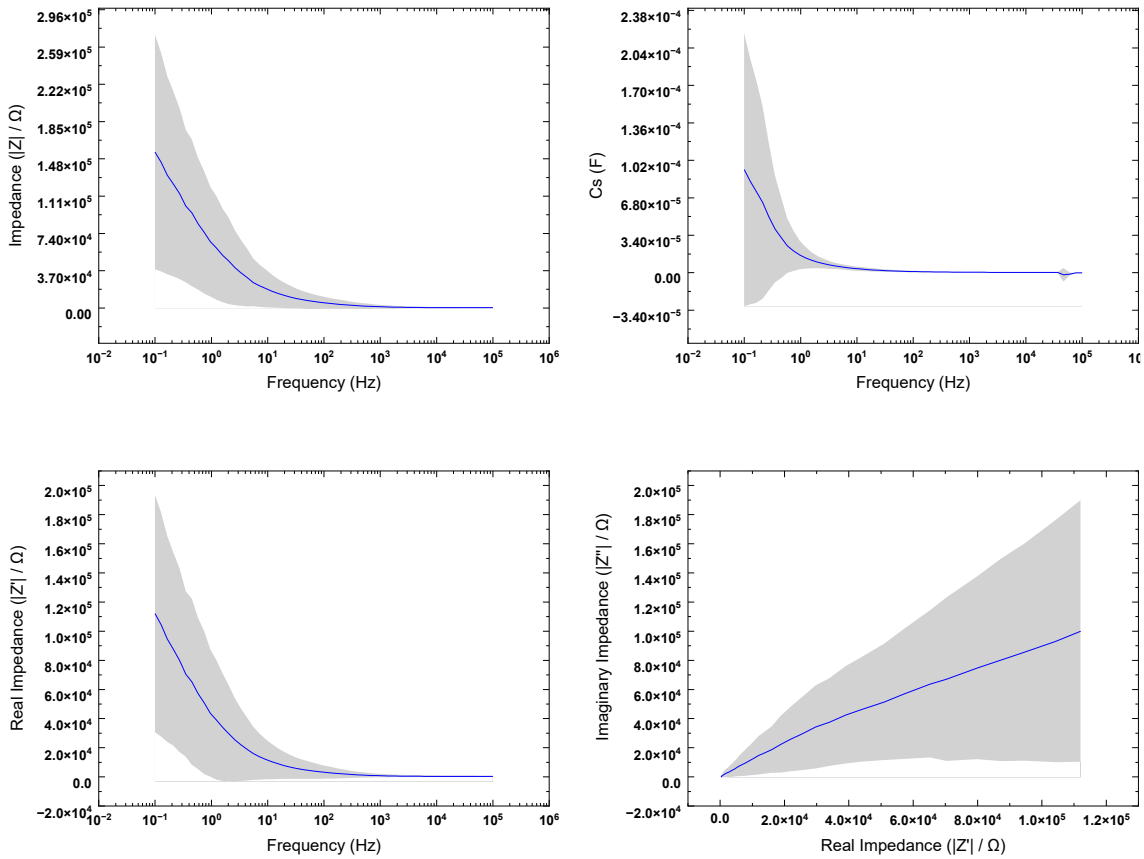


Figure A 22: Supplementary EIS analysis of PEDOT:PSS-PAA hydrogel in the gold-gold Swagelok configuration.

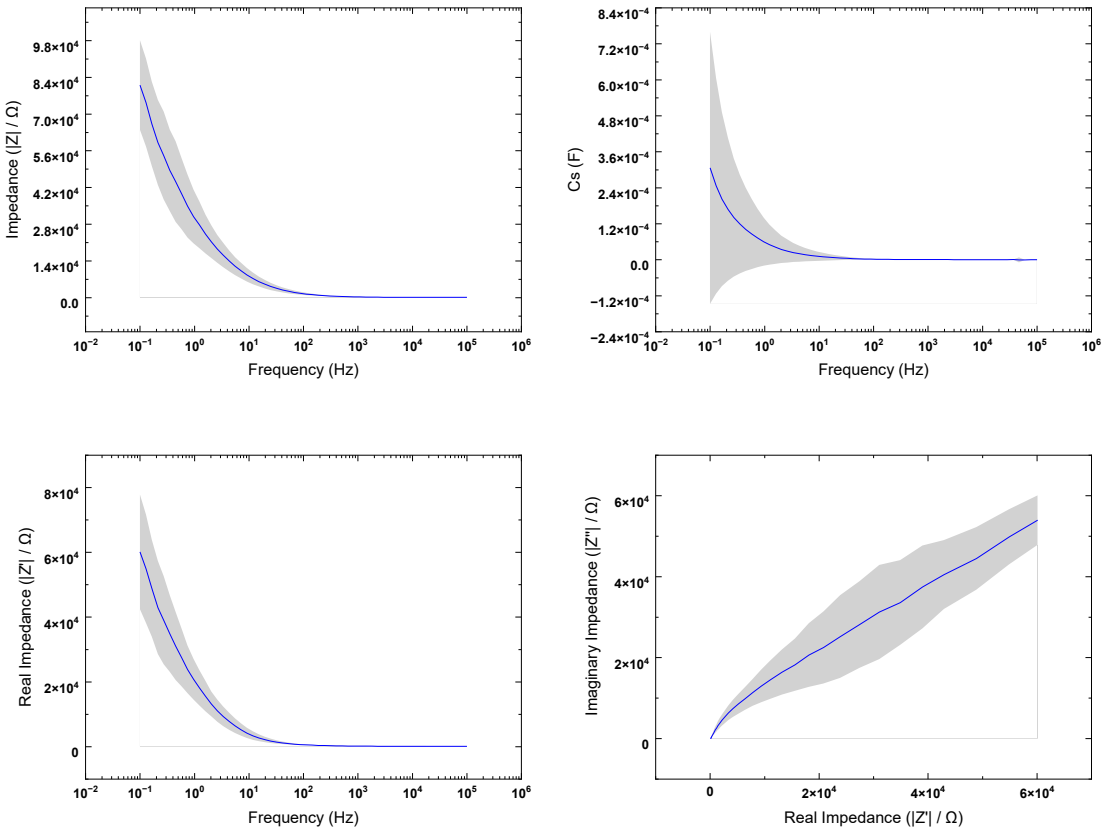


Figure A 23: Supplementary EIS analysis of PEDOT:PSS-PAA hydrogel in the platinum-platinum Swagelok configuration.

K6 Supplementary EIS analysis of PEDOT:PSS-PEGPACHI in Swagelok configurations

Supplementary EIS-derived plots were generated for PEDOT:PSS-PEGPACHI measured in the Swagelok-based configurations to compare the response obtained with different electrode materials. The hydrogel was measured between either gold-gold or platinum-platinum electrodes, and the impedance magnitude, capacitance, real impedance, and Nyquist-type response were plotted for each configuration.

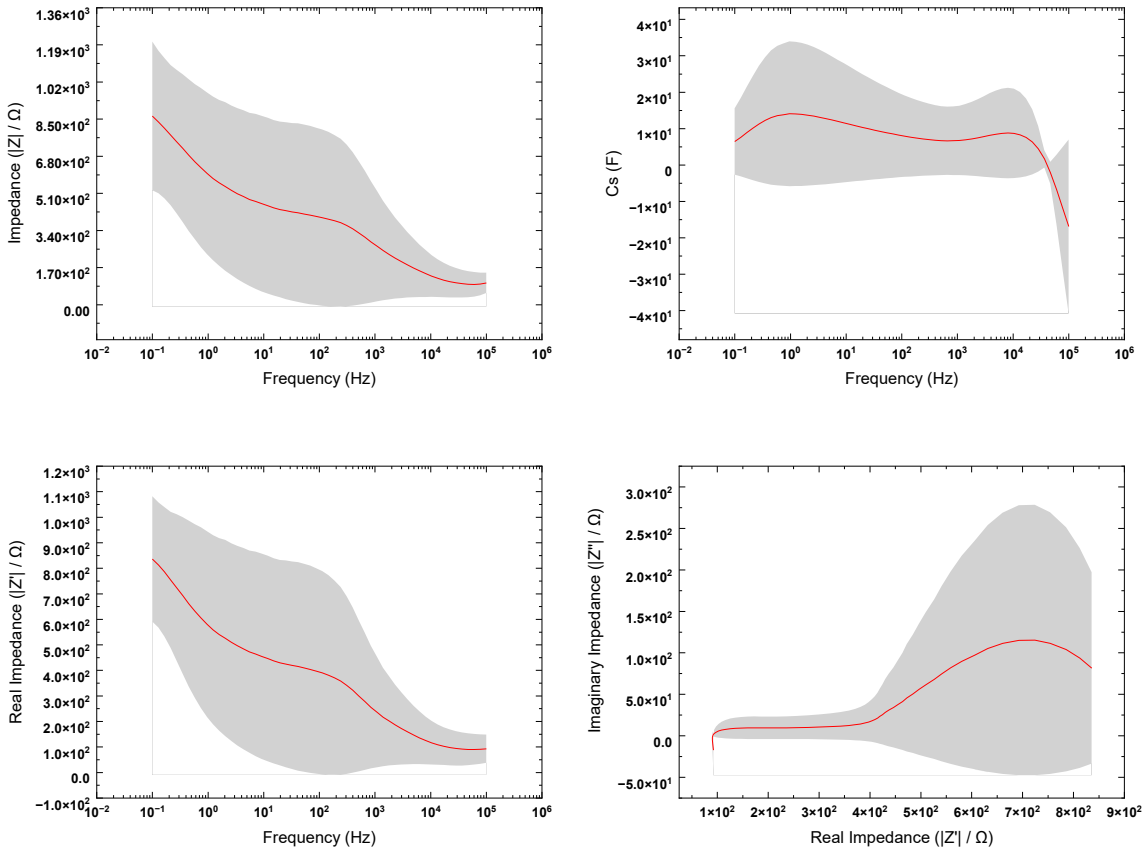


Figure A 24: Supplementary EIS analysis of PEDOT:PSS-PEGPACHI hydrogel in the gold-gold Swagelok configuration.

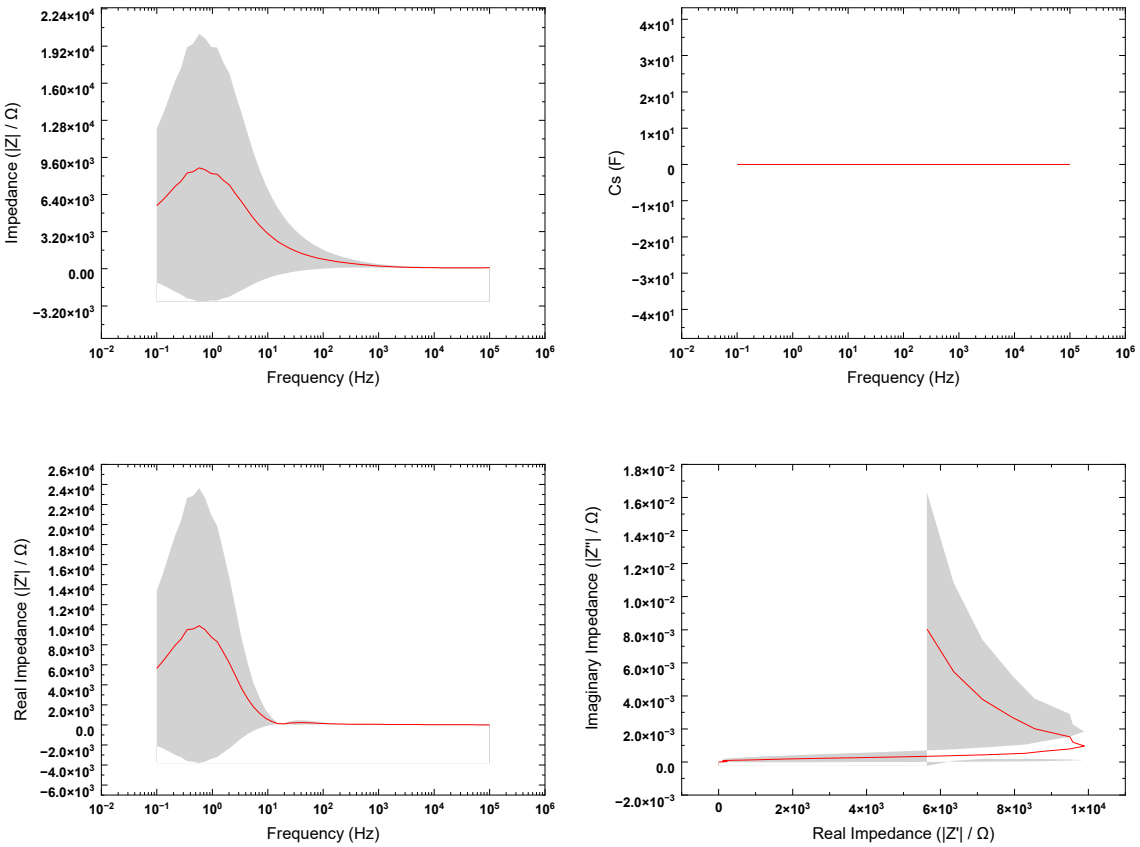


Figure A 25: Supplementary EIS analysis of PEDOT:PSS-PEGPACHI hydrogel in the platinum-platinum Swagelok configuration.

K7 Supplementary EIS analysis of PEDOT:PSS-PEGPACHI in the PDMS hydrogel-array device

Supplementary EIS-derived plots were generated for PEDOT:PSS-PEGPACHI tracks integrated into the preliminary PDMS hydrogel-array device. These plots provide additional information on the electrochemical behaviour of the patterned hydrogel tracks beyond the main impedance and CV results shown in Chapter 7. The impedance magnitude, capacitance, real impedance, and Nyquist-type response were plotted to support the interpretation of the device-level measurements.

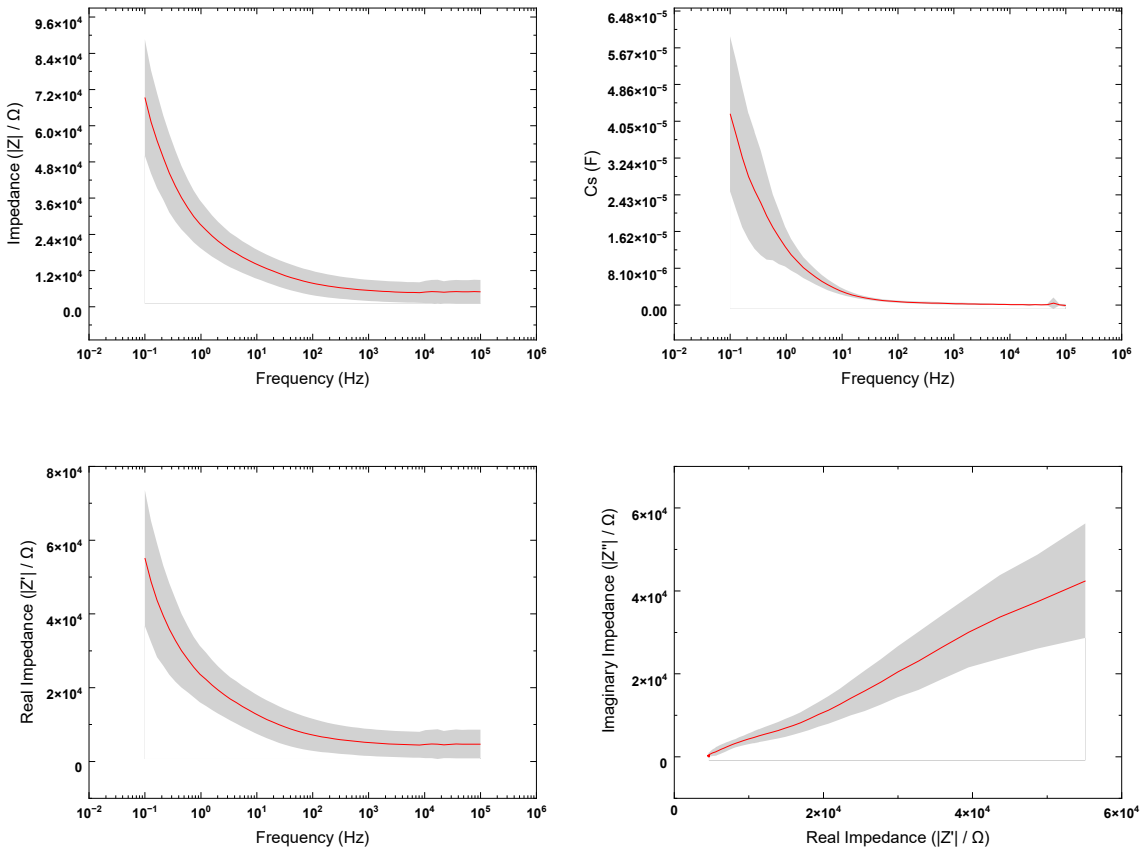


Figure A 26: Supplementary EIS analysis of PEDOT:PSS-PEGPACHI hydrogel tracks in the PDMS hydrogel-array device.

Appendix L. Supplementary Swagelok electrochemical analysis

L1 Gold-gold Swagelok configuration: PEDOT:PSS-DBSA

PEDOT:PSS-DBSA was used as the first formulation to evaluate the gold-gold Swagelok configuration because it had already shown a stable electrochemical response in the PDMS measuring platform. In this section, the purpose was not only to repeat the same measurement in a different setup, but to examine how the DBSA hydrogel behaved when measured through direct bulk contact between two gold disk electrodes. This was important because the Swagelok configuration reduces the dependence on a single local pogo-pin contact and instead probes the hydrogel as a conductive material positioned between two defined electrode surfaces.

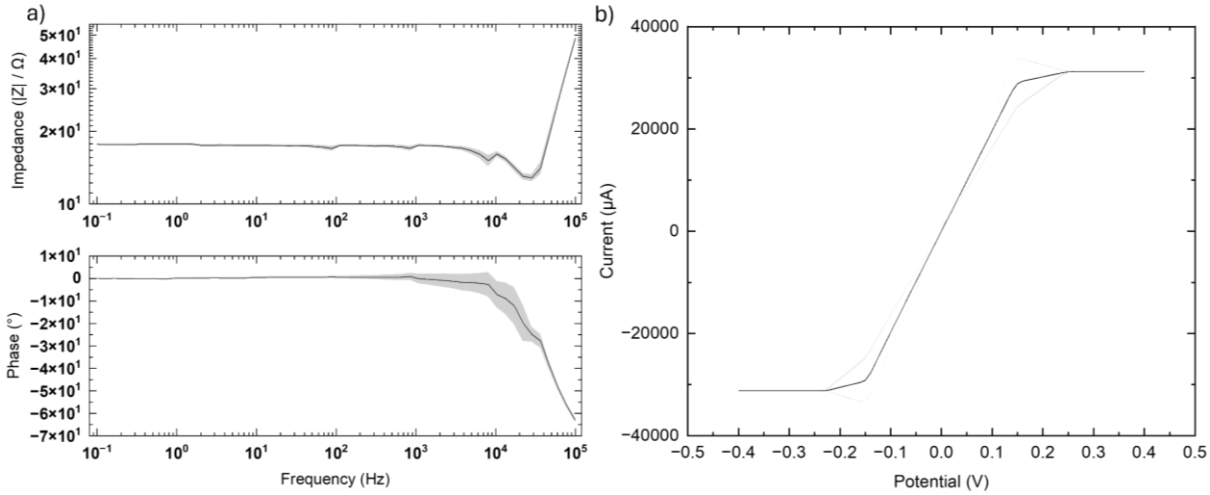


Figure A 27: Electrochemical response of PEDOT:PSS-DBSA hydrogels measured in the Swagelok-based bulk setup using gold-gold disk electrodes.
(a) Impedance magnitude |Z| and phase angle as a function of frequency measured by EIS after overnight soaking in 1x DPBS. (b) Cyclic voltammetry response recorded between −0.4 and +0.4 V. The black line represents the mean response and the grey shaded area represents mean ± SD for n = 3 hydrogel samples.

Additional Swagelok-based measurements were also performed for PEDOT:PSS-DBSA hydrogels under different measurement conditions and sample configurations. These experiments are included in **Appendix K** to document the broader electrochemical evaluation of the DBSA formulation, while Figure 5.8 presents the selected gold-gold bulk response used for comparison in the main text.

The EIS response of PEDOT:PSS-DBSA in the gold-gold Swagelok configuration was clearly different from the response measured in the PDMS measuring platform. In the Swagelok setup, the impedance magnitude remained very low across most of the measured frequency range, with values of approximately 15-17 Ω from low frequency up to the mid-frequency region. This nearly frequency-independent impedance indicates that the measurement was dominated by a highly conductive bulk pathway through the hydrated hydrogel and the two gold disk electrodes. Compared with the PDMS measuring platform, where the impedance was influenced by the local pogo-pin contact and open electrolyte geometry, the Swagelok setup provided a more direct and confined electrode-hydrogel-electrode contact.

The phase response was close to 0° over a large part of the frequency range, further supporting that the gold-gold Swagelok measurement was mainly resistive. This behaviour suggests that, under these contact conditions, the PEDOT:PSS-DBSA hydrogel behaved as a low-resistance conductive bridge between the two gold electrodes. At higher frequencies, especially above approximately 10 kHz, the phase became more negative and the impedance increased sharply near the upper end of the measured frequency range. This high-frequency deviation is unlikely to reflect only the intrinsic hydrogel behaviour. It may also include contributions from the measurement fixture, wiring, electrode geometry, and parasitic effects of the Swagelok configuration. Therefore, the most reliable interpretation of this measurement comes from the low- and mid-frequency regions, where the impedance remained low and stable.

The CV response of PEDOT:PSS-DBSA in the gold-gold Swagelok configuration showed very high current values, reaching the order of tens of milliamperes. However, the curve did not show a conventional broad and enclosed capacitive shape. Instead, the response was almost linear and was likely dominated by the very low-resistance electrode-hydrogel-electrode pathway created by confining the hydrated DBSA hydrogel directly between the two gold electrodes. Therefore, this CV response was interpreted mainly as evidence of strong electrical contact and high bulk conductivity, rather than as a clean charge-storage response of the hydrogel. The apparent capacitance-related behaviour in this configuration should therefore be interpreted with caution, as it may be strongly influenced by the measurement geometry, contact conditions, and current range limitations.

Overall, the gold-gold Swagelok measurement confirmed that PEDOT-DBSA behaved as a highly conductive bulk hydrogel when compressed between two disk electrodes. The low impedance and near-zero phase response over most of the frequency range indicate a predominantly resistive bulk pathway. However, the unusually high CV currents show that the Swagelok CV response was strongly affected by the measurement geometry, and therefore the CV results from this configuration should be interpreted cautiously.

L2 Gold-gold Swagelok configuration: PEDOT:PSS-PAA

PEDOT:PSS-PAA was measured in the gold-gold Swagelok configuration to assess whether the more robust bulk structure observed macroscopically also translated into improved electrochemical behaviour. This was particularly important because the PDMS measuring platform was not ideal for this formulation, as the hydrogel had to be post-processed before electrode contact. The Swagelok setup therefore provided a more suitable configuration for evaluating PEDOT-PAA as a bulk hydrated material.

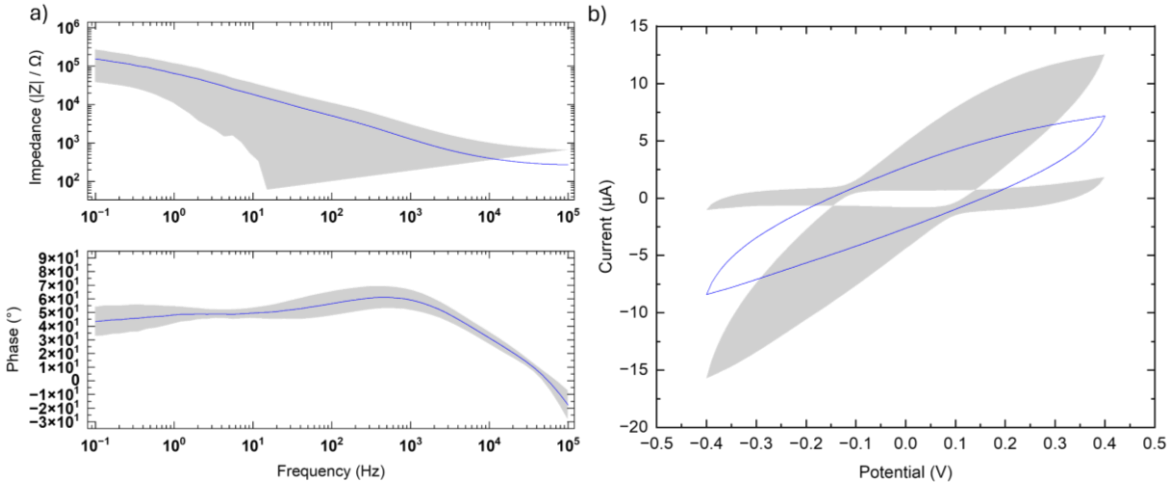


Figure A 28: Electrochemical response of PEDOT:PSS-PAA hydrogels measured in the Swagelok-based bulk setup using gold-gold disk electrodes.

(a) Impedance magnitude |Z| and phase angle as a function of frequency measured by EIS after overnight soaking in 1x DPBS. (b) Cyclic voltammetry response recorded between −0.4 and +0.4 V. The blue line represents the mean response and the grey shaded area represents mean ± SD for n = 3 hydrogel samples.

Additional Swagelok-based experiments were also performed for PEDOT:PSS-PAA hydrogels under different measurement conditions and sample configurations. These measurements are provided in **Appendix K** to document the broader evaluation of the PEDOT:PSS-PAA formulation, while Figure 5.8 presents the selected gold-gold bulk response used for comparison in the main text.

The EIS response showed that PEDOT:PSS-PAA behaved very differently from PEDOT:PSS-DBSA in the gold-gold Swagelok setup. Instead of forming a low-resistance bulk pathway, PEDOT:PSS-PAA showed a high impedance at low frequency, with values in the range of approximately 10^5 Ω. The impedance then decreased steadily with increasing frequency, reaching the 10^2-10^3 Ω range at high frequency. This large frequency dependence suggests that the response was not dominated by a simple conductive pathway between the two gold electrodes. Instead, charge transport through the PEDOT:PSS-PAA hydrogel appeared to be limited by the hydrated polymer network, internal morphology, and interfacial processes at the electrode-hydrogel contacts.

The variability in the impedance response was also much larger than for PEDOT:PSS-DBSA. The broad shaded region, especially across the low- and mid-frequency range, indicates substantial differences between samples or measurement runs. This is likely related to the heterogeneous bulk structure of the PEDOT:PSS-PAA hydrogel after post-treatment, annealing, and rehydration. During the physical characterisation, PEDOT:PSS-PAA showed a rougher and more porous structure than the other formulations, and some ionic liquid release and shape change were observed during rehydration. These factors may have caused differences in water uptake, internal connectivity, and electrode contact area between samples, which would explain the larger spread in the EIS response.

The phase behaviour supports this interpretation. The phase angle remained relatively high across a broad frequency range and reached its maximum in the mid-frequency region before decreasing at high frequency. This indicates that PEDOT:PSS-PAA did not behave as a purely resistive hydrogel in this configuration. Instead, the response included a strong frequency-dependent contribution, consistent with interfacial charging and transport limitations within the hydrated hydrogel network. Compared with PEDOT:PSS-DBSA, which showed a near-zero phase over most of the frequency range in the same gold-gold configuration, PEDOT:PSS-PAA showed a much stronger capacitive or dispersive component.

The CV response was also much weaker than that of PEDOT:PSS-DBSA in the gold-gold Swagelok setup. The measured current remained in the low microampere range, approximately within ±10 μA, and the enclosed area of the voltammogram was small. This suggests that PEDOT:PSS-PAA did not support the same level of bulk current flow or apparent charge storage under gold-gold contact conditions. The large shaded region in the CV plot also indicates considerable variability between measurements, which again points to differences in sample contact, hydration, and internal structure.

Overall, the gold-gold Swagelok measurements showed that PEDOT:PSS-PAA was physically robust but electrochemically less efficient than PEDOT:PSS-DBSA in this configuration. The hydrogel showed high low-frequency impedance, a broad phase response, low CV currents, and substantial variability between measurements. These results suggest that the PEDOT:PSS-PAA network provided mechanical stability, but its bulk electrochemical response was limited by internal transport and contact-related effects. Therefore, although the Swagelok setup was more appropriate than the PDMS measuring platform for testing PEDOT:PSS-PAA, the gold-gold measurements showed that this formulation did not provide the strongest electrochemical performance among the hydrogels tested.

L3 Gold-gold Swagelok configuration: PEDOT:PSS-PEGPACHI

PEDOT:PSS-PEGPACHI was measured in the gold-gold Swagelok configuration to evaluate its bulk electrochemical behaviour under direct contact with two gold disk electrodes. This was important because PEDOT:PSS-PEGPACHI showed strong electrochemical activity in the PDMS measuring platform, but the Swagelok setup provided a different measurement condition where the hydrogel was confined between two defined electrode surfaces. This allowed the formulation to be compared more directly with PEDOT:PSS-DBSA and PEDOT:PSS-PAA under the same bulk-contact geometry.

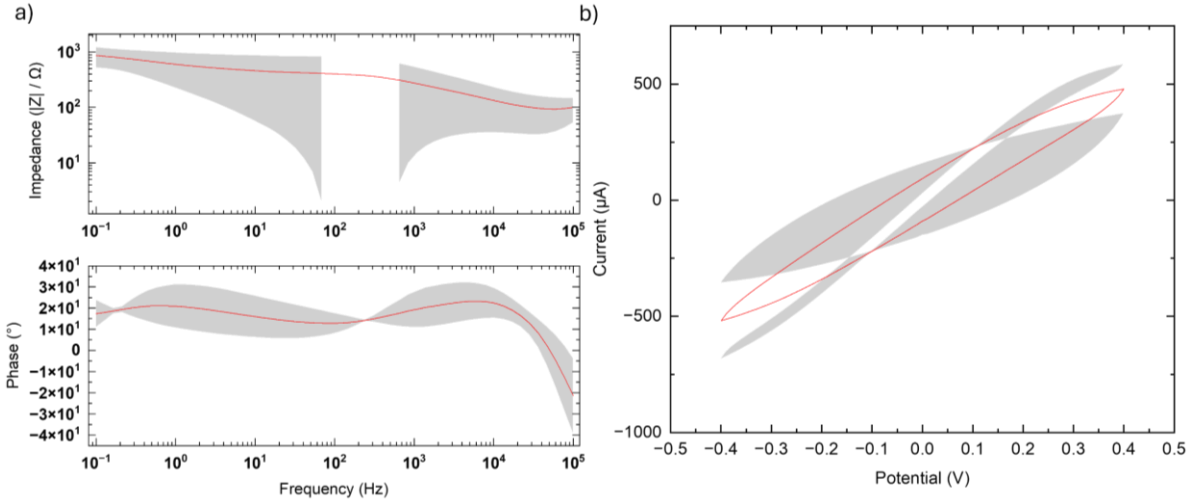


Figure A 29: Electrochemical response of PEDOT:PSS-PEGPACHI hydrogels measured in the Swagelok-based bulk setup using gold-gold disk electrodes. (a) Impedance magnitude |Z| and phase angle as a function of frequency measured by EIS after overnight soaking in 1x DPBS. (b) Cyclic voltammetry response recorded between −0.4 and +0.4 V. The red line represents the mean response and the grey shaded area represents mean ± SD for n = 3 hydrogel samples.

Additional Swagelok-based experiments were also performed for PEDOT:PSS-PEGPACHI hydrogels under different measurement conditions and sample configurations. These measurements are provided in **Appendix K** to document the broader evaluation of the PEDOT:PSS-PEGPACHI formulation, while Figure 5.8 presents the selected gold-gold bulk response used for comparison in the main text.

The EIS response of PEDOT:PSS-PEGPACHI showed an intermediate behaviour between PEDOT:PSS-DBSA and PEDOT:PSS-PAA. At low frequency, the impedance was in the order of 10^3 Ω, which was much lower than the low-frequency impedance of PEDOT:PSS-PAA but higher than the low and nearly frequency-independent impedance observed for PEDOT:PSS-DBSA in the same gold-gold configuration. As the frequency increased, the impedance gradually decreased and reached values close to 10^2 Ω at high frequency. This indicates that PEDOT:PSS-PEGPACHI formed a conductive bulk pathway between the gold electrodes, although not as strongly as PEDOT:PSS-DBSA. The impedance curve also showed a broad shaded region, especially in the low- and mid-frequency range. This suggests noticeable variability between samples or measurement runs. For PEDOT:PSS-PEGPACHI, this variability may be related to the brittle nature of the hydrogel and the fragmentation observed during handling and storage. Even when the hydrogel remained stable in DPBS, small differences in sample integrity, hydration, thickness, and electrode contact area could influence the measured impedance in the Swagelok cell. Therefore, the gold-gold Swagelok response should be interpreted as a bulk-contact measurement that is still sensitive to the physical condition of the hydrogel sample.

The phase response remained in a moderate positive range over most of the measured frequencies and showed a broad feature rather than a flat near-zero response. This behaviour indicates that PEDOT:PSS-PEGPACHI was not behaving as a purely resistive bridge between the two gold electrodes. Compared with PEDOT:PSS-DBSA, the phase response was more pronounced, suggesting a stronger contribution from interfacial charging or frequency-dependent transport within the hydrogel. However, compared with PEDOT:PSS-PAA, the impedance remained lower overall, indicating that the PEDOT:PSS-PEGPACHI network provided a more effective conductive pathway under gold-gold contact conditions.

The CV response of PEDOT:PSS-PEGPACHI was also clearly different from both PEDOT:PSS-DBSA and PEDOT:PSS-PAA. The current reached several hundred microamperes, which was higher than the PEDOT:PSS-PAA response but much lower than the very large current observed for PEDOT:PSS-DBSA in the same Swagelok configuration. The CV curve showed a broad enclosed area, indicating electrochemical charge-storage behaviour. At the same time, the curve was tilted and not ideally rectangular, showing that the response included both resistive and capacitive contributions.

Importantly, the PEDOT:PSS-PEGPACHI CV did not show the extreme current levels observed for PEDOT:PSS-DBSA in the gold-gold setup. This suggests that the PEDOT:PSS-PEGPACHI response was not dominated by a very low-resistance short bulk pathway to the same extent. Instead, the response appeared more controlled and closer to a typical conductive hydrogel response, although still affected by the bulk-contact geometry and sample-to-sample variability.

Overall, PEDOT:PSS-PEGPACHI showed promising electrochemical behaviour in the gold-gold Swagelok configuration. It had lower impedance and higher CV current than PEDOT:PSS-PAA, while avoiding the extremely high current response observed for PEDOT:PSS-DBSA. These results suggest that PEDOT:PSS-PEGPACHI provided a conductive and electrochemically active bulk hydrogel response, although its brittleness and partial fragmentation likely contributed to variability between measurements.

L4 Platinum-platinum Swagelok configuration: PEDOT:PSS-DBSA

PEDOT:PSS-DBSA was also measured in the Swagelok-based bulk setup using a platinum-platinum disk electrode configuration. This measurement was performed to evaluate whether the very low-impedance behaviour observed with gold-gold electrodes was also present when the same hydrogel was contacted using platinum electrodes. Since the hydrogel and measurement geometry were kept similar, this comparison helped separate the contribution of the hydrogel bulk response from possible electrode-material effects.

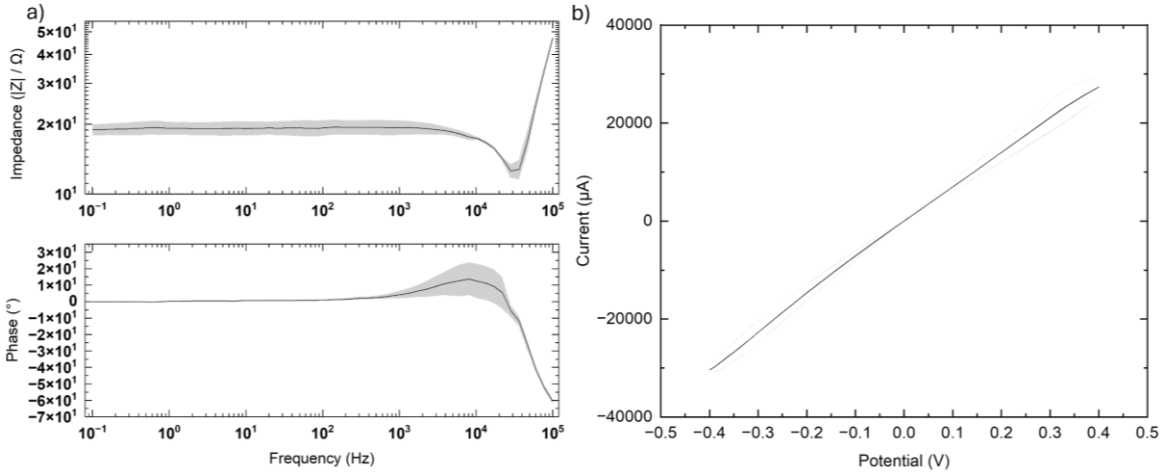


Figure A 30: Electrochemical response of PEDOT:PSS-DBSA hydrogels measured in the Swagelok-based bulk setup using platinum-platinum disk electrodes.

(a) Impedance magnitude |Z| and phase angle as a function of frequency measured by EIS after overnight soaking in 1x DPBS. (b) Cyclic voltammetry response recorded between −0.4 and +0.4 V. The black line represents the mean response and the grey shaded area represents mean ± SD for n = 3 hydrogel samples.

Additional Swagelok-based experiments were also performed for PEDOT:PSS-DBSA hydrogels under different measurement conditions and sample configurations. These measurements are provided in Appendix K to document the broader evaluation of the PEDOT:PSS-DBSA formulation, while Figure 5.9 presents the selected platinum-platinum bulk response used for comparison in the main text.

The EIS response showed that PEDOT:PSS-DBSA maintained a very low impedance in the platinum-platinum configuration. Across most of the measured frequency range, the impedance remained almost constant at approximately 18-20 Ω. This behaviour was similar to the gold-gold configuration and indicates that the PEDOT:PSS-DBSA hydrogel formed a highly conductive bulk pathway between the two disk electrodes. The low and nearly frequency-independent impedance suggests that, in this confined geometry, the measurement was dominated mainly by resistive transport through the hydrogel and the electrode-hydrogel contacts.

The phase response further supports this interpretation. Over the low- and mid-frequency range, the phase angle remained close to 0°, indicating a predominantly resistive response. This contrasts with the more frequency-dependent behaviour observed for PEDOT:PSS-PAA and PEDOT:PSS-PEGPACHI, where larger phase features were present. For PEDOT:PSS-DBSA, the near-zero phase suggests that charge transport through the hydrogel was not strongly limited by slower interfacial or capacitive processes under platinum-platinum bulk-contact conditions.

At the highest frequencies, the impedance increased sharply and the phase angle became strongly negative. This change appears only at the upper end of the frequency range and should be interpreted cautiously. It is likely influenced by the measurement setup, electrode leads, cell geometry, or other high-frequency artefacts rather than only by the intrinsic hydrogel behaviour. Therefore, the most meaningful region for interpreting the bulk response is the low- to mid-frequency range, where the impedance and phase were stable.

The CV response of PEDOT:PSS-DBSA in the gold-gold Swagelok configuration showed very high current values, reaching the order of tens of milliamperes. However, the curve did not show a conventional broad and enclosed capacitive shape. Instead, the response was almost linear and was likely dominated by the very low-resistance electrode-hydrogel-electrode pathway created by confining the hydrated DBSA hydrogel directly between the two gold electrodes. Therefore, this CV response was interpreted mainly as evidence of strong electrical contact and high bulk conductivity, rather than as a clean charge-storage response of the hydrogel. The apparent capacitance-related behaviour in this configuration should therefore be interpreted with caution, as it may be strongly influenced by the measurement geometry, contact conditions, and current range limitations.

Overall, the platinum-platinum Swagelok measurement confirmed that PEDOT:PSS-DBSA behaved as a very low-resistance bulk hydrogel under confined electrode-hydrogel-electrode contact. The EIS response was the most useful result from this configuration, showing a stable impedance of approximately 18-20 Ω over most of the frequency range. The CV confirmed strong electrical conduction, but because of the very high current and ohmic shape, it was mainly interpreted qualitatively rather than as a clean charge-storage measurement.

L5 Platinum-platinum Swagelok configuration: PEDOT:PSS-PAA

PEDOT:PSS-PAA was also evaluated in the Swagelok-based bulk setup using platinum-platinum disk electrodes. In this case, the hydrogel was measured after overnight soaking in 1x DPBS, with the sample placed between the two platinum disk electrodes in the confined bulk geometry. This

measurement was used to assess how PEDOT:PSS-PAA behaved under direct electrode-hydrogel-electrode contact and to compare its response with the other PEDOT:PSS-based hydrogel formulations examined in the same configuration.

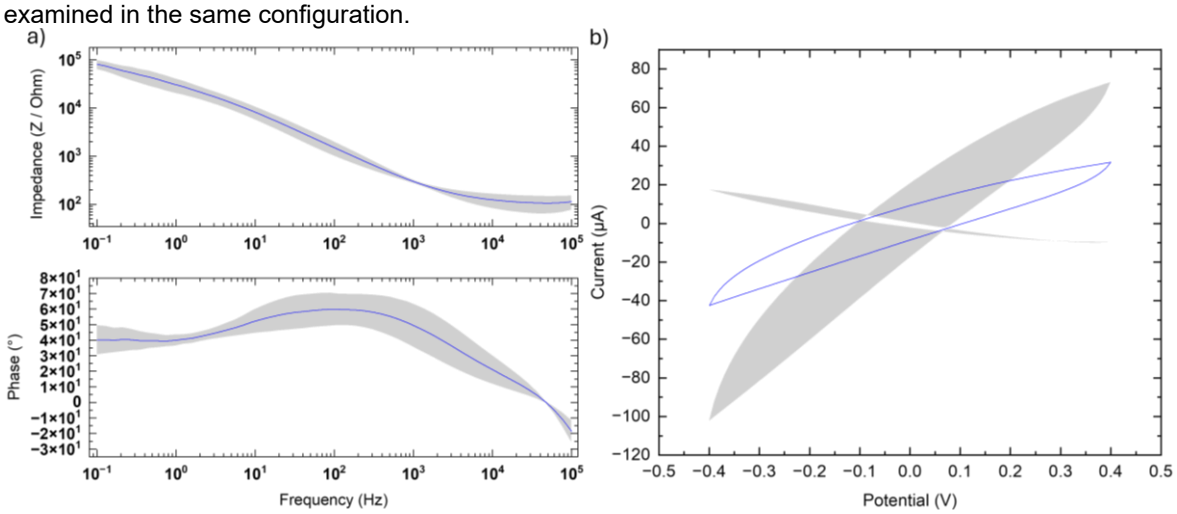


Figure A 31: Electrochemical response of PEDOT:PSS-PAA hydrogels measured in the Swagelok-based bulk setup using platinum-platinum disk electrodes. (a) Impedance magnitude |Z| and phase angle as a function of frequency measured by EIS after overnight soaking in 1x DPBS. (b) Cyclic voltammetry response recorded between −0.4 and +0.4 V. The coloured line represents the mean response and the grey shaded area represents mean ± SD for n = 3 hydrogel samples.

Additional Swagelok-based measurements were also carried out for PEDOT:PSS-PAA under different experimental conditions and with different sample preparations. These results are included in **Appendix K** to document the broader electrochemical evaluation of the PEDOT:PSS-PAA formulation, while Figure A 31 presents the representative platinum-platinum bulk response selected for the main discussion.

The EIS response of PEDOT:PSS-PAA showed a strong frequency dependence, with the impedance decreasing continuously from high values at low frequency to much lower values at high frequency. At the lowest measured frequencies, the impedance was on the order of 10^4-10^5 Ω, whereas at high frequency it decreased to approximately 10^2 Ω. This behaviour indicates that PEDOT:PSS-PAA did not behave as a simple low-resistance bulk conductor in the platinum-platinum configuration. Instead, the response suggests that slow ionic processes, interfacial effects, and bulk transport limitations all contributed significantly to the measured impedance.

The phase response supports this interpretation. At low frequency, the phase angle was already clearly positive, around 40°, and it increased further to a broad maximum of approximately 55-60° in the intermediate-frequency region. This broad phase maximum is characteristic of a mixed resistive/capacitive response and suggests that PEDOT:PSS-PAA exhibited a substantial capacitive contribution over a wide frequency range. Compared with PEDOT:PSS-DBSA in the same platinum-platinum configuration, PEDOT:PSS-PAA showed much more pronounced non-ohmic behaviour, indicating that charge transport was more strongly influenced by ionic motion within the hydrated network and by interfacial polarization effects.

At higher frequencies, the phase angle decreased steadily and eventually approached 0°, before becoming slightly negative at the upper end of the frequency range. As discussed previously for the other hydrogel systems, the transition toward lower phase angles at high frequency is consistent with increasingly resistive behaviour, while the small negative values at the highest frequencies are likely

influenced at least in part by setup-related artefacts, lead effects, or limitations of the measurement cell rather than only by the intrinsic hydrogel properties.

The cyclic voltammetry response of PEDOT:PSS-PAA was markedly different from the nearly linear, high-current behaviour observed for PEDOT:PSS-DBSA in the same bulk configuration. In the present case, the current response remained relatively low, approximately between −40 µA and +30 µA, and the voltammogram showed a narrow, tilted loop rather than a strongly expanded or highly conductive profile. This suggests that, although PEDOT:PSS-PAA was conductive enough to support charge transport across the bulk hydrogel, the response was significantly more limited and less dominated by direct ohmic conduction than in PEDOT:PSS-DBSA.

The CV shape also points to a more distributed electrochemical response, where both capacitive charging and resistive bulk transport contributed to the overall signal. The relatively small enclosed area indicates lower accessible charge transfer in this configuration, while the broad grey shaded region shows that sample-to-sample variation was considerable. This variability may arise from differences in bulk hydration, local compression between the platinum disks, slight changes in sample geometry, or variations in electrode contact quality.

Overall, the platinum-platinum Swagelok measurement showed that PEDOT:PSS-PAA behaved as a more resistive and more frequency-dependent conductive hydrogel than PEDOT:PSS-DBSA. Its electrochemical response was governed by a mixed resistive/capacitive behaviour, with a pronounced phase maximum in the intermediate-frequency region and a relatively modest CV current response. These results suggest that, in the confined bulk geometry, PEDOT:PSS-PAA provided a less direct conductive pathway than PEDOT:PSS-DBSA, but still maintained stable electrochemical behaviour characteristic of a hydrated PEDOT:PSS-based conductive hydrogel.

L6 Platinum-platinum Swagelok configuration: PEDOT:PSS-PEGPACHI

PEDOT:PSS-PEGPACHI was next evaluated using the platinum-platinum Swagelok configuration. This measurement was important because PEDOT:PSS-PEGPACHI had shown strong current response in the PDMS measuring platform, while the Swagelok setup allowed the material to be tested as a bulk hydrogel between two platinum disk electrodes. Compared with the gold-gold configuration, the platinum-platinum setup also allowed the influence of electrode material on the measured bulk response to be considered.

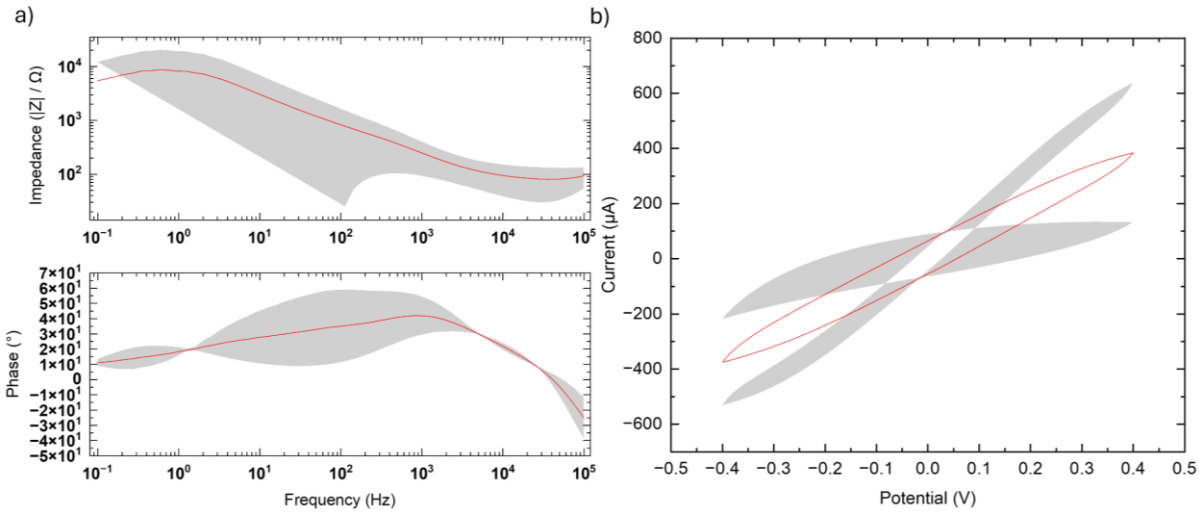


Figure A 32: Electrochemical response of PEDOT:PSS-PEGPACHI hydrogels measured in the Swagelok-based bulk setup using platinum-platinum disk electrodes. (a) Impedance magnitude |Z| and phase angle as a function of frequency measured by EIS after

overnight soaking in 1x DPBS. (b) Cyclic voltammetry response recorded between −0.4 and +0.4 V. The red line represents the mean response and the grey shaded area represents mean ± SD for n = 3 hydrogel samples.

Additional Swagelok-based experiments were also performed for PEDOT:PSS-PEGPACHI hydrogels under different experimental conditions and sample configurations. These measurements are provided in **Appendix K** to document the broader evaluation of the PEDOT:PSS-PEGPACHI formulation, while Figure 5.9 presents the selected platinum-platinum bulk response used for comparison in the main text.
The EIS response of PEDOT:PSS-PEGPACHI in the platinum-platinum configuration showed a clear decrease in impedance with increasing frequency. At low frequency, the impedance was in the order of 10^4 Ω, while at high frequency it decreased towards approximately 10^2 Ω. This indicates that PEDOT:PSS-PEGPACHI did not behave as a simple low-resistance conductor like PEDOT:PSS-DBSA, but it also did not show impedance as high as PEDOT:PSS-PAA at low frequency. Instead, the response was intermediate between the two other formulations.
The impedance response also showed considerable variability between measurements, as indicated by the broad grey shaded region. This variability was especially visible across the low- and mid-frequency range. For PEDOT:PSS-PEGPACHI, this is likely related to the physical nature of the hydrogel. Although the material remained stable when hydrated, it was also brittle and some fragmentation was observed during handling. Small differences in sample thickness, contact area, hydration state, and local compression inside the Swagelok cell could therefore strongly affect the measured impedance.
The phase response showed a broad maximum in the mid-frequency region, reaching approximately 40°, before decreasing at higher frequency and becoming negative at the upper end of the frequency range. This indicates that the platinum-platinum response of PEDOT:PSS-PEGPACHI included a stronger frequency-dependent component than PEDOT:PSS-DBSA. The behaviour suggests that the hydrogel response was influenced by both bulk transport through the hydrated PEDOT:PSS-PEGPACHI network and interfacial effects at the platinum electrode contacts.
The CV response showed a broad and tilted loop, with current values reaching several hundred microamperes. The mean current was approximately in the range of −400 to +400 µA, although the grey shaded region shows that the variability between measurements was large. Compared with PEDOT:PSS-PAA in the same platinum-platinum configuration, PEDOT:PSS-PEGPACHI showed a higher current response and a larger enclosed CV area. This suggests greater apparent charge-storage and charge-transfer capability. However, the response was still much lower than the very high current observed for PEDOT:PSS-DBSA, which behaved more like a low-resistance conductive bridge in the Swagelok setup.
The shape of the CV was not rectangular, and the loop was clearly tilted. This means that the response should not be interpreted as purely capacitive. Instead, the PEDOT:PSS-PEGPACHI hydrogel showed a mixed response where resistive bulk transport, interfacial charging, and sample-contact effects all contributed to the measured current. The large-shaded region also suggests that the platinum-platinum Swagelok measurement was sensitive to sample-to-sample differences, probably because of the brittle and partially fragmented nature of the hydrogel.
Overall, the platinum-platinum Swagelok results showed that PEDOT:PSS-PEGPACHI had a measurable and relatively strong electrochemical response compared with PEDOT:PSS-PAA, but it did not reach the very low impedance or high current levels observed for PEDOT:PSS-DBSA. The formulation therefore showed an intermediate bulk electrochemical behaviour: more electrochemically active than PEDOT:PSS-PAA, but more variable and less conductive than PEDOT:PSS-DBSA under confined platinum-platinum contact conditions.

Bibliography

[1] M. Zhang, Z. Tang, X. Liu, and J. Van der Spiegel, “Electronic neural interfaces,” Apr. 01, 2020, *Nature Research*. doi: 10.1038/s41928-020-0390-3.

[2] S. F. Cogan, “Neural stimulation and recording electrodes,” 2008. doi: 10.1146/annurev.bioeng.10.061807.160518.

[3] Kristoffer Famm, Brian Litt, Kevin J. Tracey, Edward S. Boyden, and Moncef Slaoui, “A jump-start for electroceuticals,” *Nat. Nanotechnol.*, 2013.

[4] K. Birmingham *et al.*, “Bioelectronic medicines: A research roadmap,” 2014, *Nature Publishing Group*. doi: 10.1038/nrd4351.

[5] M. E. Spira and A. Hai, “Multi-electrode array technologies for neuroscience and cardiology,” 2013, *Nature Publishing Group*. doi: 10.1038/nnano.2012.265.

[6] R. Chen, A. Canales, and P. Anikeeva, “Neural recording and modulation technologies,” Jan. 04, 2017, *Nature Publishing Group*. doi: 10.1038/natrevmats.2016.93.

[7] M. Berggren and G. G. Malliaras, “How conducting polymer electrodes operate,” Apr. 19, 2019, *American Association for the Advancement of Science*. doi: 10.1126/science.aaw9295.

[8] D. T. Simon, E. O. Gabrielsson, K. Tybrandt, and M. Berggren, “Organic Bioelectronics: Bridging the Signaling Gap between Biology and Technology,” Nov. 09, 2016, *American Chemical Society*. doi: 10.1021/acs.chemrev.6b00146.

[9] H. Yuk, B. Lu, and X. Zhao, “Hydrogel bioelectronics,” Mar. 21, 2019, *Royal Society of Chemistry*. doi: 10.1039/c8cs00595h.

[10] A. Guiseppi-Elie, “Electroconductive hydrogels: Synthesis, characterisation and biomedical applications,” Apr. 2010. doi: 10.1016/j.biomaterials.2009.12.052.

[11] Y. Shi, R. Liu, L. He, H. Feng, Y. Li, and Z. Li, “Recent development of implantable and flexible nerve electrodes,” Jan. 01, 2020, *KeAi Communications Co.* doi: 10.1016/j.smaim.2020.08.002.

[12] S. Cheng, R. Zhu, and X. Xu, “Hydrogels for next generation neural interfaces,” Dec. 01, 2024, *Springer Nature*. doi: 10.1038/s43246-024-00541-0.

[13] A. V. Volkov *et al.*, “Understanding the Capacitance of PEDOT:PSS,” *Adv. Funct. Mater.*, vol. 27, no. 28, Jul. 2017, doi: 10.1002/adfm.201700329.

[14] Y. Liang, A. Offenhäusser, S. Ingebrandt, and D. Mayer, “PEDOT:PSS-Based Bioelectronic Devices for Recording and Modulation of Electrophysiological and Biochemical Cell Signals,” Jun. 01, 2021, *John Wiley and Sons Inc*. doi: 10.1002/adhm.202100061.

[15] C. M. Proctor, J. Rivnay, and G. G. Malliaras, “Understanding volumetric capacitance in conducting polymers,” *J. Polym. Sci. B Polym. Phys.*, vol. 54, no. 15, pp. 1433-1436, Aug. 2016, doi: 10.1002/polb.24038.

[16] G. Schiavone, X. Kang, F. Fallegger, J. Gandar, G. Courtine, and S. P. Lacour, “Guidelines to Study and Develop Soft Electrode Systems for Neural Stimulation,” Oct. 28, 2020, *Cell Press*. doi: 10.1016/j.neuron.2020.10.010.

[17] K. Liu *et al.*, “The past, present, and future of in vivo-implantable recording microelectrodes: the neural interfaces,” May 10, 2024, *Royal Society of Chemistry*. doi: 10.1039/d3ma01105d.

[18] S. M. Won, E. Song, J. Zhao, J. Li, J. Rivnay, and J. A. Rogers, “Recent Advances in Materials, Devices, and Systems for Neural Interfaces,” Jul. 26, 2018, *Wiley-VCH Verlag*. doi: 10.1002/adma.201800534.

[19] P. Oldroyd and G. G. Malliaras, “Achieving long-term stability of thin-film electrodes for neurostimulation,” Feb. 01, 2022, *Acta Materialia Inc*. doi: 10.1016/j.actbio.2021.05.004.

[20] R. E. Daso *et al.*, “Standardized Electrochemical Characterisation of Conductive Hydrogels,” Apr. 10, 2025. doi: 10.26434/chemrxiv-2025-6n1bn.

[21] “hydrogel,” in *The IUPAC Compendium of Chemical Terminology*, Research Triangle Park, NC: International Union of Pure and Applied Chemistry (IUPAC), 2014. doi: 10.1351/goldbook.HT07519.

[22] K. Y. Lee and D. J. Mooney, “Hydrogels for tissue engineering,” Jul. 2001. doi: 10.1021/cr000108x.

[23] M. Gajendiran *et al.*, “Conductive biomaterials for tissue engineering applications,” Jul. 25, 2017, *Korean Society of Industrial Engineering Chemistry*. doi: 10.1016/j.jiec.2017.02.031.

[24] M. J. Donahue *et al.*, “Tailoring PEDOT properties for applications in bioelectronics,” Apr. 01, 2020, *Elsevier Ltd*. doi: 10.1016/j.mser.2020.100546.

[25] J. Ouyang, “Recent advances of intrinsically conductive polymers,” Apr. 17, 2018, *Beijing University Press*. doi: 10.3866/PKU.WHXB201804095.

[26] Y. Fang, L. Meng, A. Prominski, E. Schaumann, M. Seebald, and B. Tian, “Recent Advances in Bioelectronics Chemistry.”

[27] D. Mantione, I. del Agua, A. Sanchez-Sanchez, and D. Mecerreyes, “Poly(3,4-ethylenedioxythiophene) (PEDOT) derivatives: Innovative conductive polymers for bioelectronics,” Aug. 11, 2017, *MDPI AG*. doi: 10.3390/polym9080354.

[28] A. R. Harris and G. G. Wallace, “Organic Electrodes and Communications with Excitable Cells,” Mar. 21, 2018, *Wiley-VCH Verlag*. doi: 10.1002/adfm.201700587.

[29] C. Baker, K. Wagner, P. Wagner, D. L. Officer, and D. Mawad, “Biofunctional conducting polymers: synthetic advances, challenges, and perspectives towards their use in implantable bioelectronic devices,” 2021, *Taylor and Francis Ltd.* doi: 10.1080/23746149.2021.1899850.

[30] A. E. Ávila Ramírez, D. P. van der Laan, M. B. Shah, L. Wang, E. Zeglio, and A. Savva, “PEDOT:PSS—A Key Material for Bioelectronics,” Feb. 23, 2026, *John Wiley and Sons Inc*. doi: 10.1002/advs.202513480.

[31] L. Wang, Y. Hajee, J. P. Frimat, M. Diba, and A. Savva, “Electrically active hydrogels based on PEDOT:PSS for neural cultures,” *J. Mater. Chem. C Mater.*, vol. 14, no. 2, pp. 648-659, Jan. 2026, doi: 10.1039/d5tc02708j.

[32] D. Liu *et al.*, “Increasing the dimensionality of transistors with hydrogels,” 2025. [Online]. Available: https://www.science.org

[33] V. R. Feig *et al.*, “An Electrochemical Gelation Method for Patterning Conductive PEDOT:PSS Hydrogels,” *Advanced Materials*, vol. 31, no. 39, Sep. 2019, doi: 10.1002/adma.201902869.

[34] Q. Zeng and T. Wu, “Enhanced electrochemical performance of neural electrodes based on PEDOT:PSS hydrogel,” *J. Appl. Polym. Sci.*, vol. 139, no. 13, Apr. 2022, doi: 10.1002/app.51804.

[35] S. Zhang *et al.*, “Room-Temperature-Formed PEDOT:PSS Hydrogels Enable Injectable, Soft, and Healable Organic Bioelectronics,” *Advanced Materials*, vol. 32, no. 1, Jan. 2020, doi: 10.1002/adma.201904752.

[36] E. R. Briggs, A. X. Mendes, A. Teixeira Do Nascimento, S. E. Moulton, J. J. Blaker, and S. H. Cartmell, “Graphical Abstract Electrical Characterisation of Conductive Hydrogels for Biomedical Applications Electrical Characterisation of Conductive Hydrogels for Biomedical Applications.” [Online]. Available: https://ssrn.com/abstract=5235456

[37] Allevi, “Live/Dead Quantification Using Fiji - Step-by-Step Guide.” Accessed: Aug. 07, 2026. [Online]. Available: https://www.allevi3d.com/livedead-assay-quantification-fiji/

[38] Z. Yang *et al.*, “Free-standing PEDOT/polyaniline conductive polymer hydrogel for flexible solid-state supercapacitors,” *Electrochim. Acta*, vol. 322, Nov. 2019, doi: 10.1016/j.electacta.2019.134769.

[39] R. Borah *et al.*, “Electrically Conductive Injectable Silk/PEDOT: PSS Hydrogel for Enhanced Neural Network Formation,” *J. Biomed. Mater. Res. A*, vol. 113, no. 1, Jan. 2025, doi: 10.1002/jbm.a.37859.

[40] H. Wang *et al.*, “Flexible chitosan sensing hydrogel enabled by phytic acid coordination effect with high-conductivity and ultra-sensitivity for self-powered handwriting recognition and multimodal sensors,” *Nano Energy*, vol. 128, Sep. 2024, doi: 10.1016/j.nanoen.2024.109843.

[41] M. Solazzo, K. Krukiewicz, A. Zhussupbekova, K. Fleischer, M. J. Biggs, and M. G. Monaghan, “PEDOT:PSS interfaces stabilised using a PEGylated crosslinker yield improved conductivity and biocompatibility,” *J. Mater. Chem. B*, vol. 7, no. 31, pp. 4811-4820, 2019, doi: 10.1039/c9tb01028a.

[42] Q. Peng *et al.*, “Recent advances in designing conductive hydrogels for flexible electronics,” Sep. 01, 2020, *Blackwell Publishing Ltd*. doi: 10.1002/inf2.12113.

[43] D. Song, B. Kang, Z. Zhao, and S. Song, “Stretchable self-healing hydrogels capable of heavy metal ion scavenging,” *RSC Adv.*, vol. 9, no. 33, pp. 19039-19047, 2019, doi: 10.1039/c9ra03443a.

[44] S. M. Samani, F. Ahmadi, Z. Oveisi, and Z. Amoozgar, “Chitosan based hydrogels: characteristics and pharmaceutical applications,” 2015.

[45] S. Taokaew, W. Kaewkong, and W. Kriangkrai, “Recent Development of Functional Chitosan-Based Hydrogels for Pharmaceutical and Biomedical Applications,” Apr. 01, 2023, *MDPI*. doi: 10.3390/gels9040277.

[46] C. Pitsalidis *et al.*, “Organic Bioelectronics for In Vitro Systems,” Feb. 23, 2022, *American Chemical Society*. doi: 10.1021/acs.chemrev.1c00539.

[47] C. M. Tringides *et al.*, “Viscoelastic surface electrode arrays to interface with viscoelastic tissues,” *Nat. Nanotechnol.*, vol. 16, no. 9, pp. 1019-1029, Sep. 2021, doi: 10.1038/s41565-021-00926-z.